Moss and peat as monitors of contemporary and past rates of atmospheric dust deposition in the Athabasca Bituminous Sands Region

by

Gillian Mullan-Boudreau

A thesis submitted in partial fulfillment of the requirements for the degree of

Master of Science

in
Land Reclamation & Remediation

Department of Renewable Resources
University of Alberta

ABSTRACT

Research Problem

Since the introduction of open pit mining of the Athabasca Bituminous Sands (ABS) in 1967, this industry has generated considerable quantities of mineral dust that when released is injected into the atmosphere and settles in the surrounding environment. Despite this, a full profile of atmospheric dust deposition in the area has not been studied. The purpose of this research was to reconstruct contemporary and past rates of atmospheric dust deposition, using *Sphagnum* moss and peat cores as biomonitors respectively. To address the purpose of this research, samples were analyzed to identify the variation in natural "background" dust deposition rates in the area, and to determine the size, mineralogy, and morphology of the particulate mineral matter, in the hopes to better understand the impact of industry in the ABS region.

Methods of Investigation

Sphagnum moss samples were collected from 30 ombrotrophic (rain-fed) peat bogs surrounding ABS region and 5 ombrotrophic peat bogs in central Alberta for comparison (URSA, CMW, BMW, WAG, and EINP). Peat cores were collected from 7 ombrotrophic peat bogs (MIL, JPH4, McK, McM, ANZ, UTK, and SEB). The samples were ashed and reacted in HCl to separate the acid insoluble ash (AIA) (mineral matter) and the acid soluble ash (ASA) (macronutrients) fractions. The morphology and mineralogy of the dust mineral particles were studied using scanning electron microscopy and energy dispersive X-ray analysis, as well as the particle size distributions using a XPT (optical microscopy). Both ^{210}Pb and ^{14}C age-dating were used to create a combined age-depth model for each peat core. A major ion analysis was performed on the ASA fraction of the 2015 moss samples.

Contemporary Dust Deposition

The mean AIA content of the living layer of the moss samples increased from 0.4±0.5% to 4.7±2.0% over a 30 km distance towards industry. For comparison, the moss samples from the URSA control site had a mean value of 0.29± 0.07%. Mass accumulation rates (g/m^2 yr) were used to calculate the total amount of dust deposited within a 30km radius of industry. The result obtained using this approach (21,000 tonnes/ 4 month growing season) is beyond the current estimate (18,842 tonnes/yr) reported by the federal government (Environment and Climate Change Canada, 2015). Particle size was found to increase in variation closer to the ABS region and larger particles were more abundant. No major changes in mineralogy were found. Major ion analysis on ASA fractions showed the availability of P, Ca, Mg, Fe, Mn, S and K. Phosphorous, a growth limiting nutrient, was found to be 7 times greater at the sites with more AIA than those with background levels.

Past Dust Deposition

The concentrations of AIA and Th (a surrogate of mineral matter concentration) were determined to establish dust deposition and to calculate changes in mass accumulation rates over time. While it is uncertain if there was an increase in dust deposition since the ABS region operations began in 1967, there was a notable increase in AIA with distance from industry. Large quantities of fly ash were present in the top layers of the peat cores closest to the ABS region, but otherwise no notable changes in mineralogy were found. Near industry there was an increase in size variation of the particles and fly ash increased in abundance with depth. The average accumulation rates of AIA are up to 5x greater in the cores collected near industry. A comparison of AIA inventories with the pH of the porewaters suggest that the ASA fraction of the dusts deposited may impact the chemical composition of the bog waters.

PREFACE

The data presented here has helped to support other publications, and these are listed in Appendix 1. One of the publications, which can be found in the Appendix 2, I contributed the collection and analysis of data for pH and ash content profiles (Shotyk, W., et al. (2016), Peat bogs in northern Alberta, Canada reveal decades of declining atmospheric Pb contamination, Geophys. Res. Lett., 43, doi:10.1002/2016GL070952).

Chapter 2 and 3 were written as manuscripts to be submitted for publication. I was responsible for the data collection, analysis, and the manuscript composition for both. W. Shotyk was the supervisory author and co-author on both manuscripts, and was involved in concept formation, manuscript composition, and editing.

Chapter 2 was submitted to *Environmental Science and Technology* on December 7, 2016. The following were also co-authors on the paper: Kevin Devito, Tommy Noernberg, and Rick Pelletier. Kevin Devito took an editorial role and provided guidance on data analysis. Tommy Noernberg lead the sample collection and preformed some data collection. Rick Pelletier made Figure 1 and 2 with data I provided, and provided guidance on statistical analysis.

Chapter 3 was submitted to *Land Degradation and Development* on December 8, 2016. The following were co-authors on the paper: Lauren Davies, Duane Froese, Kevin Devito, Tommy Noernberg, and Rick Pelletier. Kevin Devito took an editorial role and provided guidance on data analysis. Tommy Noernberg lead the sample collection and preformed some data collection. Rick Pelletier made Figure 1 and 2 with data I provided. Lauren Davies, and Duane Froese made thee age dating model for each of the peat cores.

Herein the work in Chapter 2 is referred to as (Mullan-Boudreau, G., 2017a) and the work Chapter 3 is referred to as (Mullan-Boudreau, G., 2017b).

DEDICATION

"Each of us has his own special gift and you know this was meant to be true. And if you don't underestimate me, I won't underestimate you." - Bob Dylan

I dedicate this thesis to my family and friends, who have never underestimated me and have only encouraged me to strive for better. Without you this would not have been possible.

ACKNOWLEDGEMENTS

I am so grateful to everyone who helped me along the way on this project. Although I cannot thank everyone personally, I would like to say that without the support from all the wonderful people I have met in my time in Edmonton, this project would not have been nearly as wonderful!

A big thank you to Bill Shotyk. Thank you for giving me the opportunity to explore such an interesting and complex area of research. You have changed my outlook on scientific method and research for the better. Your calm and reassuring guidance throughout this whole project kept me focused, while your energizing excitement kept me wanting to learn more! You really were the best supervisor I could have possibly asked for, and I am very grateful I had the chance to work with you.

Tommy Noernberg, thanks for all your field work guidance, assistances, and sample preparation knowledge. Tracy Gartner, Melanie Bolstler, and Karen Lund thanks for providing much needed administrative support. I would like to thank several individuals for training and assistance: Nathan for SEM training, Bob Shannon for gamma spectrometry training, and Muhammad (Babar) Javed for assistance with the SPLITT. I would also like to thank Chad Cuss and Muhammad (Babar) Javed for laboratory support and instruction. Mark Donner, thanks for your help with field work. Anita Nowinka thanks for your assistance in the preparation of ash, and AIA samples of each peat core. Melissa Dergousoff and April Cormack thank you both for your hard work on moss sample cleaning and preparation. Kevin Devito thanks for acquainting our team with Utikuma, allowing me to tag along for field work to collect samples and on your help with my manuscripts. Rick Pelletier, thank you for the beautiful maps and your guidiance

on spatial modeling. Thanks to Rene Belland, Lee Foote and Claudio Zaccone for project guidance.

I would like to thank Alberta Innovates, Land Reclamation International Graduate School (LRIGS) and NSERC CREATE for providing financial support. Also, thanks to the University of Alberta, the Faculty of Agricultural, Life and Environmental Sciences, the Department of Renewable Resources for supporting the SWAMP laboratory.

Last but certainly not least, I would like to thank my friends and family who were so supportive throughout this whole journey. I would like to thank my parents and siblings who have always encouraged me to pursue my scientific aspirations. To my friends: I am very grateful to have met so many wonderful people in my time at the University of Alberta, you will be greatly missed.

My sincerest thanks to one and all!

TABLE OF CONTENTS

LIST OF TABLES

Chapter 1: Introduction

Chapter 3

LIST OF FIGURES

Chapter 1: Introduction

Chapter 2

Chapter 3

CHAPTER 1: INTRODUCTION, BACKGROUND, AND PEAT PROJECT OVERVIEW

INTRODUCTION

Background

Land Use in Northern Alberta

Northern Alberta's environment has been greatly impacted by anthropogenic activity since the turn of the 20th century when European immigrants began to settle. In the first decade of the 20th century over 59000 km^2 of undisturbed land was converted to agricultural lands (Agriculture Division of Statistics Canada, 2014), injecting large amounts of soil particulates into the atmosphere and drastically changing the composition of dust in the region. The next largest change, did not occur until 1967 with the opening of mining and upgrading operations in the Athabasca Bituminous Sands (ABS) region. The Great Canadian Oil Sands, now Suncor, was the first commercial development of mining operations in the region followed by the opening of Syncrude's operations in 1978. The ABS region has since expanded to become the third largest producer of oil in the world with 366,000 m^3/day of total bitumen production, 165,000 m^3/day of which is from open pit mining (Alberta Energy Regulator, 2015; Stringham, 2012). Of the 283.7 million m^3 of mineable oil reserves, 18% (51.3 million m^3) are accessible via open pit mining and the remaining 69% (195.9 million m^3) accessible via steam assisted gravity drainage (SAG-D) (Alberta Energy Regulator, 2015).

Figure 1: Example images of dust emissions in the ABS region (credit: William Shotyk and Mark Donner)

Effects on Air Quality

Open pit mines and tailings in Alberta produced 18842 tonnes of total particulate matter in 2015 (Figure 1)(Environment and Climate Change Canada, 2015). Once airborne, dust is deposited on the surrounding area with transport time and distance depending on factors such as wind direction, dust morphology, density, size, and height at the point of injection (Jacobson, 2002; Muhs, Prospero, Buddock, & Gill, 2014). Table 1 illustrates the time taken for particles to fall 1 km in the atmosphere as a function of their size.

Table 1: Time required for spherical particles of different sizes to fall 1 km in the atmosphere (From Table 5.4 of Jacobson, 2002).

Particle Diameter (μm)	Time to Fall 1 km
0.02	228 years
0.1	36 years
1	328 days
10	3.6 days
100	1.1 hours
1000	4.0 minutes
5000	1.8 minutes

The Wood Buffalo Environmental Association (WBEA) is a not-for-profit organization that monitors air quality in the ABS region (Percy & Davies, 2012). Their monitoring includes $PM_{2.5}$ and occasionally PM_{10} to assess human health concerns that have been found to be linked to particle size, reduction in agricultural product yields, mechanical wear on machinery, and more (Clair & Percy, 2015; Fennelly, 1976; Wang et al., 2015; Watson, Chow, Wang, Kohl, & Yatavelli, 2014). Monitoring only $PM_{2.5}$ and PM_{10} however, ignores a large fraction ($10\mu m<x<100\mu m$) of particulate matter that is also deposited into the environment (Liu & Lipták, 2000). Particulate matter in the larger size class, $10\mu m<x<100\mu m$, generally makes up a small fraction of the mass of atmospheric dusts due to their fallout rate (Table 1). Therefore, if this large size class is abundant, it is an indicator of a local sources that could be a result of a disturbance (Jacobson, 2002).

Besides the monitoring at WEBA, little work has been done on measuring dust deposition in the ABS region, although others have focused on other types of deposition: polycyclic aromatic

hydrocarbons (Bari, Kindzierski, & Cho, 2014), nitrogen and sulfur (wet and dry) (Lynam et al., 2015; Motallebi, Taylor Jr, & Croes, 2003; Watmough, Whitfield, & Fenn, 2014), base cations (Motallebi et al., 2003; Watmough et al., 2014), and heavy metals (Bari et al., 2014; Shotyk et al., 2014, 2016) . The complete size and composition profiles of mineral dust deposition in the ABS region has yet to be examined and is one of the objectives of this study.

Despite the minimal work in the ABS region, monitoring of dust generation near mines in other parts of the world has been well researched. For example, in eastern Canada dust deposited on lichen near the nickel smelting plant in Sudbury, Ontario (Neiboer et. al, 1972), as well as near the St. Lawrence North Shore (Pratte, Garneau & Vleeschouwer, 2016). Atmospheric dust deposition has also been researched in the Izery Mountains, the "Black Triangle" (heavily polluted area) on the border area of Poland, Czech Republic, and Germany using microbe communities (Fiałkiewicz-Kozieł et. al, 2015), on the East Rongbuk Glacier in the Himalayas (Burn-Nunes et. al, 2014), in Tucson, Arizona near the Ray copper mine, concentrator, smelter and tailings facilities (Félix et. al, 2015), in Northern Territory, Australia near the McArthur River zinc and lead mine (Munksgaard & Parry, 1998), and in Blenda Machado, Mexico (Csavina et. al, 2012) to name a few.

Another challenge in quantifying dust deposition rates is separating anthropogenic dust from the natural background emissions (Bargagli, 1998). Open pit mining mainly emits particulate matter from rock and soil, which is also from where natural wind erosion supplies dust into the atmosphere; resulting in both having similar compositions. Analyses in this study will focus mainly on the amount and size of the particles found to better differentiate between natural and anthropogenic sources.

Dust Composition

Dust particles are considered primary pollutants and are composed of a wide variety of substances both solid and liquid, making dust a complex mixture difficult to encompass in one category (Cooper & Alley, 2011). Mattson & Koutler-Andersson (1955) classify particulate matter into the following categories: biogenic (seeds, pollen, spores), pedogenic (wind eroded soil), oceanogenic (salt spray), pyrogenic (smoke and ashes from fire), plutogenic (volcanic eruptions), cosmogenic (comic dust) and industrial dust. This study is concerned only with the mineral dust from pedogenic and industrial sources, as biogenic dust is burned off in the ashing procedure used in this study and oceanogenic, plutogenic, and cosmogenic particles can be considered quantitatively insignificant. Pyrogenic sources include forest fires, which were considered in this study, but only contribute significantly a few times in the peat profile analysis.

Industrial dust can be created by three processes: material handling, combustion, or gas conversion reactions in the atmosphere (Cooper & Alley, 2011). Gas conversion reactions in the atmosphere occur when particles react with gas phase particles, producing aerosols. These reactions can occur through nucleation, condensation, absorption, adsorption, and coagulation (Liu & Lipták, 2000). The complexity and range of these reactions is out of the scope of this study, which focuses on particulate matter created by the material handling and combustion processes within the ABS region.

Table 2: Major elements that compose the earth's crust and their weight percentage (Klein & Dutrow, 2007)

Element	Weight Percent of Earth's Crustal Composition (%)	Element	Weight Percent of Earth's Crustal Composition (%)
O	46.60	K	2.59
Si	26.72	Mg	2.09

Al	8.13	Ti	0.44
Fe	5.00	H	0.14
Ca	3.63	P	0.10
Na	2.83	Mn	0.09
		Total	**99.17**

In the ABS region, material handling consists of haul roads, digging, tailings, coke and sulfur piles (Gosselin et al., 2010; Landis et al., 2012). Upgrading of bitumen would fall under combustion processes and is considered a point source (Liu & Lipták, 2000). Bitumen upgrading consists of two major steps: primary and secondary upgrading. Primary upgrading aims to reduce the molecular weight of bitumen by breaking down large hydrocarbon molecules at temperatures of 430-550 ^{O}C using gas or coke by-products as fuel. Secondary upgrading removes sulfur and nitrogen from bitumen (Gosselin et al., 2010).

Atmospheric dusts derived from crustal rocks are mostly composed of the elements listed in Table 2, as well as heavy metals, rare earth elements and all other elements but at lower concentrations (Klein & Dutrow, 2007; Rahn, 1976). These elements make up the bulk of the most common rock-forming minerals, listed in Table 3, that pedogenic particles are derived from. Through natural processes such as erosion, sea spray, and precipitation, particles are released into the atmosphere from <1 to 100μm, which is described in Figure 2 (Hosker & Lindberg, 1982; Willeke & Whitby, 1975). Emissions from material handling and other mechanical processes are in this size range and generally tend toward the larger end of the range (Rahn, 1976). This study focuses on the so-called “coarse” particles (Figure 2) in the 1-100 μm range to encompass the complete range of mechanically generated aerosols.

Table 3: Common rock-forming minerals (Klein & Dutrow, 2007)

Common Rock-Forming Minerals	Common Accessory Minerals
Quartz, feldspars, nepheline, sodalite, leucite, micas, pyroxenes, amphiboles, olivine	Zircon, titanite, magnetite, ilmenite, hematite, apatite, pyrite, rutile, tourmaline, monazite, garnet

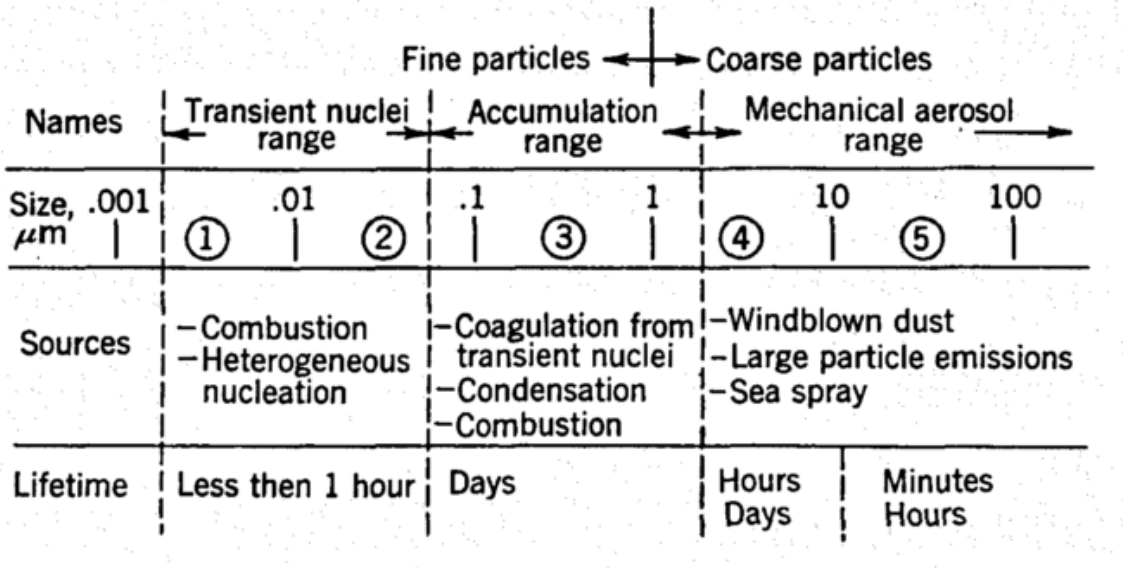

Figure 2: Size range and sources of atmospheric particles. The size range of focus is 1-100μm (Willeke & Whitby, 1975)

Methods of Collection

Contemporary Collection

There are several methods to study contemporary dust deposition rates including computer modelling, direct sampling and indirect sampling (including biomonitoring). Dry deposition models have been used, however they use only averages of particle concentrations and deposition velocities, which underestimates the impact of larger particles (Bargagli, 1998; Holsen & Noll, 1992).

Collection can occur using direct methods such as passive capture and air capture, while indirect methods include sampling snow, vegetation (tree bark), lichen, and bryophytes such as moss. Each collection style presents its own advantages and disadvantages.

Passive capture techniques use equipment set up in the desired location of collection to entrap dust particles by various means without actively disturbing the air (Bargagli, 1998) (e.g. a plate covered in adhesive, with a rain cover to prevent runoff, mounted on a 2m pole to prevent contamination from soil (Clair & Percy, 2015)). Air capture techniques are similar to passive capture, except they actively pull in air to filter out particulates (Bargagli, 1998). Capture methods can be very expensive due to the large amount of equipment needed for each location in addition to requiring electrical power. Capture instruments cannot properly illustrate how pollutants interact with the environment because their installation interrupts the natural deposition process, and data is limited by what the instruments are able to collect at one time or over a limited period of time (Bargagli, 1998). Samplers can also increase uncertainty as they change natural air flow, and interact differently with gases and particulates than natural surfaces (Bari et al., 2014).

Snow sampling has been proven to be a successful method of collection (Bari et al., 2014; Kelly et al., 2010), however it gives a limited view of deposition rates since winter has lower particulate emissions from industry than the rest of the year as snow cover suppresses particle suspension in the air.

Lichen sampling is well established as a method to assess deposition rates (Addison & Puckett, 1980). Lichen effectively accumulates dust and retains it (though not as effectively as moss (Groebner, ####)); however, lichen growth is so slow that accumulation rates cannot be

accurately determined (Nash, 1996). Without accurate ages of lichen samples, accumulation rates of pollutants cannot be calculated.

Moss sampling presents clear advantages over direct and the other indirect methods of collection. Moss is inexpensive compared to the direct sampling methods and without the large amounts of equipment needed for collection. *Sphagnum* moss (Figure 3), the moss used in this study, has a known growth rate (unlike lichen), allowing accumulation rates to be determined. Moss also captures dust deposition during the time of the year with increased amounts of dust in the atmosphere, unlike snow.

Figure 3: Sphagnum fuscum moss

Nevertheless, there are some disadvantages to consider when using moss as a biomonitor of atmospheric deposition. The health of plants or genetic bias for increased tolerance in plants, is

random and cannot be properly accounted for in samples. As well, only the effects of dust in combination with all other substances deposited on the moss surface can be analyzed, without full knowledge of how the dust particles interact with the other substances (e.g. gas phase aerosols, S, N, base cations, etc.). The biological (variation between species), meteorological and spatial-temporal variability from site to site would have to be considered. These disadvantages often introduce more error and uncertainty into studies (Bargagli, 1998).

It should be noted that deposition rates are usually assumed to be proportional to material concentrations in the air adjacent to the plant surface (Bargagli, 1998). While deposition rates cannot perfectly reflect actual concentrations in the atmosphere it does provide insight into the overall air quality as reflected by the abundance of particulates.

Temporal Collection

The WBEA monitoring program only began in 1998, limiting knowledge of any past particulate emissions to the last 18 years (Percy, 2013; Vile, Wieder, Vitt, & Berryman, 2013). There are several means to reconstruct the complete retrospective deposition of an area, for example: lake sediment cores, ice cores, or peat cores (Boutron, 1995; Norton & Kahl, 1987). For the ABS region, peat cores were the logical choice as 36% of the land cover in the surrounding area is wetland, which allowed for many possible sampling sites (Fiera Biological Consulting Ltd, 2013). Ice cores have very high temporal resolution however, there are no glaciers in the ABS region, therefore peat cores were the best option. Lake sediment cores have multiple sources of mineral matter, limiting how much knowledge can be gained about atmospheric deposition alone (Norton & Kahl, 1987).

Wetland Classifications: Bogs

There are many different types of wetlands such as fens, marshes, and bogs (Table 4 for definitions). Bogs are the wetland type sampled in this study.

Table 4: Key wetland terminology and their definitions (Alberta Environment and Sustainable Development, 2015)

Wetland	land that is saturated with water long enough to promote formation of water altered soils, growth of water tolerant vegetation, and various kinds of biological activity that are adapted to wet environments
Peatland	a wetland with more than 40 cm of accumulated peat; includes bogs and fens and some swamps
Bog	a peatland fed by ombrogenous waters originating from precipitation with low concentrations of dissolved minerals, waters generally acidic
Fen	a minerogenous peatland with surface or subsurface water flow that range from moderately-acidic to basic
Marsh	a mineral wetland with water levels near, at or above the ground surface for variable periods during the year, and which supports graminoid vegetation in the deepest portion of the wetland in the majority of years
Swamp	a mineral wetland with water levels near, at or above the ground surface for variable periods during the year which contains either more than 25% tree cover of a variety of species or more than 25% shrub cover

Ombrotrophic raised bogs present a unique opportunity for this study because they are hydrologically isolated from the surrounding ground and surface water therefore, only gaining mineral matter and water from the atmosphere (Figure 4) (Bargagli, 1998; Mattson & Koutler-Andersson, 1955; Shotyk, 1996). The amount of mineral matter present in the moss and peat samples is proportional to the atmospheric dust deposition rate of the area. Minerotrophic peat differs from ombrotrophic peat as it obtains water from groundwater and mineral particles from soil (Figure 4). These additional sources of mineral matter create a challenge in differentiating between soil/groundwater sources and atmospheric sources. Ombrotrophic peat can overlie

minerotrophic peat layers, rendering it critical to be able to differentiate between the two peat types when sampling bogs (Shotyk, 1996). There are several ways to differentiate between the classes of wetlands including morphology, chemistry (in particular using pH), and plant communities present (Gore, 1983a). The pH of porewater is a common method of peatland differentiation and is used in this study because ombrotrophic peat is characteristically acidic (pH 3.5-4.5) whereas minerotrophic peat is neutral (pH 5-7) due to the alkalinity present in groundwater, and mineralization reactions (Bragazza & Gerdol, 1999; Gore, 1983b).

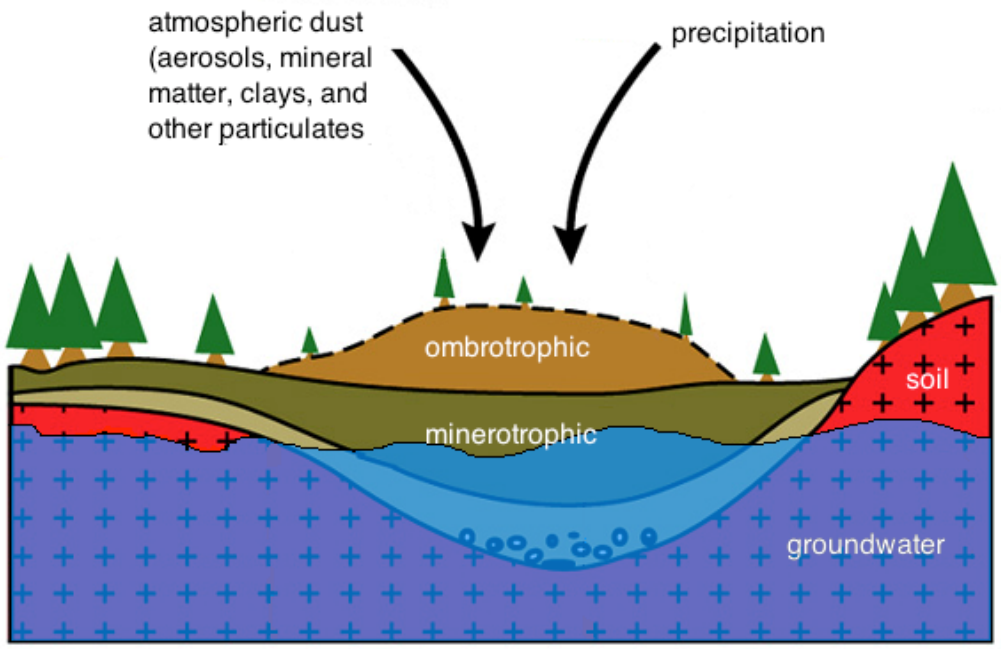

Figure 4: Illustration of the differences between ombrotrophic and minerotrophic peat (diagram adapted from figure in (Le Roux, 2009))

Moss and Peat as Biomonitors

The necessary characteristics of a biomonitor according to Bargagli (1998) are: high tolerance of a given pollutant, ability to accumulate pollutants at levels reflecting those in the environment (and in this case the atmosphere), wide distribution in the survey area, minimal mobility of the pollutant within a profile, long life cycle, and no biological uptake of the contaminant in

question. The following section discusses how *Sphagnum* moss and peat meet these qualifications.

Sphagnum moss and peat were collected at numerous sites over the ABS region (see the Materials and Methods in Chapters 1 and 2). *Sphagnum,* mainly *Sphagnum fuscum* (see S2 of Moss Paper for full list of species), was collected from ombrotrophic bogs in the area from lawns as well as the top layers of peat cores. Moss can be distinguished as the living plant material on the surface of a bog, whereas peat is the dead, sub-fossilized plant material underneath the moss layer (Figure 5).

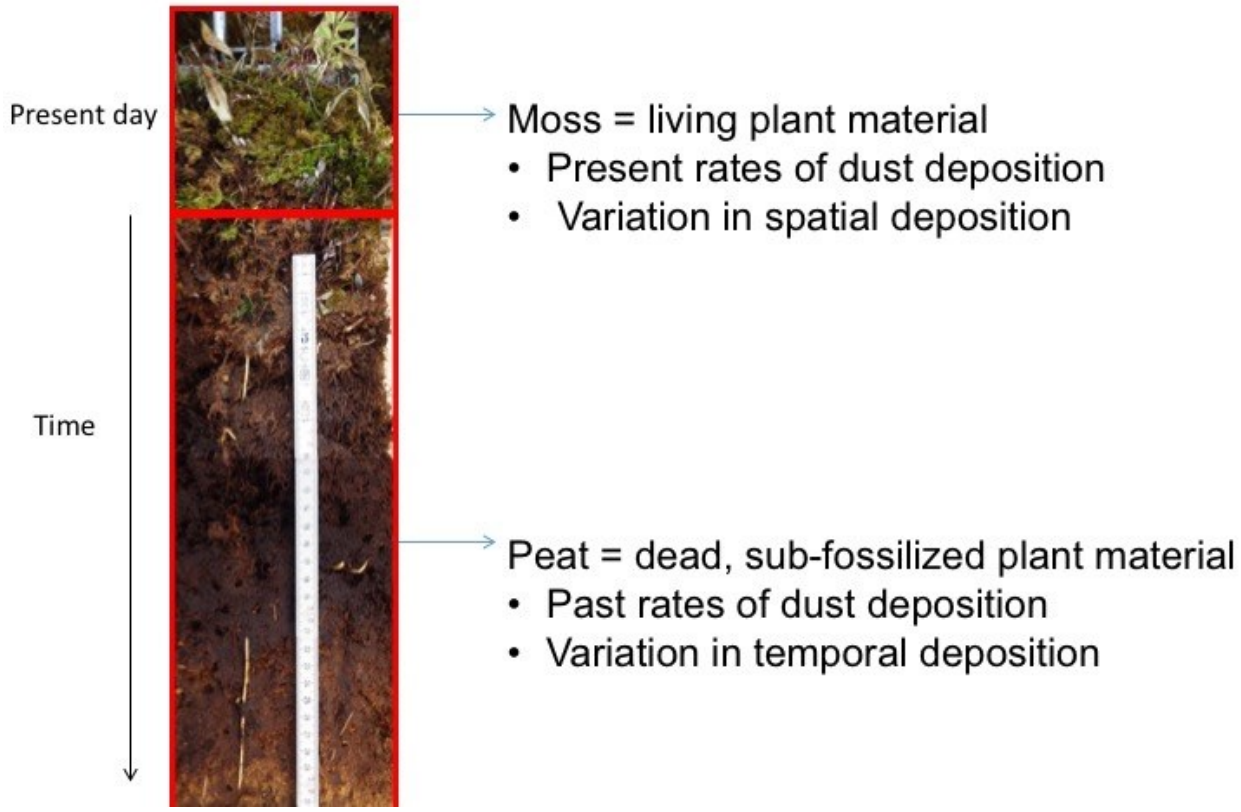

Figure 5: Moss and peat were used as monitors of dust deposition. Moss, the living plant material, was used to monitor present rates of dust deposition, while peat, dead sub-fossilized plant material, was used to monitor past rates of dust deposition.

Sphagnum has been used to determine mineral matter deposition rates for decades and has become a common tool to determine dust input to a given area (Gorham & Tilton, 1978). Dust retention of *Sphagnum* is not 100% efficient and is influenced by a number of factors including receptor surface characteristics, resuspension of particles, particle size, wind speed, particle shape, density, run off, etc. (Hosker & Lindberg, 1982). Any of these factors could change the amount of dust retained on the plant's surface; however, the efficiency of retention should be comparable for a given sphagnum species in every ombrotrophic bog. Therefore, it can be assumed that since the same species was collected throughout the study, similar biases were present at all sites and comparisons can be made between sites.

Sphagnum is commonly used as a biomonitor because of its ability to retain aerosols from the atmosphere. This is in part due to *Sphagnum*'s intricate leaf surface creating a large surface area for capture of particles (Aničić et al., 2009; Bargagli, 1998). Moss has also been found to survive and efficiently accumulate aerosols in polluted environments (Bargagli, 1998). Moss is a better medium for dust capture than artificial surfaces because it more accurately represents how dust interacts with a natural vegetation surface (Bargagli, 1998). There have been many studies done using *Sphagnum* in moss bags that illustrates its ability to retain deposited material effectively (Aničić et al., 2009). Moss has also been found to retain 2-3 times more aerosols then lichen due to more efficient retention, great density, and high leaf surface area (Taylor & Witherspoon, 1972). Particle retention by moss is a complicated process that is influenced by many factors including particle characteristics (size, water solubility, shape), moss characteristics (leaf surface, stickiness, wetness, electrical charge), and meteorology (Chamberlain, 1970; Chamberlain & Little, 1980; Little, 1979; Shotyk, Kempter, Krachler, & Zaccone, 2015)

Sphagnum dominated peat cores are very effective biomonitors and can be used to reconstruct past atmospheric dust deposition if the following three requirements are met (Krachler & Shotyk 2004). The core must be determined to be ombrotrophic (water and nutrients gained only from atmosphere), the relevant biogeochemical processes of the area have to be considered (e.g. effects of dust interacting with peat and dissolving in bogs) and the subject of the study in question (in this case, particulate mineral matter) must be immobile in the peat column. As shown later, the nature of the peat bogs sampled (MIL, JPH4, McK, McM, ANZ, UTK, SEB) were found to be at least partly ombrotrophic. Particulate mineral matter has already been shown to be immobile in peat profiles (Chapman, 1964). The major biogeochemical processes, such as deposition and dissolution of mineral matter, occur in the upper living layers of the peat column (Malmer, 1988; Pearsall, 1952). Particulate matter is deposited onto the surface of the peat bogs, on plants or in the surface waters. Ombrotrophic bogs have very acidic (pH 4) water due to lack of groundwater inputs. Thus, when soluble mineral nutrients are deposited on the bog surface they readily dissolve (Pearsall, 1952).

Methods of Analysis

Acid Insoluble Ash

Combustion is a very common method to isolate mineral dust in organic (moss and peat) samples. The ash is derived from burning off the organic matter of a sample, leaving only the residue. Ash can be examined alone, or divided further into its acid soluble (sulphates, carbonates, phosphates, and oxides) and acid insoluble fractions (quartz, aluminosilicates, zircons, etc.). This division is important to distinguish between the atmospheric mineral dust (AIA), nutrient salts created during the uptake and recycling of plants (ASA), as well as any compounds created during the combustion process (ASA) (Shotyk, 1996). Also included in the

AIA fraction are biological silicates in the forms of diatoms and testate amoebae skeletons, with a structure of amorphous SiO_2 (Malmer, 1988). Acid insoluble ash (AIA) has been used frequently to measure the mineral matter inputs in both moss and peat (Damman, Tolonen, & Sallantaus, 1992; Malmer, 1988; Sapkota, 2006; Steinmann & Shotyk, 1997; Urban, Verry, & Eisenreich, 1995; C. Zaccone, Miano, & Shotyk, 2012; Claudio Zaccone, Pabst, Senesi, Shotyk, & Miano, 2013). However, it was originally used in feed digestibility studies for fish, pigs and ruminants (Atkinson, Hilton, & Slinger, 1984; McCarthy, Aherne, & Okai, 1974; Van Keulen & Young, 1977).

Mineralogy

There are many methods to analyze the mineralogical and chemical composition of dusts both directly and indirectly. Indirect methods include ICP-OES and laser ablation ICP-MS (Suzuki, 2006) that analyze elemental composition and used normative calculations to estimate minerals present. Direct methods of mineral identification include X-ray diffraction (Jeong, 2008), and scanning electron microscope (SEM) with electron dispersive x-ray (EDX) (Marx, et al., 2009; Williamson et al., 2004). Each method has its own merits, but since mineralogy was not the focus of this study, qualitative analysis using SEM and EDX was chosen. The SEM utilizes a high intensity electron beam finely focused on a sample to gather information on its morphology and surface features (Klein & Dutrow, 2007). In this study backscattered electron detection was used, which relates the average atomic number of a specimen, its crystallographic orientation, and surface topography to create images. EDX analyzes the x-rays generated from the specimen directly from the electron beam using fluorescence spectroscopy, allowing for a compositional analysis alongside the morphological assessment (Klein & Dutrow, 2007).

Particle Size Distributions

Particle size distributions can be obtained using several techniques: photomicrographs (Coe & Lindberg, 1987), laser particle size analysis (Jeong, 2008), sedimentation (Wadge, Hutton, & Peterson, 1996), and dynamic image analysis (Roberson & Weltje, 2014). A dynamic image analysis instrument (XPT-C) was chosen for this study due to the small mass of samples available (average mass ~0.005g). Laser particle size analysis would have been the most reliable method of analysis to a 95% confidence interval (Roberson & Weltje, 2014), but sample size was insufficient for this method. Dynamic image analysis can be compared to laser particle size analysis by using homogenized regression models as outlined elsewhere (Roberson & Weltje, 2014).

Previous studies of dusts in peat from bogs reported the following distribution: 45% of particles are less than 2μm, 15% between 2-6μm, 6-20μm is about 30% of material, and 10% of material greater than 20μm (Finney & Farnham, 1968).

Objectives

One of the greater challenges with determining the anthropogenic effects on atmospheric dust deposition is to establish the underlying natural background levels (Bargagli, 1998). There are two possible approaches: collect samples remote from the impacted area or sample back in time; we used both. The main objectives of this study were to 1) understand the contemporary atmospheric dust deposition rates and 2) understand the past atmospheric dust deposition rates. In order to do so, a third objective was established: 3) determine background rates of dust deposition, which to compare the findings from the ABS region.

Within the main set of objectives, secondary objectives were established to best address the main objectives. To evaluate contemporary atmospheric dust deposition rates the following questions were posed: 1a) Do bogs closer to the ABS region have greater amounts of ash than bogs further away? 1b) Do bogs closer to the ABS region have larger particles than bogs further away? 1c) What is the impact of industry on the relative importance of AIA versus ASA? 1d) What is the morphology and mineralogy of the dust and how is this affected by industry? 1e) How has deposition of ASA to the bogs affected inputs of plant nutrients such as P and Ca in the ABS region?

To evaluate past atmospheric dust deposition rates the following questions were addressed: 2a) How does ash content vary over time and between the peat cores? 2b) How has industry impacted deposition of AIA and ASA over time? 2c) What is the variation in particle size within and between peat cores? 2d) What is the morphology and mineralogy of the dusts and how has it changed over time?

Moss and Peat Project Overview

This thesis project is part of a larger project funded by Alberta Innovates. There are several different teams working to analyze different components of the moss and peat samples collected from the ABS region. Each team (Table 5) had an integral part in the success of this project and have collaborated in numerous ways to better understand the data collected.

Table 5: Peat Project Breakdown

Project Members	Area of Study for Project
Jon Martin & Yifeng Zhang	Organic Compounds (PAHs)
Tommy Noernberg, Bob Shannon, & Peter Appleby	^{210}Pb measurement using gamma spectroscopy and calculation of ^{210}Pb age dates
Duane Froese & Lauren Davies	Calculated ^{14}C age dates and combined ^{210}Pb and ^{14}C age models. Lauren also measured volcanic ash input
Simon van Bellen	Plant macrofossils, vegetation, and climate change
Beatriz Bicalho & Iain Grant-Weaver	Metals
Gabriela Gonzalez Arismendi, Steve Larter, Thomas Oldenburg, & Haiping Huang	Bitumen compounds in basal peat layers
Rick Pelletier	Maps and spatial modeling
Melanie Vile	Recommending sample locations and providing 2013 moss samples
Gillian Mullan-Boudreau	pH, EC, atmospheric dust deposition (ash content, AIA, and ASA), mineral ID, particle size analyses, calculation of dust deposition rates
William Shotyk	Project leader and coordinator

References

Addison, P. A., & Puckett, K. J. (1980). Deposition of atmospheric pollutants as measured by lichen element content in the Athabasca oil sands area. *Canadian Journal of Botany*, *58*(22), 2323–2334. http://doi.org/10.1139/b80-269

Agriculture Division of Statistics Canada. (2014). Table M23-33: Area of land in farm holdings, census data, Canada and by province, 1871-1971. Retrieved September 6, 2016, from http://www.statcan.gc.ca/pub/11-516-x/sectionm/4057754-eng.htm#1

Alberta Energy Regulator. (2015). *Alberta's Energy Reserves 2014 and Supply/Demand Outlook 2015-2024* (Vol. ST98-2015). Calgary.

Alberta Environment and Sustainable Development. (2015). *Alberta wetland classification system*. Water Policy Branch, Policy and Planning Division, Alberta Government. Edmonton, AB. ISBN: 9781460122570

Aničić, M., Tomašević, M., Tasić, M., Rajšić, S., Popović, A., Frontasyeva, M. V., Lierhagen, S., Steinnes, E. (2009). Monitoring of trace element atmospheric deposition using dry and wet moss bags: Accumulation capacity versus exposure time. *Journal of Hazardous Materials*, *171*(1–3), 182–188. http://doi.org/10.1016/j.jhazmat.2009.05.112

Atkinson, L., Hilton, J. W., & Slinger, S. J. (1984). Evaluation of acid-insoluble ash as an indicator of feed digestibility in rainbow trout (salmo gairdneri). *Can, J. Fish. Aquat. Sci.*, *41*, 1384–1386.

Bargagli, R. (1998). *Trace Elements in Terrestrial Plants: An Ecophysiological Approach to Biomonitoring and Biorecovery*. Verlag Berlin Heidelberg New York: Springer. ISBN:3540645519

Bari, M. A., Kindzierski, W. B., & Cho, S. (2014). A wintertime investigation of atmospheric deposition of metals and polycyclic aromatic hydrocarbons in the Athabasca Oil Sands Region, Canada. *Science of The Total Environment*, *485–486*, 180–192. http://doi.org/10.1016/j.scitotenv.2014.03.088

Boutron, C. F. (1995). Historical reconstruction of the earth's past atmospheric environment from Greenland and Antarctic snow and ice cores. *Environmental Reviews*, *3*(1), 1–28. http://doi.org/10.1139/a95-001

Bragazza, L., & Gerdol, R. (1999). Hydrology, groundwater chemistry and peat chemistry in relation to habitat conditions in a mire on the South Eastern Alps of Italy. *Plant Ecology*, *144*, 243–256. Retrieved from http://dx.doi.org/10.1023/A:1009868113976

Burn-Nunes, L., Vallelonga, P., Lee, K., Hong, S., Burton, G., Hou, S., Moy, A., Edwards, R., Loss, R., Rosman, K. (2014). Seasonal variations in the sources of natural and anthropogenic lead deposited at the East Rongbuk Glacier in the high-altitude Himalayas. *Science of the Total Environment*, *487*(1), 407–419. http://doi.org/10.1016/j.scitotenv.2014.03.120

Chamberlain, A. C. (1970). Interception and retention of radioactive aerosols by vegetation. *Atmospheric Environment (1967)*, *4*(1), 57–78. http://doi.org/10.1016/0004-6981(70)90054-5

Chamberlain, A. C., & Little, P. (1980). Transport & capture of particles by vegetation. In J. Grace, E. D. Ford, & P. Javiss (Eds.), *Plants and their Atmopsheric Environment* (pp. 147–173). Blackwell: Oxford.

Chapman, S. B. (1964). The Ecology of Coom Rigg Moss , Northumberland : II . The Chemistry of Peat Profiles and the Development of the Bog System. *Journal of Ecology*, *52*(2), 315–321.c

Clair, T. A., & Percy, K. E. (2015). Assessing forest health in the Alberta Oil Sands Region. *Wood Buffalo Enironmental Association*, 1-180

Coe, J. M., & Lindberg, S. E. (1987). The Morphology and Size Distribution of Atmospheric Particles Deposited on Foliage and Inert Surfaces. *Japca*, *37*(3), 237–243. http://doi.org/10.1080/08940630.1987.10466218

Cooper, C. D., & Alley, F. C. (2011). *Air pollution control : a design approach.* Long Grove, Ill. : Waveland Press, c2011. Retrieved from http://login.ezproxy.library.ualberta.ca/login?url=http://search.ebscohost.com/login.aspx?direct=true&db=cat03710a&AN=alb.4851511&site=eds-live&scope=site

Csavina, J., Field, J., Taylor, M. P., Gao, S., Landázuri, A., Betterton, E. A., & Sáez, A. E. (2012). A review on the importance of metals and metalloids in atmospheric dust and aerosol from mining operations. *Science of the Total Environment*, *433*, 58–73. http://doi.org/10.1016/j.scitotenv.2012.06.013

Damman, A. W. H., Tolonen, K., & Sallantaus, T. (1992). Element Retention and Removal in Ombrotrophic Peat of Haadetkeidas, a Boreal Finnish Peat Bog. *Suo (Helsinki)*, *43*(4–5), 137–145.

Environment and Climate Change Canada. (2015). PM - Total Particulate Matter (NA - M08). Retrieved November 9, 2016, from http://ec.gc.ca/inrp-npri/donnees-data/index.cfm?do=results&lang=en&opt_facility_name=&opt_facility=&opt_npri_id=&opt_report_year=2015&opt_chemical_type=ALL&opt_industry=&opt_cas_name=NA+-+M08&opt_cas_num=&opt_location_type=ALL&opt_province=AB&opt_postal_code=&opt_community=&opt_csic=&opt_csi2=&opt_asic=&opt_naics3=&opt_naics4=&opt_naics6=9&opt_nai6code=&community1=&opt_urban_center=&opt_province_comm=&opt_media=all&opt_sort_order=A.CITY&opt_sort_direction=ASC&submit=Sort

Félix, O. I., Csavina, J., Field, J., Rine, K. P., Sáez, A. E., & Betterton, E. A. (2015). Use of lead isotopes to identify sources of metal and metalloid contaminants in atmospheric aerosol from mining operations. *Chemosphere*, *122*, 219–226.

http://doi.org/10.1016/j.chemosphere.2014.11.057

Fennelly, P. (1976). The Origin and Influence of Airborne Particulates. *American Scientist*, *64*(1), 46–56.

Fialkiewicz-Koziel, B., Smieja-Krol, B., Ostrovnaya, T. M., Frontasyeva, M., Sieminska, A., & Lamentowicz, M. (2015). Peatland microbial communities as indicators of the extreme atmospheric dust deposition. *Water, Air, and Soil Pollution*, *226*(4). http://doi.org/10.1007/s11270-015-2338-1

Fiera Biological Consulting Ltd. (2013). *State of the Watershed Report - Phase 3: Water Quantity and Basic Water Quality in the Athabasca WatershedReport prepared for the Athabasca Watershed Council. Fiera Biological Consulting Report #1234*.

Finney, H. R., & Farnham, R. S. (1968). Mineralogy of the Inorganic Fraction of Peat from Two Raised Bogs in Northern Minnesota. *Proceedings of the Third International Peat Congress*, 102–108.

Gore, A. J. P. (Ed.). (1983a). *Ecosystems of the World 4A, Mires: Swamp, Bog, Fen and Moor General Studies*. Amsterdam, Netherlands; New York, N.Y., USA: Elsevier Scientific Publishing Co.

Gore, A. J. P. (Ed.). (1983b). *Ecosystems of the World 4B, Mires: Swamp, Bog, Fen and Moor Regional Studies* (4B ed.). Amsterdam, Netherlands; New York, N.Y., USA: Elsevier Scientific Publishing Co.

Gorham, E., & Tilton, D. L. (1978). The mineral content of Sphagnum fuscum as affected by human settlement. *Canadian Journal of Botany*, *56*(180), 2755–2759.

Gosselin, P., Hrudey, S. E., Naeth, M. A., Plourde, A., Therrien, R., Van Der Kraak, G., & Xu, Z. (2010). *Environmental and Health Impacts of Canada 's Oil Sands Industry*. Retrieved from http://rsc-src.ca/sites/default/files/pdf/RSC Oil Sands Panel Main Report Oct 2012.pdf

Holsen, T. M., & Noll, K. E. (1992). Dry deposition of atmospheric particles: application of current models to ambient data. *Environmental Science & Technology*, *26*(9), 1807–1815. http://doi.org/10.1021/es00033a015

Hosker, R. P., & Lindberg, S. E. (1982). Review: Atmospheric deposition and plant assimilation of gases and particles. *Atmospheric Environment (1967)*, *16*(5), 889–910. http://doi.org/10.1016/0004-6981(82)90175-5

Jacobson, M. Z. (2002). *Atmospheric Pollution : History, Science, and Regulation*. Cambridge, UK: Cambridge University Press. Retrieved from http://login.ezproxy.library.ualberta.ca/login?url=http://search.ebscohost.com/login.aspx?direct=true&db=nlebk&AN=304527&site=ehost-live&scope=site

Jeong, G. Y. (2008). Bulk and single-particle mineralogy of Asian dust and a comparison with its source soils. *Journal of Geophysical Research Atmospheres*, *113*(2), 1–16.

http://doi.org/10.1029/2007JD008606

Kelly, E. N., Schindler, D. W., Hodson, P. V, Short, J. W., Radmanovich, R., & Nielsen, C. C. (2010). Oil sands development contributes elements toxic at low concentrations to the Athabasca River and its tributaries. *Proceedings of the National Academy of Sciences of the United States of America*, *107*(37), 16178–16183. http://doi.org/10.1073/pnas.1008754107

Klein, C., & Dutrow, B. (2007). *The 23rd Edition of the Manual of Mineral Science* (23rd ed.). New Delhi: John Wiley & Sons, Inc.

Krachler, M., & Shotyk, W. (2004). Natural and anthropogenic enrichments of molybdenum, thorium, and uranium in a complete peat bog profile, Jura Mountains, Switzerland. *Journal of Environmental Monitoring : JEM*, *6*(5), 418–426. http://doi.org/10.1039/b313300a

Landis, M. S., Pancras, J. P., Graney, J. R., Stevens, R. K., Percy, K. E., & Krupa, S. (2012). *Receptor Modeling of Epiphytic Lichens to Elucidate the Sources and Spatial Distribution of Inorganic Air Pollution in the Athabasca Oil Sands Region*. *Developments in Environmental Science* (1st ed., Vol. 11). Elsevier Ltd. http://doi.org/10.1016/B978-0-08-097760-7.00018-4

Little, P. (1979). Particle capture by natural surfaces. *Agricultural Aviation*, *20*(3), 129–144.

Lynam, M. M., Dvonch, J. T., Barres, J. A., Morishita, M., Legge, A., & Percy, K. (2015). Oil sands development and its impact on atmospheric wet deposition of air pollutants to the Athabasca Oil Sands Region, Alberta, Canada. *Environmental Pollution*, *206*, 469–478. http://doi.org/10.1016/j.envpol.2015.07.032

Malmer, N. (1988). Patterns in the growth and the accumulation of inorganic constituents in the Sphagnum cover on ombrotrophic bogs in Scandinavia. *Oikos*, *53*(1), 105–120.

Marx, S. K., McGowan, H. a., & Kamber, B. S. (2009). Long-range dust transport from eastern Australia: A proxy for Holocene aridity and ENSO-type climate variability. *Earth and Planetary Science Letters*, *282*(1–4), 167–177. http://doi.org/10.1016/j.epsl.2009.03.013

Mattson, S., & Koutler-Andersson, E. (1955). Geochemistry of a Raised Bog. *Annals of the Royal Agricultural College*, *21*, 321–356.

McCarthy, J. F., Aherne, F. X., & Okai, D. B. (1974). Use of HCl insoluble ash as an index material for determining apparent digestibility with pigs. *Canadian Journal of Animal Science*, *54*(1), 107–109. http://doi.org/10.4141/cjas74-016

Motallebi, N., Taylor Jr, C. A., & Croes, B. E. (2003). Particulate matter in California: Part 2-Spatial, temporal, and compositional patterns of PM2.5, PM10-2.5, and PM10. *Journal of the Air & Waste Management Association*, *53*(12), 1517–1530. http://doi.org/10.1080/10473289.2003.10466322

Muhs, D. R., Prospero, J. M., Buddock, M. C., & Gill, T. E. (2014). *Identifying Sources of Aeolian Mineral Dust: Present and Past*. http://doi.org/10.1007/978-94-017-8978-3

Munksgaard, N. C., & Parry, D. L. (1998). Lead isotope ratios determined by ICP-MS: Monitoring of mining-derived metal particulates in atmospheric fallout, Northern Territory, Australia. *Science of the Total Environment*, *217*(1–2), 113–125. http://doi.org/10.1016/S0048-9697(98)00170-3

Nash, T. H. (1996). Growth. In *Lichen Biology* (2nd ed., p. p.79-82). Cambridge University Press.

Nieboer, E., Ahmed, H. M., Puckett, K. J., & Richardson, D. H. S. (1972). Heavy Metal Content of Lichens in Relation to Distance from a Nickel Smelter in Sudbury, Ontario. *The Lichenologist*, *5*, 292. http://doi.org/10.1017/S0024282972000301

Norton, S. A., & Kahl, J. S. (1987). A Comparison of Lake Sediments and Ombrotrophic Peat Deposits as Long- Term Monitors of Atmosplieric Pollution. In T. . Boyle (Ed.), *New approaches to monitoring aquatic ecosystem* (pp. 40--57). Philadelphia: American Society for Testing and Materials. http://doi.org/10.1038/nbt0987-872

Pearsall, W.H. (1952). The pH of Natural Soils and its Ecological Significance. *Journal of Soil Science*, *3*(1), 41–51. http://doi.org/10.1017/CBO9781107415324.004

Percy, K. E. (2013). Ambient Air Quality and Linkage to Ecosystems in the Athabasca OIl Sands. *Geosicence of Climate and Engery*, *11*, 182–201.

Percy, K. E., & Davies, M. J. E. (2012). *Air Quality Modeling in the Athabasca Oil Sands Region*. *Developments in Environmental Science* (1st ed., Vol. 11). Elsevier Ltd. http://doi.org/10.1016/B978-0-08-097760-7.00004-4

Pratte, S., Garneau, M., & De Vleeschouwer, F. (2016). Late-Holocene atmospheric dust deposition in eastern Canada (St. Lawrence North Shore). *The Holocene*. http://doi.org/10.1177/095968361664618

Rahn, K. A. (1976). Silicon and aluminium in atmospheric aerosols: crust-air fractionations? *Atmospheric Environment*, *10*(1966), 597–601.

Roberson, S., & Weltje, G. J. (2014). Inter-instrument comparison of particle-size analysers. *Sedimentology*, *61*(4), 1157–1174. http://doi.org/10.1111/sed.12093

Sapkota, A. (2006). *Mineralogical, Chemical, and Isotopic (Sr, Pb) Composition of Atmospheric Mineral Dusts in an Ombrotrophic Peat Bog, Southern South America*. Ruprecht-Karls-Universität, Hiedelberg.

Shotyk, W. (1996). Peat bog archives of atmospheric metal deposition : geochemical evaluation of peat profiles, natural variations in metal concentrations, and metal enrichment factors. *Environmental Reviews*, *4*, 149–183. http://doi.org/10.1139/a96-010

Shotyk, W., Belland, R., Duke, J., Kempter, H., Krachler, M., Noernberg, T., Pelletier, R., Vile, M. A., Wieder, K., Zaccone, C., Zhang, S. (2014). Sphagnum mosses from 21 ombrotrophic bogs in the athabasca bituminous sands region show no significant atmospheric

contamination of "heavy metals." *Environmental Science and Technology*, *48*(21), 12603–12611. http://doi.org/10.1021/es503751v

Shotyk, W., Bicalho, B., Cuss, C. W., Duke, M. J. M., Noernberg, T., Pelletier, R., Steinnes, E., Zaccone, C. (2016). Dust is the dominant source of "heavy metals" to peat moss (Sphagnum fuscum) in the bogs of the Athabasca Bituminous Sands region of northern Alberta. *Environment International*, *92–93*, 494–506. http://doi.org/10.1016/j.envint.2016.03.018

Shotyk, W., Kempter, H., Krachler, M., & Zaccone, C. (2015). Stable (^{206}Pb, ^{207}Pb, ^{208}Pb) and radioactive (^{210}Pb) lead isotopes in 1year of growth of Sphagnum moss from four ombrotrophic bogs in southern Germany: Geochemical significance and environmental implications. *Geochimica et Cosmochimica Acta*, *163*, 101–125. http://doi.org/10.1016/j.gca.2015.04.026

Steinmann, P., & Shotyk, W. (1997). Geochemistry, mineralogy, and geochemical mass balance on major elements in two peat bog profiles (Jura Mountains, Switzerland). *Chemical Geology*, *138*(1–2), 25–53. http://doi.org/10.1016/S0009-2541(96)00171-4

Stringham, G. (2012). *Energy Developments in Canada's Oil Sands*. *Developments in Environmental Science* (1st ed., Vol. 11). Elsevier Ltd. http://doi.org/10.1016/B978-0-08-097760-7.00002-0

Suzuki, K. (2006). Characterisation of airborne particulates and associated trace metals deposited on tree bark by ICP-OES, ICP-MS, SEM-EDX and laser ablation ICP-MS. *Atmospheric Environment*, *40*(14), 2626–2634. http://doi.org/10.1016/j.atmosenv.2005.12.022

Taylor, F. G., & Witherspoon, J. P. (1972). Retention of simulated fallout particles by lichens and mosses. *Health Physics*, *23*, 867–869.

Le Roux, G. (2009). Survey years of lead. University of Liège. Retrieved June 29, 2015, from http://reflexions.ulg.ac.be/cms/c_19292/fr/enquete-sur-les-annees-de-plomb?portal=j_55&printView=true

Urban, N. R., Verry, E. S., & Eisenreich, S. J. (1995). Retention and mobility of cations in a small peatland: trends and mechanisms. *Water, Air and Soil Pollution*, *79*, 201–224.

Van Keulen, J., & Young, B. A. (1977). Evaluation of acid-insoluble ash as a natural marker in ruminant digestibility studies. *Journal of Animal Science*, *44*(2), 282–287.

Vile, M. A., Wieder, R. K., Vitt, D. H., & Berryman, S. (2013). *Final Report: Development of monitoring protocols for nitrogen-sensitive bog ecosystems, including further development of lichen monitoring tools*. *WBEA Final Report* (Vol. 1–87).

Wadge, A., Hutton, M., & Peterson, P. J. (1996). The Concentrations and Particle Size Relationships of Selected Trace Elements in Fly Ashes from U.K. Coal-Fired Power Plants and a Refuse Incinerator. *The Science of the Total Environment*, *54*, 13–27.

Wang, X., Chow, J. C., Kohl, S. D., Yatavelli, L. N. R., Percy, K. E., Legge, A. H., & Watson, J.

G. (2015). Wind erosion potential for fugitive dust sources in the Athabasca Oil Sands Region. *Aeolian Research*, *18*, 121–134. http://doi.org/10.1016/j.aeolia.2015.07.004

Watmough, S. A., Whitfield, C. J., & Fenn, M. E. (2014). The importance of atmospheric base cation deposition for preventing soil acidification in the Athabasca Oil Sands Region of Canada. *Science of the Total Environment*, *493*, 1–11. http://doi.org/10.1016/j.scitotenv.2014.05.110

Watson, J. G., Chow, J. C., Wang, X., Kohl, S. D., & Yatavelli, L. N. R. (2014). *Windblown Fugitive Dust Characterization in the Athabasca Oil Sands Region*. *Wood Buffalo Environmental Association*. McMurray.

Willeke, K., & Whitby, K. T. (1975). Atmospheric Aerosols: Size Distribution Interpretation. *Journal of the Air Pollution Control Association*, *25*(5), 529–534. http://doi.org/10.1080/00022470.1975.10470110

Williamson, B. J., Mikhailova, I., Purvis, O. W., & Udachin, V. (2004). SEM-EDX analysis in the source apportionment of particulate matter on Hypogymnia physodes lichen transplants around the Cu smelter and former mining town of Karabash, South Urals, Russia. *Science of the Total Environment*, *322*(1–3), 139–154. http://doi.org/10.1016/j.scitotenv.2003.09.021

Zaccone, C., Miano, T. M., & Shotyk, W. (2012). Interpreting the ash trend within ombrotrophic bog profiles: atmospheric dust depositions vs. mineralization processes. The Etang de la Gruère case study. *Plant and Soil*, *353*(1–2), 1–9. http://doi.org/10.1007/s11104-011-1055-9

Zaccone, C., Pabst, S., Senesi, G. S., Shotyk, W., & Miano, T. M. (2013). Comparative evaluation of the mineralogical composition of Sphagnum peat and their corresponding humic acids, and implications for understanding past dust depositions. *Quaternary International*, *306*, 80–87. http://doi.org/10.1016/j.quaint.2013.04.017

CHAPTER 2: *SPHAGNUM* MOSS AS AN INDICATOR OF CONTEMPORARY RATES OF ATMOSPHERIC DUST DEPOSITION IN THE ATHABASCA BITUMINOUS SANDS REGION

A version of this manuscript has been submitted to the journal *Environmental Science and Technology* for publication.

ABSTRACT

Open pit mining of the Athabasca Bituminous Sands (ABS) generates enormous quantities of mineral dusts, yet the full profile of dust deposition in the area has not been studied. Using *Sphagnum* moss as a biomonitor, samples were collected from 30 ombrotrophic peat bogs surrounding the ABS region and 5 ombrotrophic peat bogs in central Alberta for comparison. The ashed samples were reacted in HCl to separate the acid-insoluble ash (AIA) (mineral matter) and the acid-soluble acid (ASA) (macronutrients). The AIA content increased from 0.4±0.5% to 4.7±2.0% over a 30km distance towards industry. For comparison the Utikuma control site had a value of 0.29±0.07%. Mass accumulations rates were calculated and yielded similar trends. Dust deposition estimates were calculated to be 21000 tonnes in a 4-month growth period which is considerably greater than the existing estimate of 18842 tonnes per year.

The morphology and mineralogy of the AIA particles were studied using scanning electron microscopy and energy dispersive X-ray analysis, and the particle size distributions using optical microscopy. Particle size was more variable closer to the ABS region. Major ion analysis performed on the ASA fraction showed elevated concentrations of Ca, K, Mg, P, and S, with P up to 7 times more abundant in samples nearest industry. Since P is regarded as the growth limiting nutrient in bogs, fugitive fertilization of nutrient-poor ecosystems such as these, may have long-term ecological ramifications.

INTRODUCTION

The Athabasca Bituminous Sands (ABS) region currently produces over 165000 m^3/day of bitumen from its open pit mining and steam assisted gravity drainage (SAGD) operations [1,2]. Estimates suggest that, 18842 tonnes of total particulate matter in 2015 was produced and injected into the surrounding atmosphere from the industrial activities such as open pit mining, gravel roads, bitumen upgrading, and by-product piles in 2014 [3]. Once airborne, the dust may travel considerable distances depending on such factors as wind speed, particle size, density, and composition [4].

Dust in the form of particulate matter is considered a primary pollutant and can be composed of a wide variety of substances both solid and liquid [5]; however, for this study dust composed of mineral particles will be the focus. Mineral dust is largely composed of pedogenic particles derived from wind erosion; however, it can also be composed of particles from pyrogenic and industrial sources [6]. It has been found that dust is also the dominant source of heavy metals [7] and PAHs (in particular coke dust) in the ABS region [8]. Increased deposition of mineral dust can cause health risks and impact growth of vegetation in the surrounding environment [9].

Dust deposition in the ABS region is currently being monitored by the Wood Buffalo Environmental Association (WBEA), which studies $PM_{2.5}$ and PM_{10} in detail. Yet, they do not monitor the full range of particulate matter sizes emitted [9,10]. To date, there has been no published research on total dust deposition in the ABS region. To investigate dust deposition of the ABS region, *Sphagnum* moss was collected from 35 ombrotrophic bogs, 30 of which are in the surrounding area of the ABS region, and 5 in other regions in Alberta (control sites).

The main objective of this study was to quantify total deposition of mineral dusts to terrestrial ecosystems in the ABS region, and to estimate contemporary impacts from industry and their spatial variation. The content of mineral matter within the living layer of *Sphagnum* moss was obtained by distinguishing the acid-insoluble (AIA) and acid-soluble (ASA) ash fractions. Concentrations of ash, AIA and ASA were combined with estimated growth rates[17] of the moss to calculate current mass accumulation rates of dust deposition. A second objective was to characterize the dusts in respect to particle size, mineralogical composition, and morphology. A third objective was to understand the potential ecological significance of these dusts for terrestrial ecosystems, by estimating the availability of plant nutrients (P, Ca, Mg, K, S, Fe, Mn) in the ASA fraction.

MATERIALS AND METHODS

Sample Collection

The samples used in this study were collected between 2013 and 2015.

2013 Moss

Three replicate samples per site were collected from 21 bogs in 2013 by Melanie Vile surrounding the ABS region (Figure S1). These samples were collected for a separate study, but part of each sample was given to this project. The volume of the samples collected from each site is unknown, so density could not be calculated.

2014 Moss

Three replicate samples per site were collected from 7 bogs (MIL, JPH4, McK, McM, ANZ, URSA, SEB), see Figure S1. The samples from MIL, JPH4, McK, ANZ, and SEB were collected by hand using polypropylene gloves and polypropylene bags by Dr. Shotyk. McM and URSA were collected later in the year and the same handling procedure was used as the 2015 moss samples (see below).

2015 Moss

Three replicate samples per site were collected from 30 bogs in 2015. The bogs ranged from 7 to 50 km from the reference point which is defined as the midpoint between the two central upgraders (Figure 1). The samples were collected in open sections of the bogs to minimize interference from the tree canopies. While *Sphagnum fuscum* was the preferred moss species, a list of all species collected can be found in Table S1. A medical grade stainless steel knife and polypropylene container (462.25 cm^2 surface area) were used to collect the samples while wearing polypropylene gloves. Once the sample location was selected, the polypropylene container was inverted into the moss layer and the knife was used to trace around the container creating a cut-out of the container in the moss mat. The container was then pushed down so the moss cut-out filled the container. To extract the sample, the knife was used to cut the moss level with the container opening (underneath the sample cut-out). The sample now free of the mat could be sealed in the container with a polypropylene lid. See Table S2 for GPS coordinates.

2015 Control Sites

Samples were also collected from the URSA region (264 km from the reference point) home to long-term studies of peatland hydrology and biogeochemistry [11–13]. The Birch Mountain Wildlands site (BMW, 101 km) and Caribou Mountain Wildlands site (CMW, 321 km) are extremely remote and could only be accessed using helicopter. The URSA, BMW, and CMW sites provide baseline values for the abundance of ash and AIA in *Sphagnum* moss.

All sites were chosen with distance from the nearest road in mind, to reduce road dust exposure. Dust deposition is known to be impacted within 100 m of roads [9,14]; therefore, all samples were collected at a minimum of 100 m from the nearest road. The distances from the nearest roads for all collection sites can be found in Table S2.

Cleaning, Drying and Ashing of Samples

Each moss sample was cut so that only the living layer was used for study; these were then cleaned to remove all foreign material [15]. Determining the length of living layer to be used was a challenge as annual growth increases in *Sphagnum* are reported to vary [16]. To account for varying growth rates from site to site in the region, a standard length of 2-2.5 cm was chosen for consistency in order to ensure that only the living material was retained [17].

The cleaned samples were dried at 105^{O}C overnight in 120 mL polypropylene jars and weighed to determine water content. One gram of each dried sample was then ashed at 550 ^{O}C for 16 hours in a muffle furnace (Pyro High Temperature Microwave Muffle Furnace, Milestone, Italy) to determine ash content. The samples were then placed into a desiccator for 24 hours to prevent moisture uptake while cooling. The complete procedure schematic is featured in Figure S2.

Acid Insoluble Ash

To obtain the AIA, each ashed sample was reacted in 1M HCl for 15 minutes. After the reaction, the solution was filtered using 10 ml polypropylene syringes and 0.45μm syringe filters (PTFE Teflon in polypropylene casing) to collect the insoluble ash residue [18]. The filters were dried using a vacuum pump (Air Admiral diaphragm vacuum/pressure pump, Cole-Parmer, Canada). To access the AIA remaining on the filters, the casings of the syringe filters were removed using a cleaned, precision mechanical lathe (Schaublin 135, Bevilard, Switzerland) covered in plastic film to minimize contamination.

Scanning Electron Microscopy and Energy Dispersive X-ray Analysis

Selected AIA samples were analyzed using scanning electron microscopy (SEM) and energy dispersive x-ray spectroscopy (EDX) to determine the mineralogy and morphology of the particles. Specifically, a Zeiss EVO LS15 EP-SEM with Bruker EDX was used under the

following operating conditions: x-ray resolution of 123 eV and a 10 mm^2 window area, gun conditions of 25 kV and 200 pA, in variable pressure (VP) mode, using backscattered electron detector (BSD) imaging.

Particle Size Distribution

A XenParTec (XPT-C) Optical Particle Analysis System was used to determine particle size distribution profiles for selected AIA samples. Portions of selected samples were diluted in 10 mL of surfactant (1% Fisherbrand™ FL-70™ concentrate solution), stirred, and allowed to run through the device for 1 minute before taking a measurement to ensure a representative analysis. Each sample was run for 15 minutes to stabilize the distribution and provide statistically significant particle counts. After each run the XPT-C was cleaned using 18.2 Milli-Q water to remove any remaining particles in the line.

ICP-OES Analysis of ASA

An inductively coupled plasma optical emission spectrometer (ICP-OES) in the Natural Resources Analytical Laboratory (NRAL) at the University of Alberta was used to perform a major ion analysis on one ASA sample from each site of the 2015 collection of moss samples. The concentrations of a long list of elements were determined (Table S4), but here we focus on selected plant macronutrients, namely Ca, K, Mg, P, and S. For more information on the ICP-OES results and QA/QC procedure see Table S3 and Appendix S1.

Statistical Analyses

The average ash and AIA content were calculated using three replicate samples from each bog. To test for first order spatial autocorrelation, Global Moran's I and the Mantel test were performed using the R studio, on the average values of both ash and AIA data for each site. Moran's I for both data sets was close to zero (0.005 and -0.002), and the large p-values (0.7 and 0.8) indicated that the null hypothesis of zero spatial autocorrelation could not be rejected at $\alpha=$

0.05. The Mantel test indicates that no significant correlation was present because the observed values were close to zero (0.003 and 0.006) and the p-values were very large (0.5 and 0.5). Since no significant spatial autocorrelation was detected in the data sets, independent statistical analysis of each site was performed as described below.

The average of the three replicate samples was used as the data point for that site. The standard deviation of the three replicate samples was used to find a confidence interval with α=0.05 for each site location. Some irregularity and variation in AIA concentrations is expected due to the inherent differences between samples in terms of growth rate, productivity, and site conditions [16]. For a complete full list of ash, AIA, and MAR data values, confidence intervals and ranges for the 2015 moss samples see Tables S5 and S6.

Utikuma Control Site

The Utikuma region study area (URSA) is made up of a complex mosaic of wetlands, making it possible to sample at 3 bogs located on different glacial landforms located within a few kilometers of each other. At each of the 3 bogs, 10 *Sphagnum* moss samples were collected using random number assignments in a 10X10 grid (Figure S3). A total of 30 samples from the URSA allowed for a significant background control value to be calculated for ash (1.95 ± 0.11%) and AIA (0.29± 0.07%). The samples from URSA provide the contemporary background values for the both ash and AIA, to serve as a reference level, against which the moss samples from the ABS region may be compared.

RESULTS AND DISCUSSION

Ash and Acid Insoluble Ash

2013-2014 Moss

The mean values of the 3 samples taken from each bog were calculated for ash, AIA, and ASA. The spatial variation in ash, AIA, and ASA is shown in Figure S4. As distance increases from the industrial reference point the amount of ash decreases, with higher concentrations leading to the southeast following wind direction trends (see Figure S5). The highest percentages of AIA (2.3-2.8%) were in a zone 20-25 kilometers from the upgrader midpoint, whereas beyond this distance the ash and AIA values decrease to background values comparable to those found at URSA. In the 2013-2014 sample set there are greater ASA than AIA values, especially at the bogs closer to the industrial reference point.

2015 Moss

The 2015 data for ASA and AIA are shown in Figure 2. Again, the amount of ash and AIA in the moss decreases with distance from the reference point. There is a notable decrease in the size of the AIA fraction relative to the ASA as distance increases from the reference point. The largest values of AIA (2.3-4.7%) and ash content (6.3-10.1%) are all located within proximity to the industrial area (15-20 km), beyond which the values level off to background values. In comparison to the background values established at URSA (ash: 1.95 ± 0.11% and AIA: 0.29± 0.07%), BMW (ash: 1.69 ± 0.31% and AIA: 0.16± 0.23%), and CMW (ash: 1.19 ± 0.34% and AIA: 0.33± 0.06%) the values closest to the ABS region are clearly elevated. In Saskatchewan, *Sphagnum fuscum* was found to have an ash content ranging from 1.6% (remote wilderness area) to 5.5% (predominantly agricultural area) [19], supporting this study's results. An average value calculated for ash content values taken from studies undertaken at other locations (see Table S6 for ash content values) was 3.0% ash, which is slightly greater than URSA and much lower than

the values found closest to the ABS region [15,16,19–24]. Compared to background sites in Alberta and published studies from other areas, the bogs near the ABS region are clearly impacted by dusts.

Colour Variation

While determining ash content, it was observed that the ash samples displayed a large variation in colour from light blue to rust brown. The colours were recorded using microscope imaging and mapped (Figure S6). It was found that there is a correlation between the colour of the ash sample and the AIA content. Brown ash samples correspond to elevated concentrations of AIA, whereas blue ash samples correspond to low concentrations of AIA. The reason for the differences in colour is unknown, but appears to be related to the differences in dust deposition.

Mass accumulation rates

The mass accumulation rates (MAR) of ash and AIA were calculated (see Appendix S2 for calculation example) and mapped (Figure 3). The values calculated represent one growing season of collection (4 months), but for simplicity will be denoted as per year. The range of MAR for ash was determined to be 6.0 – 27.3 g/m^2 yr and 1.0 – 11.9 g/m^2 yr for AIA, with the values decreasing with distance from industry, which agree with findings in Mullan-Boudreau (2017b). In comparison, the background values calculated at URSA (ash: 3.65 ± 0.36 g/m^2 yr and AIA: 0.53± 0.12 g/m^2 yr), BMW (ash: 6.27 ± 3.18 g/m^2 yr and AIA: 0.58± 0.73 g/m^2 yr), and CMW (ash: 4.51 ± 3.28 g/m^2 yr and AIA: 1.16± 0.37 g/m^2 yr) are lower than those nearest the ABS industry. The Oreste bog, located in Southern Isla Navarino, Chile, was found to have an average AIA mineral matter accumulation rate of 0.43 ± 0.12 g/m^2 yr [18], which is consistent with the values calculated at URSA, BMW, and CMW. It is clear that values as great as 11.9 ± 21.2 g/m^2 yr of AIA are well beyond "background values" and result from industrial activity.

Major Ions present in ASA

Major ions analyses were performed on the ASA fraction of the 2015 moss samples to understand inputs of elements essential to plant growth [4]. Phosphorus ranged from 45 mg/L to 336 mg/L (Figure 4) with values clearly increasing with proximity to industrial activity. In ombrotrophic bogs P is naturally limited due to the low concentrations typically found in wet and dry deposition, and typical concentrations in peat from bogs is less than 16 mg/kg[25]. The ASA fraction of mineral dust is therefore the primary supply of available P. Phosphorus can occur in several different forms in dust: authigenic-biogenic minerals of the apatite family, Fe oxides to which P is adsorbed, anthropogenic particles, organic P compounds, and $CaCO_3$-associated P [4,26], most of which would dissolve in an acid bog environment. An increase in P from anthropogenic sources may act as a fertilizer, promoting plant growth and potentially increasing plant competition [26]. Increased competition in an environment where there is naturally very little, could have consequences for the species that dominate ombrotrophic bogs, such as *Sphagnum fuscum*. In fact, a 2014 study found base cation deposition, primarily from dust, was preventing soil acidification due to N and S deposition [27]. These authours also found that these dusts have the potential to increase porewater pH in the environments they studied, if deposition rates continued to increase.

Calcium in the ASA ranges from 200 mg/L to 1200 mg/L, and again, is clearly elevated in the vicinity of industry (Figure 4). Calcium has also been found to be correlated to increased *Sphagnum* growth, although there is no evidence of cause or effect [28]. In a 2013 report for the WBEA on some of the same bogs used in this study (MIL, JPH4, McK, ANZ, and McM), Ca deposition rates in the area ranged from 2.02 kg/ha yr to 7.1 kg/ha yr [28]. Using the Ca concentrations found in this study (200 mg/L to 1200 mg/L) and considering the growth increment of moss used here (2.5cm) for analysis, we obtain Ca fluxes in the range 2 to 12

kg/ha/yr which is comparable to the values reported in Vile et al. (2013). Another study similarly found that base cation (Ca^{2+}, Mg^{2+} and Na^{+}) deposition decreased logarithmically with distance from the industrial center in the ABS region [27]. Potassium, Fe, Mg, and S (Figure S7) display spatial trends similar to those of Ca.

Mineralogy and Physical Characterization

Two of the sources of dust in the ABS region are open pit mining and dust generating gravel roads. This creates a challenge in differentiating between these sources of mineral matter from the natural background from wind erosion of soils. In general, the AIA samples contained quartz, feldspars, micas (biotite), amphiboles, zircons, and clay minerals which are consistent with previous studies of dust source mineralogy profiles in the ABS region [29,30]. In addition, some samples of AIA contained gypsum crystals (Figure 5c), which did not dissolve in the HCl reaction as it is only partly soluble in HCl [31]. Spherical fly ash particles were found in some of the near-site samples (Figure 5d). The majority of the spherical fly ash were silicates or aluminosilicates with some containing trace elements such as Fe, and Ti. These particles are typical of fly ash particle composition [32,33]. In contrast to early studies [34], no trace metals were found in the fly ash analyzed using EDX (LOD ~1000 mg/kg).

The SEM imaging also illustrated that there was larger diversity in particle sizes in samples from sites closer to industry (Figure 5a) than in samples further away (Figure 5b). The variability in particle size was confirmed with particle size distributions performed on selected samples (Figure S8). The size distributions found in the AIA samples indicated that sites closer to industry have much more variation in particle sizes than the distal and background samples.

Estimating dust deposition in the ABS region using Sphagnum moss

A current estimate of total particulate matter emissions from the ABS industry in 2015 is 18,842 tonnes [3]. Since the statistical test, Moran's I, did not show spatial-autocorrelation, an average mass accumulation rate for the 18 sites within a 30 km radius of the reference point was calculated using ash (11.0 g/m^2) and AIA (3.5 g/m^2). To correct for natural background dust deposition, the accumulation rates obtained of the URSA samples were subtracted from the averages to obtain the average anthropogenic dust accumulation rates of 7.4 g/m^2 (ash) and 3.0 g/m^2 (AIA). Using these approaches, we obtain 21,000 tonnes of total anthropogenic dust (based on ash contents) consisting of 8,500 tonnes of insoluble material (AIA) and 12,500 tonnes of soluble material (ASA). For context, the natural background of contemporary dust deposited within a 30 km radius of the URSA was determined to be 10,300 tonnes total dust (ash), 1,500 tonnes of insoluble material (AIA), and 8,800 tonnes of soluble matter (ASA).

It should be noted that the arrangement and small number of samples (Moran's I requires 30 points as a minimum) could make the result of no spatial-autocorrelation contestable. Given the location of industrial activity (roads and stacks) it is possible that spatial structure exists at a larger scale but remains undetected by the statistic. If this is the case, then a spatial autocorrelation based interpolation would be used to estimate the total dust deposition in the ABS region. Therefore, ordinary kriging was used to create a simple prediction surface of ash and AIA deposition. The sum of the area based prediction surface values suggest anthropogenic activities in the region add 23,000 tonnes of dust (ash), 9,300 tonnes of insoluble material (AIA) and 13,700 tonnes of soluble material (ASA).

The amount of dust calculated by Environment and Climate Change Canada, represents one full year of emissions for the Fort McMurray area. However as previously stated, the data

presented in this paper represents mineral matter found in the living layer of *Sphagnum* moss representing one growing season i.e. approximately 4 months. Over the course of one year, within 30 km of industry, both of our calculations above infer annual deposition greater than Environment and Climate Change Canada reports. Using the average mass accumulation rates 63,000 tonnes of total dust, with 25,500 tonnes of insoluble matter and 37,500 tonnes of soluble material is calculated per year, while using ordinary kriging results in 69,000 tonnes of total dust, with 27,900 tonnes of insoluble matter and 41,100 tonnes of soluble material. While our findings are based upon a single year (2015) of plant collection at only 30 sites, they are consistent with the data obtained from the samples collected during 2014 at a smaller number of sites. And while the calculated dust inputs to these bogs are not definitive, both scenarios do suggest that the extent of dust deposition may have been considerably underestimated, and that the amount of mineral matter in *Sphagnum* moss might be a useful tool in future monitoring studies.

Consequences of elevated dust deposition

Increased mineral dust deposition in the ABS region, could have consequences for surrounding ecosystems. Naturally acidic ecosystems, such as bogs, are home to plants accustomed to (and dependent upon) acidic (pH 4) low ionic strength waters. The bogs with the greatest dust deposition rates are at risk due to elevated inputs of soluble minerals: their dissolution increases the availability of plant nutrients and may increase the pH thereby creating an environment more welcoming for competition by plants normally unable to grow in that environment [35]. Studies have shown that bogs closer to a significant source of dust deposition will have less *Sphagnum* and other acidophilus mosses present. For example, these effects were seen with dust deposition rates ranging from 25.6 – 912.5 g/m^2 yr of road dust, with notable declines in the population becoming apparent at 365 g/m^2 yr [6,14,15,36]. While the mass accumulation rates of dust in the ABS region today are at least a factor of ten below this value,

further expansion of the industry and the cumulative inputs of dust deposition may have an impact on the surrounding acidophilus mosses and other vegetation. Establishing current deposition rates are important to help understand potential changes in the future. Understanding the significance of dust deposition today and in the future can become part of a strategy to reduce emissions, e.g. by watering or minimizing surface disturbances [9,37].

ACKNOWLEDGMENTS

Thanks to Alberta Innovates for funding, to the University of Alberta, the Faculty of Agricultural, Life and Environmental Sciences, the Department of Renewable Resources for supporting the SWAMP laboratory. Thanks to the Land Reclamation International Graduate School (LRIGS) and NSERC CREATE for providing financial support. Thanks to Natural Resources Analytical Laboratory (NRAL) for performing the major ion analysis on the 2015 ASA samples. Tracy Gartner, Melanie Bolstler, and Karen Lund provided administrative support, and Chad Cuss and Muhammad (Babar) Javed provided laboratory support and instruction. Anita Nowinka aided in preparation of ash, and AIA samples of the moss samples. Thanks to Melissa Dergousoff and April Cormack for their hard work on sample cleaning and preparation. Also a big thanks to Melanie Vile for acquainting our team with the bogs sites used in this study. Thanks to Rene Belland for species identification and project instruction, to Lee Foote and Claudio Zaccone for project guidance, and to Emer Mullan for reviewing this manuscript.

REFERENCES

(1) Alberta Energy Regulator. Alberta's Energy Reserves 2014 and Supply/Demand Outlook 2015-2024. Alberta Energy Regulator: Calgary **2015**, pp 3–12.

(2) Stringham, G. *Energy Developments in Canada's Oil Sands*, 1st ed.; Elsevier Ltd., **2012**; Vol. 11.

(3) Environment and Climate Change Canada. PM - Total Particulate Matter (NA - M08) http://ec.gc.ca/inrp-npri/donnees-data/index.cfm?do=results&lang=en&opt_facility_name=&opt_facility=&opt_npri_id=&opt_report_year=2015&opt_chemical_type=ALL&opt_industry=&opt_cas_name=NA+-+M08&opt_cas_num=&opt_location_type=ALL&opt_province=AB&opt_postal_ (accessed Nov 9, 2016).

(4) Muhs, D. R.; Prospero, J. M.; Buddock, M. C.; Gill, T. E. Identifying sources of aeolian mineral dust: Present and past. In *Mineral Dust: A Key Player in the Earth System*; Springer Science & Business Media: Dordrecht, **2014**; pp 385–409.

(5) Cooper, C. D.; Alley, F. C. *Air pollution control : a design approach.*, 4th ed.; Long Grove, Ill. : Waveland Press, **2011**.

(6) Mattson, S.; Koutler-Andersson, E. Geochemistry of a raised bog. *Annals of the Royal Agricultural College*. Sweden. **1955**, pp 321–356.

(7) Shotyk, W.; Bicalho, B.; Cuss, C. W.; Duke, M. J. M.; Noernberg, T.; Pelletier, R.; Steinnes, E.; Zaccone, C. Dust is the dominant source of "heavy metals" to peat moss (*Sphagnum fuscum*) in the bogs of the Athabasca Bituminous Sands region of northern Alberta. *Environ. Int.* **2016**, *92–93*, 494–506.

(8) Zhang, Y.; Shotyk, W.; Zaccone, C.; Noernberg, T.; Pelletier, R.; Bicalho, B.; Froese, D. G.; Davies, L.; Martin, J. W. Airborne petcoke dust is a major source of polycyclic aromatic hydrocarbons in the Athabasca oil sands region. *Environ. Sci. Technol.* **2016**, *50* (4), 1711–1720.

(9) Watson, J. G.; Chow, J. C.; Wang, X.; Kohl, S. D.; Yatavelli, L. N. R. Windblown Fugitive Dust Characterization in the Athabasca Oil Sands Region. *Wood Buffalo Environmental Association*. Desert Research Institute: McMurray. **2014**, pp 1-1-4–19.

(10) Wang, X.; Chow, J. C.; Kohl, S. D.; Percy, K. E.; Legge, A. H.; Watson, J. G. Characterization of PM 2.5 and PM 10 fugitive dust source profiles in the Athabasca Oil Sands Region. *J. Air Waste Manage. Assoc.* **2015**, *65* (12), 1421–1433.

(11) Devito, K.; Mendoza, C.; Qualizza, C. Conceptualizing water movement in the Boreal Plains: Implications for watershed reconstruction. Canadian Oil Sands Network for Research and Development, Environmental and Reclamation Research Group: Edmonton, AB. **2012**, p 164.

(12) Petrone, R.; Devito, K. J.; Mendoza, C. Utikuma Region Study Area (URSA) - Part 2: Aspen Harvest and Recovery Study. *For. Chron.* **2016**, *92* (1), 62–65.

(13) Devito, K. J.; Mendoza, C.; Petrone, R. M.; Kettridge, N.; Waddington, J. M. Utikuma Region Study Area (URSA) - Part 1: Hydrogeological and ecohydrological studies (HEAD). *For. Chron.* **2016**, *92* (1), 57–61.

(14) Walker, D. A.; Everett, K. R. Road dust and its environmental impact on Alaskan taiga and tundra. *Arct. Alp. Res.* **1987**, *19* (4), 479–489.

(15) Santelmann, M. V; Gorham, E. The influence of airborne road dust on the chemistry of *Sphagnum* mosses. *J. Ecol.* **1988**, *76* (4), 1219–1231.

(16) Malmer, N. Patterns in the growth and the accumulation of inorganic constituents in the *Sphagnum* cover on ombrotrophic bogs in Scandinavia. *Oikos* **1988**, *53* (1), 105–120.

(17) Vile, M. A.; Wieder, R. K.; Berryman, S.; Vitt, D. H. WBEA 2010 Annual Report: Development of Monitoring Protocols for N & S Sensitive Bog Ecosystems. Wood Buffalo Enironmental Association. **2010**.

(18) Sapkota, A. Mineralogical, Chemical, and Isotopic (Sr, Pb) Composition of Atmospheric Mineral Dusts in an Ombrotrophic Peat Bog, Southern South America, Ruprecht-Karls-Universität, **2006**.

(19) Gorham, E.; Tilton, D. L. The mineral content of *Sphagnum fuscum* as affected by human settlement. *Can. J. Bot.* **1978**, *56* (180), 2755–2759.

(20) Shotyk, W. Review of the inorganic geochemistry of peats and peatland waters. *Earth-Science Rev.* **1988**, *25* (2), 95–176.

(21) Shotyk, W. Natural and anthropogenic enrichments of As, Cu, Pb, Sb, and Zn in ombrotrophic versus minerotrophic peat bog profiles, Jura Mountains, Switzerland. *Water. Air. Soil Pollut.* **1996**, *90*, 375–405.

(22) Damman, A. W. H.; Tolonen, K.; Sallantaus, T. Element retention and removal in ombrotrophic peat of Haadetkeidas, a boreal Finnish peat bog. *Suo* **1992**, *43* (4–5), 137–145.

(23) Vuorela, I. Field erosion by wind as indicated by fluctuations in the ash content of *Sphagnum* peat. *Bull. Geol. Soc. Finl.* **1983**, *55* (1978), 25–33.

(24) Gorham, E. Water, ash, nitrogen and acidity of some bog peats and other organic soils. *J. Ecol.* **1961**, *49*, 103–106.

(25) Small, E. Ecological significance of four critical elements in plants of raised spagnum peat bogs. *Ecology* **1972**, *53* (3), 498–503.

(26) Hudson-Edwards, K. A.; Bristow, C. S.; Cibin, G.; Mason, G.; Peacock, C. L. Solid-phase

phosphorus speciation in Saharan Bodélé Depression dusts and source sediments. *Chem. Geol.* **2014**, *384*, 16–26.

(27) Watmough, S. A.; Whitfield, C. J.; Fenn, M. E. The importance of atmospheric base cation deposition for preventing soil acidification in the Athabasca Oil Sands Region of Canada. *Sci. Total Environ.* **2014**, *493*, 1–11.

(28) Vile, M. A.; Wieder, R. K.; Vitt, D. H.; Berryman, S. Final Report: Development of monitoring protocols for nitrogen-sensitive bog ecosystems, including further development of lichen monitoring tools. *WBEA Final Report*. Wood Buffalo Enironmental Association. **2013**, pp 1–91.

(29) Bichard, J. A. AOSTRA technical publication series #4: Oil sands composition and behaviour research. Alberta Oil Sands Technology & Research Authority (AOSTRA): Edmonton, Alberta. **1987**, pp 3–2 & 3–14.

(30) Welton, J. E. *SEM petrology Atlas*; The American Association of Petroleum Geologists: Tulsa, Oklahoma, **2003**.

(31) Azimi, G.; Papangelakis, V. G.; Dutrizac, J. E. Development of an MSE-based chemical model for the solubility of calcium sulphate in mixed chloride-sulphate solutions. *Fluid Phase Equilib.* **2008**, *266* (1–2), 172–186.

(32) Yoo, J. G.; Jo, Y. M. Utilization of coal fly ash as a slow-release granular medium for soil improvement. *J. Air Waste Manag. Assoc.* **2003**, *53* (1), 77–83.

(33) Jang, H.; Etsell, T. H. Morphological and mineralogical characterization of oil sands fly ash morphological and mineralogical characterization of oil. *Energy & Fuels* **2005**, *19* (5), 2121–2128.

(34) Shelfentook, W. An inventory system for atmospheric emissions in the AOSERP study area. SNC Tottrup Services Ltd.: Edmonton, AB **1978**.

(35) Pearsall, W. . The pH of natural soils and its ecological significance. *J. Soil Sci.* **1952**, *3* (1), 41–51.

(36) Farmer, A. M. The effects of dust on vegetation - a review. *Environ. Pollut.* **1993**, *79*, 63–75.

(37) Wang, X.; Chow, J. C.; Kohl, S. D.; Yatavelli, L. N. R.; Percy, K. E.; Legge, A. H.; Watson, J. G. Wind erosion potential for fugitive dust sources in the Athabasca Oil Sands Region. *Aeolian Res.* **2015**, *18*, 121–134.

(38) Government of Canada. Historical Data http://climate.weather.gc.ca/historical_data/search_historic_data_e.html (accessed Oct 1, 2016).

(39) R Development Core Team. R: A language and environment for statistical computing. R

Foundation for Statistical Computing: Vienna, Austria **2008**.

(40) Carslaw, D. C.; Ropkins, K. openair. Environmental Modelling & Software **2012**.

(41) Fennelly, P. The origin and influence of airborne particulates. *Am. Sci.* **1976**, *64* (1), 46–56.

LIST OF FIGURES

Figure 1: 2015 moss sampling bogs (30 bogs within the ABS region, MIL, JPH4, McK, McM, URSA, EINP, WAG, CMW, BMW). Active upgraders, Wabamum Transalta Sundance Coal-fired Generating Station, and the upgrader midpoint (reference point) are also depicted.

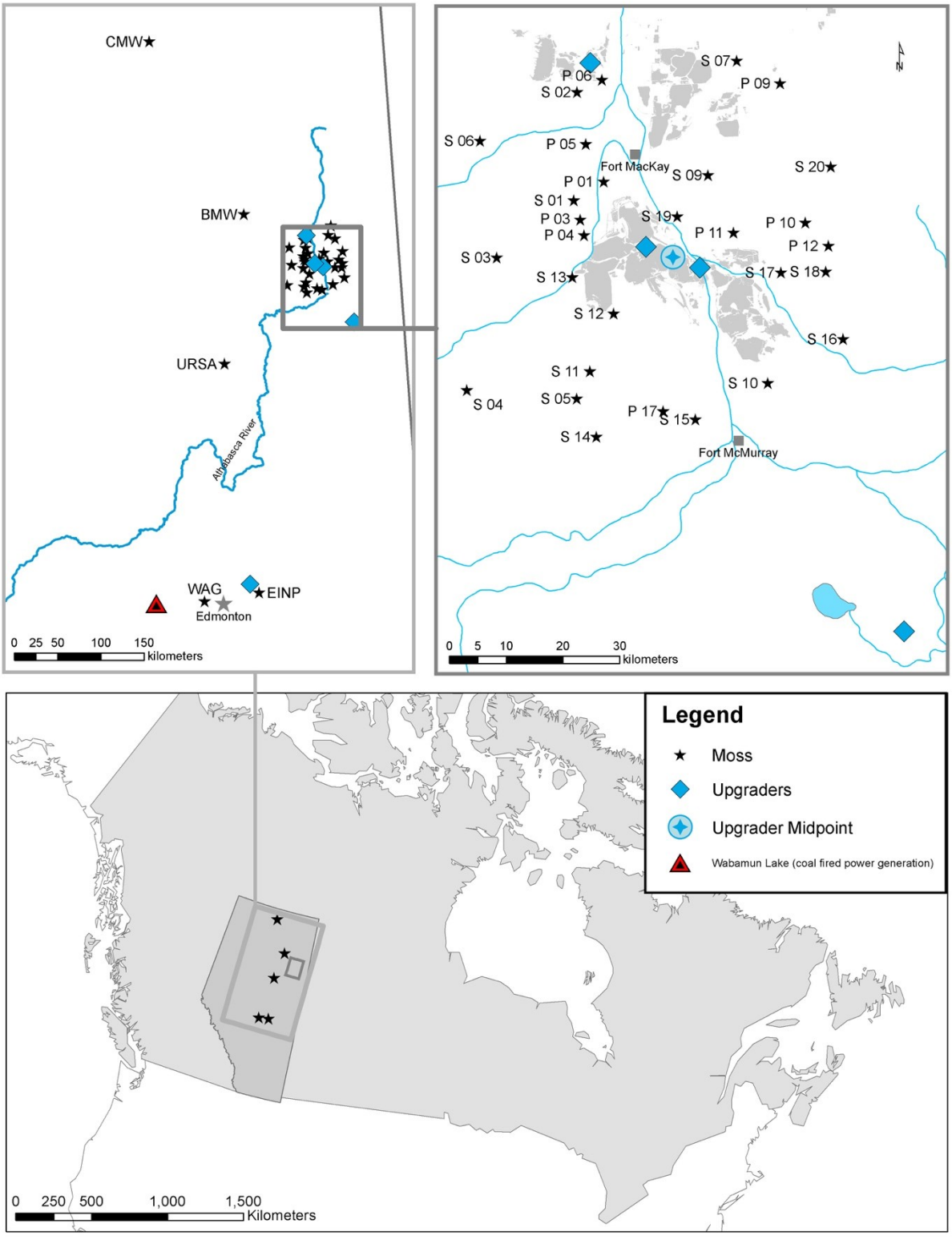

Figure 2: Average Ash and AIA values of moss sampled during 2015 (30 bogs with the ABS region, URSA, EINP, WAG, CMW, & BMW). Active upgraders and upgrader midpoint (reference point) are also depicted. The circle size represents the ash content (%), while the fractions of each circle represent AIA (orange) and ASA (cream).

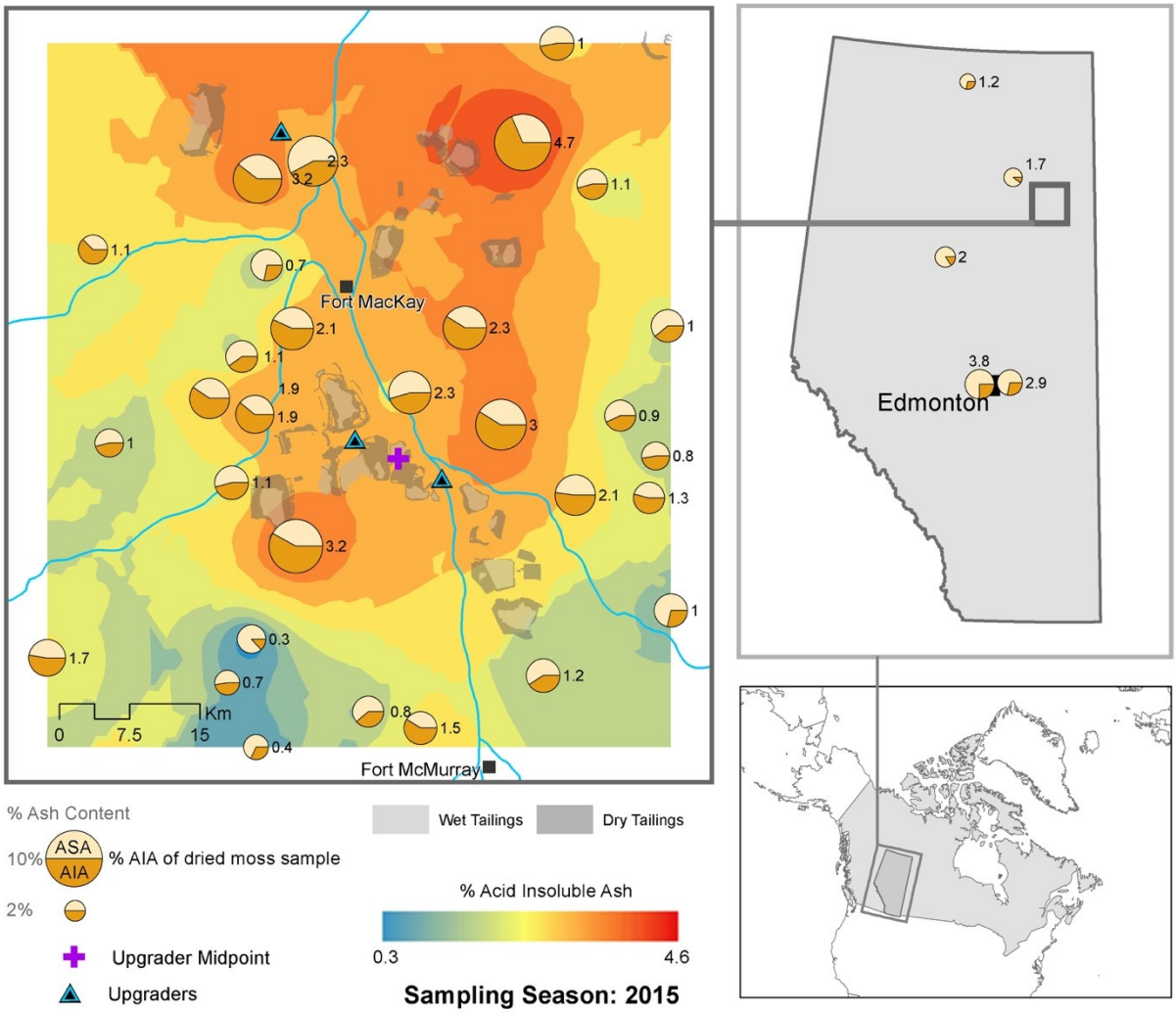

Figure 3: Map of mass accumulation rates (g/m^2 yr) of ash and AIA for moss sampled during 2015. Calculated using moss accumulation rates determined from volumetric dry weights. Main image depicts 2015 ABS region samples, square inset image on left depict URSA samples, and rectangle inset image on right depict CMW & BMW samples.

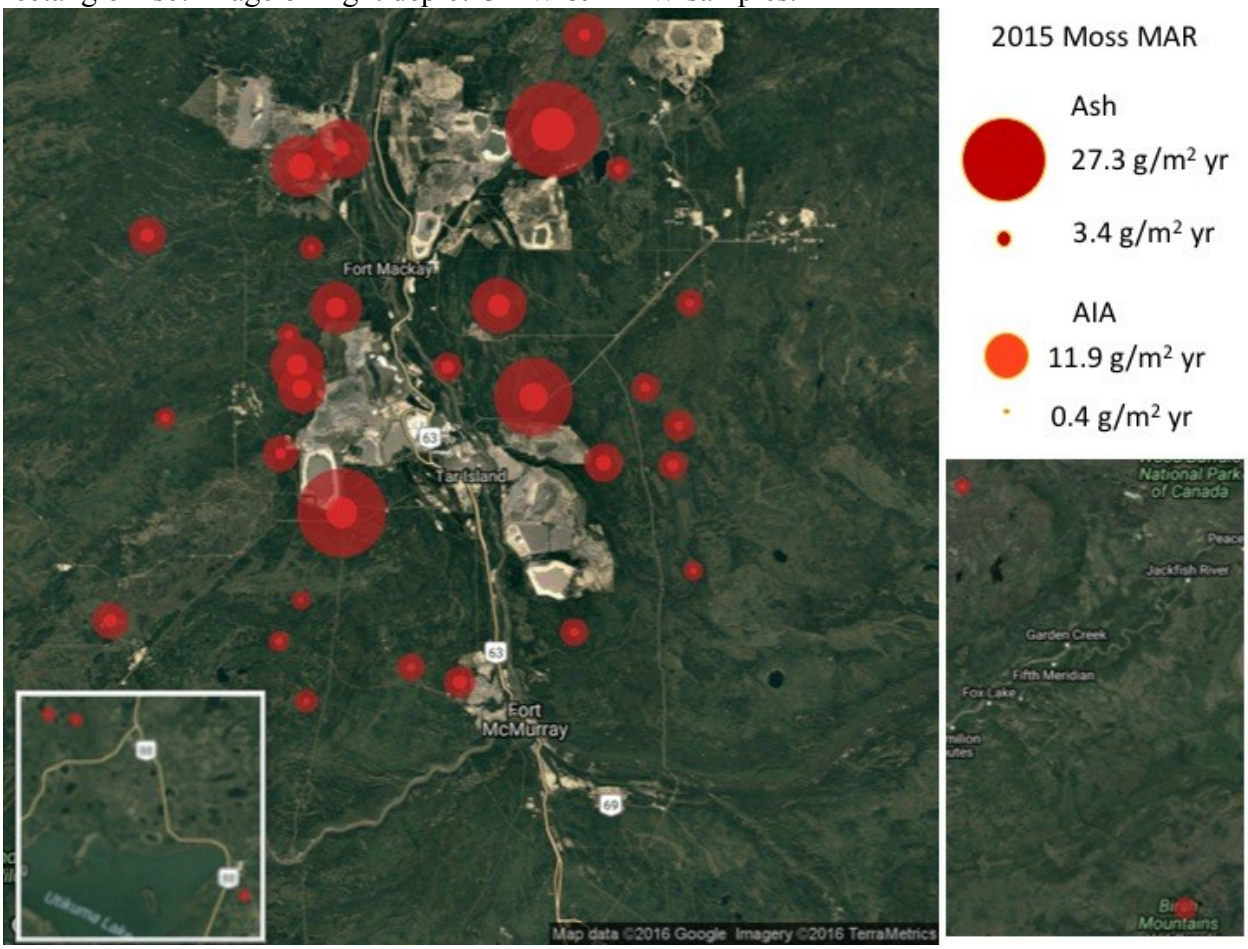

Figure 4: Phosphorus and calcium concentrations in ASA of moss sampled in 2015. One out of three samples (sample "a") was analyzed from each site. Main image depicts 2015 ABS region samples, square inset image on left depict URSA samples, and rectangle inset image on right depict CMW & BMW samples.

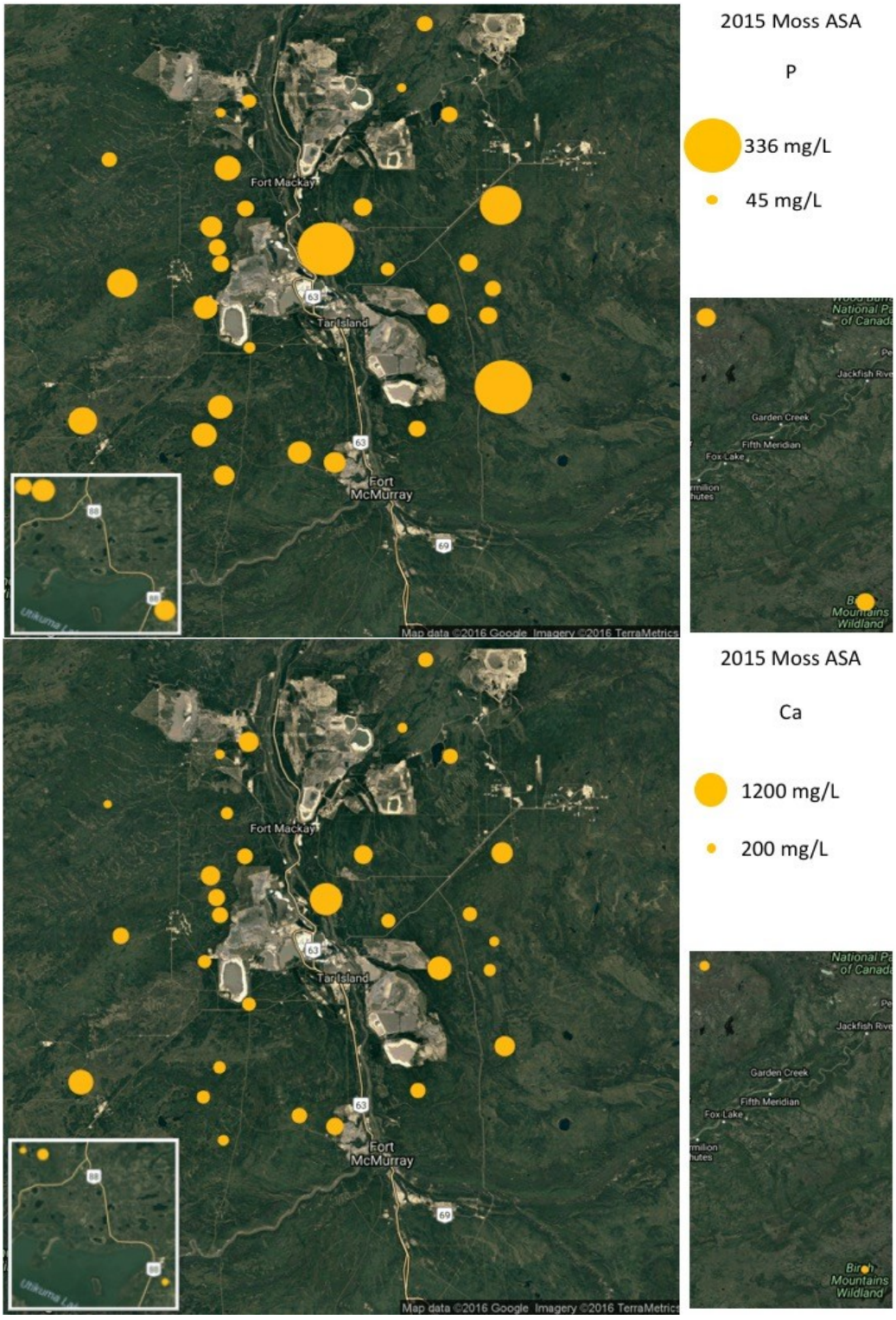

Figure 5: SEM images highlighting morphology and mineralogy of AIA a) high variation in morphology and size from a site close to industry. Aluminosilicates typical of all the samples are depicted (sample S07-a) b) smaller variation in morphology and size from a site far from industry. A quartz particle is depicted (sample S14-a) c) gypsum crystals found in some samples (sample URSA 524-a) d) spherical fly ash particles present in proximal sites. An iron aluminosilicate is depicted (sample S02-c). Mineralogy of several particles to highlight typical particles found in most samples.

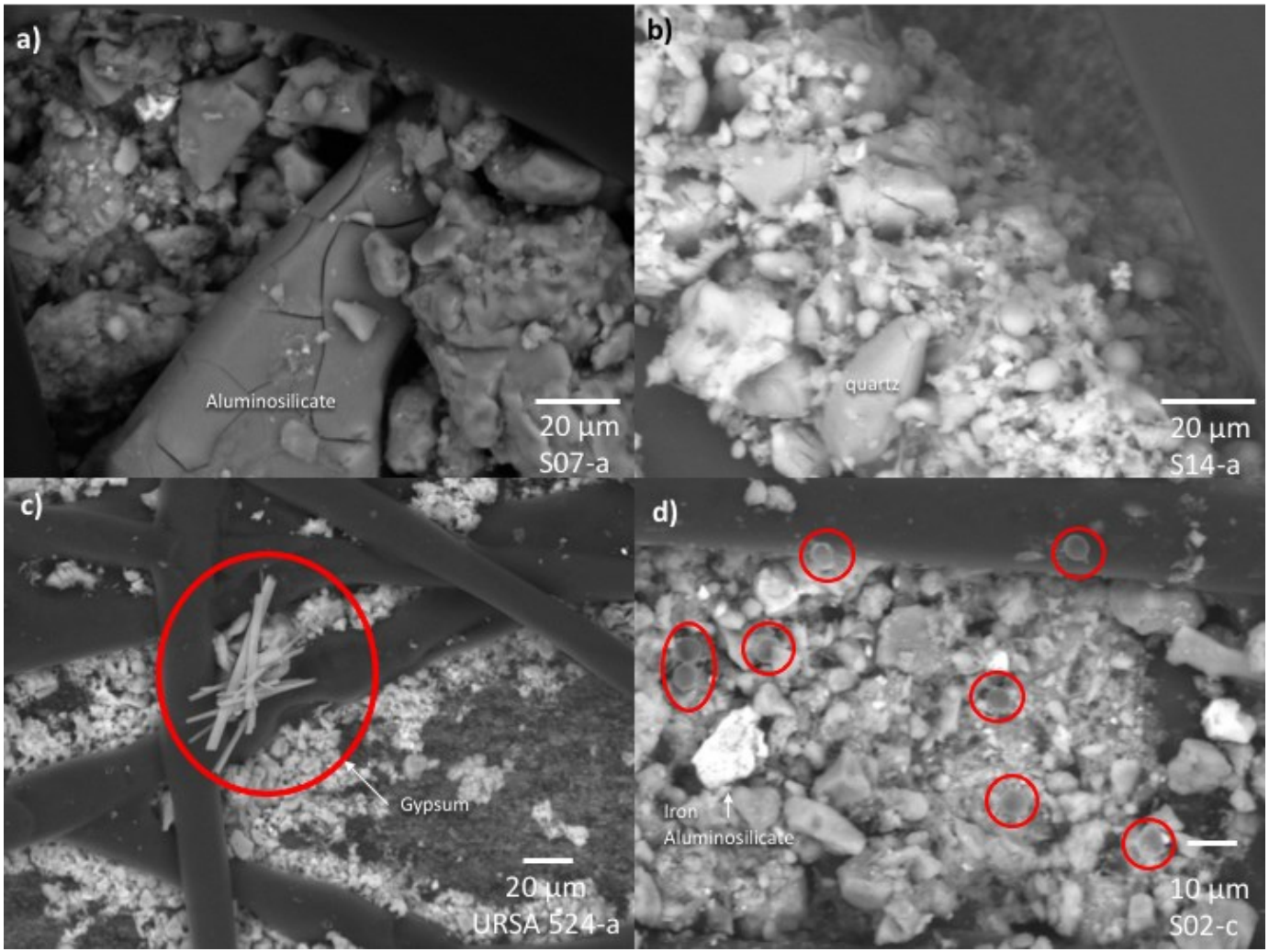

SUPPORTING INFORMATION

List of Figures

List of Tables

List of Appendix

Supporting Information Figures

Figure S1: 2013-2014 moss sampling locations (21 sites within the ABS region plus MIL, JPH4, McK, McM, ANZ, URSA). Active upgraders, Wabamum Transalta Sundance Coal-fired Generating Station, and the midpoint between the two central upgraders (reference point) are also depicted.

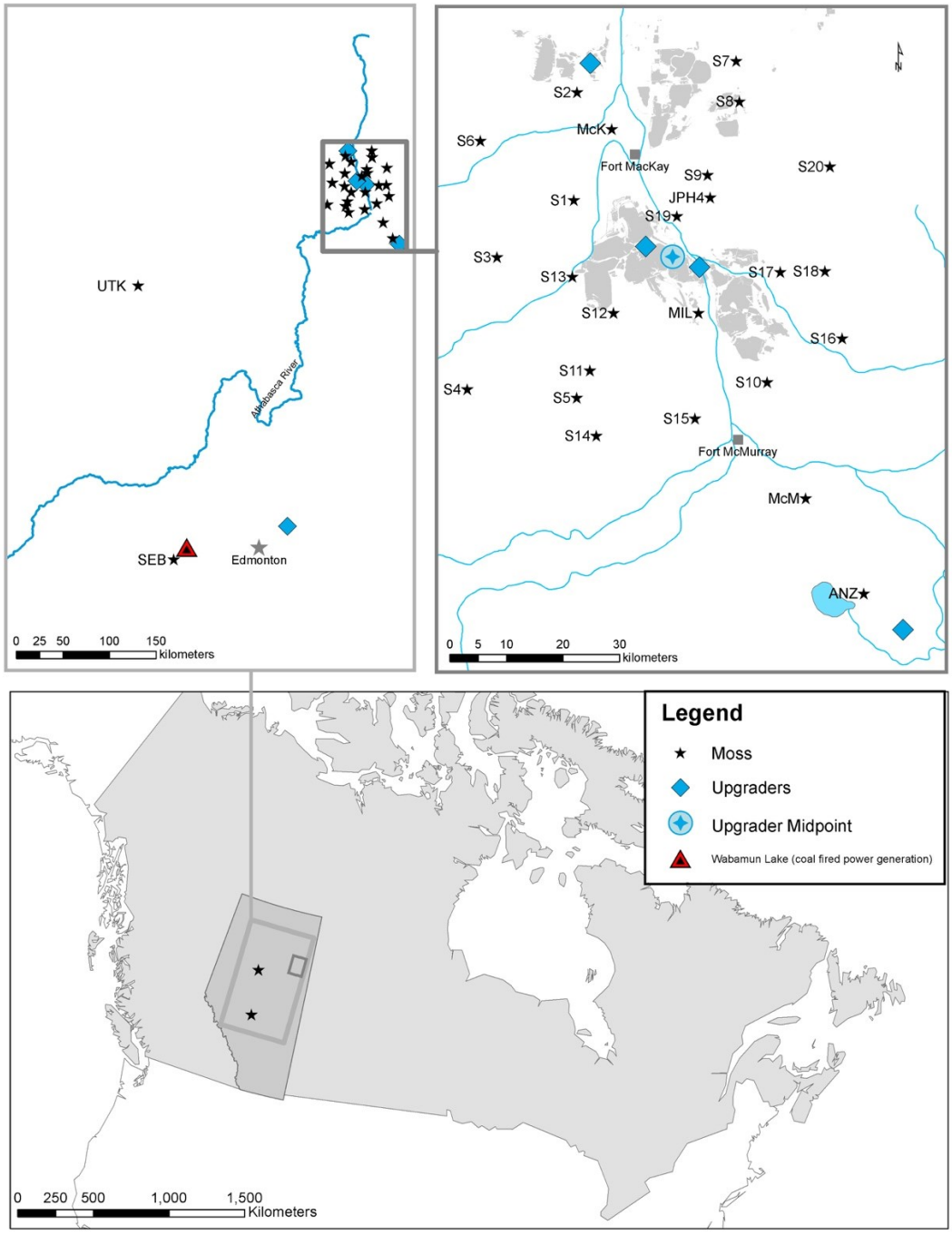

Figure S2: Moss Sample Preparation and Analysis Schematic

Figure S3: Sampling grids used at the three bogs in the Utikuma Region Study Area. Each bog had 10 samples collected (a-j) that were selected using a randomized grid method. The circle size represents the ash content (%), while the fractions of each circle represent AIA (orange) and ASA (cream). The coloured squares represent the colour of each ash sample.

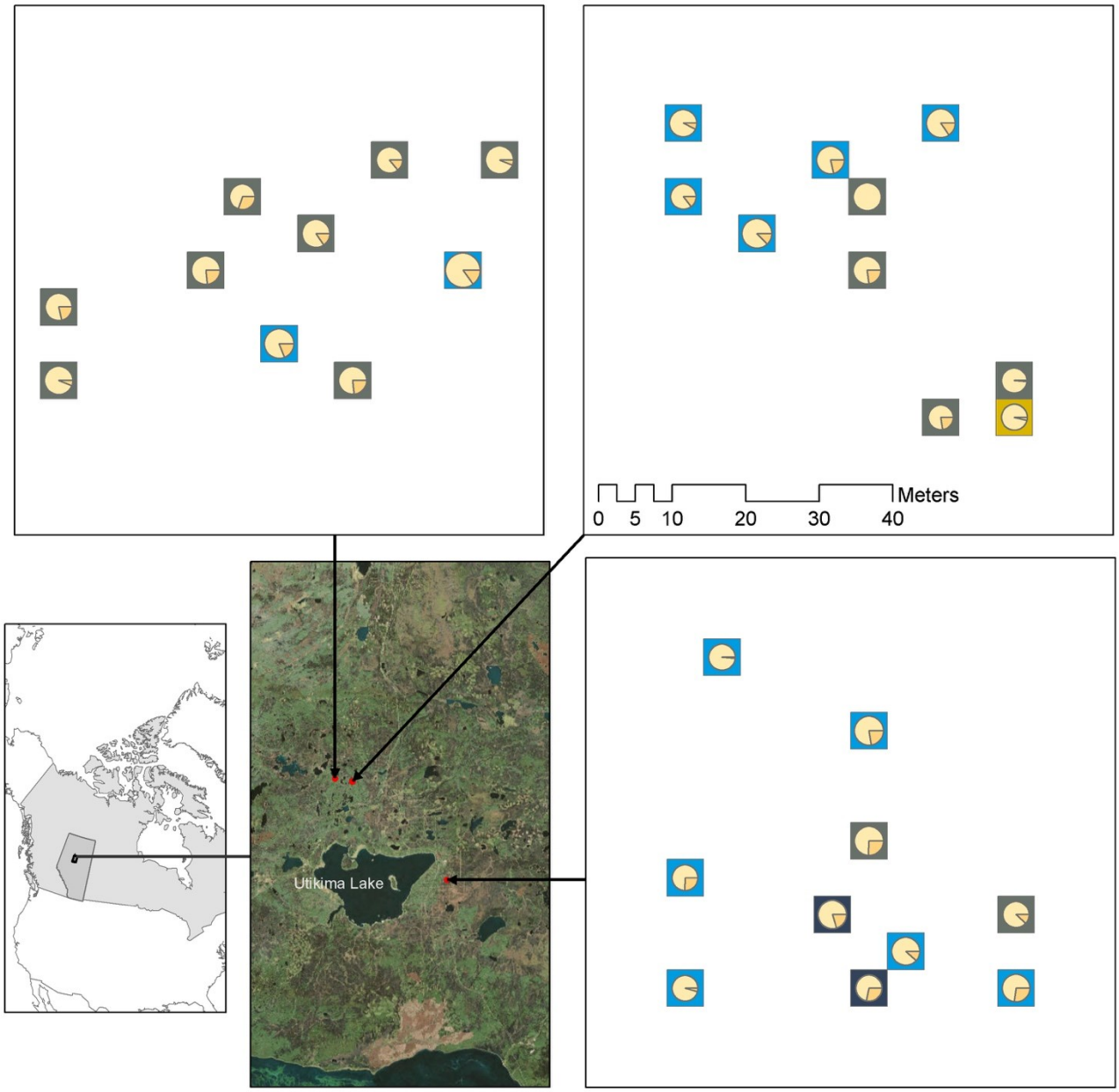

Figure S4: 2013-2014 map illustrating ash and AIA content (%). The circle size represents the ash content (%), while the fractions of each circle represent AIA (orange) and ASA (cream). The increase in ASA may be due to samples being milled prior to ashing, reducing the particle sizes and thus, allowing more of each sample to move through the 0.45µm filters.

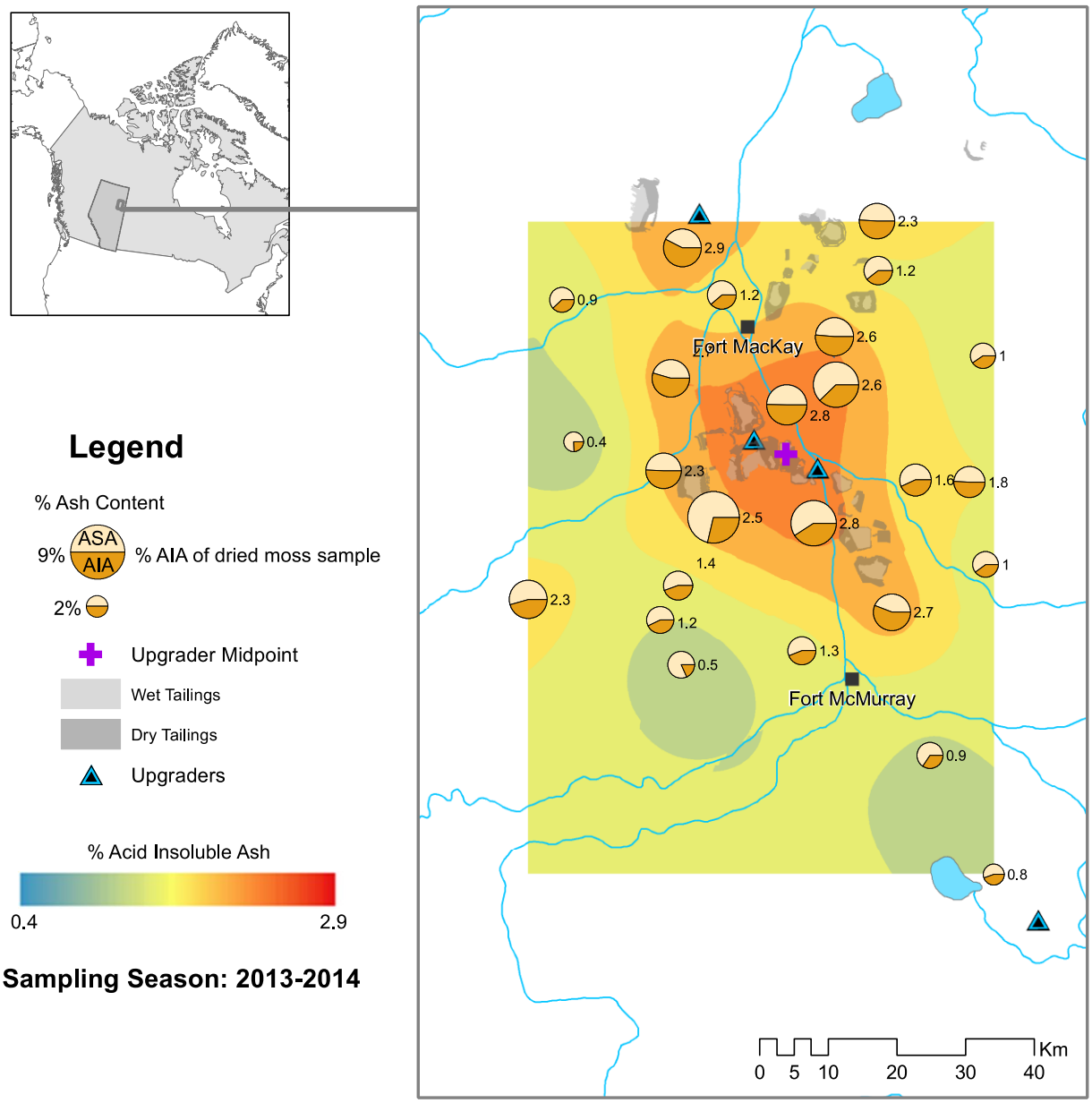

Figure S5: Wind rose diagrams for 2014 & 2015 at Mildred Stations. Historic hourly weather data from May 1, 2014 through July 31, 2014 and May 1 to August 31, 2015 was downloaded [38] from the Government of Canada climate station: Mildred Lake (latitude: 57°02'28.000" N, longitude: 111°33'32.000" W, elevation: 310.00 m, Climate ID: 3064528, WMO ID: 71255) Data was formatted with python, processed in R [39] and wind roses created with the R openair package [40].

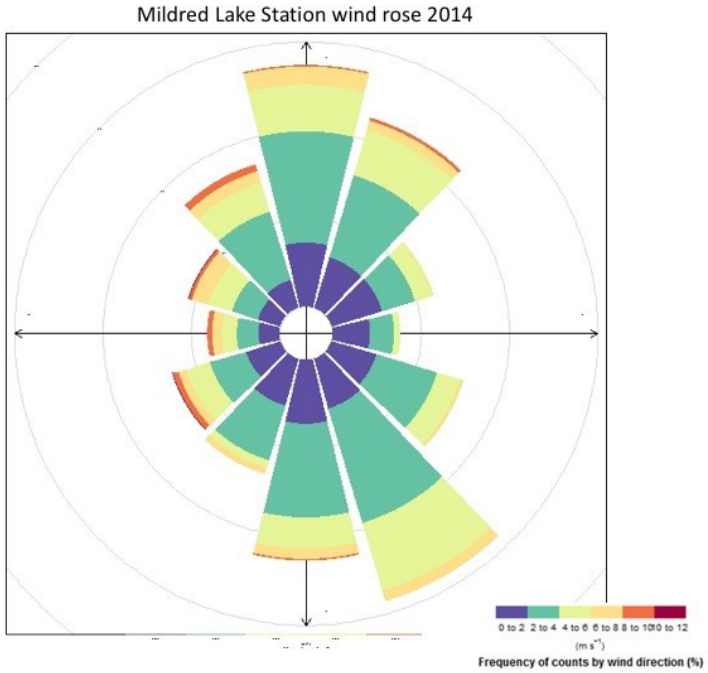

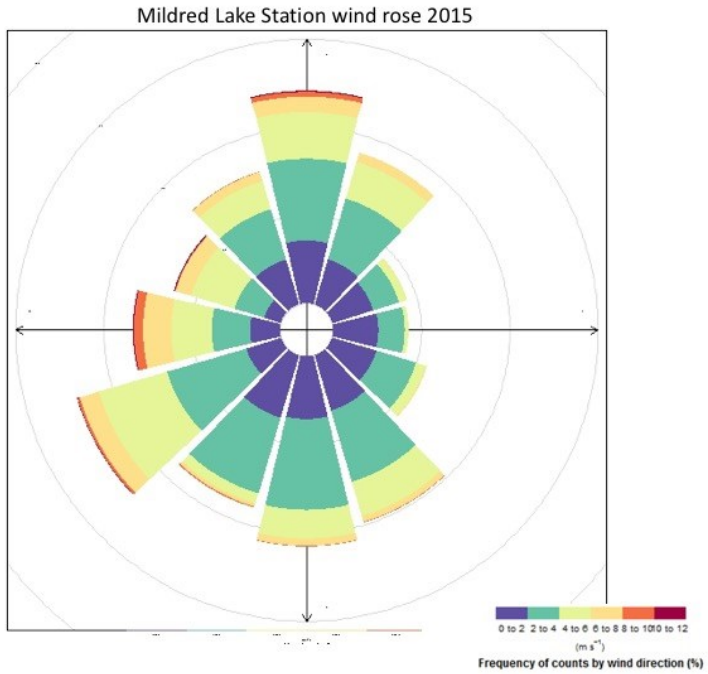

Figure S6: The range of colour observed in all 2015 ash samples. Brown ash samples correspond to elevated concentrations of AIA, whereas blue ash samples correspond to low concentrations of AIA. Image examples of the colour variation within the 2015 moss samples are shown below.

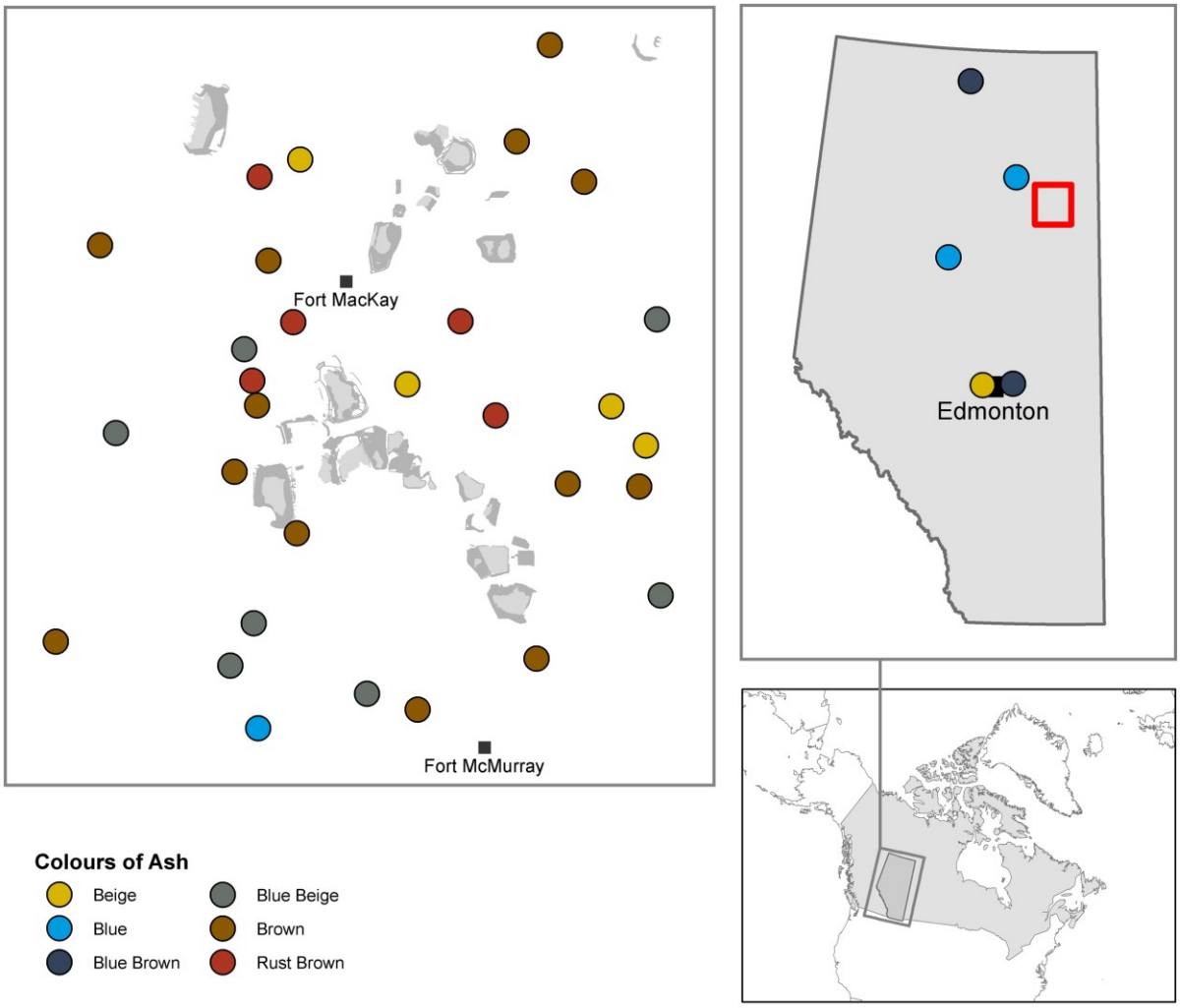

Examples of the colour variation within the 2015 moss samples

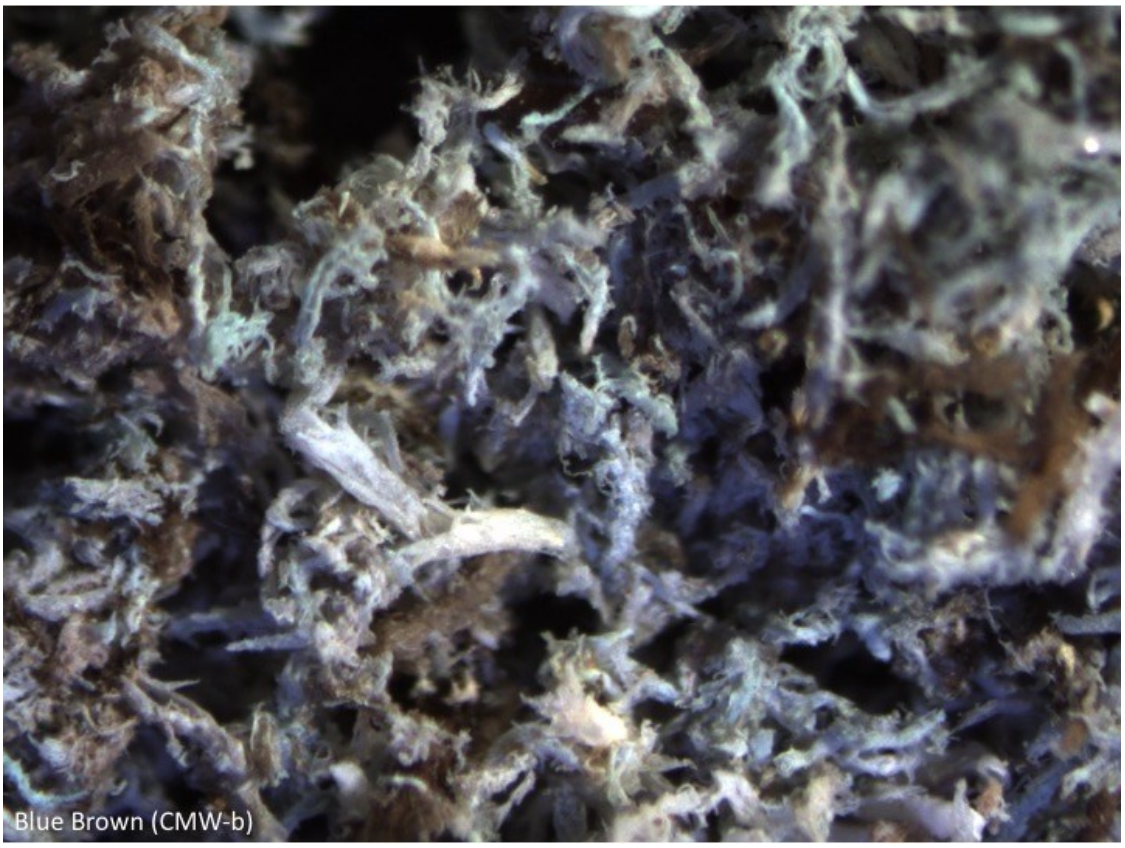
Blue Brown (CMW-b)


Beige (WAG-a)


Blue-Beige (URSA19/21-a)


Brown (PU5-a)


Blue (URSA524-g)

Figure S7: Potassium, Mg, Fe, and S concentrations (mg/L) in ASA of 2015 moss samples

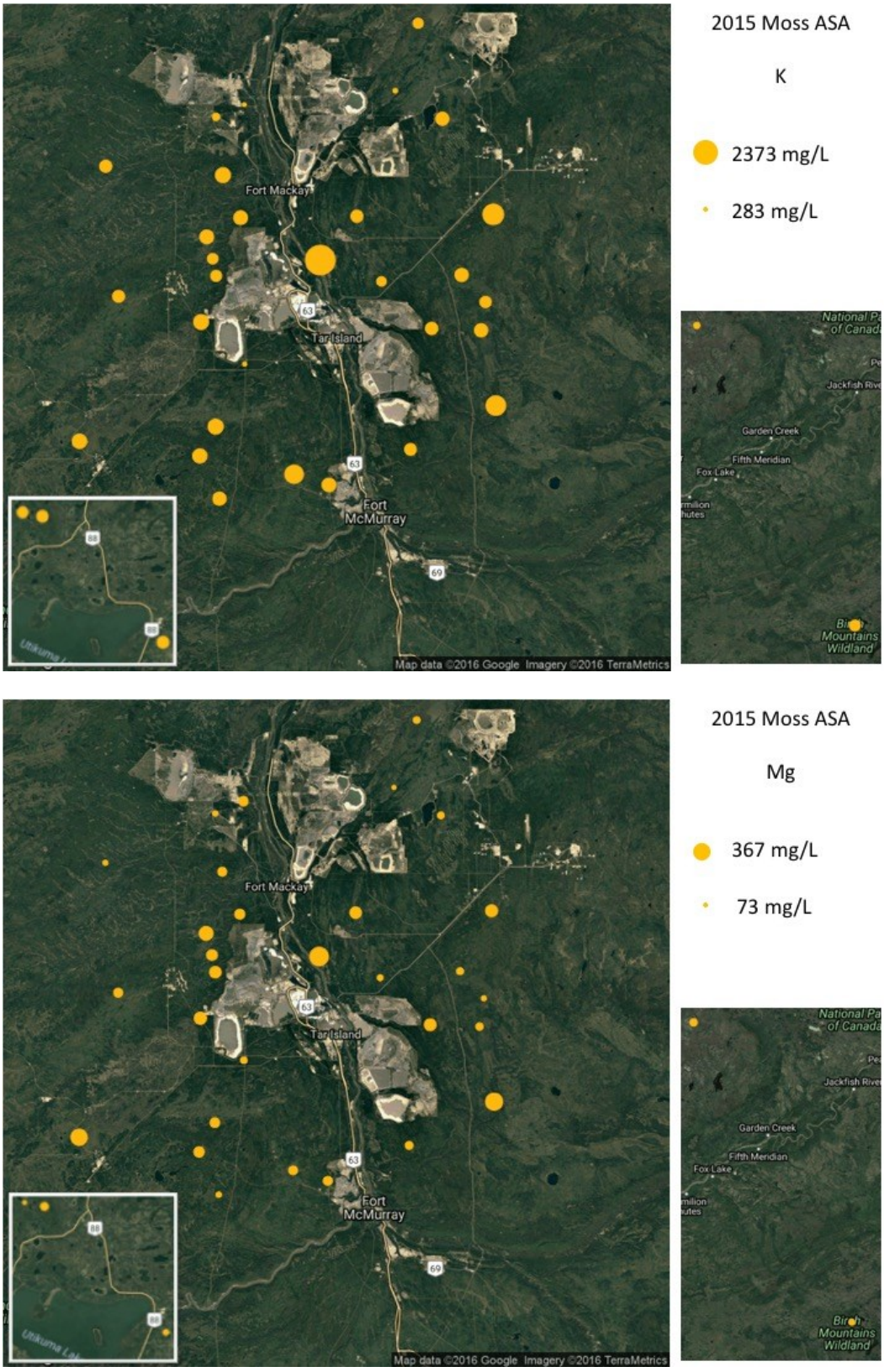

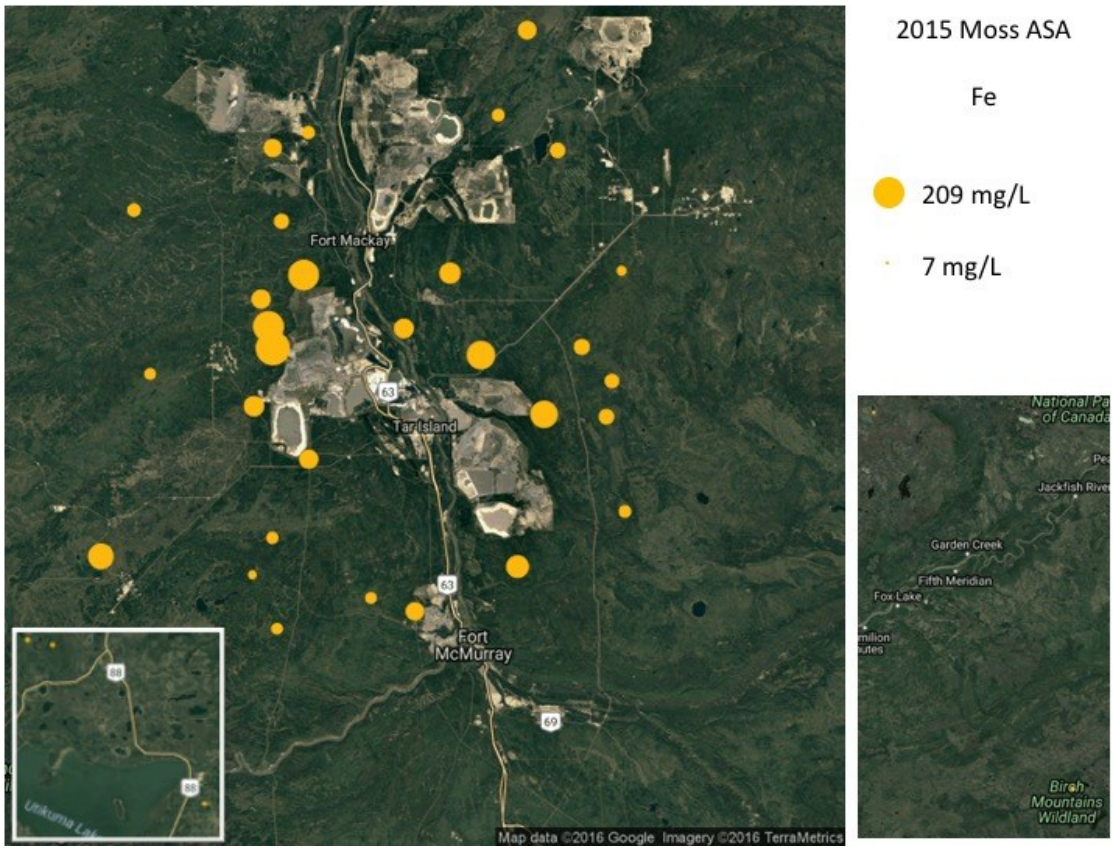
2015 Moss ASA
Fe
209 mg/L
7 mg/L
Fort Mackay
Tar Island
Fort McMurray
Map data ©2016 Google Imagery ©2016 TerraMetrics
Garden Creek
Fifth Meridian
Fox Lake
Jackfish River
Birch Mountains Wildland

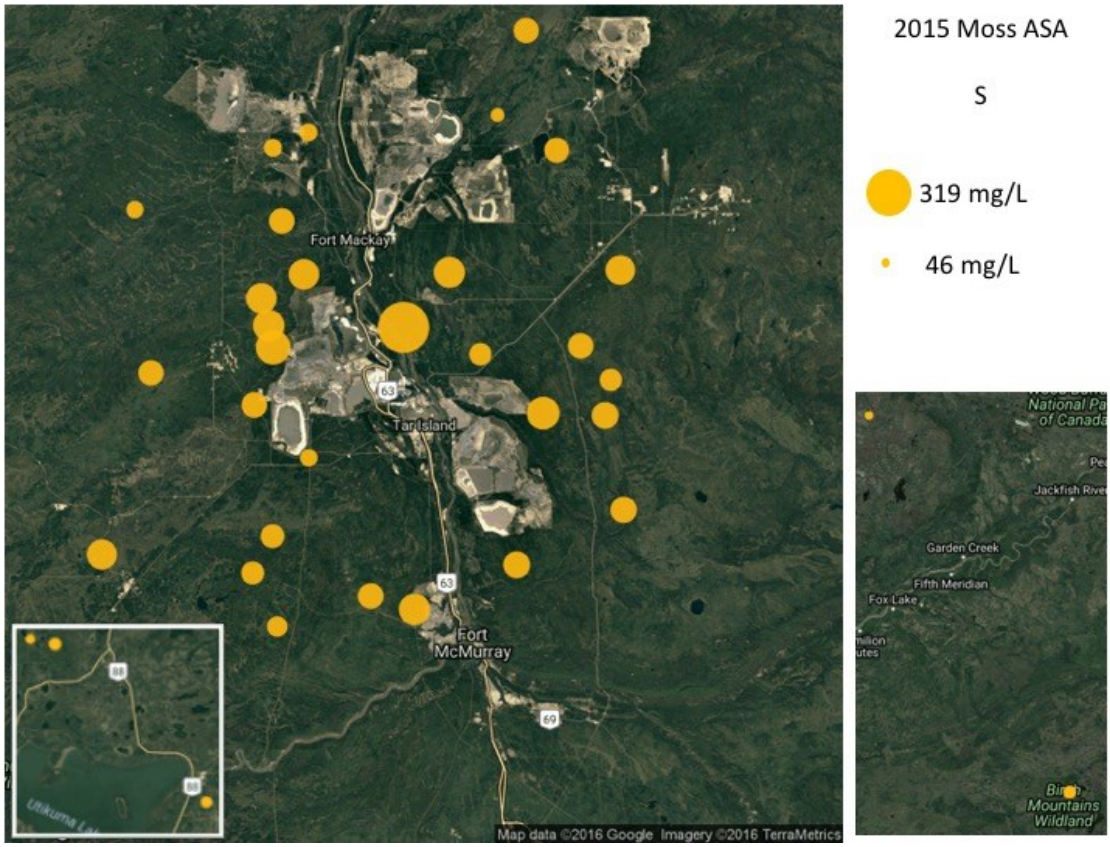
2015 Moss ASA
S
319 mg/L
46 mg/L
Fort Mackay
Tar Island
Fort McMurray
Map data ©2016 Google Imagery ©2016 TerraMetrics
Garden Creek
Fifth Meridian
Fox Lake
Jackfish River
Birch Mountains Wildland

Figure S8: Percent volume particle size distributions at a) 6 proximal sites (<16 km) and b) 5 distal sites (>19 km). The farthest sites (Figure S8b) display relatively uniform particle size distributions typical of atmospheric aerosols [34,41], with peaks at 7µm that decreases below 5% volume at 20µm and remains there until about 70µm where a handful of larger particles are represented in some peaks (larger volume per particle). On the other hand, in Figure S8a, the distributions display high variability but generally do not level out below 5% volume until 45µm. See Appendix S3 for calculations of percent volume.

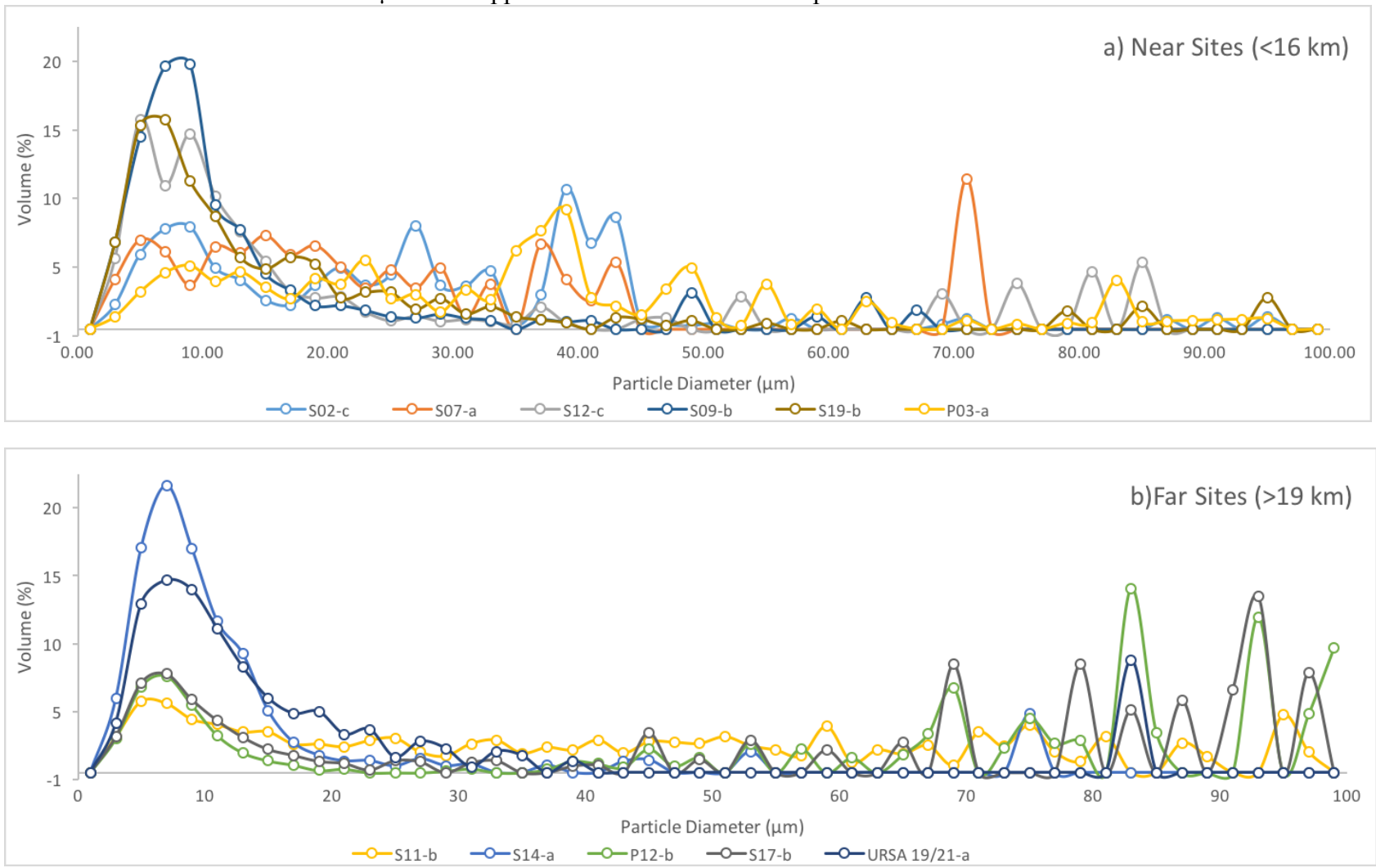

Supporting Information Tables

Table S1: Complete list of moss species in 2015 samples. All moss samples are of the genus *Sphagnum.*

Sample	Species	Sample	Species
BMW-a	Fuscum	P 11-a	Fuscum
BMW-b	Fuscum	P 11-b	Magellanicum & Angustifolium
BMW-c	Fuscum	P 11-c	Warnstorfii
CMW-a	Fuscum	P 12-a	Fuscum
CMW-b	Fuscum	P 12-b	Fuscum
CMW-c	Fuscum	P 12-c	Fuscum
EINP-a	Fuscum	P 17-a	Fuscum
EINP-b	Fuscum	P 17-b	Fuscum
EINP-c	Fuscum	P 17-c	Fuscum
WAG-a	Fuscum	S 01-a	Fuscum
WAG-b	Fuscum	S 01-b	Fuscum
WAG-c	Fuscum	S 01-c	Fuscum
URSA 19/21-a	Fuscum	S 02-a	Fuscum
URSA 19/21-b	Fuscum	S 02-b	Fuscum
URSA 19/21-c	Fuscum	S 02-c	Fuscum
URSA 19/21-d	Fuscum	S 03-a	Fuscum
URSA 19/21-e	Fuscum	S 03-b	Fuscum
URSA 19/21-f	Fuscum	S 03-c	Fuscum
URSA 19/21-g	Fuscum	S 04-a	Fuscum
URSA 19/21-h	Fuscum	S 04-b	Fuscum
URSA 19/21-i	Fuscum	S 04-c	Fuscum
URSA 19/21-j	Fuscum	S 05-a	Capillifolium
URSA 300-a	Fuscum	S 05-b	Fuscum
URSA 300-b	Fuscum	S 05-c	Fuscum
URSA 300-c	Fuscum	S 06-a	Fuscum
URSA 300-d	Fuscum	S 06-b	Fuscum
URSA 300-e	Fuscum	S 06-c	Fuscum
URSA 300-f	Fuscum	S 07-a	Fuscum
URSA 300-g	Fuscum	S 07-b	Fuscum
URSA 300-h	Fuscum	S 07-c	Fuscum
URSA 300-i	Fuscum	S 09-a	Fuscum
URSA 300-j	Fuscum	S 09-b	Capillifolium
URSA 524-a	Fuscum	S 09-c	Fuscum
URSA 524-b	Fuscum	S 10-a	Fuscum

URSA 524-c	Fuscum	S 10-b	Fuscum
URSA 524-d	Fuscum	S 10-c	Fuscum
URSA 524-e	Fuscum	S 11-a	Fuscum
URSA 524-f	Fuscum	S 11-b	Fuscum
URSA 524-g	Fuscum	S 11-c	Warnstorfii
URSA 524-h	Fuscum	S 12-a	Fuscum
URSA 524-i	Fuscum	S 12-b	Capillifolium
URSA 524-j	Fuscum	S 12-c	Fuscum
P 01-a	Fuscum	S 13-a	Fuscum
P 01-b	Fuscum	S 13-b	Fuscum
P 01-c	Fuscum	S 13-c	Fuscum
P 03-a	Fuscum	S 14-a	Fuscum
P 03-b	Fuscum	S 14-b	Fuscum
P 03-c	Fuscum	S 14-c	Teres
P 04-a	Fuscum	S 15-a	Fuscum
P 04-b	Fuscum	S 15-b	Fuscum
P 04-c	Capillifolium	S 15-c	Fuscum
P 05-a	Fuscum	S 16-a	Warnstorfii
P 05-b	Fuscum	S 16-b	Magellanicum
P 05-c	Fuscum	S 16-c	Fuscum
P 06-a	Russowii	S 17-a	Fuscum
P 06-b	Warnstorfii	S 17-b	Fuscum
P 06-c	Warnstorfii	S 17-c	Fuscum
P 08-a	Fuscum	S 18-a	Fuscum
P 08-b	Fuscum	S 18-b	Fuscum
P 08-c	Fuscum	S 18-c	Fuscum
P 09-a	Fuscum	S 19-a	Fuscum
P 09-b	Fuscum	S 19-b	Fuscum
P 09-c	Fuscum	S 19-c	Fuscum
P 10-a	Fuscum	S 20-a	Fuscum
P 10-b	Fuscum	S 20-b	Fuscum
P 10-c	Fuscum	S 20-c	Fuscum

Table S2: List of GPS coordinates of the 2015 moss locations and distances to nearest road. Effects of road dust are limited to 100 m [14]. All sites are sufficiently removed from roads (at least 100 m), such that road dust should not be a major contributor to dust input.

Site Name	Latitude	Longitude	Distance from Nearest Road (km)
P 01	57.14609	-111.73227	2.6
P 03	57.08775	-111.80556	4.1
P 04	57.06323	-111.79662	1.9
P 05	57.20668	-111.77855	1.5
P 06	57.30690	-111.72284	0.1
P 08	57.42187	-111.26675	6.4
P 09	57.28675	-111.20317	3.6
P 10	57.06467	-111.15269	2.3
P 11	57.05528	-111.36288	1.2
P 12	57.02599	-111.08999	5.1
P 17	56.77908	-111.59211	2.3
S 01	57.11879	-111.82107	5.1
S 02	57.28937	-111.79685	0.4
S 03	57.03401	-112.05236	7.8
S 04	56.82660	-112.15509	5.4
S 05	56.80544	-111.83947	1.7
S 06	57.21935	-112.08611	10.2
S 07	57.32645	-111.32666	4.8
S 09	57.14824	-111.42753	3.8
S 10	56.81480	-111.28670	4.0
S 11	56.84755	-111.79790	4.0
S 12	56.93714	-111.72176	0.9
S 13	56.99745	-111.83602	2.0
S 14	56.74397	-111.78785	4.7
S 15	56.76378	-111.50061	0.8
S 16	56.87767	-111.06291	3.8
S 17	56.98812	-111.23141	4.4
S 18	56.98551	-111.10171	3.6
S 19	57.08565	-111.52352	4.1
S 20	57.15089	-111.06978	0.1
BMW	57.56691	-112.91694	59.3
CMW	59.38345	-114.75002	88.8
URSA1921	56.08208	-115.53153	0.3
URSA300	55.87600	-115.13053	0.3
URSA524	56.07581	-115.47492	5.3

EINP	53.614444	-112.86611	0.1
WAG	53.56641	-113.827972	0.5

Table S3: ICP-OES major ion analysis results and QA/QC for ASA sample from all 30 ABS region sites plus the 3 URSA sites, BMW, and CMW.

		Ca 317.933	Cu 324.754	Fe 259.940	K 766.490	Mg 279.079	Mn 257.610	Na 589.592	Zn 213.856	P	S
sample ID	Lab ID	mg/L	mg/L	mg/L	mg/L	mg/L	mg/L	mg/L	mg/L	mg/L	mg/L
BMW	1	262.7	0.194	18.0	942.9	123.2	35.035	59.361	2.139	114.9	80.144
CMW	2	368.7	0.212	7.0	530.7	156.9	36.130	18.870	1.761	120.0	46.939
URSA1921	3	226.9	0.244	21.3	919.3	76.9	19.993	14.707	1.717	103.2	53.194
URSA300	4	246.7	0.288	17.5	1033.4	115.0	32.454	9.012	2.571	132.6	67.421
URSA524	5	428.1	0.324	18.3	978.2	162.4	28.158	9.000	3.685	144.0	75.47
S01	6	711.0	0.458	112.2	1084.7	272.4	53.645	31.685	4.240	122.4	184.8
S02	7	315.2	0.046	105.8	559.8	99.4	17.743	26.019	1.436	49.1	103.3
S03	8	592.0	0.321	63.1	935.8	173.0	43.585	25.739	3.057	173.9	151.4
S04	9	928.8	0.248	153.9	1132.9	320.6	46.891	32.571	3.051	164.2	182.7
S05	10	460.5	0.212	42.8	1116.5	201.3	38.218	16.774	3.097	142.0	136.9
S06	11	253.8	0.276	74.9	953.5	92.7	26.412	23.554	1.891	83.5	97.9
S07	12	329.1	0.246	71.0	332.3	73.2	18.706	13.475	1.088	45.7	75.2
S09	13	680.8	0.149	125.5	944.8	225.5	33.607	38.285	2.452	103.0	188.3
S10	14	541.6	0.151	134.7	917.4	148.0	35.180	52.265	2.425	93.4	161.9
S11	15	431.3	0.204	66.4	1182.9	187.9	39.076	28.162	2.587	139.6	141.6
S12	16	473.8	0.066	111.7	300.0	121.8	21.381	14.419	2.174	60.8	99.4
S13	17	463.1	0.256	120.0	1169.4	239.0	34.256	36.640	3.048	136.3	154.2
S14	18	367.3	0.163	62.6	1035.5	100.6	32.097	22.243	2.501	115.7	120.0
S15	19	627.8	0.310	105.8	1071.5	171.1	39.472	31.195	3.273	122.6	190.4
S16	20	752.6	0.226	68.8	1551.1	338.8	58.448	25.923	3.961	336.6	158.7
S17	21	884.7	0.358	164.4	969.0	230.3	34.276	46.903	3.190	119.5	199.8
S18	22	421.0	0.274	88.5	1036.9	136.9	26.091	28.598	2.139	98.7	161.3

S19	23	1228.6	0.590	116.0	2373.1	367.3	48.969	50.247	5.471	333.1	319.0
S20	24	786.0	0.280	51.6	1643.3	232.6	49.999	23.830	4.347	242.5	178.6
P01	25	566.1	0.649	186.1	1081.3	191.9	43.895	46.442	3.065	92.6	184.5
P03	26	619.0	0.302	187.2	818.4	204.7	37.650	210.374	3.366	94.8	192.0
P04	27	574.1	0.224	209.4	857.2	226.2	29.371	184.964	2.984	92.5	212.4
P05	28	427.6	0.342	85.8	1182.4	170.2	37.690	33.887	3.355	147.5	153.5
P06	29	735.9	0.026	73.3	283.2	182.6	23.214	18.852	1.410	75.6	103.0
P08	30	530.1	0.163	108.2	785.0	126.0	33.666	25.949	2.274	87.1	150.9
P09	31	540.3	0.488	87.3	1034.4	126.5	27.767	20.611	1.988	89.7	149.1
P10	32	502.0	0.389	91.3	1041.2	130.3	27.439	39.671	3.034	102.1	152.1
P11	33	499.4	0.241	171.5	734.9	109.1	12.548	33.553	2.016	74.1	133.2
P12	34	327.5	0.413	81.2	877.8	92.5	25.798	30.926	1.594	88.2	131.0
P17	35	550.7	0.551	62.0	1461.3	170.3	34.392	19.843	3.498	132.3	152.8

		Ca	Cu	Fe	K	Mg	Mn	Na	Zn	P	S
sample ID	Lab ID	mg/L	mg/L	mg/L	mg/L	mg/L	mg/L	mg/L	mg/L	mg/L	mg/L
	qc	0.2	0.203	0.2	1.0	0.2	0.201	0.210	0.202	1.003	1.015
	qc	0.2	0.207	0.2	1.0	0.2	0.205	0.213	0.204	0.993	1.011
	qc	0.2	0.203	0.2	1.0	0.2	0.201	0.210	0.203	0.999	1.021
	qc	0.2	0.205	0.2	1.0	0.2	0.203	0.214	0.203	1.007	1.024
	Qc expected	0.2	0.2	0.2	1.0	0.2	0.2	0.2	0.2	1.0	1.0
	detection limit	0.0	0.007	0.0	0.0	0.0	0.001	0.002	0.001	0.02	0.03

Table S4: 2015 moss sample ash and AIA content values, confidence intervals, and ranges

Site Name	Ash Content	Confidence Interval Ash	AIA Content	Confidence Interval AIA	Ash Range	AIA Range
	%	%	%	%	%	%
BMW	1.69	0.31	0.16	0.23	1.56-1.82 (0.26)	0.10-0.27 (0.17)
CMW	1.19	0.34	0.33	0.06	1.12-1.37 (0.25)	0.30-0.04 (0.09)
EINP	2.91	0.95	0.83	1.23	2.59-3.33 (0.74)	0.36-1.39 (1.03)
WAG	3.79	0.42	0.92	0.53	3.64-3.96 (0.32)	0.70-1.08 (0.38)
URSA	1.95	0.11	0.29	0.07	1.59-3.06 (1.47)	0-0.056 (0.056)
P 01	6.10	1.94	2.18	2.98	5.43-6.96 (1.53)	1.24-3.63 (2.40)
P 03	5.50	2.35	1.93	2.52	4.42-6.15 (1.74)	0.76-2.75 (1.99)
P 04	5.06	1.12	1.93	0.92	4.73-557 (0.84)	1.51-2.25 (0.74)
P 05	3.65	1.26	0.60	0.83	2.89-4.08 (1.18)	0.66-0.83 (0.17)
P 06	8.28	2.21	2.27	0.83	6.96-8.99 (2.02)	1.91-2.62 (0.71)
P 08	4.09	0.20	1.02	0.84	4.00-4.16 (0.16)	0.72-1.40 (0.69)
P 09	3.45	0.19	1.09	0.66	3.36-3.51 (0.15)	0.75-1.27 (0.52)
P 10	3.55	1.09	0.95	1.14	3.23-4.05 (0.82)	0.50-1.43 (0.93)
P 11	8.31	3.48	3.03	1.57	6.78-9.53 (2.74)	2.60-3.70 (1.10)
P 12	2.94	0.19	0.78	1.33	2.87-3.02 (0.16)	0.30-1.36 (1.06)
P 17	3.53	1.54	0.88	1.52	3.01-4.21 (1.21)	0.48-1.61 (1.13)
S 01	3.69	1.86	1.05	0.79	2.89-4.38 (1.48)	0.71-1.30 (0.59)
S 02	7.74	4.06	3.11	2.42	6.11-9.38 (3.27)	2.37-4.29 (1.92)
S 03	3.01	0.50	0.93	1.25	2.80-319 (0.40)	0.39-1.40 (1.01)
S 04	4.74	1.12	1.65	0.78	4.25-5.14 (0.89)	1.30-1.95 (0.65)
S 05	2.39	0.52	0.70	0.61	2.20-2.62 (0.42)	0.48-0.99 (0.50)
S 06	3.16	1.78	1.08	0.81	2.56-3.95 (1.39)	0.75-1.45 (0.70)
S 07	10.13	10.75	4.43	4.94	7.26-15.11 (7.85)	2.98-6.91 (3.92)
S 09	6.28	4.54	2.35	2.90	4.25-7.79 (3.55)	1.25-3.65 (2.40)
S 10	4.05	1.56	1.17	0.61	3.38-4.62 (1.24)	0.89-1.40 (0.52)
S 11	3.06	0.50	0.32	0.63	2.85-3.12 (0.27)	0.13-0.59 (0.46)
S 12	9.17	4.78	3.21	3.34	7.58-11.31 (3.73)	2.17-4.82 (2.65)
S 13	4.10	1.85	1.10	1.27	3.51-4.94 (1.43)	0.64-1.68 (1.04)
S 14	2.42	0.42	0.41	0.50	2.31-2.62 (0.31)	0.19-0.63 (0.43)
S 15	3.92	2.75	1.58	2.04	2.74-4.94 (2.20)	0.61-2.15 (1.54)
S 16	4.20	0.74	1.00	0.76	3.44-4.54 (1.10)	0.61-1.20 (0.59)
S 17	5.65	1.00	2.12	1.60	5.19-5.93 (0.74)	1.43-2.72 (1.29)
S 18	3.61	0.50	1.29	0.96	3.48-3.84 (0.36)	0.91-1.73 (0.82)
S 19	6.08	1.67	2.15	2.62	5.32-6.58 (1.27)	0.93-2.92 (1.99)
S 20	3.83	0.53	0.94	0.80	3.58-3.97 (0.38)	0.66-1.35 (0.68)

Table S5: 2015 moss sample ash and AIA mass accumulation rates, confidence intervals, and ranges

Site Name	Accumulation Rate (MAR) Ash	Accumulation Rate (MAR) AIA	Standard Deviation Ash	Confidence Interval Ash	Standard Deviation AIA	Confidence Interval AIA
	g/m^2 yr	g/m^2 yr		g/m^2 yr		g/m^2 yr
P 01	14.29	5.27	4.87	12.10	4.07	10.10
P 03	15.20	5.36	5.40	13.41	3.27	8.13
P 04	13.37	4.87	2.37	5.89	0.55	1.36
P 05	6.28	1.10	2.20	5.47	0.43	1.06
P 06	16.41	4.33	6.09	15.14	1.58	3.92
P 08	11.88	2.76	0.72	1.79	0.77	1.91
P 09	6.54	2.01	0.98	2.42	0.72	1.80
P 10	7.51	2.00	2.56	6.35	1.36	3.38
P 11	22.25	7.59	7.57	18.80	1.28	3.18
P 12	8.42	1.98	0.68	1.68	1.30	3.22
P 17	7.31	1.73	1.77	4.40	1.31	3.26
S 01	5.93	1.75	2.45	6.09	1.00	2.49
S 02	17.23	6.96	4.68	11.62	2.66	6.62
S 03	5.25	1.74	1.50	3.74	1.22	3.04
S 04	9.72	3.40	2.19	5.43	0.99	2.47
S 05	5.34	1.52	0.69	1.71	0.35	0.87
S 06	10.01	3.42	3.31	8.21	1.33	3.31
S 07	27.28	11.87	19.01	47.22	8.53	21.20
S 09	15.46	5.78	7.95	19.76	4.01	9.96
S 10	7.36	1.97	1.93	4.80	0.11	0.28
S 11	4.75	0.42	0.64	1.59	0.39	0.96
S 12	25.22	8.38	2.13	5.28	2.54	6.31
S 13	9.76	2.59	3.98	9.89	1.70	4.23
S 14	6.02	0.95	1.08	2.68	0.68	1.70
S 15	8.60	3.42	4.33	10.76	2.23	5.53
S 16	4.96	1.22	2.08	5.16	0.65	1.61
S 17	10.58	3.79	0.74	1.84	0.74	1.84
S 18	7.74	2.69	0.97	2.42	1.01	2.51
S 19	7.70	3.15	3.97	9.87	2.38	5.91
S 20	7.10	1.81	2.36	5.87	1.21	2.99
BMW	6.27	0.58	1.28	3.18	0.29	0.73
CMW	4.51	1.16	1.32	3.28	0.15	0.37
URSA1921	3.85	0.60	2.04	5.07	0.37	0.93

URSA300	3.43	0.58	2.29	5.69	0.28	0.69
URSA524	3.69	0.40	2.31	5.74	0.32	0.79

Site Name	MAX Ash MAR	MIN Ash MAR	Range Ash MAR	MAX AIA MAR	MIN AIA MAR	Range AIA MAR
	%	%	%	%	%	%
P 01	19.83	10.69	9.15	9.92	2.36	7.56
P 03	20.29	9.54	10.75	7.43	1.58	5.84
P 04	15.28	10.71	4.57	5.50	4.53	0.97
P 05	8.64	4.29	4.35	1.44	0.62	0.81
P 06	20.99	9.49	11.50	5.25	2.51	2.74
P 08	12.67	11.24	1.42	3.62	2.12	1.49
P 09	7.63	5.73	1.89	2.62	1.21	1.41
P 10	9.97	4.86	5.11	3.44	0.74	2.70
P 11	30.96	17.30	13.66	9.04	6.63	2.41
P 12	9.16	7.83	1.33	3.42	0.91	2.51
P 17	8.88	5.39	3.49	3.24	0.88	2.36
S 01	8.66	3.91	4.74	2.87	0.93	1.94
S 02	22.38	13.24	9.14	9.97	4.92	5.06
S 03	6.98	4.30	2.68	2.98	0.54	2.45
S 04	11.74	7.40	4.34	4.01	2.25	1.76
S 05	5.85	4.55	1.30	1.77	1.12	0.65
S 06	13.78	7.60	6.18	4.83	2.18	2.65
S 07	48.94	13.40	35.54	21.51	5.27	16.23
S 09	22.18	6.68	15.50	9.91	1.91	8.00
S 10	9.21	5.35	3.86	2.10	1.89	0.22
S 11	5.41	4.13	1.28	0.86	0.16	0.70
S 12	27.64	23.65	3.99	11.30	6.66	4.64
S 13	13.35	5.48	7.87	4.37	0.97	3.40
S 14	6.85	4.80	2.05	1.72	0.44	1.28
S 15	13.23	4.65	8.58	5.35	0.98	4.37
S 16	6.93	2.79	4.14	1.70	0.48	1.22
S 17	11.36	9.88	1.48	4.42	2.97	1.45
S 18	8.86	7.12	1.74	3.74	1.73	2.01
S 19	11.62	3.68	7.95	5.08	0.49	4.58
S 20	8.83	4.41	4.42	3.09	0.71	2.39
BMW	7.73	5.33	2.40	0.89	0.32	0.58
CMW	5.38	3.48	1.90	1.33	1.04	0.29

URSA1921	5.85	2.09	3.76	1.30	0.00	1.30
URSA300	4.45	2.68	1.76	0.97	0.17	0.80
URSA524	5.03	2.03	3.00	1.10	0.00	1.10

Table S6: List of ash and AIA values from studies outside Alberta using *Sphagnum* moss

Publication	Location	Ash content (%)
Damman, et al. (1992)	Finland	1.5-20
Gorham & Tilton, (1978)	Minnesota, USA	1.6-5.5
Santelmann & Gorham (1988)	New Brunswick	1.7-3.0
Gorham (1961)	England	3.2
Shotyk (1996)	Switzerland	1.5-2.5
Vuorela (1983)	Finland	1-4.2

Damman, A. W. H.; Tolonen, K.; Sallantaus, T. Element retention and removal in ombrotrophic peat of Haadetkeidas, a boreal Finnish peat bog. *Suo* **1992**, *43* (4–5), 137–145.

Gorham, E. Water, ash, nitrogen and acidity of some bog peats and other organic soils. *J. Ecol.* **1961**, *49*, 103–106.

Gorham, E.; Tilton, D. L. The mineral content of Sphagnum fuscum as affected by human settlement. *Can. J. Bot.* **1978**, *56* (180), 2755–2759.

Santelmann, M. V; Gorham, E. The influence of airborne road dust on the chemistry of Sphagnum mosses. *J. Ecol.* **1988**, *76* (4), 1219–1231.

Shotyk, W. Natural and anthropogenic enrichments of As, Cu, Pb, Sb, and Zn in ombrotrophic versus minerotrophic peat bog profiles, Jura Mountains, Switzerland. *Water. Air. Soil Pollut.* **1996**, *90*, 375–405.

Vuorela, I. Field erosion by wind as indicated by fluctuations in the ash content of Sphagnum peat. *Bull. Geol. Soc. Finl.* **1983**, *55* (1978), 25–33.

Supporting Information Appendices

Appendix S1: NRAL notes on ICP-OES major ion analysis results and QA/QC for ASA sample from all 30 ABS region sites plus the 3 URSA sites, BMW, and CMW.

Repeat analyses of unknown samples are performed on approximately 10% of submitted samples. 5 % RPD (relative percent difference) between analysis repeats is normally considered the maximum acceptable tolerance.

Continuous Calibration Verification (CCV) checks are performed every 10 samples using a NIST-traceable standard reference solution to ensure calibration accuracy. 95-105 % recovery of the certified value is considered the maximum acceptable tolerance. Data reported in "RESULTS" tabs has passed QA/QC checks. QC values and recoveries are shown in raw data tabs.

An internal standard solution (Yttrium) is used to correct for matrix effects in samples. Final analyte values are reported after this correction factor has been applied.

For sample digests, an external reference material QC check is also performed periodically (at least once per data set).

Appendix S2: Calculating the mineral Mass Accumulation Rates (MAR) for moss samples

1. Calculation of water content

The total weight of the living layer was measured, $m_{LL,}$ before a smaller portion of the living layer was separated, weighed to give m_w, and then dried at 105^{O}C for 36 hours. The dried material was weighed (m_d). Using Equation 1 the water content, WC, was calculated.

$$\left(1 - \frac{m_d}{m_w}\right) * 100 \qquad (1)$$

2. Calculation of dry matter accumulation rate

Accumulation rate (AR) is calculated by Equation 2:

$$\frac{m}{A \cdot t} \qquad (2)$$

Where: m=mass of sample (g)

A= area of collection (m^2)

t= time of growth (y)

The area of collection of the whole living layer is known, however not the entire living layer was dried. To account for this, the dried sample, m_{dry}, must be related to the whole living layer mass, m_{LL}, using a conversion factor. The conversion factor, CF, can be calculated using Equation 3.

$$CF = \frac{m_{dry}}{(1-WC)} \Big/ m_{LL} \qquad (3)$$

The conversion factor illustrates the percentage of living layer mass, and therefore what percentage of the area collected, was used to yield m_{dry}. Therefore, the new equation for accumulation rate becomes:

$$AR = \frac{m_{dry}}{CF \cdot A \cdot t} \qquad (4)$$

The conversion factor, CF, in Equation 4 allows for the correct amount of area to be accounted for in the calculation.

3. Calculation of ash content

The dried sample mass, m_{dry}, was then ashed at 550^{o}C for 16 hours. The material remaining after ashing was then weighed (m_{ash}). Using Equation 5 ash content was found.

$$Ash\ content\ (\%) = \left(\frac{m_{ash}}{m_{dry}}\right) * 100 \qquad (5)$$

4. Calculation of ash accumulation rate

Ash accumulation rate was calculated using Equation 6:

$$Ash\ AR = \frac{m_{ash}}{CF \cdot A \cdot t} \qquad (6)$$

5. Calculation of AIA content

The ashed sample mass, m_{ash}, was then soaked in HCl for 15 mins and vacuum filtered. The material remaining on the filter was then weighed (m_{AIA}). Using Equation 7 AIA content was found.

$$AIA\ (\%) = \left(\frac{m_{AIA}}{m_{ash}}\right) * 100 \qquad (7)$$

4. Calculation of AIA accumulation rate

AIA accumulation rate was calculated using Equation 8:

$$AIA\ AR = \frac{m_{AIA}}{CF \cdot A \cdot t} \qquad (8)$$

Appendix S3: Calculating the percent volume of particle size distributions

1. Calculation of average particle volume

Particle sizes were separated into bins upon measurement, each 2µm wide (i.e. 0-2µm, 2-4µm, etc.). Average diameters (d_p) were used for each bin in these calculations (i.e. for the bin 0-2µm a diameter of 1µm was used). An average volume per bin (V_p) was calculated assuming all particles were spherical, using Equation 1.

$$V_p = \frac{4}{3}\pi\left(\frac{(d_p)}{2}\right)^3 \quad (1)$$

2. Calculation of the volume of the total number of particles in each particle size bin (V) was calculated by Equation 2, multiplying the average volume per bin (V_p) and the number of particles (x_p) measured:

$$V = V_p \times x_p \quad (2)$$

3. Calculation of percent volume

The total volume (V_t) of all particles measured was calculated with Equation 3.

$$V_t = \sum_{i=1}^{n} V_{pi} \times x_{pi} \quad (3)$$

Then the percent volume was calculated using Equation 4:

$$Volume\ (\%) = \left(\frac{V}{V_t}\right) * 100 \quad (4)$$

CHAPTER 3: RECONSTRUCTING PAST RATES OF ATMOSPHERIC DUST DEPOSITION IN THE ATHABASCA BITUMINOUS SANDS REGION USING PEAT CORES

A version of this manuscript has been submitted to the journal *Land Degradation and Development* for publication.

ABSTRACT

Open pit mining of the Athabasca Bituminous Sands (ABS) generates considerable quantities of mineral dusts, but there is no published record of the amount of material deposited in the surrounding environment via the atmosphere since industry began in 1967. Contemporary as well as past rates of atmospheric dust deposition were reconstructed using ^{210}Pb and ^{14}C age-dated peat cores collected from five bogs in the vicinity of mines and upgraders (MIL, JPH4, McK, McM, ANZ) and from two bogs far removed from industrial activities (UTK and SEB). The main objective was to quantify the impact of industry on dust emissions and to do this, the variation in natural "background" rates of mineral matter accumulation also had to be determined. A second goal was to characterize the size, mineralogical composition, and morphology of the particulate matter emitted, to better understand potential environmental consequences of dust emissions.

The concentrations of acid insoluble ash (AIA) and Th (mineral matter surrogate) were determined to calculate dust accumulation rates. Scanning electron microscopy with energy dispersive x-ray analysis failed to reveal much variation in mineralogical composition, but near industry there was an increase in size variation of the particles and fly ash increased in abundance with depth. The average accumulation rates of AIA are up to 5x greater in the cores collected near industry. A comparison of AIA inventories with the pH of the porewaters suggest that the acid-soluble ash (ASA) fraction of the dusts deposited may impact the chemical composition of the bog waters.

Keywords: (max 5) AIA, ash content, peat cores, Athabasca bituminous sands region, ombrotrophic bogs

INTRODUCTION

The environment in northern Alberta has been impacted by human activities since the late 1800s when immigration from Europe first started to occur. In the first decade of the 20th century over 59000 km^2 of forest was converted to agricultural lands, injecting large amounts of soil particles into the atmosphere and drastically changing the composition of dust in the region (Agriculture Division of Statistics Canada, 2014). After introducing agriculture, the largest change to the environment in northern Alberta has been the opening of the Athabasca Bituminous Sands (ABS) mines and upgraders. Operation first began in 1967 when the Great Canadian Oil Sands, now Suncor, opened for commercial development. This was followed by the opening of Syncrude's operations in 1978. The ABS is currently the third largest source of accessible oil in the world, producing 165000 m^3/day of bitumen from open pit mining (Alberta Energy Regulator, 2015; Stringham, 2012). It is estimated that the ABS region produced 18842 tonnes of total particle matter in 2015 (Environment and Climate Change Canada, 2015). Once airborne, dust is deposited on the surrounding area with transport time and distance depending on such factors as dust composition, particle size, density, and height at the point of injection (Jacobson, 2002; Muhs *et al.*, 2014). Elevated emissions of mineral dusts can lead to adverse health effects, reduce visibility, and may impact vegetation growth in the vicinity of deposition (Watson *et al.*, 2014).

Sphagnum dominated peat cores are very effective biomonitors and can be used to reconstruct past atmospheric dust deposition (Krachler & Shotyk, 2004; Le Roux *et al.*, 2006, 2012; Sapkota *et al.*, 2007; Zaccone *et al.*, 2012, 2013). For a peat core to serve as a record of dust deposition, it must be ombrotrophic (water and nutrients gained only from atmosphere), the relevant biogeochemical processes of the area have to be considered (such as mineral dissolution

in acidic bog waters) and the particles must be immobile in the peat column (Krachler & Shotyk, 2004). Mineral matter, has already been shown to be immobile in peat profiles (Chapman, 1964). While the acid-soluble ash (ASA) fraction will certainly dissolve in acid bog waters (Le Roux *et al.*, 2006), the acid-insoluble ash (AIA) fraction will not (Sapkota, 2006; Steinmann & Shotyk, 1997).

To use a peat core as an archive of atmospheric deposition, its trophic status or peat development must first be determined to be ombrotrophic or ombrogenic (rain-fed) (Kempter & Frenzel, 2000; Shotyk *et al.*, 1997). Ombrotrophic peat receives mineral matter exclusively from the atmosphere (Bargagli, 1998; Damman, 1978; Shotyk, 1996). Unlike, minerotrophic peat which also receives mineral matter from surface and groundwaters (Shotyk, 1988). There are several ways to differentiate between ombrotrophic and minerotrophic peat, the simplest being the pH of surface water (Gore, 1983a). Ombrotrophic peat is characteristically acidic (pH 3.5-4.5) due to its limited access to alkaline surface and groundwaters (Pearsall, 1952) and acidification by *Sphagnum* moss. Minerotrophic peat is less acid (pH 5-7) and mineral-rich, particularly in Ca (Bragazza & Gerdol, 1999; Gore, 1983b). Since ombrotrophic peat is deficient in mineral nutrients, the electrical conductivity (EC) is lower than other peatlands (Gore, 1983b). Here, pH and EC the of each core was measured to distinguish ombrotrophic from minerotrophic peat layers.

The ash content of peat is derived from the combustion of the organic matter of a sample, leaving only the residue (Andrejko *et al.*, 1983). As noted above, ash can be divided further into its acid soluble ash (ASA) and acid insoluble ash (AIA) fractions. ASA is composed of mineral artifacts (sulphates, carbonates, phosphates, and oxides) that were created during combustion from plant nutrients such as Ca, Mg, P, Fe, Mn, and S. In contrast, AIA contains the deposited

mineral particles such as silicates, aluminosilicates, and refractory oxides including quartz, zircons, and clays. Biological structures such as diatoms and testate amoebae, which are skeletons made up of amorphous silica are also found in the AIA fraction (Malmer, 1988).

AIA has been used frequently to measure the mineral particulate matter input in peat cores across Europe (Steinmann & Shotyk, 1997; Vile *et al.*, 1995; Vile *et al.*, 2000; Zaccone *et al.*, 2012; Zaccone *et al.*, 2013). There has been little work performed on dust deposition in North America (outside of Alberta) with only a few studies published: the influence of road dust examined in New Brunswick, Canada (Santelmann & Gorham, 1988), Alaska, USA (Walker & Everett, 1987), and minerology of AIA in Minnesota (Finney & Farnham, 1968).

There have been some studies in northern Alberta that address dust deposition, including: $PM_{2.5}$ and PM_{10} source profiles were characterized in the ABS region (Wang *et al.*, 2015 ; Wang *et al*., 2015), atmospheric emissions assessments (Gosselin *et al.*, 2010; Shelfentook, 1978; Watson *et al.*, 2010), deposition of atmospheric pollutants using lichen (Addison & Puckett, 1980), air quality modelling (Percy & Davies, 2012), and Th peat profiles used as an indicator of mineral particles (Shotyk *et al.*, 2016). The Wood Buffalo Environmental Association (WBEA), the monitoring program that tracks atmospheric emissions in the ABS region, presently measures particulate deposition exclusively in the $PM_{2.5}$ and PM_{10} ranges. The air quality monitoring program began in 1998, which limits the depth of knowledge of past emissions to the last 18 years (Percy, 2013; Watson *et al.*, 2014). In consequence, there is a lack of information about bulk dust deposition, and no published records of long-term changes over time. In Alberta there are no published peat core profiles of AIA available to determine dust deposition for comparison with the data in this paper.

Objectives

The main of objective of this study was to quantify the rates of dust deposition and how they may have changed in response to bitumen mining and upgrading. To do this, peat cores from ombrotrophic bogs were used to compare 1) spatial variations in contemporary rates of dust deposition (obtained from the surface layer of each peat core), 2) rates of dust deposition since 1967 when the mines first opened (using the peat layers which have accumulated since this time), and 3) rates of dust deposition prior to 1967 (using peat from deeper, older layers). A secondary objective was to document changes, if any, in the particle size and mineralogical composition of dusts emitted from mining and upgrading activities. Finally, changes in dust deposition, expressed using both the ASA and AIA concentrations and fluxes, were compared with the pH value of the surface waters, to identify any environmental impacts these dusts may be having on naturally acidic ecosystems.

MATERIALS AND METHODS

Sample Collection

Peat cores were collected from 7 sites: 5 sites within the ABS region and 2 sites in other areas of Alberta to use for comparison. The 5 cores with the ABS region were collected at increasing distances from the reference point (the mid-point between the Syncrude and Suncor upgraders) to give insight into both spatial and temporal variation. The distance from the reference point to each peat core collected is respectively: MIL-W1 11.0km, JPH4-W1 12.0km, McK-W2 24.9km, McM-W3 48.7km, ANZ-W3 68.7km, UTK-W2 263.8km, and SEB-W1 447.0km (Figure 1). UTK is the control site, located 263.8km southwest of the reference point. Although the peat core collected in central Alberta (SEB-W1) is far from the ABS industry, it is only 21 km from Wabamum Transalta Sundance Coal-fired Generating Station. All peat cores were collected more than 100 m from the nearest road to prevent contamination from road dust (Walker &

Everett, 1987; Watson *et al.*, 2014). The GPS coordinates for each core, and the distance to the nearest road, is given in Table S1. See supporting information Methods S1, Figure S1, and Figure S2 for sample collection and preparation details.

Sample Analysis

The pH and EC (Methods S2) of the porewaters was used to determine the ombrotrophic zones of each peat core. Ash content (Methods S3) and AIA (Methods S4) were determined to allow the atmospheric dust deposition rates to be calculated. Scanning electron microscopy (SEM) and energy dispersive x-ray spectroscopy (EDX) was used to determine the mineralogy and morphology of the particles (Methods S5). A XenParTec (XPT-C) Optical Particle Analysis System was used to determine particle size distribution profiles for selected AIA samples (Methods S6). Peat samples were dated using ^{14}C and ^{210}Pb as described briefly in Methods S7 and in more detail elsewhere (Shotyk *et al.*, 2016).

Statistical Analysis

Due to the limited mass of each sample, most samples do not have replicates. To account for statistical variation in these samples, an average confidence interval was determined by calculating an average standard deviation of the mass ratios (mass of AIA/mass of dry peat) for the samples with sufficient material for replicates. The standard deviation was then used to calculate the average confidence interval at α=0.05.

RESULTS and DISCUSSION

Ombrotrophic Versus Minerotrophic Peat Layers

Six of the seven cores (JPH4-W1, McK-W2, McM-W3, ANZ-W3, UTK-W2, & SEB-W1) were found to be ombrotrophic throughout the entire core. The ombrotrophic zone at MIL-W1 is restricted to the top 18cm. As a consequence, ash data collected from depths below 18cm in the MIL-W1 core includes mineral matter from both atmospheric as well as non-atmospheric sources

(such as groundwater). However, while the ASA profile is clearly affected by the transition from ombrotrophic to minerotrophic peat (Figure 2), the AIA profile of MIL-W1 is not. Thus, the abundance of AIA in the uppermost part of the minerotrophic section of the core can still be used to quantify atmospheric deposition rates for the insoluble fraction of mineral dusts. The pH and EC values of peat accumulated after 1900 (Figure S3 & S4 respectively) and before 1900 (Figure S5 & S6 respectively) are provided in the Supporting Information. For more information on determining the ombrotrophic zones see Appendix S1.

UTK Control Site

The Utikuma region (UTK) is a well-established research study area in Alberta for environmental science (Devito *et al.*, 2016; Devito *et al.*, 2012; Petrone *et al.*, 2016). The region is isolated from the urban and industrial areas (300 km from Edmonton and 250 km from Fort McMurray) minimizing anthropogenic atmospheric contamination. As displayed in Figure 2, UTK-W2 has low ash (1-3%,) and AIA (0.2-1.39%) contents which are below the averages of 3.0% and 0.6% respectively calculated from previous studies (Damman *et al.*, 1992; Gorham & Tilton, 1978; Shotyk, 1988, 1996; Vuorela, 1983). In fact, UTK-W2 values are comparable to the values found in the ancient layers of the Swiss bog at Etang de la Gruère (EGR) (ash average: 3.0% and AIA average: 1.5%) (Steinmann & Shotyk, 1997). As a result, the UTK-W2 core provides background reference values to compare with all other sites.

Ash contents of ombrotrophic peat in Alberta

Ash is commonly used to study atmospheric deposition of mineral dusts in moss and peat. Shotyk (1988) summarized ash contents of *Sphagnum* peat from studies throughout Europe with a range of 0.6-5.5% and an average value of 3.2%. Ombrotrophic peat commonly has ash contents below 5%, with pristine peat estimated to have ~1% ash (Vuorela, 1983). In the peat layers formed since 1900 (Figure 3), five of the peat cores in the ABS region (McK-W2, McM-

W3, ANZ-W3, UTK-W2, and SEB-W3) yielded average ash contents within the common range given for ombrotrophic peat (Table S2). During the same time interval, the two peat cores nearest industry (MIL-W1 and JPH4-W1) have average values of 9.1% and 5.4% respectively. In general, the ash values range from 1% (at the control site UTK-W2:1983 and as well as at ANZ-W3:1973-1984) to 14% (in the ombrotrophic layers of MIL-W1: 2002). Some of the peaks in ash content (McK-W2: 1956, ANZ-W3:1962, and UTK-W2: 1960-1977) coincide with charcoal peaks that could be a result of local fires (Magnan *et al.*, 2017).

AIA contents of ombrotrophic peat in Alberta

The distribution of AIA in the peat cores follows trends similar to the ash content profiles (Figure 3), with values as low as 0.2% (UTK-W2: 2013, 2014 and ANZ-W3:1991, 2003, 2004) to values as high as 9.6% (MIL-W1:2002). As seen in the ash content data, peat samples since 1900 show similar average values for AIA except for MIL-W1 and JPH4-W1 which are elevated compared to the rest (Table S2). There is a notable difference between UTK-W2 (0.6%) and SEB-W1 (2.8%), which is most likely due to SEB's proximity to the Wabamum Transalta Sundance coal-fired Generating Station (Wabamum Station – Figure 1). For more information on ash and AIA values before 1900 see Figure S7.

Mass Accumulation Rates

To describe the changing dust fluxes, mass accumulation rates (MAR) were calculated for six of the seven peat cores. MAR, depicted in Figure 4, were calculated for ash content, AIA and ASA using peat accumulation rates and the ash, AIA and ASA contents. An overall average living layer peat accumulation rate (1084 g/m^2 yr) taken from the 6 peat cores (MIL-W1, JPH4-W1, McK-W2, McM-W3, ANZ-W3, and UTK-W2) and their 6 duplicate cores (not discussed in this paper) was used to calculate the living layer MAR of each peat core. The actual calculated

peat accumulate rate for each living layer is displayed in Table S3. The age date model for SEB is incomplete and therefore the MAR could not be accurately compared to the other peat cores.

MAR for ash, AIA and ASA are relatively consistent in all six peat cores since the ABS region opened in 1967, with a few exceptions (Figure 4). JPH4-W1 has a peak in ash and AIA with a jump from in 1979 to 1984 in ash content and AIA. ANZ-W3 and UTK-W2 have peaks in ash, AIA and ASA in 1962 and 1973-1977 respectively. Peaks in mineral matter accumulation rates can be caused by one of two situations: 1) the rate of dust deposition is constant over time but the rate of peat growth decreases or 2) the rate of dust deposition increases while the rate of peat growth stays consistent. These peaks in dust are most likely due to decreases in growth rate, not an increase in dust deposition rate since the age date in the samples below have a much longer gap than the rest of the samples in the profiles. For example, the ANZ-W3 layer below the peak in 1943 is a 19-year gap and below the peak in UTK-W2 there is an 18-year gap, whereas the next youngest layers in these cores there are only 4-5 year gaps. The average MAR are listed in Table 1 exclude these peaks to improve accuracy. The averages all fall within the range of AIA accumulation rates (0.4 g/m^2 yr to 8.4 g/m^2 yr) found in the literature (Damman *et al.*, 1992; Wieder *et al.*, 1994), except for MIL-W1 with an average of 16.2 ± 9.6 g/m^2 yr.

Although the peat cores show only slight differences in MARs throughout the cores, the living layers (i.e. first slice removed from the top of each peat core) show distinct differences. Specifically, the living layers show a decrease in the MAR with distance from industry (Figure 4). This finding is consistent with the 2015 *Sphagnum* moss data, presented in Mullan-Boudreau (2017a), for MAR obtained using ash, AIA and ASA. In the living layers of the peat cores, the MARs obtained from AIA values increased from 1.0±0.7 g/m^2 to 11.9 ± 21.2 g/m^2 yr over a

30km distance towards industry. For comparison, the AIA values for the UTK control site (labeled as URSA in Mullan-Boudreau (2017a)) yielded a MAR of 0.53± 0.12 g/m^2 yr.

Cumulative Dust Inputs

To gain a clearer picture of how the accumulation rates have changed since the opening of the ABS mines and upgraders, the cumulative mass of dust deposition since 1985 were calculated for ash, AIA and ASA (Figure 5a), as well as the cumulative mass of dust deposition from 1900-1960 for comparison (Figure 5b). The range of 1985-present was chosen to illustrate any changes since the beginning industrial activities, while still being able to include ash and ASA profiles of MIL-W1, which has only been ombrotrophic since 1985. Therefore, the ash and ASA profiles of MIL-W1 were not included in the Figure 5b (1900-1960).

Figure 5a shows a general decline in cumulative mass of dust deposition for ash, AIA and ASA with distance from industry. Comparing Figure 5a to 5b, there is a dramatic increase in the cumulative mass of dust deposited since 1985 versus 1900-1960 for MIL-W1 (AIA:162.1 g/m^2 versus 15.2 g/m^2), JPH4-W1(AIA: 55.9 g/m^2 versus 9.9 g/m^2) and McK-W2 (AIA: 95.4 g/m^2 versus 4.0 g/m^2). Smaller increases in McM-W3 (AIA: 30.1 g/m^2 versus 17.6 g/m^2), ANZ-W3 (AIA: 33.8 g/m^2 versus 19.7 g/m^2), and UTK-W2 (AIA: 22.3 g/m^2 versus 2.5 g/m^2) suggest there is additional dust loads for MIL-W1, JPH4-W1, and McK-W2 which can be attributed to the open pit mines and upgraders.

Accumulation rates are very useful tools to quantify changes in dust deposition; however, these results are dependent on the age dating models they are derived from. The age dating models used in this study are extremely robust, using ^{14}C, ^{210}Pb, humification, volcanic ash and macrofossils to fit the data (Shotyk *et al.*, 2016). Precision, however, varies with age: at 1900 the confidence intervals range from ±14-46 years between cores, whereas the modern layers range

from 1-2 years. These errors however are small compared to the changes in dust inputs, so the interpretation of dust fluxes having increased over time in the ABS region is well founded.

The effect of dust deposition on bog surface water pH and trophic status

The average pH values for the porewaters and average MAR of AIA since 1967 are compared in Figure 6. The average MAR of AIA decreases with distance from industry; however, pH shows a similar trend. As previously discussed, atmospheric dust is partially composed of ASA (sulphates, carbonates, phosphates, and oxides), which will dissolve in the acidic oligotrophic bog waters because of their low alkalinity and high H+ ion content. The high H+ ion content results from decomposition of organic matter that produces carbonic and organic acids (Shotyk, 1986a, 1986b, 1987, 1989). For example, carbonate minerals such as calcite would be rapidly dissolved, consuming H+ ions through Equation 1 and releasing Ca^{2+} cations into solution (Shotyk, 1989).

$$CaCO_3\ (s) + H_2CO_3\ (aq) \rightarrow Ca^{2+} + 2\ HCO_3^- \qquad (1)$$

An increase in deposition of ASA to the point that the dissolution of bases exceeds the rate of supply of carbonic and organic acids would increase cation concentrations and increase the pH in the bog waters (Shotyk, 1989).

Some of these cations are also important nutrients for plant growth (e.g. P, Ca, Mg, K). Increases in bog water pH could lead to increased competition for existing bog vegetation as they are best adapted to thrive in acidic oligotrophic environments (Chapman, 1964). These findings agree with a 2014 study that found elevated base cation deposition, primarily derived from dust, close to industry in the ABS region, which was counteracting the acidic effects of N and S deposition and had the potential to increase soil pH (Watmough *et al.*, 2014). Although the

average MAR of AIA over the last 30 years shows a decline with distance from industry, pH only slightly declines and stays within the normal pH range of bog surface water (Shotyk, 1988; Wieder *et al.*, 2010). Despite the increase in dust deposition closer to industry, there are only minor changes in pH, which suggests that the amount of dust deposited has yet to exceed the buffer capacity of bog surface water.

Thorium Accumulation Rates

To calculate the Thorium (Th) accumulation rates, Th values (mg/kg) where used from a comparison study (Shotyk *et al.*, 2016). Thorium has been used as an indicator of dust contamination because it is abundant in accessory minerals, such as zircons, that are known to be abundant in the ABS themselves. Moreover, these are stable minerals resistant to weathering (Goldich, 1938). Thorium in peat bogs is used as an immobile lithophile element (Krachler & Shotyk, 2004); therefore, it can be assumed that the host minerals are also immobile (Kamber *et al.*, 2005). The Th accumulation rate profiles are displayed in Figure 7a, along with their enrichment factor (EF) (Th concentration: AIA concentration in sample divided by the same ratio in the earth's crust) profiles in Figure 7b. The Th accumulation rate profiles resemble the MAR, ash, and AIA profiles, with corresponding peaks. The peaks at 1960 in McK-W2, ANZ-W3, and UTK-W2 also correspond with charcoal>1mm peaks (Magnan *et al.*, 2017) again indicating they are most likely the result of local burns (forest fires, peatland fires or both). Otherwise, the abundance of Th in these peat cores is consistent with the expected Th value of the Upper Continental Crust (Wedepohl, 1995), only a few sections of the peat cores with EF values above 1. In particular, McK-W2 has an elevated EF between 1874-1937 ranging from 5.12-6.50. For more information on the Th enrichment factors before 1900, see Figure S8.

Particle Size Distributions

Selected samples from each of the 7 peat cores were analyzed (Figure S9). The peat core from JPH4 was selected for a detailed analysis of particle size because of the abundance of AIA in these samples as well as the proximity of this site to industry.

Particle size distributions were measured for every odd layer and the living layer of JPH4-W1 for the period 1912-2013. The particle counts, for each layer analyzed and the percentage of particles in the different size classes ranging from 1μm to 100μm, are shown in Figure 8. The JPH4-W1 profile suggests that while larger particles >40μm are present, their relative abundance decreases over time, compared to the smaller (<10μm) particles. There appears to be elevated inputs of large particles in the sample dating from 1967 and as well as in the top layers. There are also inputs of relatively larger particles earlier in the 20th century that could be due to other land use activities such as agriculture or construction. The decrease in relative abundance of larger particles may indicate that the dusts generated by industry today are mainly composed of particles in the smaller size classes. However, more detailed interpretation is not possible, mainly due to the small quantities of sample that were available.

Morphology and Mineralogy

A select number of samples from JPH4-W1 were assessed for particle size and composition using SEM and EDX analysis, to complement the size distribution analysis (Figure 9). 54 SEM images of 5 AIA samples were studied to elevate the morphology and mineralogy. It is difficult to differentiate natural particles from soil erosion versus particulate emissions from mines simply because their mineralogical composition is similar.

The particle sizes seen in the SEM images are consistent with the measured particle size distributions, with majority of particles <15μm. Most particles appear to be poorly sorted and of

blocky or massive structures, with some platy particles (Figure 9 a, c, d, e, g). Spherical fly ash particles (Figure 9 e, g), as described by Fisher *et al.,* (1976), were also found, and increased in abundance with depth as described in Table S4. The spherical fly ash particles were ~20μm or less in diameter. The morphology of these spheres, particularly the roughness of the particles surface, may be a reflection of the temperature the fly ash reached before it was injected into the atmosphere. The rougher the sample, the lower the temperature of injection (Jang & Etsell, 2005). Three trace metals are known to be enriched in bituminous sands namely V, Ni, and Mo (Hodgson, 1954). Vanadium was the only element of these three that was found using EDX in the dust particles, and then only in the 1984 sample (Figure 9g), and only in the fly ash. The 1984 sample is also where there is a peak in AIA, and MAR in JPH4-W1.

The composition of particulate matter in the samples investigated were mostly silicates and aluminosilicates (Figure 9a, c) such as quartz, feldspars, and some Fe-rich silicates which agrees with previous studies of mineralogy of the ABS (Bichard, 1987; Jang & Etsell, 2005; Welton, 2003), as well as other studies of dust in the area (Kaminsky, 2009; Wang *et al.*, 2015a). TiO_2 (Figure 9b) and zircons (Figure 9f) were also present throughout all core layers. Testate amoeba were found in some of the samples (Figure 9e). Gypsum crystals (Figure 9c) was also found in the samples. Gypsum had been assumed to dissolve in HCl with other reactive minerals; however upon investigation it was discovered that gypsum is only partly soluble in HCl (Azimi *et al.*, 2008).

CONCLUSION

Peat cores from seven bogs in the ABS region were analyzed to reconstruct rates of atmospheric dust deposition over the last century. A recent increase in dust deposition, expressed as the AIA accumulation rate, was observed near industry. There is an increase in cumulative mass of dust deposition during the past 30 years compared to between 1900-1960 in each peat core, with larger increases in MIL-W1, JPH4-W1, and McK-W2. There appears to be a connection between elevated dust inputs to bogs near industry, and increasing surface water pH. If chemically reactive minerals are dissolving in the surface waters of these bogs, the availability of plant nutrients (Ca, Mg, K, P, S, Fe, Mn, etc.) may also be increasing and this may impact vegetation.

While there is limited variation in mineral size and composition, fly ash particles are only found near industry and some of these contain detectable levels of V. The morphology and composition of the fly ash particles links them to the bitumen upgraders.

ACKNOWLEDGMENTS

I would like to thank Alberta Innovates for funding, to the University of Alberta, the Faculty of Agricultural, Life and Environmental Sciences, the Department of Renewable Resources for supporting the SWAMP laboratory. Thanks to the Land Reclamation International Graduate School (LRIGS) and NSERC CREATE for providing financial support. Tracy Gartner, Melanie Bolstler, and Karen Lund provided administrative support, and Chad Cuss and Muhammad (Babar) Javed for laboratory support and instruction. Anita Nowinka aided in preparation of ash, and AIA samples of each peat core. Also a big thanks to Melanie Vile for acquainting our team with the bogs sites used in this study. Thanks to Rene Belland, Lee Foote and Claudio Zaccone for project guidance, and Emer Mullan for reviewing this manuscript.

REFERENCES

Addison PA, Puckett KJ. 1980. Deposition of atmospheric pollutants as measured by lichen element content in the Athabasca oil sands area. *Canadian Journal of Botany* **58**: 2323–2334. DOI: 10.1139/b80-269

Agriculture Division of Statistics Canada. 2014. *Table M23-33: Area of land in farm holdings, census data, Canada and by province, 1871-1971*. *Statistics Canada*

Alberta Energy Regulator. 2015. *Alberta's Energy Reserves 2015 and Supply/Demand Outlook 2015-2024*. ST98-2015. Calgary, 3-12.

Andrejko MJ, Fiene F, Cohen AD. 1983. Comparison of Ashing Techniques for Determination of the Inorganic Content of Peats. *Testing of Peats and Organic Soils, ASTM STP 820* 5–20

Azimi G, Papangelakis VG, Dutrizac JE. 2008. Development of an MSE-based chemical model for the solubility of calcium sulphate in mixed chloride-sulphate solutions. *Fluid Phase Equilibria* **266**: 172–186. DOI: 10.1016/j.fluid.2008.01.027

Bargagli R. 1998. *Trace Elements in Terrestrial Plants: An Ecophysiological Approach to Biomonitoring and Biorecovery*. Springer: Verlag Berlin Heidelberg New York

Bichard JA. 1987. AOSTRA technical publication series #4: Oil sands composition and behaviour research. Alberta Oil Sands Technology & Research Authority (AOSTRA): Edmonton, Alberta, 3–2 & 3–14

Bragazza L, Gerdol R. 1999. Hydrology, groundwater chemistry and peat chemistry in relation to habitat conditions in a mire on the South Eastern Alps of Italy. *Plant Ecology* **144**: 243–256

Chapman SB. 1964. The ecology of Coom Rigg Moss , Northumberland : II . The chemistry of peat profiles and the development of the bog system. *Journal of Ecology* **52**: 315–321

Damman AWH. 1978. Distribution and movement of elements in ombrotrophic peat bogs. *Oikos* **30**: 480–495. DOI: 10.2307/3543344

Damman AWH, Tolonen K, Sallantaus T. 1992. Element retention and removal in ombrotrophic peat of Haadetkeidas, a boreal Finnish peat bog. *Suo (Helsinki)* **43**: 137–145

Devito K, Mendoza C, Qualizza C. 2012. Conceptualizing water movement in the Boreal Plains. Implications for watershed reconstruction. Canadian Oil Sands Network for Research and Development, Environmental and Reclamation Research Group, 164

Devito KJ, Mendoza C, Petrone RM, Kettridge N, Waddington JM. 2016. Utikuma Region Study Area (URSA) - Part 1: Hydrogeological and ecohydrological studies (HEAD). *Forestry Chronicle* **92**: 57–61. DOI: 10.5558/tfc2016-017

Environment and Climate Change Canada. 2015. *PM - Total Particulate Matter (NA - M08)*. *National Pollutant Release Inventory* Retrieved: November 6, 2016 from http://ec.gc.ca/inrp-npri/donnees-data/index.cfm?do=results&lang=en&opt_facility_name=&opt_facility=&opt_npri_id=&opt_report_year=2015&opt_chemical_type=ALL&opt_industry=&opt_cas_name=NA+-+M08&opt_cas_num=&opt_location_type=ALL&opt_province=AB&opt_postal_

Finney HR, Farnham RS. 1968. Mineralogy of the inorganic fraction of peat from two raised bogs in northern Minnesota. *Proceedings of the Third International Peat Congress* **3**: 102–108

Fisher GL, Chang DPY, Brummer M. 1976. Fly ash collected from electrostatic precipitators: Microcrystalline structures and the mystery of the spheres. *Science* **192**: 553–555

Goldich S. 1938. A study in rock-weathering. *The Journal of Geology* **46**: 17–58

Gore AJP (ed). 1983a. *Ecosystems of the World 4A, Mires: Swamp, Bog, Fen and Moor General Studies*. Elsevier Scientific Publishing Co.: Amsterdam, Netherlands; New York, N.Y., USA

Gore AJP (ed). 1983b. *Ecosystems of the World 4B, Mires: Swamp, Bog, Fen and Moor Regional Studies*. Elsevier Scientific Publishing Co.: Amsterdam, Netherlands; New York, N.Y., USA

Gorham E, Tilton DL. 1978. The mineral content of *Sphagnum* fuscum as affected by human settlement. *Canadian Journal of Botany* **56**: 2755–2759

Gosselin P, Hrudey SE, Naeth MA, Plourde A, Therrien R, Van Der Kraak G, Xu Z. 2010. *Environmental and Health Impacts of Canada 's Oil Sands Industry*.

Hodgson W. 1954. Vanadium, nickel, and iron trace metals in crude oils of western Canada. *Bulletin of the American Association of Petroleum Geologists* **38**: 2537–2554

Jacobson MZ. 2002. *Atmospheric Pollution : History, Science, and Regulation*. Cambridge University Press: Cambridge, UK

Jang H, Etsell TH. 2005. Morphological and mineralogical characterization of oil sands fly ash morphological and mineralogical characterization of oil. *Energy & Fuels* **19**: 2121–2128. DOI: 10.1021/ef050123a

Kamber BS, Greig A, Collerson KD. 2005. A new estimate for the composition of weathered young Upper Continental Crust from alluvial sediments, Queensland, Australia. *Geochimica et Cosmochimica Acta* **69**: 1041–1058. DOI: 10.1016/j.gca.2004.08.020

Kaminsky HA. 2009. Characterization of an Athabasca oil sand ore and process streams. *Dissertation Abstracts International, Section B* **70**: 9–18

Kempter H, Frenzel B. 2000. The impact of early mining and smelting on the local tropospheric aerosol detected in ombrotrophic peat bogs in the Harz, Germany. *Water, Air, and Soil Pollution* **121**: 93–108

Krachler M, Shotyk W. 2004. Natural and anthropogenic enrichments of molybdenum, thorium, and uranium in a complete peat bog profile, Jura Mountains, Switzerland. *Journal of environmental monitoring : JEM* **6**: 418–426. DOI: 10.1039/b313300a

Le Roux G, Fagel N, De Vleeschouwer F, Krachler M, Debaille V, Stille P, Mattielli N, van der Knaap WO, van Leeuwen JFN, Shotyk W. 2012. Volcano- and climate-driven changes in atmospheric dust sources and fluxes since the late glacial in Central Europe. *Geology* **40**: 335–338. DOI: 10.1130/G32586.1

Le Roux G, Laverret E, Shotyk W. 2006. Fate of calcite, apatite and feldspars in an ombrotrophic peat bog, Black Forest, Germany. *Journal of the Geological Society* **163**: 641–646. DOI: 10.1144/0016-764920-035

Malmer N. 1988. Patterns in the growth and the accumulation of inorganic constituents in the *Sphagnum* cover on ombrotrophic bogs in Scandinavia. *Oikos* **53**: 105–120

Muhs DR, Prospero JM, Buddock MC, Gill TE. 2014. Identifying sources of aeolian mineral dust: Present and past. *Mineral Dust: A Key Player in the Earth System*. Springer Science & Business Media: Dordrecht, 385–409. DOI: 10.1007/978-94-017-8978-3

Pearsall W. 1952. The pH of natural soils and its ecological significance. *Journal of Soil Science* **3**: 41–51. DOI: 10.1017/CBO9781107415324.004

Percy KE. 2013. Ambient air quality and linkage to ecosystems in the Athabasca oil sands, Alberta. *Geosicence of Climate and Engery* **11**: 182–201

Percy KE, Davies MJE. 2012. *Air quality modeling in the Athabasca oil sands region*. *Developments in Environmental Science*. Elsevier Ltd. DOI: 10.1016/B978-0-08-097760-7.00004-4

Petrone R, Devito KJ, Mendoza C. 2016. Utikuma Region Study Area (URSA) - Part 2: Aspen Harvest and Recovery Study. *Forestry Chronicle* **92**: 62–65. DOI: 10.5558/tfc2016-018

Santelmann M V, Gorham E. 1988. The influence of airborne road dust on the chemistry of *Sphagnum* mosses. *The Journal of Ecology* **76**: 1219–1231. DOI: 10.2307/2260644

Sapkota A. 2006. Mineralogical, Chemical, and Isotopic (Sr, Pb) Composition of Atmospheric Mineral Dusts in an Ombrotrophic Peat Bog, Southern South America. Ruprecht-Karls-Universität

Sapkota A, Cheburkin AK, Bonani G, Shotyk W. 2007. Six millenia of atmospheric dust depostion in southern South America (Isla Navarino, Chile). *The Holocene 17* **5**: 561–572

Shelfentook W. 1978. An inventory system for atmospheric emissions in the AOSERP study

area. SNC Tottrup Services Ltd.: Edmonton, AB

Shotyk W. 1897. European contributions to the geochemistry of peatland waters, 1890-1940. *Symposium '87 Wetlands/Peatlands*. Canadian Society of Wetlands and Peatlands, and Canadian National Committee, International Peat Society: Edmonton, Alberta, 115–125

Shotyk W. 1986a. Overview of the geochemistry of peatland waters. *Advances in Peatlands Engineering*. National Research Council Canada: Ottawa Ontario, 159–171

Shotyk W. 1986b. Overview of the inorganic geochemistry of peats. *Advances in Peatlands Engineering*. National Research Council Canada: Ottawa Ontario, 249–258

Shotyk W. 1988. Review of the inorganic geochemistry of peats and peatland waters. *Earth-Science Reviews* **25**: 95–176. DOI: 10.1016/0012-8252(88)90067-0

Shotyk W. 1989. The chemistry of peatland waters. *Water-Quality Bulletin* **14**: 47–57

Shotyk W. 1996. Natural and anthropogenic enrichments of As, Cu, Pb, Sb, and Zn in ombrotrophic versus minerotrophic peat bog profiles, Jura Mountains, Switzerland. *Water, Air, and Soil Pollution* **90**: 375–405. DOI: 10.1007/BF00282657

Shotyk W, Appleby PG, Bicalho B, Davies L, Froese DG, Grant-Weaver I, Krachler M, Magnan G, Mullan-Boudreau G, Noernberg T, Pelletier R, Shannon B, van Bellen S, Zaccone C. 2016. Peat bogs in northern Alberta, Canada reveal decades of declining atmospheric Pb contamination. *Geophysical Research Letters* **43**: 1–11. DOI: 10.1002/2016GL070952

Shotyk W, Norton SA, Farmer JG. 1997. Summary of the workshop of Peat Bog Archives of Atmospheric Metal Deposition. *Water, Air, and Soil Pollution*, 213–219. DOI: 10.1023/A:1018336828640

Steinmann P, Shotyk W. 1997. Geochemistry, mineralogy, and geochemical mass balance on major elements in two peat bog profiles (Jura Mountains, Switzerland). *Chemical Geology* **138**: 25–53. DOI: 10.1016/S0009-2541(96)00171-4

Stringham G. 2012. *Energy Developments in Canada's Oil Sands*. *Developments in*

Environmental Science. Elsevier Ltd. DOI: 10.1016/B978-0-08-097760-7.00002-0

Vile MA, Novak MJ V, Brizova E, Wieder RK, Schell WR. 1995. Historical rates of atmospheric Pb deposition using ^{210}Pb dated peat cores: Corroboration, computation, and interpretation. *Water, Air, and Soil Pollution* **79**: 89–106. DOI: 10.1007/BF01100432

Vile MA, Wieder RK, Novák M. 2000. 200 years of Pb deposition throughout the Czech Republic: Patterns and sources. *Environmental Science and Technology* **34**: 12–21. DOI: 10.1021/es990032q

Vuorela I. 1983. Field erosion by wind as indicated by fluctuations in the ash content of *Sphagnum* peat. *Bulletin of the Geological Society of Finland* **55**: 25–33

Walker DA, Everett KR. 1987. Road dust and its environmental impact on Alaskan taiga and tundra. *Arctic and Alpine Research* **19**: 479–489. DOI: 10.2307/1551414

Wang X, Chow JC, Kohl SD, Percy KE, Legge AH, Watson JG. 2015a. Characterization of PM 2.5 and PM 10 fugitive dust source profiles in the Athabasca Oil Sands Region. *Journal of the Air & Waste Management Association* **65**: 1421–1433. DOI: 10.1080/10962247.2015.1100693

Wang X, Chow JC, Kohl SD, Yatavelli LNR, Percy KE, Legge AH, Watson JG. 2015b. Wind erosion potential for fugitive dust sources in the Athabasca Oil Sands Region. *Aeolian Research* **18**: 121–134. DOI: 10.1016/j.aeolia.2015.07.004

Watmough SA, Whitfield CJ, Fenn ME. 2014. The importance of atmospheric base cation deposition for preventing soil acidification in the Athabasca Oil Sands Region of Canada. *Science of the Total Environment* **493**: 1–11. DOI: 10.1016/j.scitotenv.2014.05.110

Watson JG, Chow JC, Wang X, Kohl SD. 2010. Emission characterization plans for the Athabasca oil sands region. In: Tropp RJ and Legge AH (eds) *Proceedings, 103rd Annual Meeting of the Air & Waste Management Association*. Air & Waste Management Association: Pittsburgh, PA, 1–6

Watson JG, Chow JC, Wang X, Kohl SD, Yatavelli LNR. 2014. Windblown Fugitive Dust

Characterization in the Athabasca Oil Sands Region. *Wood Buffalo Environmental Association*. Desert Research Institute: McMurray, 1-1-4–19

Wedepohl KH. 1995. Composition of the Continental Crust. *Geochimica et Cosmochimica Acta* **59**: 11217–1232. DOI: 10.1016/B978-0-08-095975-7.00301-6

Welton JE. 2003. *SEM petrology Atlas*. The American Association of Petroleum Geologists: Tulsa, Oklahoma

Wieder RK, Novák M, Schell WR, Rhodes T. 1994. Rates of peat accumulation over the past 200 years in five *Sphagnum*-dominated peatlands in the United States. *Journal of Paleolimnology* **12**: 35–47. DOI: 10.1007/BF00677988

Wieder RK, Vitt DH, Burke-Scoll M, Scott KD, House M, Vile MA. 2010. Nitrogen and sulphur deposition and the growth of *Sphagnum* fuscum in bogs of the Athabasca Oil Sands Region, Alberta. *Journal of Limnology* **69**: 161–170. DOI: 10.3274/JL10-69-S1-16

Zaccone C, Miano TM, Shotyk W. 2012. Interpreting the ash trend within ombrotrophic bog profiles: atmospheric dust depositions vs. mineralization processes. The Etang de la Gruère case study. *Plant and Soil* **353**: 1–9. DOI: 10.1007/s11104-011-1055-9

Zaccone C, Pabst S, Senesi GS, Shotyk W, Miano TM. 2013. Comparative evaluation of the mineralogical composition of *Sphagnum* peat and their corresponding humic acids, and implications for understanding past dust depositions. *Quaternary International* **306**: 80–87. DOI: 10.1016/j.quaint.2013.04.017

List of Figures

List of Tables

Figure 1: Map of 7 peat core sampling sites (MIL-W1, JPH4-W1, McK-W2, McM-W3, ANZ-W3, UTK-W2, and SEB-W1). The 4 active upgraders, Wabamum Transalta Sundance Coal-fired Generating Station, and the upgrader midpoint (reference point) are also depicted.

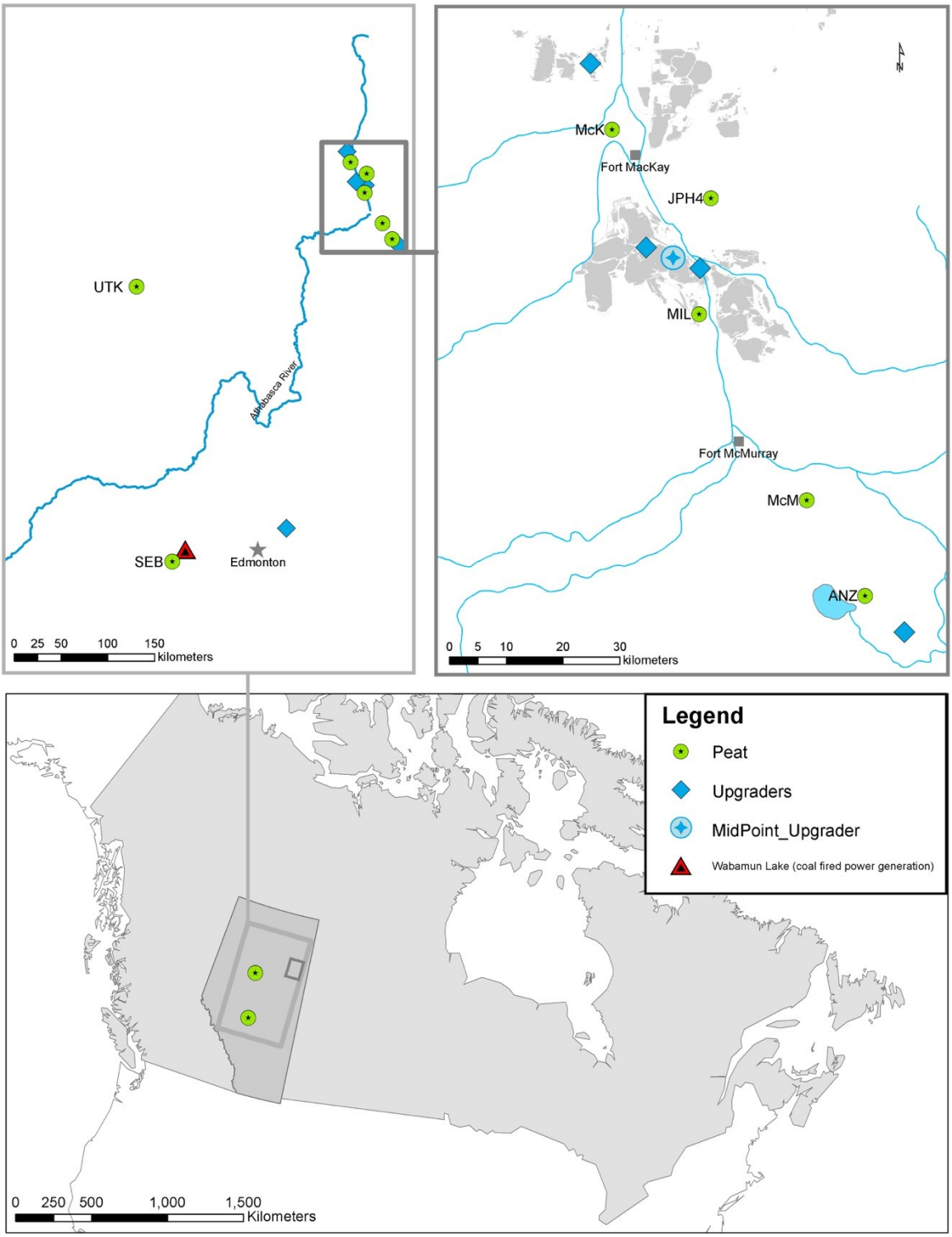

Figure 2: MIL-W1 ash, AIA and ASA (%) profiles, that indicate that ASA, not AIA, is effected by the transition from ombrotrophic to minerotrophic; therefore, AIA values can be used beyond 1985 where the transition begins. MIL-W1 was included in the comparison because the AIA inventory does not appear to be effected by the transition from ombrotrophic to minerotrophic peat (linear correlation coefficient between AIA and ash: R=0.46). The ASA follows the ash trend (linear correlation coefficient between ASA and ash: R=0.86) indicating that any mineral input from other sources is minimal and of soluble origin.

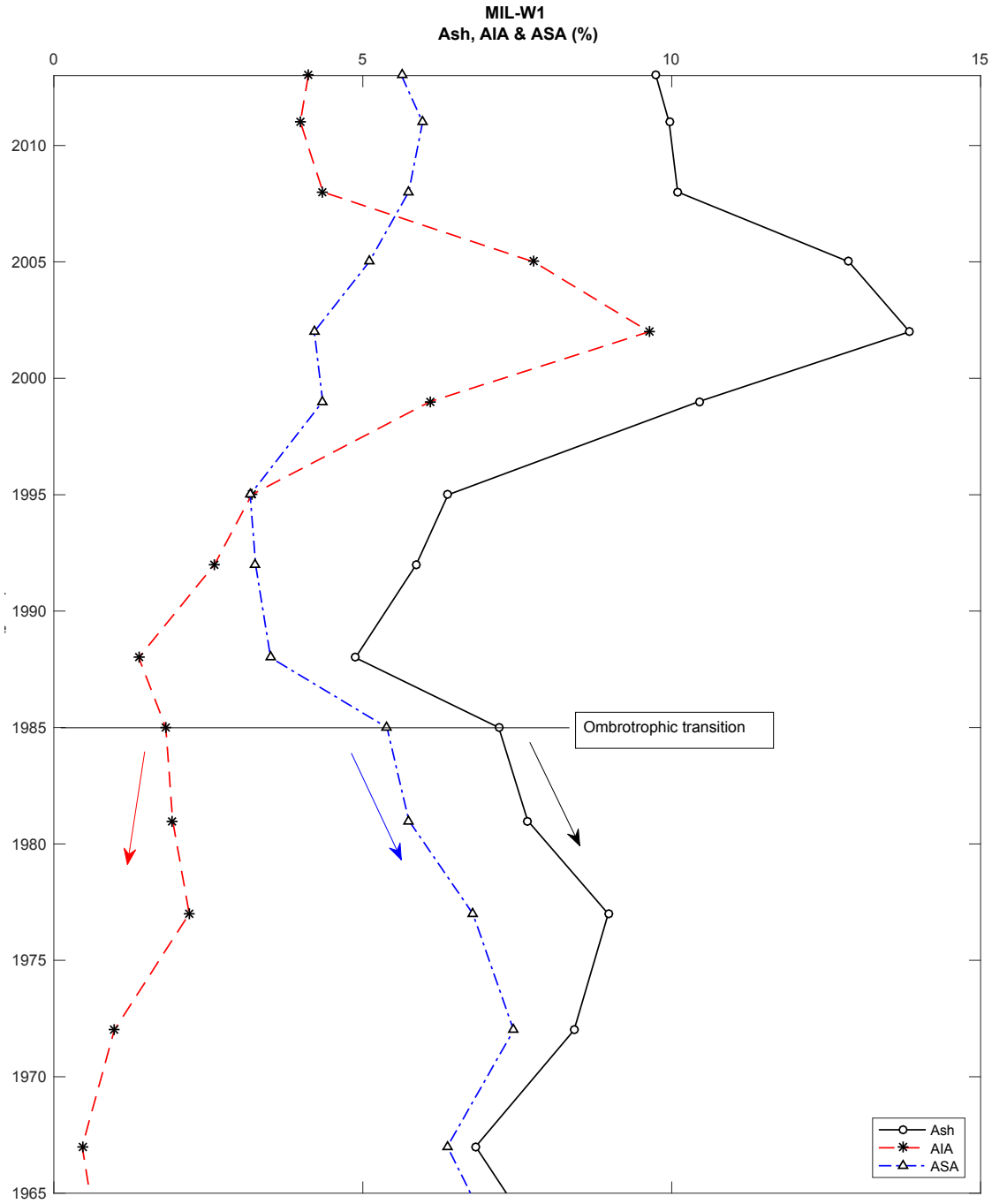

Figure 3: Ash and AIA (%) profiles from 1900 to the time of collection for MIL-W1, JPH4-W1, McK-W2, McM-W3, ANZ-W3, UTK-W2, and SEB-W1.

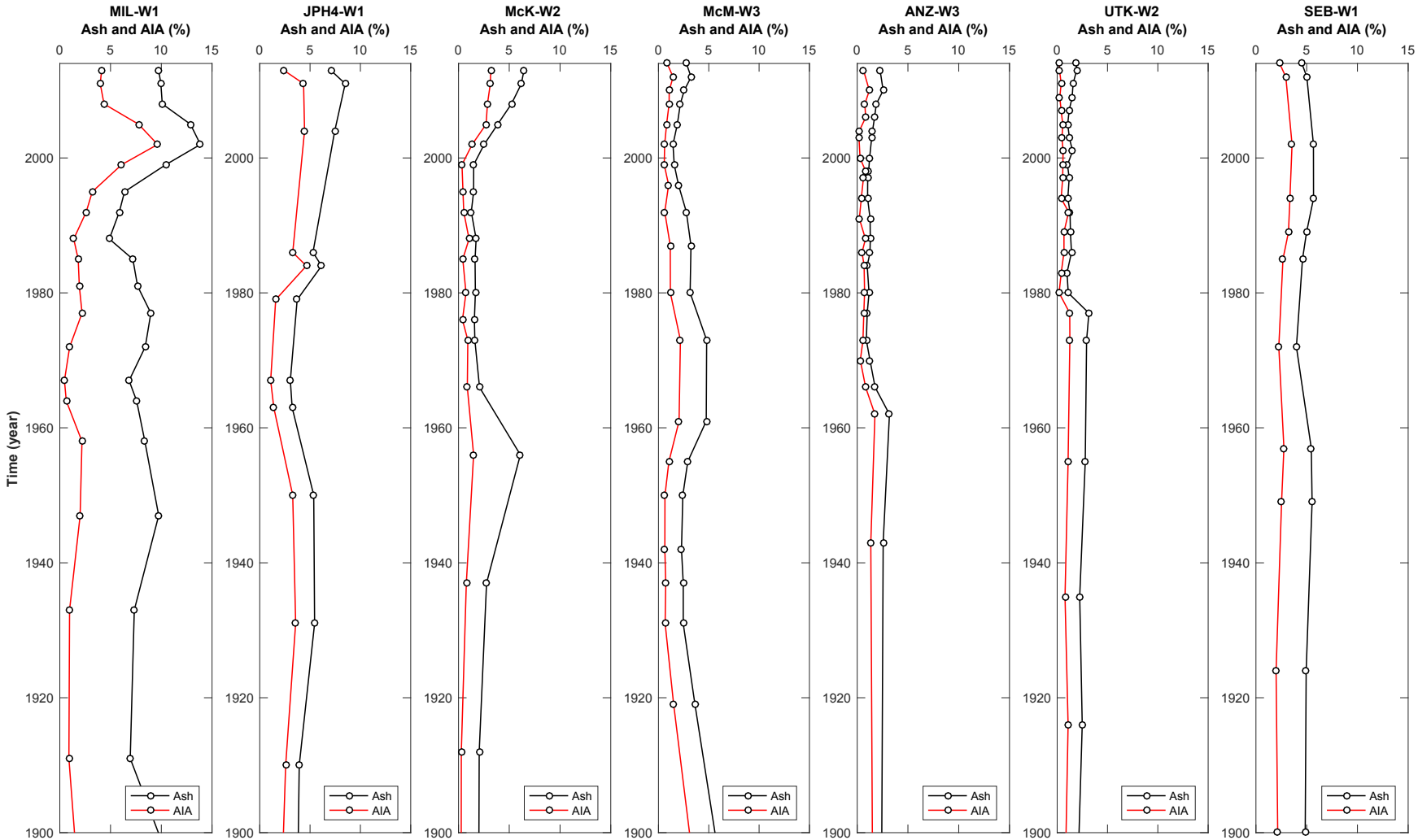

Figure 4: MAR profiles from 1900 to time of collection for each of the 6 peat cores with completed age-date models (MIL-W1, JPH4-W1, McK-W2, McM-W3, ANZ-W3, and UTK-W2). The average was used to minimize error from the determination of living layer thickness, which can have a high degree of error if there is no clear transition visible when cutting the peat core. Using the average peat accumulation rate for the living layers is thought to give more realistic values; however, decreases the degree of confidence in any trends discussed.

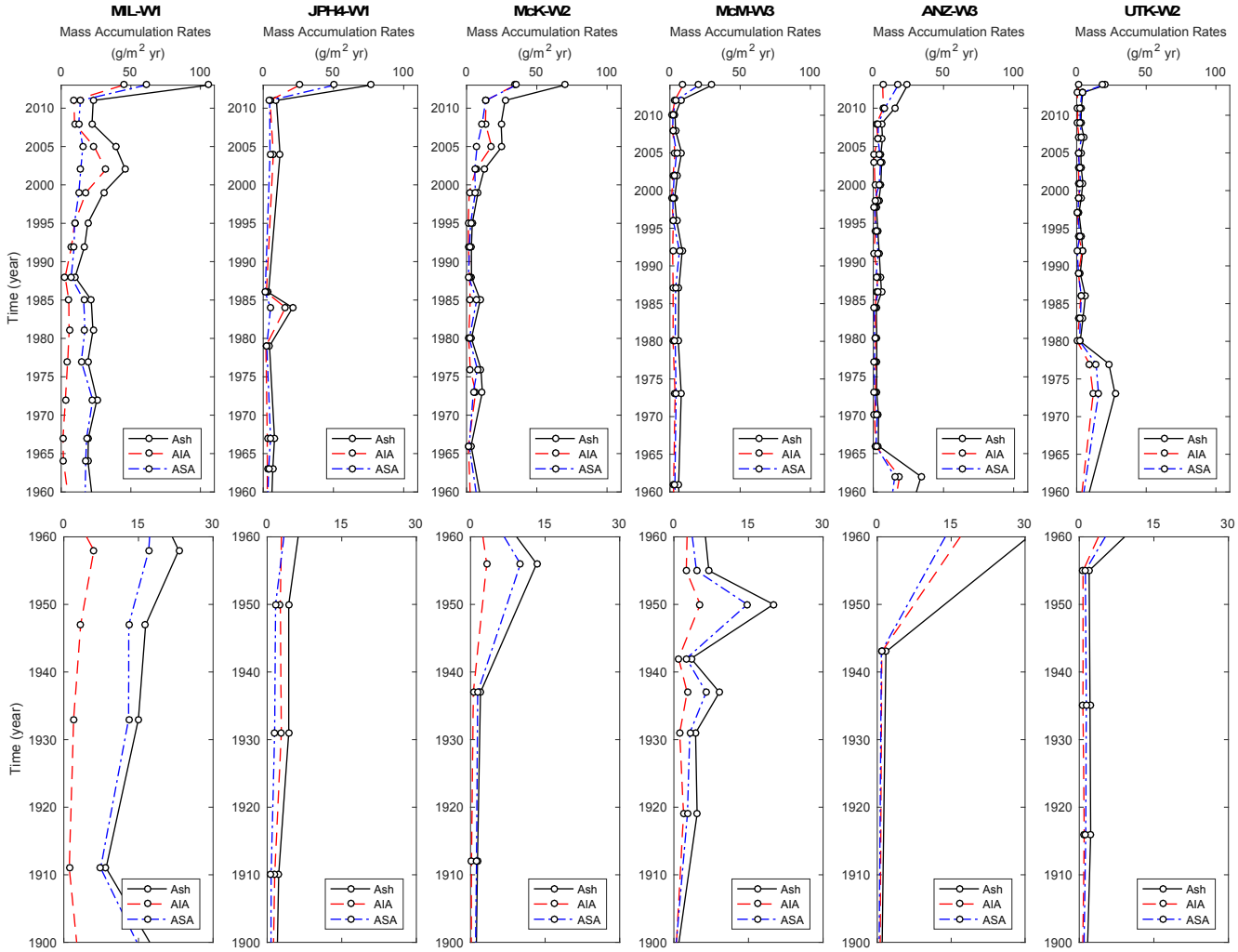

Figure 5: a) Cumulative mass of dust deposition of ash, AIA and ASA over the top 30 years (1985 to the time of collection) and **b)** Cumulative mass of dust deposition of ash, AIA and ASA from 1900 to 1960.

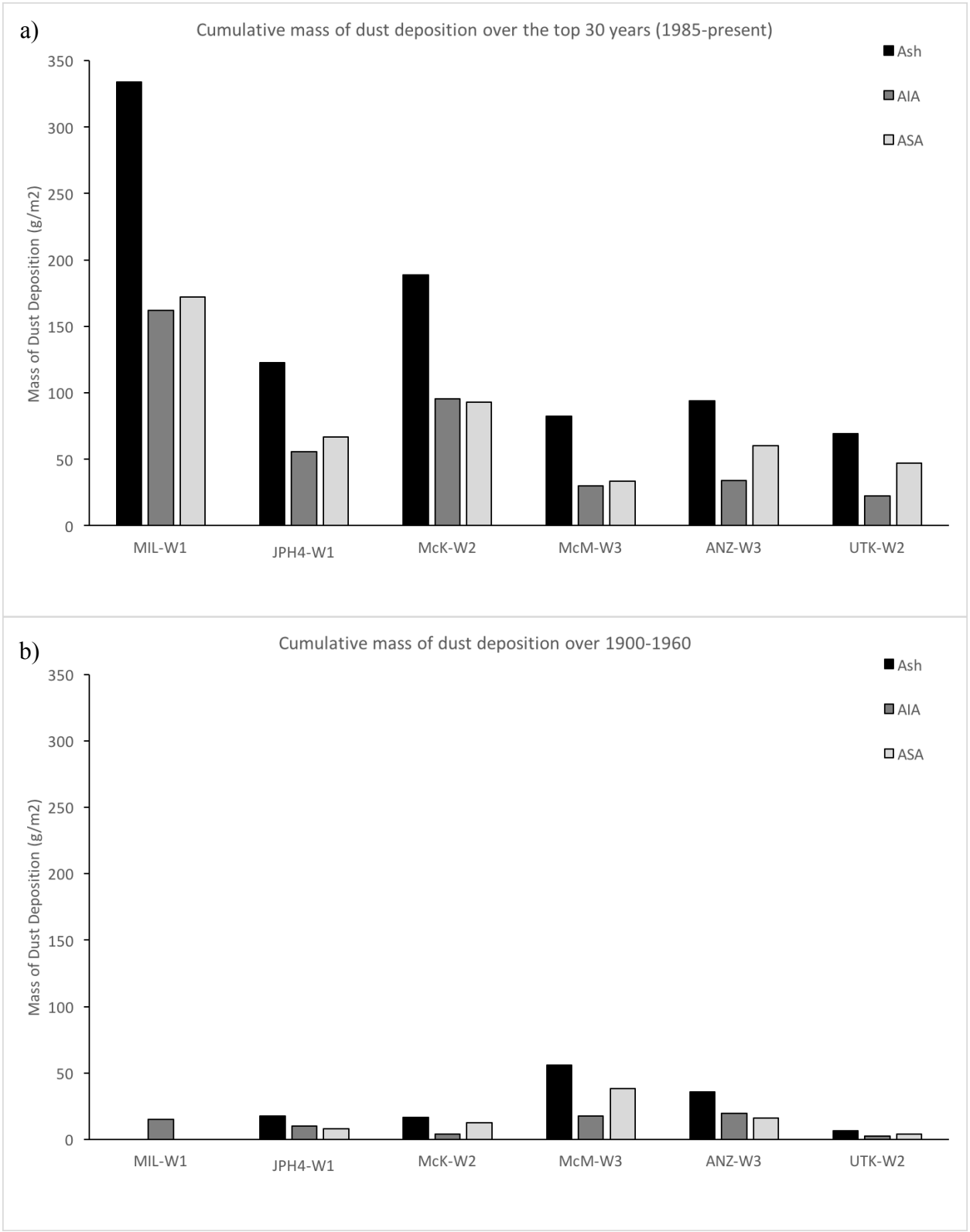

Figure 6: The average MAR of AIA (g/m^2 yr) and pH of peat pore water over top 46 years (1967 to time of collection).

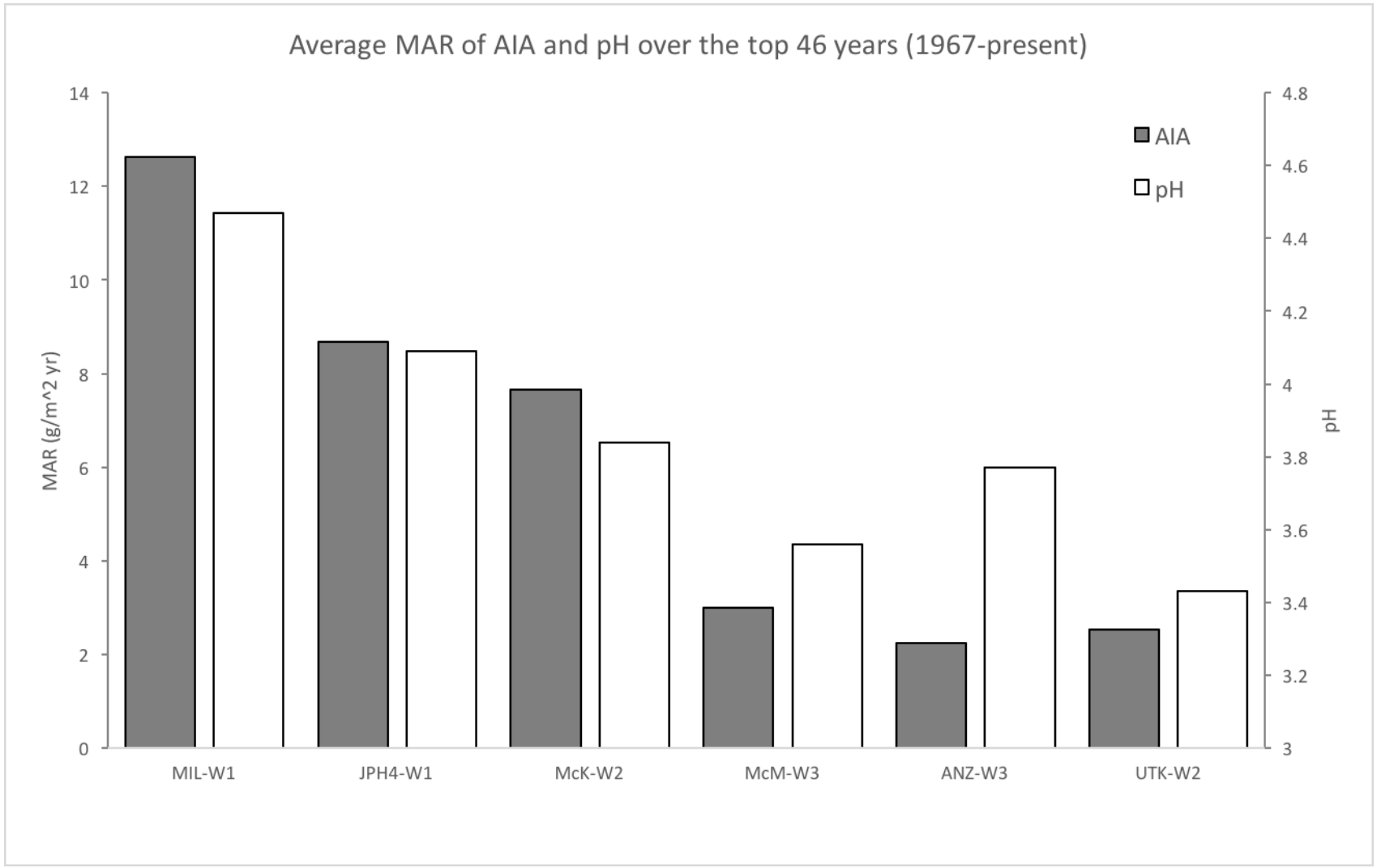

Figure 7: Thorium accumulation rate profiles (1900 to time of collection) and Th enrichment factor (EF) profiles for MIL-W1, JPH4-W1, McK-W2, McM-W3, ANZ-W3, and UTK-W2. An average living layer peat accumulation rate (1084 g/m^2 yr) was used to calculate the Th accumulation rates, as was for the MAR, to reduce error from the determination of living layer thickness.

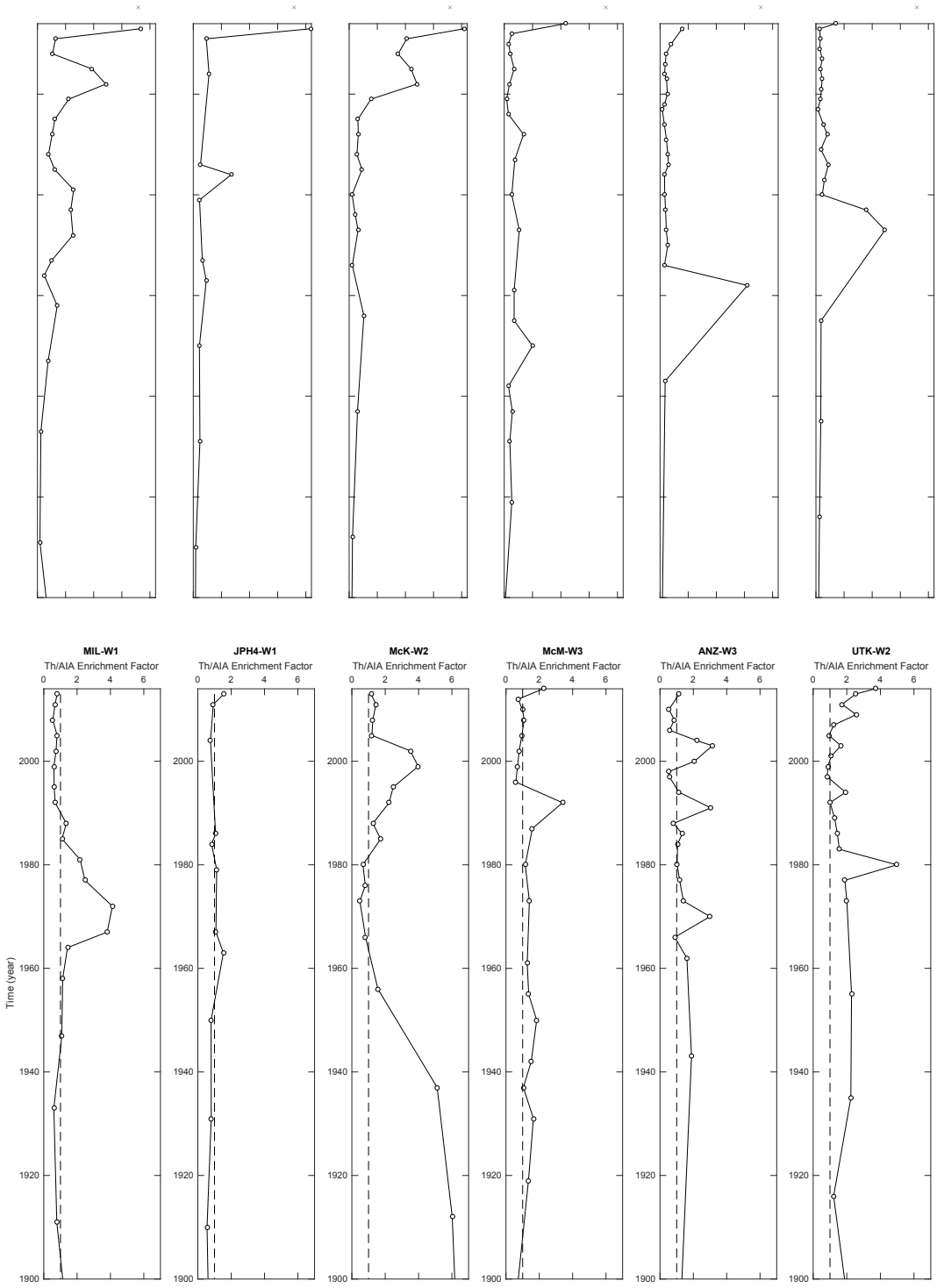

Figure 8: The size distribution profile of JPH4-W1 from 1900 to time of collection. The profile illustrates the percentage of particles in each size class from 1-100µm over time.

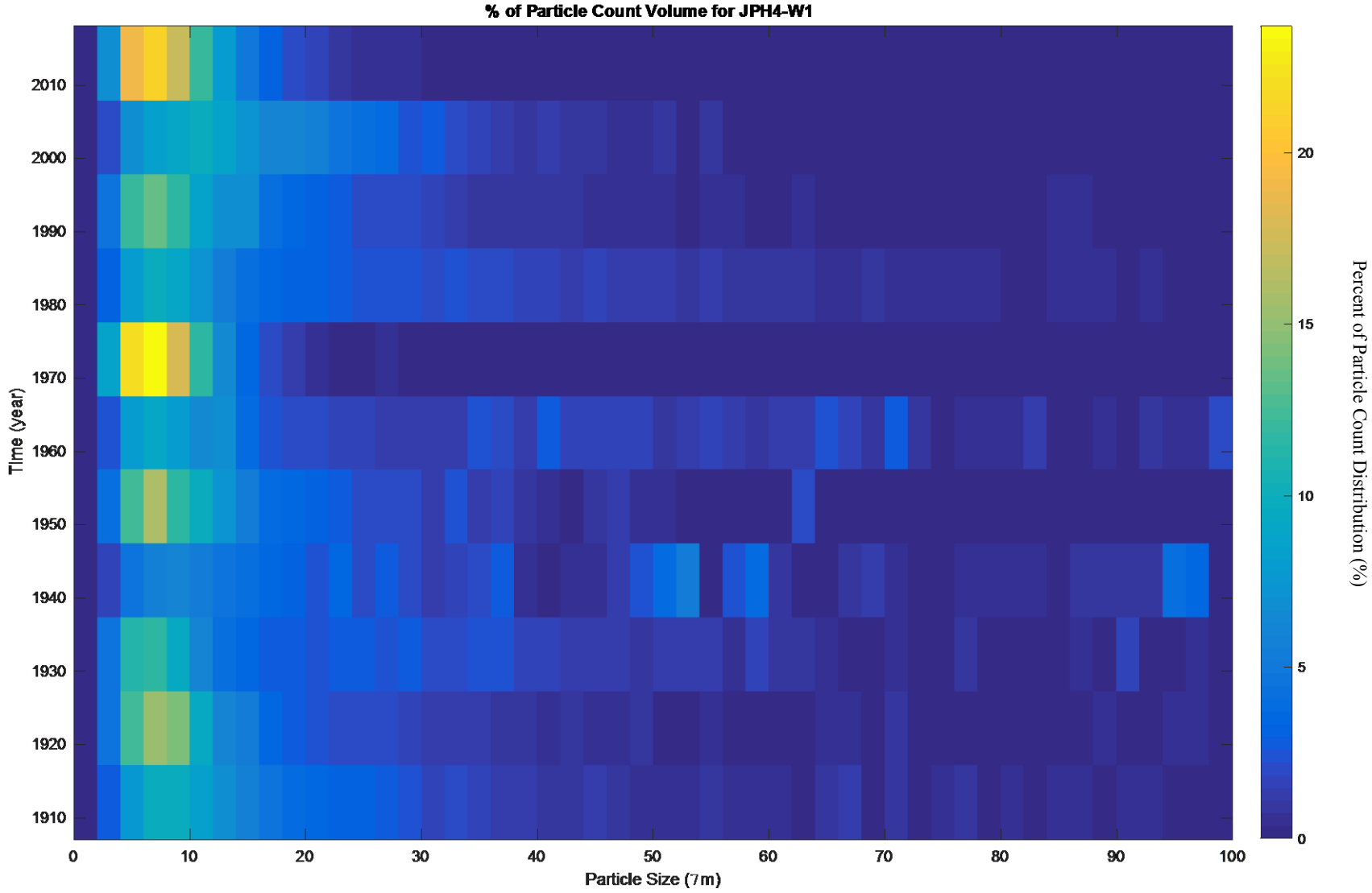

Figure 9: SEM images of selected samples of JPH4-W1 core. a) 2013: depicts typical Fe silicate particles abundant in all samples as well as blocky and massive structures b) 2013: depicts a typical TiO_2 particle found in most layers of the peat cores c) 1967: highlights gypsum crystals found as well as typical aluminosilicate particle d) 1950: depicts platy particles e)1967: pure glass SiO_2 fly ash with a testate amoebae f)1984: example of a typical zircon particle found in most layers of the peat cores g)1984: shows the fly ash sphere with traces of V alongside other small fly ash particles with its EDX spectrum

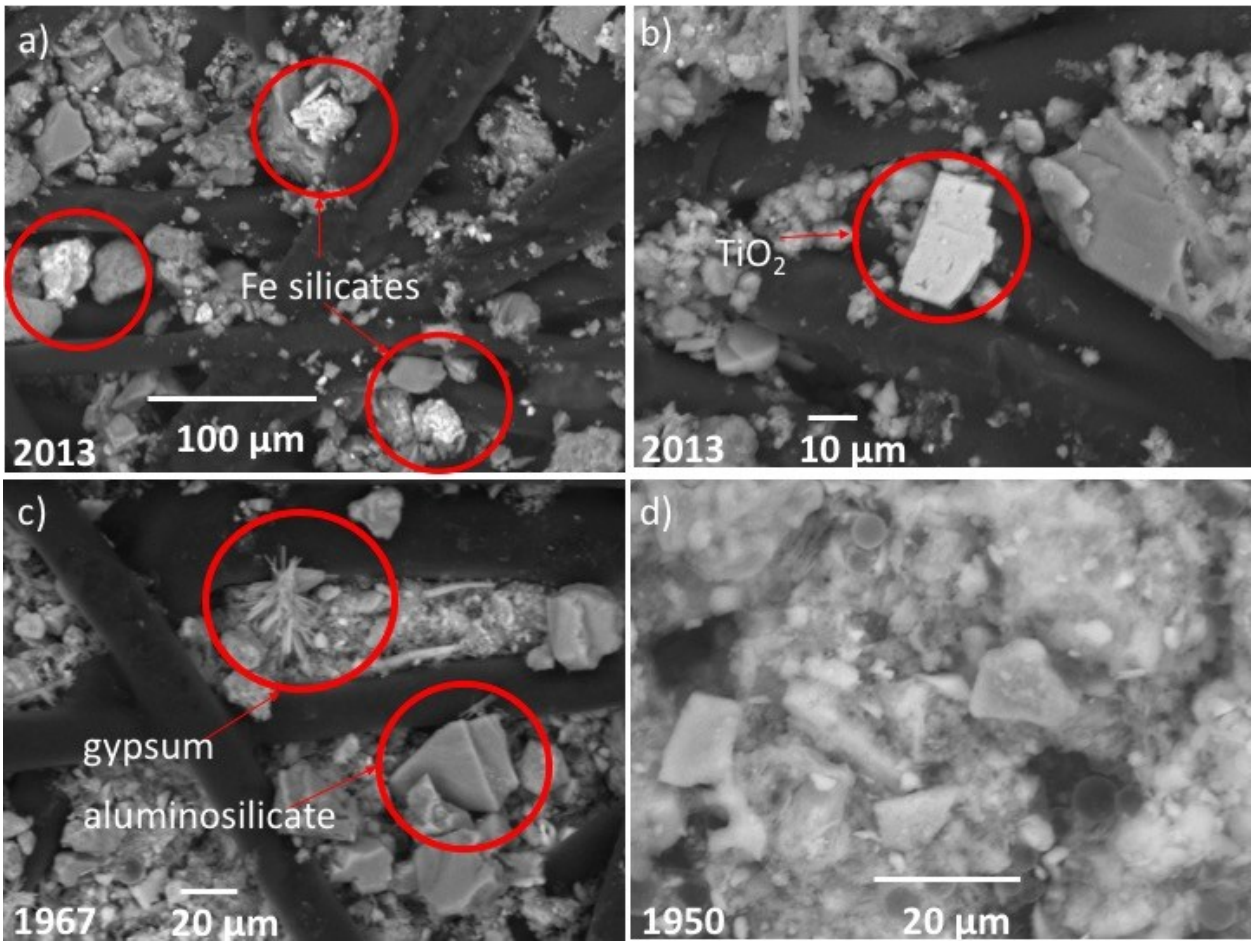

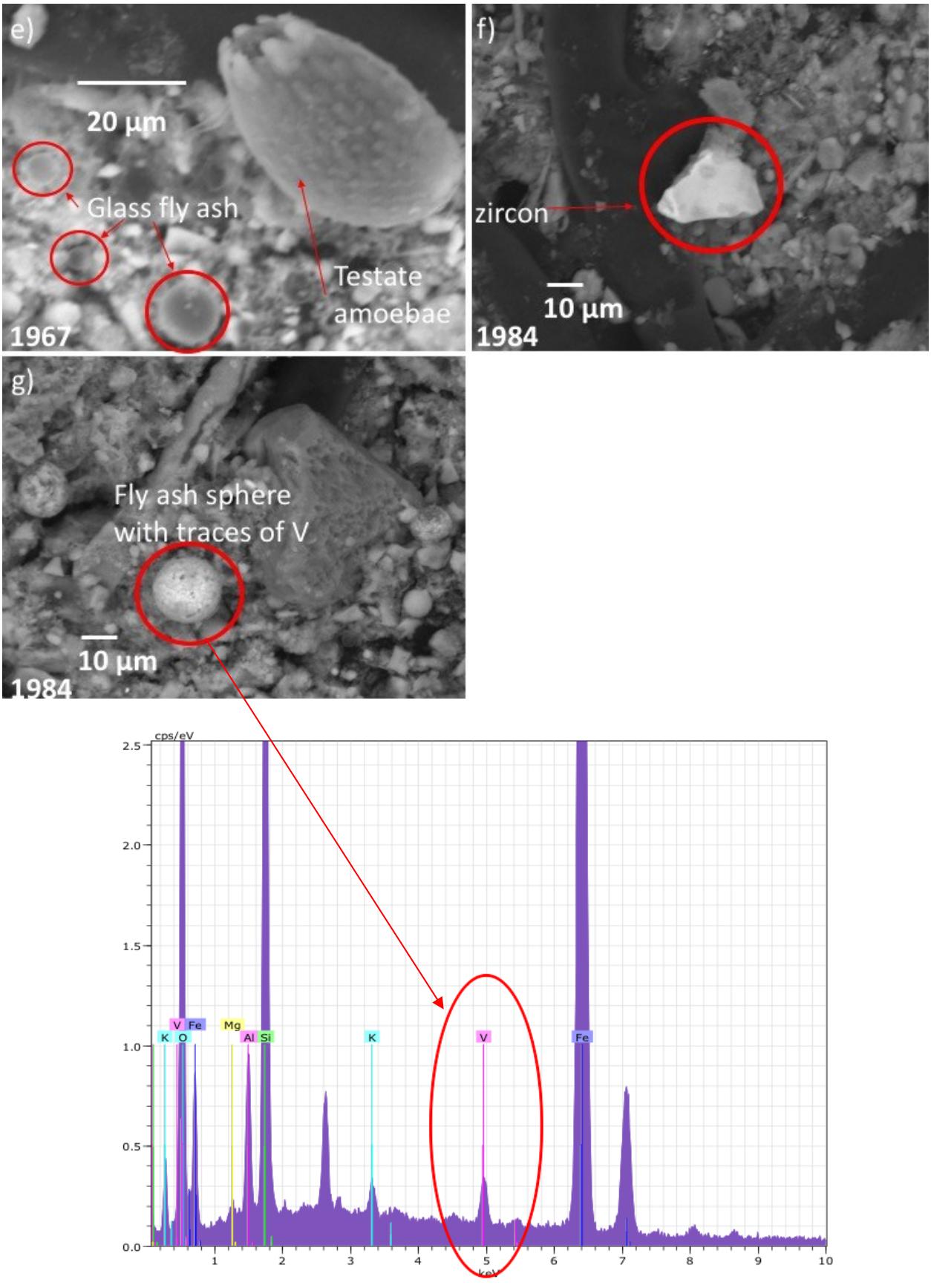
e)
20 µm
Glass fly ash
Testate amoebae
1967
f)
zircon
10 µm
1984
g)
Fly ash sphere with traces of V
10 µm
1984
cps/eV
2.5
2.0
1.5
1.0
0.5
0.0
V Fe
K O
Mg
Al Si
K
V
Fe
1 2 3 4 5 6 7 8 9 10

Table 1: Average MARs for ash, AIA and ASA of MIL-W1, JPH4-W1, McK-W2, McM-W3, ANZ-W3, and UTK-W2 from 1900 to time of collection. MIL-W1 was averaged from 1985 to time of collection for ash and ASA because of the transition from ombrotrophic.

	Ash (g/m^2 yr)		**AIA (g/m^2 yr)**		**ASA (g/m^2 yr)**	
	MARs	+/-	MARs	+/-	MARs	+/-
MIL-W1	33.4	19.7	16.2	9.6	17.2	11.2
JPH4-W1	13.2	16.0	5.5	5.2	7.7	10.8
McK-W2	13.7	8.6	6.5	4.6	7.2	4.2
McM-W3	7.3	3.0	2.7	0.9	3.6	0.7
ANZ-W3	5.6	2.5	2.2	0.8	3.4	1.8
UTK-W2	4.4	2.0	1.4	0.4	2.9	1.9

Supporting Information

List of Figures

List of Tables

List of Methods

List of Appendices

Supporting Information Figures

S1: Peat layer subsampling preparation schematic that illustrates how much sample was used for which analysis in the peat project.

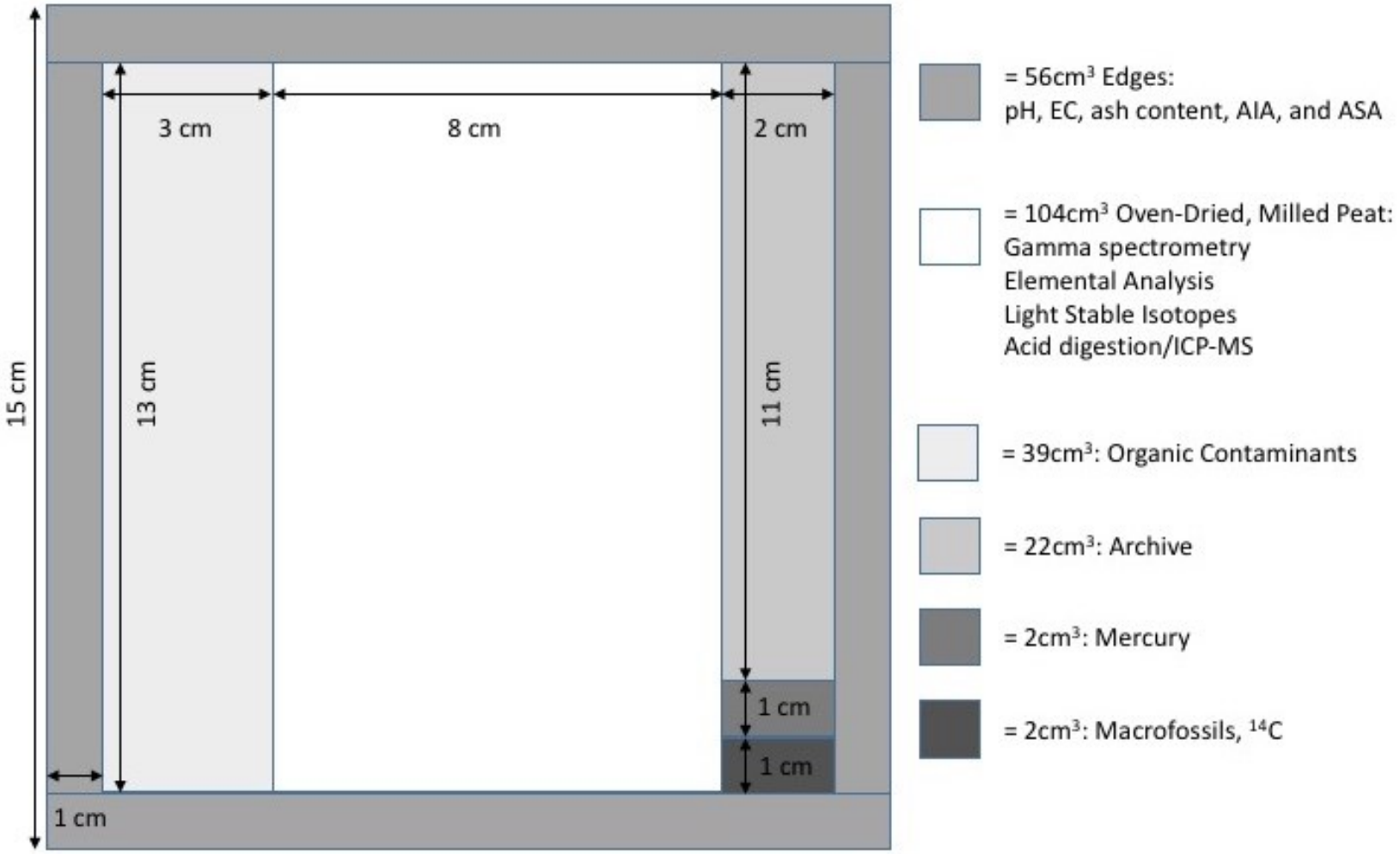

S2: Sample Preparation and Analysis Schematic


Peat core


Cut into 1 cm layers


Dry at 105°C for 24 hours


Dried peat


Ash at 550°C for 16 hours


Peat ash

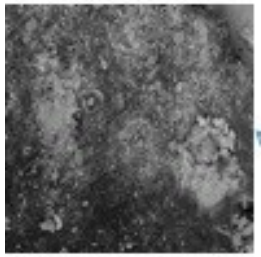
SEM and EDX


Measure pH and Electrical Conductivity (EC)

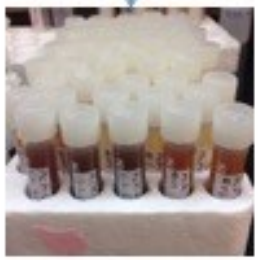
Reacted in 1M HCl (15 min)


Laser Particle Size Distribution Analysis using XPT-C

Suspend AIA in 0.1% surfactant solution


AIA on filter membrane


Cut open filters to remove PTFE membrane filter


Drying filters using vacuum pump


Filter to separate ASA from AIA

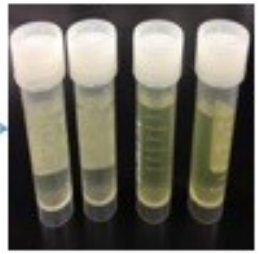
ASA

S3: pH profiles for MIL-W1, JPH4-W1, McK-W2, McM-W3, ANZ-W3, UTK-W2, and SEB-W1 (Shotyk *et al.*, 2016)

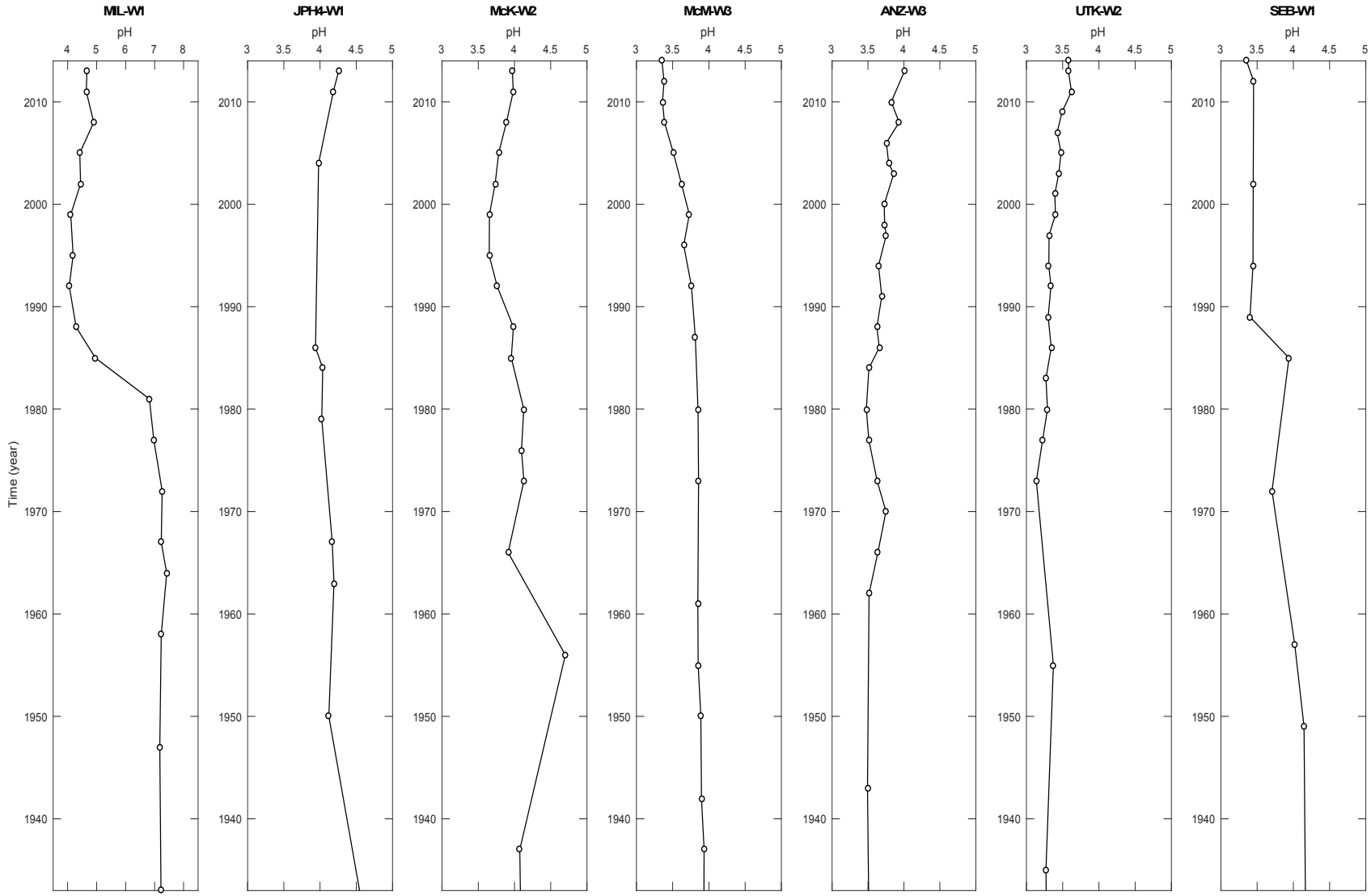

S4: EC profiles for MIL-W1, JPH4-W1, McK-W2, McM-W3, ANZ-W3, UTK-W2, and SEB-W1 (Shotyk *et al.*, 2016)

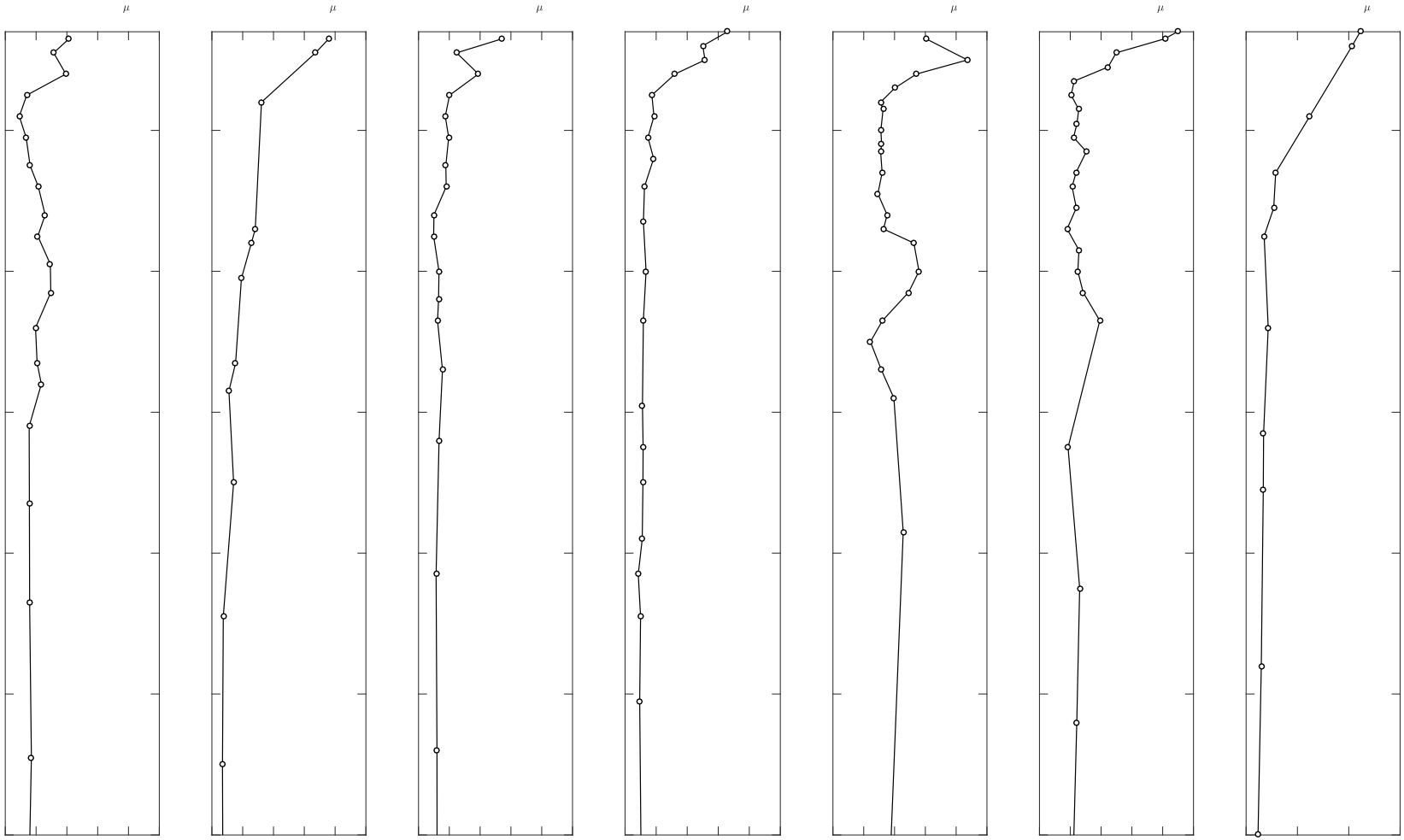

S5: pH profiles (pre-1900) for MIL-W1, JPH4-W1, McK-W2, McM-W3, ANZ-W3, UTK-W2, and SEB-W1

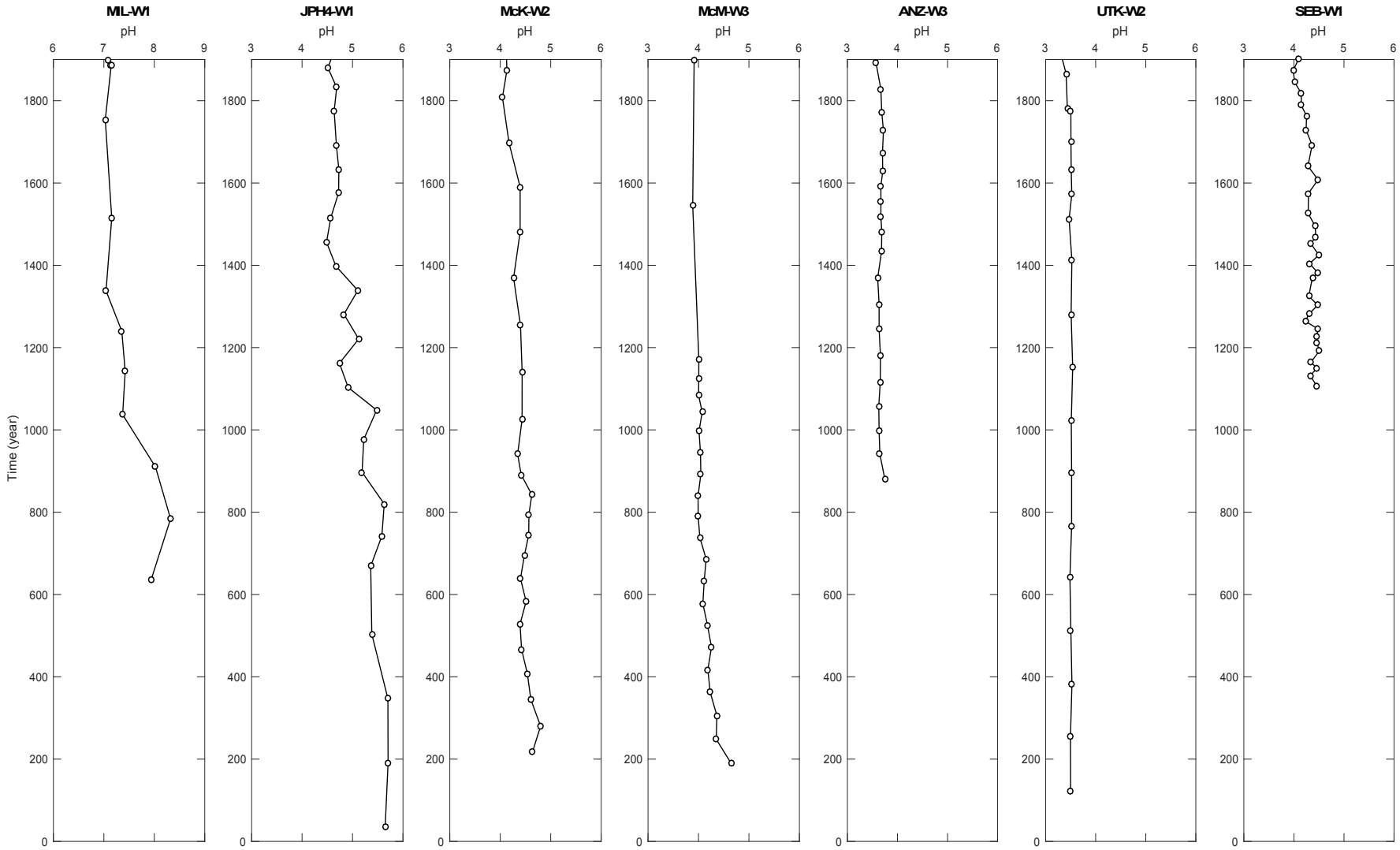

S6: EC profiles (pre-1900) for MIL-W1, JPH4-W1, McK-W2, McM-W3, ANZ-W3, UTK-W2, and SEB-W1

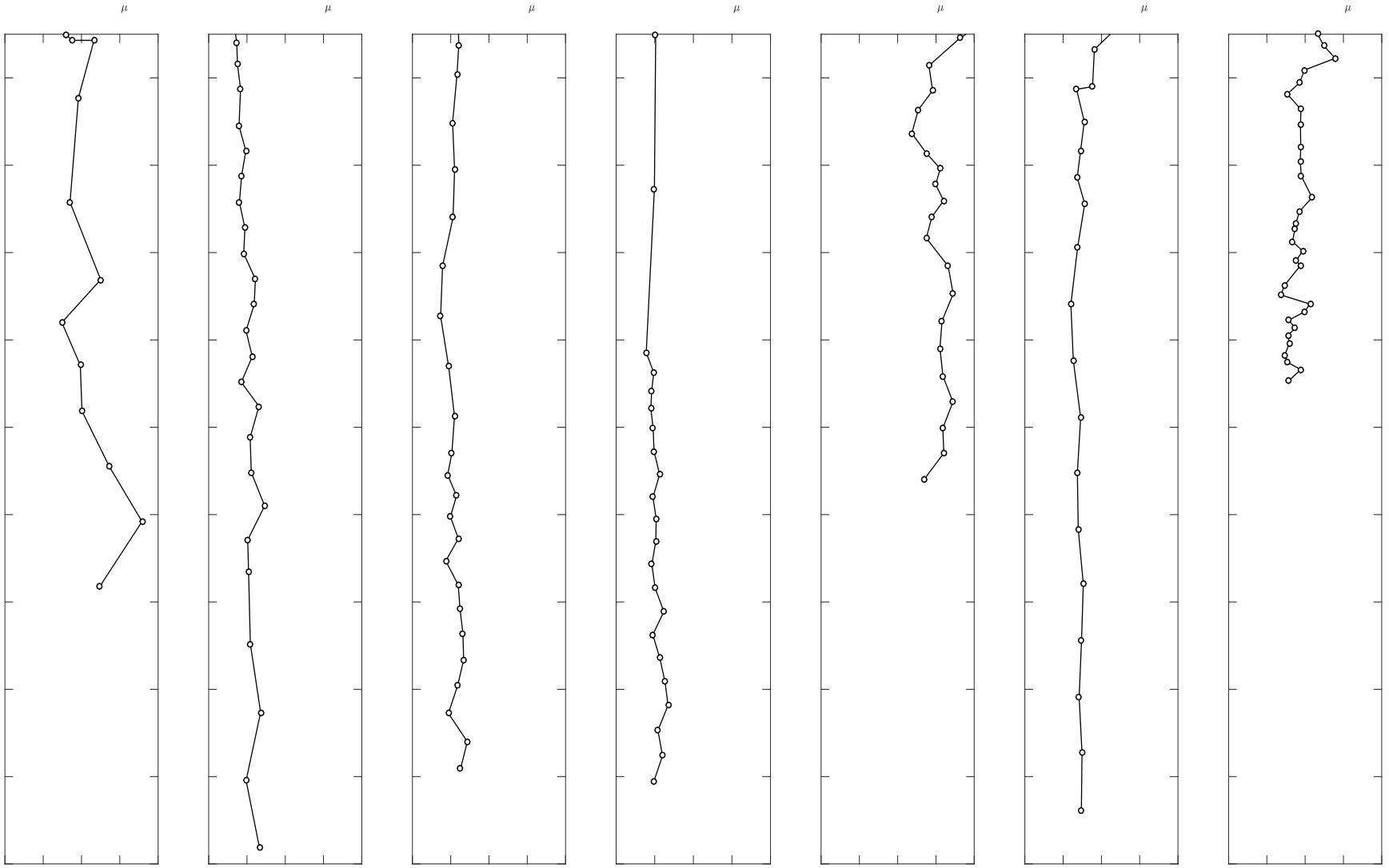

S7: Ash and AIA profiles (pre1900) for MIL-W1, JPH4-W1, McK-W2, McM-W3, ANZ-W3, UTK-W2, and SEB-W1

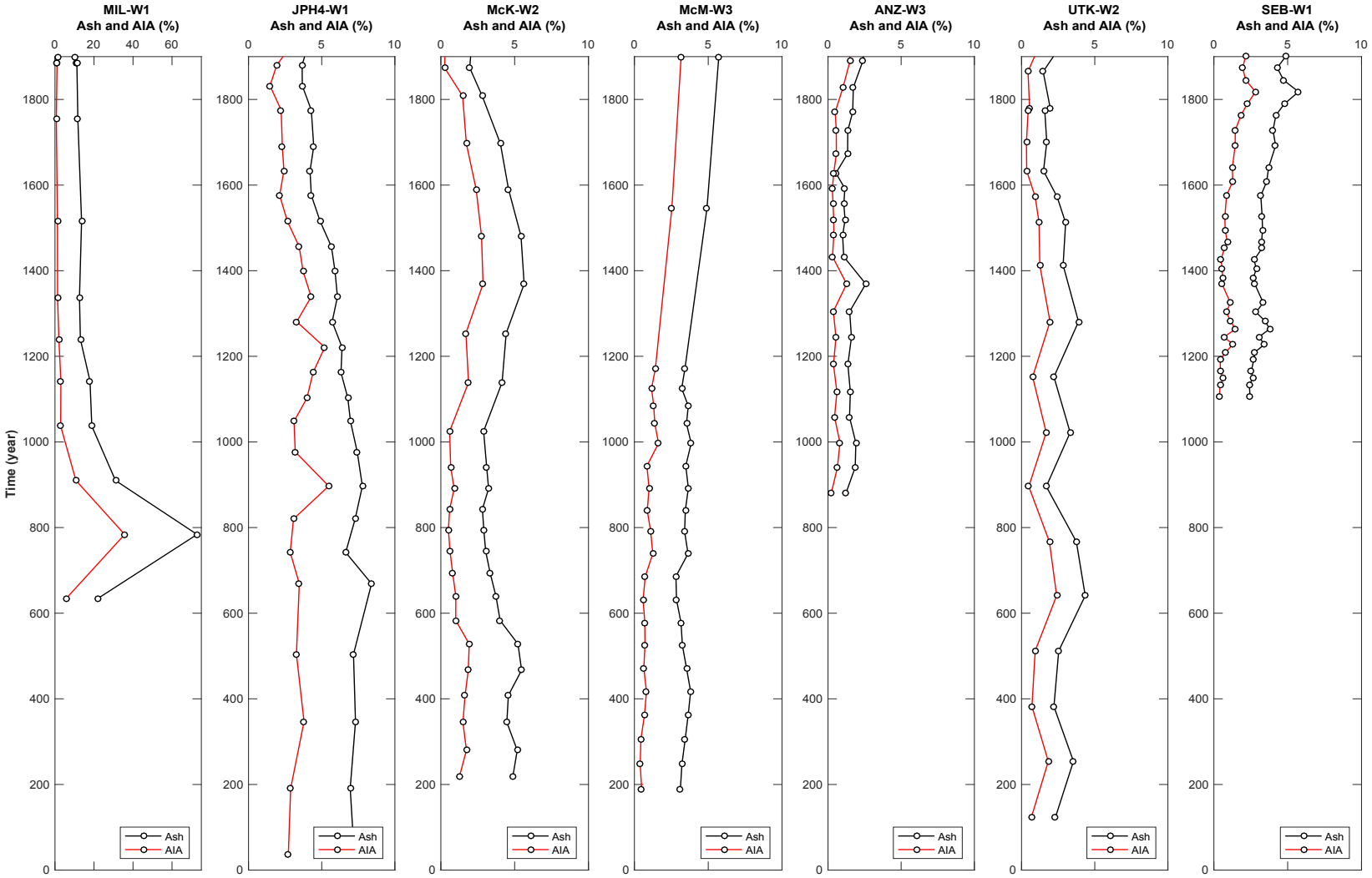

S8: Th Enrichment Factor profiles (pre1900) for MIL-W1, JPH4-W1, McK-W2, McM-W3, ANZ-W3, UTK-W2, and SEB-W1

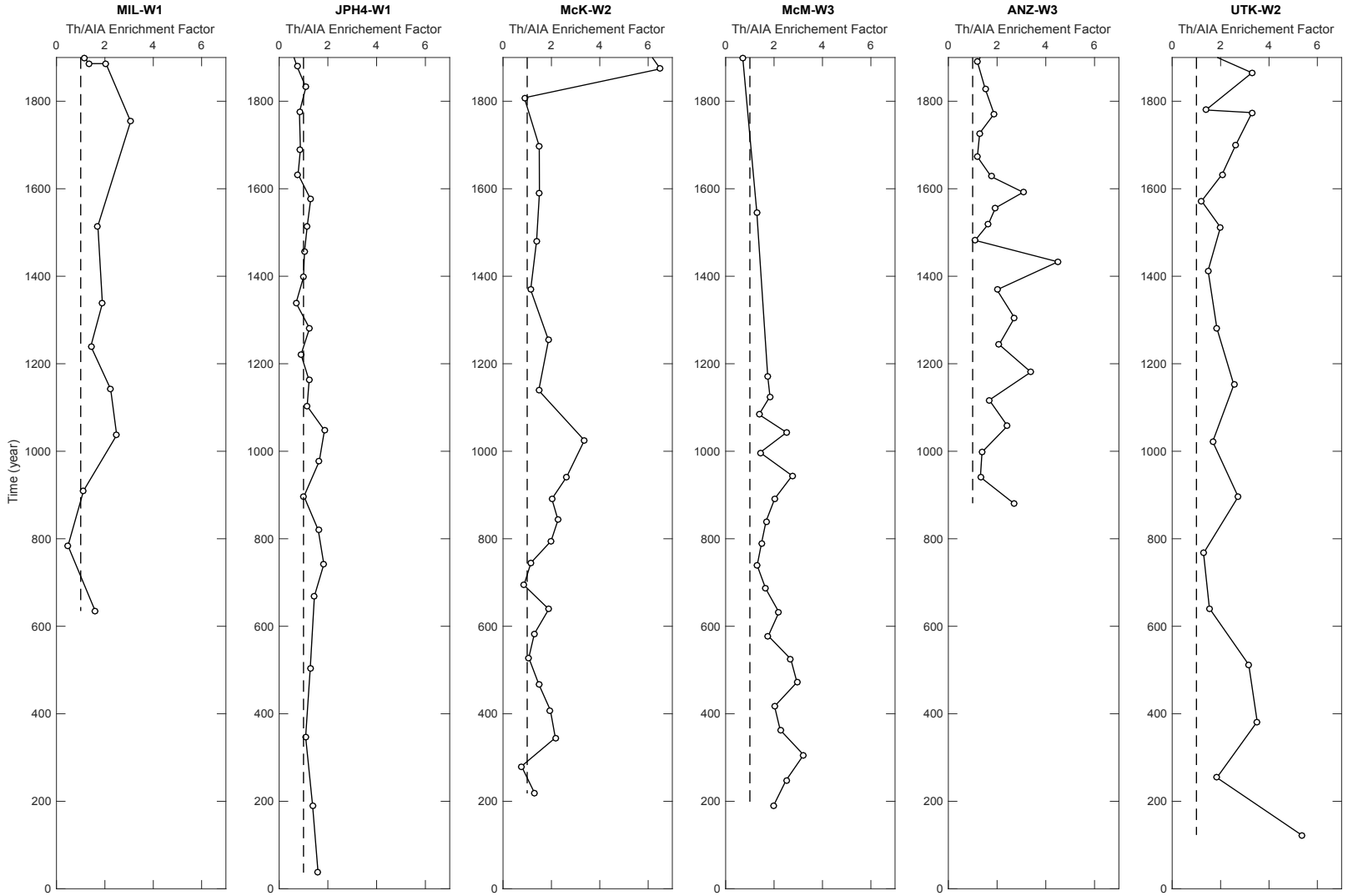

S9: Abundance of large (>7μm) particles in AIA for MIL, McK, McM, ANZ, UTK, and SEB

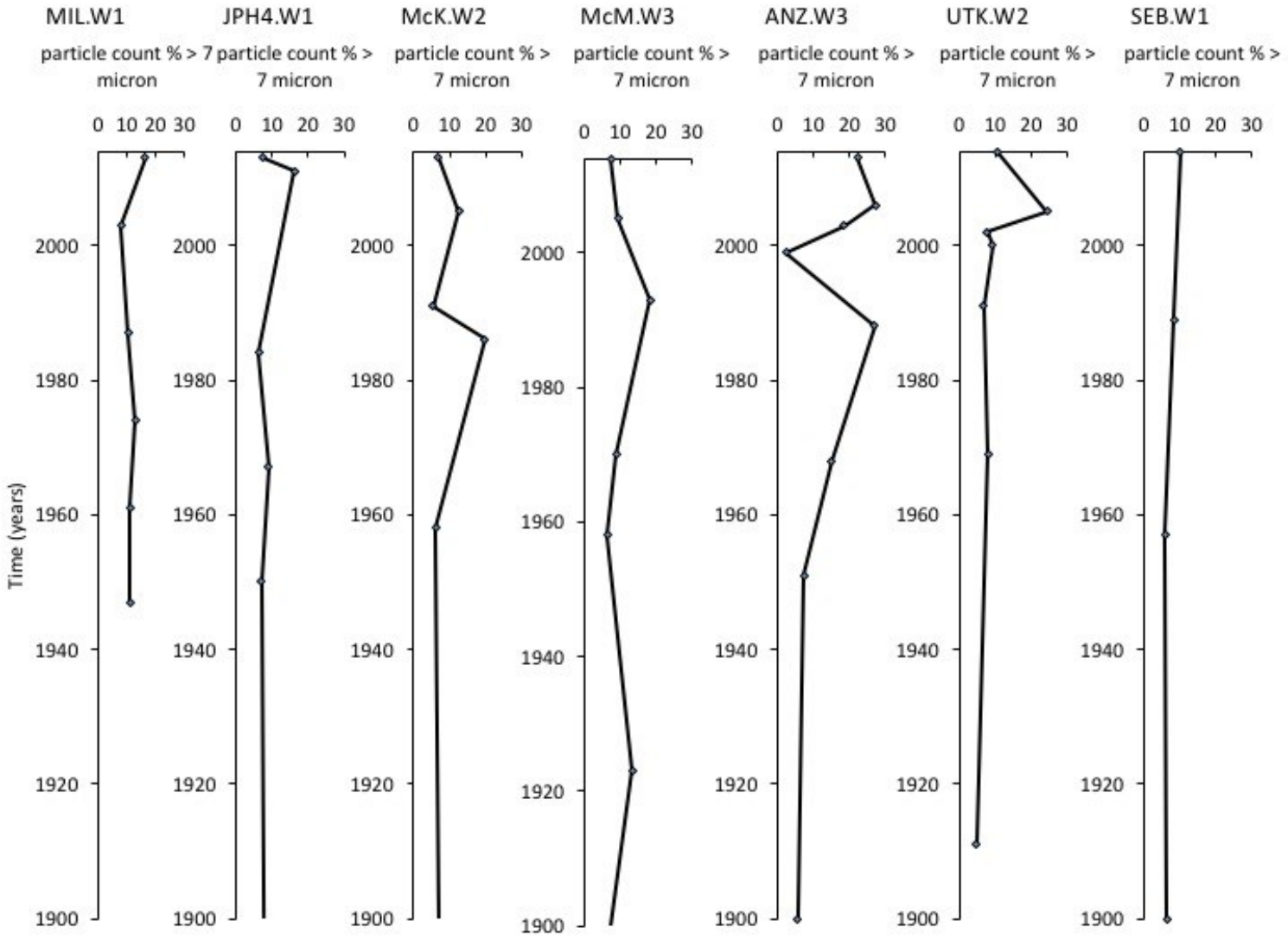

Supporting Information Tables

S1: The list of peat cores GPS coordinates and distances to the nearest road from each site. Effects of road dust are documented between 30-100 m, indicating that the sites are not affected by it (Walker & Everett, 1987). Table of distances from each peat core site to the nearest road.

Site Name	Latitude	Longitude	Distance to Nearest Road (km)
JPH4	57.100227	-111.4167964	0.2
MIL	56.9168953	-111.46681	0.3
McK	57.2168658	-111.7000869	0.6
McM	56.6168503	-111.1835267	0.6
ANZ	56.4666978	-111.0335058	0.1
UTK	55.9834014	-115.1833558	6.0
SEB	53.468397	-114.868467	0.2

S2: Average ash and AIA content values for each peat core since 1900. The number of samples used for each average are displayed as n=#.

Peat Core	Average Ash Content (%)	Average AIA Content (%)
MIL-W1 (n_{ash}= 10, n_{AIA}=19)	9.1	3.0
JPH4-W1 (n=5)	5.4	3.0
McK-W2 (n=17)	2.9	1.3
McM-W3 (n=19)	2.8	1.0
ANZ-W3 (n= 21)	1.5	0.7
UTK-W2 (n= 21)	1.7	0.6
SEB-W3 (n=10)	5.0	2.8

S3: Table of actual living layer MAR for MIL, JPH4, McK, McM, ANZ, and UTK

Peat Core	Accumulation Rate (MAR) Ash	Accumulation Rate (MAR) AIA	Accumulation Rate (MAR) ASA
	g/m^2 yr	**g/m^2 yr**	**g/m^2 yr**
MIL-W1	21.3	9.0	12.3
JPH4-W1	216.1	73.1	143.0
McK-W2	61.2	30.2	31.0
McM-W3	8.8	2.7	2.0
ANZ-W3	13.6	3.7	9.9
UTK-W2	2.3	0.2	2.1

S4: Qualitative description of the quantity of fly ash particles present in JPH4-W1 AIA samples

Sample Name and Year	**Amount of fly ash particles per sample**
JPH4-LL (2013)	absent
JPH4-01 (2011)	common
JPH4-07 (1984)	very common
JPH4-11 (1967)	abundant
JPH4-15 (1950)	abundant

Supporting Information Methods
Methods S1

Sample Collection

Three replicate peat cores were collected from each of 7 sites using a titanium 15 cm x 15cm x 100cm Wardenaar corer (Wardenaar, 1987). The cores were collected in open sections of the bogs to minimize interference from the tree canopies. Each core was wrapped in plastic film then placed in a wooden crate for transport.

Sample Preparation

Each core was frozen upon collection then cut precisely into 1 cm slices using a stainless steel band saw with stainless steel blades. Each slice was divided into subsamples using a stainless steel knife while using polypropylene gloves. The subsample volume used for dust deposition was taken from the edges of each slice and was approximately 56 cm^3. The subsamples were kept frozen until the next step in preparation. The complete subsampling schematic is featured in Figure S1.

Methods S2

pH and Electrical Conductivity (EC) Measurements

The pH and EC were determined for the living layer, every odd layer and the last layer of each peat core. After the edge subsamples were warmed to room temperature over 24 hours, 2mL of pore water was extracted from the subsamples using Luer-Slip Plastic Syringes (10mL) into Microcentrifuge tubes (1.5 mL Graduated Tube with Flat Cap) through a syringe filter (Teflon 0.45 microns, 30mm). EC and then the pH were measured with the Mettler Toledo Seven

Excellence pH/ORP/Ion/Conductivity/DO Meter. The meter was calibrated before each core was analyzed (approximately every 40 samples) using the corresponding standards.

Methods S3

Drying and Ashing of Samples

Once the pore water was extracted, the remaining peat was dried in 4 oz. polypropylene jars for 24 hours at 105 ^{O}C and weighed to determine water content. Each dried sample was ashed at 550 ^{O}C for 16 hours in a muffle furnace to determine ash content. Samples were placed into a desiccator for 24 hours in between drying and ashing to prevent moisture uptake. For more information, see the sample preparation procedure schematic in Figure S2.

Methods S4

AIA

To obtain the AIA, each ashed sample was reacted in 1M HCl for 15 minutes. After the reaction, the solution was filtered using 10 ml polypropylene syringes and Teflon 0.45μm syringe filters in polypropylene casing to collect insoluble ash residue (Sapkota, 2006). The filters were dried using a vacuum pump (Air Admiral diaphragm vacuum/pressure pump, Cole-Parmer, Canada). To access the AIA remaining on the filters, the casings of the syringe filters were removed using a cleaned lathe (Schaublin 135, Bevilard, Switzerland) that was covered in plastic film to minimize possible contamination. For more information, see the sample preparation procedure schematic in Figure S2.

Methods S5

Scanning Electron Microscopy and Energy Dispersive X-ray Analysis

Selected AIA samples were analyzed using scanning electron microscopy (SEM) and energy dispersive x-ray spectroscopy (EDX) to determine the mineralogy and morphology of the particles. Specifically, a Zeiss EVO LS15 EP-SEM and Bruker EDX with an x-ray resolution of 123 eV and a 10 mm2 window area, gun conditions of 25 kV and 200 pA, in variable pressure (VP) mode, using backscattered electron detector (BSD) imaging, was used.

Methods S6

Particle Size Distribution Analysis

XenParTec (XPT-C) Optical Particle Analysis System was used to determine particle size distribution profiles for selected AIA samples. Portions of selected samples were diluted in 10 mL of surfactant (1% Fisherbrand™ FL-70™ Concentrate solution), stirred, and allowed to run through the device for 1 minute before taking a measurement to ensure a representative analysis. Each sample was run for 15 minutes to stabilize the distribution and provide statistically significant particle counts. After each run the XPT-C was cleaned using 18.2 Milli-Q water to remove any remaining particles in the line. There was not enough sample at all sites to perform a different and more accurate particle sizing protocol, since it is recommended to have at least 1 g of sample to do so and this study had an average of 0.03 g of sample.

Methods S7

Age-Depth Models

Sample depth does not provide a reliable reference level to compare peat cores due to spatial and temporal variations in growth and decomposition rates (Damman *et al.*, 1992); therefore, peat samples were dated using 14C and 210Pb as described elsewhere (Shotyk *et al.*, 2016). Briefly, 210Pb was determined using ultralow background gamma spectrometry, and 14C using accelerator mass spectrometry. Unsupported 210Pb was used to calculate ages using the constant rate of supply model (Shotyk *et al.*, 2016). The 14C age dates included those derived using the atmospheric bomb pulse curve (Goodsite *et al.*, 2001). For more information, see (Shotyk *et al.*, 2016).

Supporting Information Appendix
Appendix S1

Ombrotrophic Versus Minerotrophic Peat Layers

Six of the seven cores (JPH4-W1, McK-W2, McM-W3, ANZ-W3, UTK-W2, & SEB-W1) were found to be ombrotrophic throughout the entire core with pH values ranging from 3.1-5.8. The larger values (4.5-5.8) were found in the deeper layers of JPH4-W1 and McK-W2, suggesting the beginning of a transition to minerotrophic peat. The ombrotrophic zone of the seventh peat core, MIL-W1, was determined to be restricted to the top 18cm (with a pH of 4.2): below this depth there is a suddenly change to minerotrophic peat at 21cm with a pH of 6.8 (Figure S3).

Six cores (MIL-W1, JPH4-W1, McK-W2, McM-W3, ANZ-W3, & UTK-W2) followed a similar trend of elevated EC values (300 to 800 μS/cm) within the top 3-4 layers (Figure S5), while SEB-W1 had anomalously high EC values in the top 3 layers (mean = 1843 μS/cm). Elevated EC values in the upper layers are caused by uptake and recycling of ions by the living moss (Malmer, 1988; Mattson & Koutler-Andersson, 1955; Pearsall, 1952). Below the surface (living) layer, the EC values for all seven peat cores were in the range 144-325 μS/cm, consistent with ombrotrophic bog waters (Shotyk, 1988). In contrast, greater values of EC in the deeper layers of MIL-W1 reflect increases in minerotrophic conditions (Figure S6). For more information on EC values before 1900 see Figure S6.

Supporting Information References

Damman AWH, Tolonen K, Sallantaus T. 1992. Element retention and removal in ombrotrophic peat of Haadetkeidas, a boreal Finnish peat bog. *Suo (Helsinki)* **43**: 137–145

Goodsite ME, Rom W, Heinemeier J, Lange T, Ooi S, Appleby PG, Shotyk W, Van Der Knapp WO, Lohse C, Hansen TS. 2001. High-resolution AMS ^{14}C dating of post-bomb peat archives of atmospheric pollutants. *Radiocarbon* **43**: 495–515

Malmer N. 1988. Patterns in the growth and the accumulation of inorganic constituents in the *Sphagnum* cover on ombrotrophic bogs in Scandinavia. *Oikos* **53**: 105–120

Mattson S, Koutler-Andersson E. 1955. Geochemistry of a raised bog. *Annals of the Royal Agricultural College*. Sweden, 321–356

Pearsall W. 1952. The pH of natural soils and its ecological significance. *Journal of Soil Science* **3**: 41–51. DOI: 10.1017/CBO9781107415324.004

Sapkota A. 2006. Mineralogical, Chemical, and Isotopic (Sr, Pb) Composition of Atmospheric Mineral Dusts in an Ombrotrophic Peat Bog, Southern South America. Ruprecht-Karls-Universität, Heidelberg.

Shotyk W. 1988. Review of the inorganic geochemistry of peats and peatland waters. *Earth-Science Reviews* **25**: 95–176. DOI: 10.1016/0012-8252(88)90067-0

Shotyk W, Appleby PG, Bicalho B, Davies L, Froese DG, Grant-Weaver I, Krachler M, Magnan G, Mullan-Boudreau G, Noernberg T, Pelletier R, Shannon B, van Bellen S, Zaccone C. 2016. Peat bogs in northern Alberta, Canada reveal decades of declining atmospheric Pb contamination. *Geophysical Research Letters* **43**: 1–11. DOI: 10.1002/2016GL070952

Walker DA, Everett KR. 1987. Road dust and its environmental impact on Alaskan taiga and tundra. *Arctic and Alpine Research* **19**: 479–489. DOI: 10.2307/1551414

Wardenaar ECP. 1987. A new hand tool for cutting peat profiles. *Canadian Journal of Botany* **65**: 1772–1773. DOI: 10.1139/b87-243

CHAPTER 4: CONCLUSIONS

Research Synthesis

The focus of this project was to understand contemporary and past atmospheric dust deposition rates in the ABS region. To do so, moss and peat samples collected around the ABS region were used as biomonitors. Samples were also taken from the remote sites of Utikuma (moss and peat), CMW (moss), and BMW (moss) to establish background values with which to compare.

The contemporary rates of atmospheric dust deposition expressed using ash, AIA, and ASA, were found to decrease as distance from the ABS region increased. The dust deposition rates farthest from the ABS region (>20 km) were comparable to the background values determined at Utikuma, CMW, and BMW. Bogs closer to the ABS region were found to have more variation in particle size than bogs farther away. Generally, the samples had similar mineral compositions, near and far, with the exception of spherical fly ash particles that were found in some bogs closer to the ABS region. Finally, it was also found that P, Ca, K, Fe, Mg, and S were elevated in the ASA at sites near industrial activity. In particular, P was found to be up to 7 times higher in the ASA of moss collected when compared to background values.

It was observed that a colour variation in the moss ash, ranging from light blue to rust brown, correlated with changes in AIA content. Brown samples had elevated concentrations of AIA, while blue samples correlated with low concentrations of AIA. It is unknown as to why the colour variation exists, yet it is postulated that variation in dust deposition plays a role.

The results for past rates of atmospheric dust deposition were a little more complex. There was a decrease in ash, AIA, and ASA content in the surface layers of the peat profile as distance from ABS region increases, which agreed with the findings in Chapter 1 (Mullan-Boudreau, G.

2017a); however, within the peat cores there was no obvious trend in the ash and AIA profiles over time since the opening of the ABS region (1967). An increase in cumulative mass of dust deposition was found when peat accumulation during the periods 1900-1960 and 1985-present were compared. There appeared to be elevated inputs of large particles when the ABS region opened and again today, but it is unknown what other land-use activities (e.g. agriculture, construction, etc.) could have had an impact. The mineralogy of the particles and morphology were consistent, with the exception of fly ash particles found in the samples from JPH4-W1: these increased in quantity with depth indicating greater rates of deposition of fly ash in the past. Vanadium was found in a few fly ash particles one sample (JPH4-W1 1984).

A positive correlation between average mass accumulations rates in the peat cores (since 1985) and pH was also found, which suggests increased dust deposition closer to the ABS region (Mullan-Boudreau, G. 2017a) may be starting to impact wetland water chemistry. An increase in soluble mineral matter deposition into an acidic nutrient-deficient environment (such as an ombrotrophic bog) allows for increased mineral dissolution that in turn causes increased pH and elevated concentrations of nutrients such as P and Ca. With an increase in soluble mineral matter deposition, there is a risk of shifting the buffering capacity of these bogs, increasing pH and stressing the existing vegetation that is dependent upon the acidic, oligotrophic environment. The shift in pH could also increase competition from plants unable to grow in the otherwise acidic environment.

Study Limitations

The greatest limitation in this study was the amount of sample available. On average, only 1-2% by weight of each dried sample (moss or peat) was AIA, creating a challenge in producing enough sample to perform all desired analysis. The average AIA sample had a mass of only 16 mg. To better examine the particle size distributions of contemporary and past rates of dust deposition, the sample size would have to increase to at least 1g of AIA. To obtain that much AIA more than 60g of dried moss would be needed per sample. Using that much sample for one analysis would greatly reduce the number of other analysis could be performed on the same moss sample. To produce 1g of AIA using the current peat corer and existing slicer size (15cmx15cmx1cm), peat samples would have to be 9 cm thick with a volume of more than 2000 cm^3 and with a dry mass of over 500g. To obtain enough sample the chronological resolution would be greatly reduced and this would limit the amount of information that could be gained from the particle size distribution analysis. Another option would be to increase the size of the peat corer, but this would be impractical. In the end, tradeoffs must be made.

Future Work and Recommendations

Recommendations to improve the methods of this study would be to at least increase (triple) the amount of initial peat sample available to allow for 3 replicates samples to be analyzed for ash content, AIA, etc. The extra sample would increase precision and accuracy of the ash, AIA, and ASA profiles. Additional elemental work (ICP-MS analysis) on AIA and ASA fractions to better understand compositional differences and where contaminants may reside would also be valuable. More precise mineral composition analysis via x-ray diffraction (XRD) analysis, could present more insight into differences in mineralogy with distance from the ABS region (in moss) or changes over time (in peat).

Further study should examine how much dust input would be required to produce greater shifts in pH levels of bogs and the other surrounding ecosystems, as well as how much of an increase in soluble nutrient availability would cause vegetation change. Research into the interaction of mineral dust with other material deposited (i.e. N, S, PAHs, etc.) and how these interactions affect the availability of contaminants would also be beneficial.

BIBLIOGRAPHY

Addison, P. A., & Puckett, K. J. (1980). Deposition of atmospheric pollutants as measured by lichen element content in the Athabasca oil sands area. *Canadian Journal of Botany*, *58*(22), 2323–2334. http://doi.org/10.1139/b80-269

Agriculture Division of Statistics Canada. (2014). Table M23-33: Area of land in farm holdings, census data, Canada and by province, 1871-1971. Retrieved September 6, 2016, from http://www.statcan.gc.ca/pub/11-516-x/sectionm/4057754-eng.htm#1

Alberta Energy Regulator. (2015). Alberta's Energy Reserves 2014 and Supply/Demand Outlook 2015-2024. *Alberta Energy Regulator*: Calgary, pp 3–12.

Alberta Environment and Sustainable Development. (2015). Alberta wetland classification system. *Water Policy Branch, Policy and Planning Division, Alberta Government* Edmonton, AB. p.38. ISBN: 9781460122570

Andrejko MJ, Fiene F, Cohen AD. (1983). Comparison of Ashing Techniques for Determination of the Inorganic Content of Peats. *Testing of Peats and Organic Soils, ASTM STP 820* 5–20

Aničić, M., Tomašević, M., Tasić, M., Rajšić, S., Popović, A., Frontasyeva, M. V., Lierhagen, S., Steinnes, E. (2009). Monitoring of trace element atmospheric deposition using dry and wet moss bags: Accumulation capacity versus exposure time. *Journal of Hazardous Materials*, *171*(1–3), 182–188. http://doi.org/10.1016/j.jhazmat.2009.05.112

Atkinson, L., Hilton, J. W., & Slinger, S. J. (1984). Evaluation of acid-insoluble ash as an indicator of feed digestibility in rainbow trout (salmo gairdneri). *Can, J. Fish. Aquat. Sci.*, *41*, 1384–1386.

Azimi G, Papangelakis VG, Dutrizac JE. (2008). Development of an MSE-based chemical model for the solubility of calcium sulphate in mixed chloride-sulphate solutions. *Fluid Phase Equilibria 266,* 172–186. DOI: 10.1016/j.fluid.2008.01.027

Bargagli R. (1998). *Trace Elements in Terrestrial Plants: An Ecophysiological Approach to Biomonitoring and Biorecovery*. Springer: Verlag Berlin Heidelberg New York

Bari, M. A., Kindzierski, W. B., & Cho, S. (2014). A wintertime investigation of atmospheric deposition of metals and polycyclic aromatic hydrocarbons in the Athabasca Oil Sands Region, Canada. *Science of The Total Environment*, *485–486*, 180–192. http://doi.org/10.1016/j.scitotenv.2014.03.088

Bichard JA. (1987). AOSTRA technical publication series #4: Oil sands composition and behaviour research. *Alberta Oil Sands Technology & Research Authority (AOSTRA)*. Edmonton, Alberta, 3–2 & 3–14

Bragazza, L., & Gerdol, R. (1999). Hydrology, groundwater chemistry and peat chemistry in relation to habitat conditions in a mire on the South Eastern Alps of Italy. *Plant Ecology*, *144*, 243–256. Retrieved from http://dx.doi.org/10.1023/A:1009868113976

Boutron, C. F. (1995). Historical reconstruction of the earth's past atmospheric environment from Greenland and Antarctic snow and ice cores. *Environmental Reviews*, *3*(1), 1–28. http://doi.org/10.1139/a95-001

Burn-Nunes, L., Vallelonga, P., Lee, K., Hong, S., Burton, G., Hou, S., Moy, A., Edwards, R., Loss, R., Rosman, K. (2014). Seasonal variations in the sources of natural and anthropogenic lead deposited at the East Rongbuk Glacier in the high-altitude Himalayas. *Science of the Total Environment*, *487*(1), 407–419. http://doi.org/10.1016/j.scitotenv.2014.03.120

Carslaw, D. C.; Ropkins, K. openair. Environmental Modelling & Software 2012.

Chamberlain, A. C. (1970). Interception and retention of radioactive aerosols by vegetation. *Atmospheric Environment (1967)*, *4*(1), 57–78. http://doi.org/10.1016/0004-6981(70)90054-5

Chamberlain, A. C., & Little, P. (1980). Transport & capture of particles by vegetation. In J. Grace, E. D. Ford, & P. Javiss (Eds.), *Plants and their Atmopsheric Environment*. Blackwell: Oxford. p. 147–173.

Chapman, S. B. (1964). The Ecology of Coom Rigg Moss , Northumberland : II . The Chemistry of Peat Profiles and the Development of the Bog System. *Journal of Ecology*, *52*(2), 315–321.

Clair, T. A., & Percy, K. E. (2015). Assessing forest health in the Alberta Oil Sands Region. Wood Buffalo Enironmental Association Technical Report.

Coe, J. M., & Lindberg, S. E. (1987). The Morphology and Size Distribution of Atmospheric Particles Deposited on Foliage and Inert Surfaces. *Japca*, *37*(3), 237–243. http://doi.org/10.1080/08940630.1987.10466218

Cooper, C. D., & Alley, F. C. (2011). Air pollution control : a design approach. *Waveland Press.* Long Grove, Ill. Retrieved from http://login.ezproxy.library.ualberta.ca/login?url=http://search.ebscohost.com/login.aspx?direct=true&db=cat03710a&AN=alb.4851511&site=eds-live&scope=site

Csavina, J., Field, J., Taylor, M. P., Gao, S., Landázuri, A., Betterton, E. A., & Sáez, A. E. (2012). A review on the importance of metals and metalloids in atmospheric dust and aerosol from mining operations. *Science of the Total Environment*, *433*, 58–73. http://doi.org/10.1016/j.scitotenv.2012.06.013

Damman AWH. (1978). Distribution and movement of elements in ombrotrophic peat bogs. *Oikos. 30*, 480–495. DOI: 10.2307/3543344

Damman AWH, Tolonen K, Sallantaus T. (1992). Element retention and removal in ombrotrophic peat of Haadetkeidas, a boreal Finnish peat bog. *Suo.* Helsinki. *43*, 137–145.

Devito K, Mendoza C, Qualizza C. (2012). Conceptualizing water movement in the Boreal Plains. Implications for watershed reconstruction. *Canadian Oil Sands Network for Research and Development, Environmental and Reclamation Research Group*. Edmonton. 164.

Devito KJ, Mendoza C, Petrone RM, Kettridge N, Waddington JM. (2016). Utikuma Region Study Area (URSA) - Part 1: Hydrogeological and ecohydrological studies (HEAD). *Forestry Chronicle 92*, 57–61. DOI: 10.5558/tfc2016-017

Environment and Climate Change Canada. (2015). PM - Total Particulate Matter (NA - M08). Retrieved November 9, 2016, from http://ec.gc.ca/inrp-npri/donnees-data/index.cfm?do=results&lang=en&opt_facility_name=&opt_facility=&opt_npri_id=&opt_report_year=2015&opt_chemical_type=ALL&opt_industry=&opt_cas_name=NA+-+M08&opt_cas_num=&opt_location_type=ALL&opt_province=AB&opt_postal_code=&opt_community=&opt_csic=&opt_csi2=&opt_asic=&opt_naics3=&opt_naics4=&opt_naics6=9&opt_nai6code=&community1=&opt_urban_center=&opt_province_comm=&opt_media=all&opt_sort_order=A.CITY&opt_sort_direction=ASC&submit=Sort

Farmer, A. M. (1993). The effects of dust on vegetation - a review. *Environ. Pollut. 79*, 63–75.

Félix, O. I., Csavina, J., Field, J., Rine, K. P., Sáez, A. E., & Betterton, E. A. (2015). Use of lead isotopes to identify sources of metal and metalloid contaminants in atmospheric aerosol from mining operations. *Chemosphere*, *122*, 219–226. http://doi.org/10.1016/j.chemosphere.2014.11.057

Fennelly, P. (1976). The Origin and Influence of Airborne Particulates. *American Scientist*, *64*(1), 46–56.

Fialkiewicz-Koziel, B., Smieja-Krol, B., Ostrovnaya, T. M., Frontasyeva, M., Sieminska, A., & Lamentowicz, M. (2015). Peatland microbial communities as indicators of the extreme atmospheric dust deposition. *Water, Air, and Soil Pollution*, *226*(4). http://doi.org/10.1007/s11270-015-2338-1

Fiera Biological Consulting Ltd. (2013). State of the Watershed Report - Phase 3: Water Quantity and Basic Water Quality in the Athabasca Watershed. *Fiera Biological Consulting Report #1234*.

Finney HR, Farnham RS. (1968). Mineralogy of the inorganic fraction of peat from two raised

bogs in northern Minnesota. *Proceedings of the Third International Peat Congress 3*, 102–108.

Fisher GL, Chang DPY, Brummer M. (1976). Fly ash collected from electrostatic precipitators: Microcrystalline structures and the mystery of the spheres. *Science. 192*, 553–555.

Goldich S. (1938). A study in rock-weathering. *The Journal of Geology. 46*, 17–58.

Goodsite ME, Rom W, Heinemeier J, Lange T, Ooi S, Appleby PG, Shotyk W, Van Der Knapp WO, Lohse C, Hansen TS. (2001). High-resolution AMS ^{14}C dating of post-bomb peat archives of atmospheric pollutants. *Radiocarbon. 43*, 495–515.

Gore, A. J. P. (Ed.). (1983). *Ecosystems of the World 4A, Mires: Swamp, Bog, Fen and Moor General Studies*. Amsterdam, Netherlands; New York, N.Y., USA: Elsevier Scientific Publishing Co.

Gore, A. J. P. (Ed.). (1983). *Ecosystems of the World 4B, Mires: Swamp, Bog, Fen and Moor Regional Studies* (4B ed.). Amsterdam, Netherlands; New York, N.Y., USA: Elsevier Scientific Publishing Co.

Gorham, E. (1961). Water, ash, nitrogen and acidity of some bog peats and other organic soils. *Journal of Ecol. 49*, 103–106.

Gorham, E., & Tilton, D. L. (1978). The mineral content of Sphagnum fuscum as affected by human settlement. *Canadian Journal of Botany*, *56*(180), 2755–2759.

Gosselin, P., Hrudey, S. E., Naeth, M. A., Plourde, A., Therrien, R., Van Der Kraak, G., & Xu, Z. (2010). *Environmental and Health Impacts of Canada 's Oil Sands Industry*. Retrieved from http://rsc-src.ca/sites/default/files/pdf/RSC Oil Sands Panel Main Report Oct 2012.pdf

Government of Canada. (2016). Historical Data. *Past Weather and Climate.*Retrived Oct 1, 2016 from: http://climate.weather.gc.ca/historical_data/search_historic_data_e.html

Hodgson W. (1954). Vanadium, nickel, and iron trace metals in crude oils of western Canada. *Bulletin of the American Association of Petroleum Geologists. 38*, 2537–2554.

Hudson-Edwards, K. A., Bristow, C. S., Cibin, G., Mason, G., Peacock, C. L. (2014). Solid-phase phosphorus speciation in Saharan Bodélé Depression dusts and source sediments. *Chem. Geol. 384*, 16–26.

Holsen, T. M., & Noll, K. E. (1992). Dry deposition of atmospheric particles: application of current models to ambient data. *Environmental Science & Technology*, *26*(9), 1807–1815. http://doi.org/10.1021/es00033a015

Hosker, R. P., & Lindberg, S. E. (1982). Review: Atmospheric deposition and plant assimilation of gases and particles. *Atmospheric Environment (1967)*, *16*(5), 889–910. http://doi.org/10.1016/0004-6981(82)90175-5

Jacobson, M. Z. (2002). *Atmospheric Pollution : History, Science, and Regulation*. Cambridge, UK: Cambridge University Press. Retrieved from http://login.ezproxy.library.ualberta.ca/login?url=http://search.ebscohost.com/login.aspx?direct=true&db=nlebk&AN=304527&site=ehost-live&scope=site

Jang H, Etsell TH. (2005). Morphological and mineralogical characterization of oil sands fly ash morphological and mineralogical characterization of oil. *Energy & Fuels. 19*, 2121–2128. DOI: 10.1021/ef050123a

Jeong, G. Y. (2008). Bulk and single-particle mineralogy of Asian dust and a comparison with its source soils. *Journal of Geophysical Research Atmospheres*, *113*(2), 1–16. http://doi.org/10.1029/2007JD008606

Kamber BS, Greig A, Collerson KD. (2005). A new estimate for the composition of weathered young Upper Continental Crust from alluvial sediments, Queensland, Australia. *Geochimica et Cosmochimica Acta. 69*, 1041–1058. DOI: 10.1016/j.gca.2004.08.020

Kaminsky HA. (2009). Characterization of an Athabasca oil sand ore and process streams. *Dissertation Abstracts International, Section B. 70*, 9–18.

Kelly, E. N., Schindler, D. W., Hodson, P. V, Short, J. W., Radmanovich, R., & Nielsen, C. C. (2010). Oil sands development contributes elements toxic at low concentrations to the Athabasca River and its tributaries. *Proceedings of the National Academy of Sciences of the United States of America*, *107*(37), 16178–16183. http://doi.org/10.1073/pnas.1008754107

Kempter H, Frenzel B. (2000). The impact of early mining and smelting on the local tropospheric aerosol detected in ombrotrophic peat bogs in the Harz, Germany. *Water, Air, and Soil Pollution. 121*, 93–108.

Klein, C., & Dutrow, B. (2007). *The 23rd Edition of the Manual of Mineral Science*. New Delhi: John Wiley & Sons, Inc.

Krachler, M., & Shotyk, W. (2004). Natural and anthropogenic enrichments of molybdenum, thorium, and uranium in a complete peat bog profile, Jura Mountains, Switzerland. *Journal of Environmental Monitoring : JEM*, *6*(5), 418–426. http://doi.org/10.1039/b313300a

Landis, M. S., Pancras, J. P., Graney, J. R., Stevens, R. K., Percy, K. E., & Krupa, S. (2012). Receptor Modeling of Epiphytic Lichens to Elucidate the Sources and Spatial Distribution of Inorganic Air Pollution in the Athabasca Oil Sands Region. *Developments in*

Environmental Science Elsevier Ltd (1st ed.). *11*. http://doi.org/10.1016/B978-0-08-097760-7.00018-4

Le Roux G, Fagel N, De Vleeschouwer F, Krachler M, Debaille V, Stille P, Mattielli N, van der Knaap WO, van Leeuwen JFN, Shotyk W. (2012). Volcano- and climate-driven changes in atmospheric dust sources and fluxes since the late glacial in Central Europe. *Geology. 40*, 335–338. DOI: 10.1130/G32586.1

Le Roux G, Laverret E, Shotyk W. (2006). Fate of calcite, apatite and feldspars in an ombrotrophic peat bog, Black Forest, Germany. *Journal of the Geological Society. 163*, 641–646. DOI: 10.1144/0016-764920-035

Little, P. (1979). Particle capture by natural surfaces. *Agricultural Aviation*, *20*(3), 129–144.

Lynam, M. M., Dvonch, J. T., Barres, J. A., Morishita, M., Legge, A., & Percy, K. (2015). Oil sands development and its impact on atmospheric wet deposition of air pollutants to the Athabasca Oil Sands Region, Alberta, Canada. *Environmental Pollution*, *206*, 469–478. http://doi.org/10.1016/j.envpol.2015.07.032

Malmer, N. (1988). Patterns in the growth and the accumulation of inorganic constituents in the Sphagnum cover on ombrotrophic bogs in Scandinavia. *Oikos*, *53*(1), 105–120.

Marx, S. K., McGowan, H. a., & Kamber, B. S. (2009). Long-range dust transport from eastern Australia: A proxy for Holocene aridity and ENSO-type climate variability. *Earth and Planetary Science Letters*, *282*(1–4), 167–177. http://doi.org/10.1016/j.epsl.2009.03.013

Mattson, S., & Koutler-Andersson, E. (1955). Geochemistry of a Raised Bog. *Annals of the Royal Agricultural College*, *21*, 321–356.

McCarthy, J. F., Aherne, F. X., & Okai, D. B. (1974). Use of HCl insoluble ash as an index material for determining apparent digestibility with pigs. *Canadian Journal of Animal Science*, *54*(1), 107–109. http://doi.org/10.4141/cjas74-016

Motallebi, N., Taylor Jr, C. A., & Croes, B. E. (2003). Particulate matter in California: Part 2-Spatial, temporal, and compositional patterns of PM2.5, PM10-2.5, and PM10. *Journal of the Air & Waste Management Association*, *53*(12), 1517–1530. http://doi.org/10.1080/10473289.2003.10466322

Muhs DR, Prospero JM, Buddock MC, Gill TE. (2014). Identifying sources of aeolian mineral dust: Present and past. *Mineral Dust: A Key Player in the Earth System*. Springer Science & Business Media: Dordrecht, 385–409. DOI: 10.1007/978-94-017-8978-3

Munksgaard, N. C., & Parry, D. L. (1998). Lead isotope ratios determined by ICP-MS:

Monitoring of mining-derived metal particulates in atmospheric fallout, Northern Territory, Australia. *Science of the Total Environment*, *217*(1–2), 113–125. http://doi.org/10.1016/S0048-9697(98)00170-3

Nash, T. H. (1996). Growth. *Lichen Biology* (2nd ed.). Cambridge University Press. p.79-82.

Nieboer, E., Ahmed, H. M., Puckett, K. J., & Richardson, D. H. S. (1972). Heavy Metal Content of Lichens in Relation to Distance from a Nickel Smelter in Sudbury, Ontario. *The Lichenologist*, *5*, 292. http://doi.org/10.1017/S0024282972000301

Norton, S. A., & Kahl, J. S. (1987). A comparison of lake sediments and ombrotrophic peat deposits as longterm monitors of atmosplieric pollution. *New approaches to monitoring aquatic ecosystem*. Philadelphia: American Society for Testing and Materials. p. 40-57. http://doi.org/10.1038/nbt0987-872

Pearsall, W. (1952). The pH of Natural Soils and its Ecological Significance. *Journal of Soil Science*, *3*(1), 41–51. http://doi.org/10.1017/CBO9781107415324.004

Percy, K. E. (2013). Ambient Air Quality and Linkage to Ecosystems in the Athabasca OIl Sands. *Geosicence of Climate and Engery*, *11*, 182–201.

Percy, K. E., & Davies, M. J. E. (2012). *Air Quality Modeling in the Athabasca Oil Sands Region*. *Developments in Environmental Science* (1st ed.). Elsevier Ltd., *11*, http://doi.org/10.1016/B978-0-08-097760-7.00004-4

Petrone R, Devito KJ, Mendoza C. (2016). Utikuma Region Study Area (URSA) - Part 2: Aspen Harvest and Recovery Study. *Forestry Chronicle., 92*, 62–65. DOI: 10.5558/tfc2016-018

Pratte, S., Garneau, M., & De Vleeschouwer, F. (2016). Late-Holocene atmospheric dust deposition in eastern Canada (St. Lawrence North Shore). *The Holocene*. http://doi.org/10.1177/0959683616646185

R Development Core Team. (2008). R: A language and environment for statistical computing. *R Foundation for Statistical Computing*: Vienna, Austria.

Rahn, K. A. (1976). Silicon and aluminium in atmospheric aerosols: crust-air fractionations? *Atmospheric Environment*, *10*(1966), 597–601.

Roberson, S., & Weltje, G. J. (2014). Inter-instrument comparison of particle-size analysers. *Sedimentology*, *61*(4), 1157–1174. http://doi.org/10.1111/sed.12093

Santelmann M V, Gorham E. (1988). The influence of airborne road dust on the chemistry of *Sphagnum* mosses. *The Journal of Ecology., 76*, 1219–1231. DOI: 10.2307/2260644

Sapkota, A. (2006). *Mineralogical, Chemical, and Isotopic (Sr, Pb) Composition of Atmospheric Mineral Dusts in an Ombrotrophic Peat Bog, Southern South America*. Ruprecht-Karls-Universität, Hiedelberg.

Sapkota A, Cheburkin AK, Bonani G, Shotyk W. (2007). Six millenia of atmospheric dust depostion in southern South America (Isla Navarino, Chile). *The Holocene., 5*(17), 561–572.

Shelfentook W. (1978). An inventory system for atmospheric emissions in the AOSERP study area. *SNC Tottrup Services Ltd.*: Edmonton, AB.

Shotyk W. (1987). European contributions to the geochemistry of peatland waters, 1890-1940. *Symposium '87 Wetlands/Peatlands*. Canadian Society of Wetlands and Peatlands, and Canadian National Committee, International Peat Society: Edmonton, Alberta, 115–125.

Shotyk W. (1986). Overview of the geochemistry of peatland waters. *Advances in Peatlands Engineering*. National Research Council Canada: Ottawa Ontario, 159–171.

Shotyk W. (1986). Overview of the inorganic geochemistry of peats. *Advances in Peatlands Engineering*. National Research Council Canada: Ottawa Ontario, 249–258.

Shotyk W. (1988). Review of the inorganic geochemistry of peats and peatland waters. *Earth-Science Reviews., 25*, 95–176. DOI: 10.1016/0012-8252(88)90067-0

Shotyk W. (1989). The chemistry of peatland waters. *Water-Quality Bulletin., 14*, 47–57.

Shotyk W. (1996). Natural and anthropogenic enrichments of As, Cu, Pb, Sb, and Zn in ombrotrophic versus minerotrophic peat bog profiles, Jura Mountains, Switzerland. *Water, Air, and Soil Pollution., 90*, 375–405. DOI: 10.1007/BF00282657

Shotyk, W. (1996). Peat bog archives of atmospheric metal deposition : geochemical evaluation of peat profiles , natural variations in metal concentrations , and metal enrichment factors. *Environmental Reviews*, *4*, 149–183. http://doi.org/10.1139/a96-010

Shotyk, W., Norton, S.A., Farmer, J.G. (1997). Summary of the workshop of Peat Bog Archives of Atmospheric Metal Deposition. *Water, Air, and Soil Pollution*, 213–219. DOI: 10.1023/A:1018336828640

Shotyk, W., Belland, R., Duke, J., Kempter, H., Krachler, M., Noernberg, T., Pelletier, R., Vile, M., Wieder, K., Zaccone, C., Zhang, S. (2014). Sphagnum mosses from 21 ombrotrophic bogs in the athabasca bituminous sands region show no significant atmospheric contamination of "heavy metals." *Environmental Science and Technology*, *48*(21), 12603–12611. http://doi.org/10.1021/es503751v

Shotyk, W., Kempter, H., Krachler, M., & Zaccone, C. (2015). Stable (^{206}Pb, ^{207}Pb, ^{208}Pb) and radioactive (^{210}Pb) lead isotopes in 1year of growth of Sphagnum moss from four ombrotrophic bogs in southern Germany: Geochemical significance and environmental implications. *Geochimica et Cosmochimica Acta*, *163*, 101–125. http://doi.org/10.1016/j.gca.2015.04.026

Shotyk, W., Appleby, P.G., Bicalho, B., Davies, L., Froese, D.G., Grant-Weaver, I., Krachler, M., Magnan, G., Mullan-Boudreau, G., Noernberg, T., Pelletier, R., Shannon, B., van Bellen, S., Zaccone, C. (2016). Peat bogs in northern Alberta, Canada reveal decades of declining atmospheric Pb contamination. *Geophysical Research Letters., 43*, 1–11. DOI: 10.1002/2016GL070952

Shotyk, W., Bicalho, B., Cuss, C. W., Duke, M. J. M., Noernberg, T., Pelletier, R., Steinnes, E., Zaccone, C. (2016). Dust is the dominant source of "heavy metals" to peat moss (*Sphagnum fuscum*) in the bogs of the Athabasca Bituminous Sands region of northern Alberta. *Environment International*, *92–93*, 494–506. http://doi.org/10.1016/j.envint.2016.03.018

Small, E. (1972). Ecological significance of four critical elements in plants of raised spagnum peat bogs. *Ecology*., *53* (3), 498–503.

Steinmann, P., & Shotyk, W. (1997). Geochemistry, mineralogy, and geochemical mass balance on major elements in two peat bog profiles (Jura Mountains, Switzerland). *Chemical Geology*, *138*(1–2), 25–53. http://doi.org/10.1016/S0009-2541(96)00171-4

Stringham, G. (2012). *Energy Developments in Canada's Oil Sands*. *Developments in Environmental Science* (1st ed., Vol. 11). Elsevier Ltd. http://doi.org/10.1016/B978-0-08-097760-7.00002-0

Suzuki, K. (2006). Characterisation of airborne particulates and associated trace metals deposited on tree bark by ICP-OES, ICP-MS, SEM-EDX and laser ablation ICP-MS. *Atmospheric Environment*, *40*(14), 2626–2634. http://doi.org/10.1016/j.atmosenv.2005.12.022

Taylor, F. G., & Witherspoon, J. P. (1972). Retention of simulated fallout particles by lichens and mosses. *Health Physics*, *23*, 867–869.

University of Liège. (2009). Survey years of lead. Retrieved June 29, 2015, from http://reflexions.ulg.ac.be/cms/c_19292/fr/enquete-sur-les-annees-de-plomb?portal=j_55&printView=true

Urban, N. R., Verry, E. S., & Eisenreich, S. J. (1995). Retention and mobility of cations in a small peatland: trends and mechanisms. *Water, Air and Soil Pollution*, *79*, 201–224.

Van Keulen, J., & Young, B. A. (1977). Evaluation of acid-insoluble ash as a natural marker in

ruminant digestibility studies. *Journal of Animal Science*, *44*(2), 282–287.

Vile, M.A., Novak, M.J.V., Brizova, E., Wieder, R.K., Schell, W.R. (1995). Historical rates of atmospheric Pb deposition using ^{210}Pb dated peat cores: Corroboration, computation, and interpretation. *Water, Air, and Soil Pollution., 79*, 89–106. DOI: 10.1007/BF01100432

Vile, M.A., Wieder, R.K., Novák, M. (2000). 200 years of Pb deposition throughout the Czech Republic: Patterns and sources. *Environmental Science and Technology., 34*, 12–21. DOI: 10.1021/es990032q

Vile, M. A., Wieder, R. K., Berryman, S., Vitt, D. H. (2010). WBEA 2010 Annual Report: Development of Monitoring Protocols for N & S Sensitive Bog Ecosystems. *Wood Buffalo Enironmental Association*. Villanova Univesity.

Vile, M. A., Wieder, R. K., Vitt, D. H., Berryman, S. (2013). Final Report: Development of monitoring protocols for nitrogen-sensitive bog ecosystems, including further development of lichen monitoring tools. *Wood Buffalo Environmental Association*., p.1–91.

Vuorela, I. (1983). Field erosion by wind as indicated by fluctuations in the ash content of *Sphagnum* peat. *Bulletin of the Geological Society of Finland, 55*, 25–33.

Walker, D.A., Everett, K.R. (1987). Road dust and its environmental impact on Alaskan taiga and tundra. *Arctic and Alpine Research., 19*, 479–489. DOI: 10.2307/1551414

Wadge, A., Hutton, M., & Peterson, P. J. (1996). The Concentrations and Particle Size Relationships of Selected Trace Elements in Fly Ashes from U.K. Coal-Fired Power Plants and a Refuse Incinerator. *The Science of the Total Environment*, *54*, 13–27.

Wang, X., Chow, J.C., Kohl, S.D., Percy, K.E., Legge, A.H., Watson, J.G. (2015). Characterization of PM 2.5 and PM 10 fugitive dust source profiles in the Athabasca Oil Sands Region. *Journal of the Air & Waste Management Association., 65*, 1421–1433. DOI: 10.1080/10962247.2015.1100693

Wang, X., Chow, J.C., Kohl, S.D., Yatavelli, L.N.R., Percy, K.E., Legge, A.H., Watson, J.G. (2015). Wind erosion potential for fugitive dust sources in the Athabasca Oil Sands Region. *Aeolian Research., 18*, 121–134. DOI: 10.1016/j.aeolia.2015.07.004

Watmough, S.A., Whitfield, C.J., Fenn, M.E. (2014). The importance of atmospheric base cation deposition for preventing soil acidification in the Athabasca Oil Sands Region of Canada. *Science of the Total Environment, 493*, 1–11. DOI: 10.1016/j.scitotenv.2014.05.110

Watson, J.G., Chow, J.C., Wang, X., Kohl, S.D. (2010). Emission characterization plans for the

Athabasca oil sands region. In: Tropp RJ and Legge AH (eds)., *Proceedings, 103rd Annual Meeting of the Air & Waste Management Association*. Air & Waste Management Association: Pittsburgh, PA, 1–6

Watson, J.G., Chow, J.C., Wang, X., Kohl, S.D., Yatavelli, L.N.R. (2014). Windblown Fugitive Dust Characterization in the Athabasca Oil Sands Region. *Wood Buffalo Environmental Association*. Desert Research Institute: McMurray, 1-1-4–19

Wardenaar, E.C.P. (1987). A new hand tool for cutting peat profiles. *Canadian Journal of Botany., 65*, 1772–1773. DOI: 10.1139/b87-243

Wedepohl, K.H. (1995). Composition of the Continental Crust. *Geochimica et Cosmochimica Acta., 59*, 11217–1232. DOI: 10.1016/B978-0-08-095975-7.00301-6

Welton, J.E. (2003). *SEM petrology Atlas*. The American Association of Petroleum Geologists: Tulsa, Oklahoma

Wieder, R.K., Novák, M., Schell, W.R., Rhodes, T. (1994). Rates of peat accumulation over the past 200 years in five *Sphagnum*-dominated peatlands in the United States. *Journal of Paleolimnology., 12*, 35–47. DOI: 10.1007/BF00677988

Wieder, R.K., Vitt, D.H., Burke-Scoll, M., Scott, K.D., House, M., Vile, M.A. (2010). Nitrogen and sulphur deposition and the growth of *Sphagnum fuscum* in bogs of the Athabasca Oil Sands Region, Alberta. *Journal of Limnology., 69*, 161–170. DOI: 10.3274/JL10-69-S1-16

Willeke, K., & Whitby, K. T. (1975). Atmospheric Aerosols: Size Distribution Interpretation. *Journal of the Air Pollution Control Association*, *25*(5), 529–534. http://doi.org/10.1080/00022470.1975.10470110

Williamson, B. J., Mikhailova, I., Purvis, O. W., & Udachin, V. (2004). SEM-EDX analysis in the source apportionment of particulate matter on Hypogymnia physodes lichen transplants around the Cu smelter and former mining town of Karabash, South Urals, Russia. *Science of the Total Environment*, *322*(1–3), 139–154. http://doi.org/10.1016/j.scitotenv.2003.09.021

Yoo, J. G., Jo, Y. M. (2003). Utilization of coal fly ash as a slow-release granular medium for soil improvement. *Journal of the Air Waste Management Association*, *53* (1), 77–83.

Zaccone, C., Miano, T. M., & Shotyk, W. (2012). Interpreting the ash trend within ombrotrophic bog profiles: atmospheric dust depositions vs. mineralization processes. The Etang de la Gruère case study. *Plant and Soil*, *353*(1–2), 1–9. http://doi.org/10.1007/s11104-011-1055-9

Zaccone, C., Pabst, S., Senesi, G. S., Shotyk, W., & Miano, T. M. (2013). Comparative

evaluation of the mineralogical composition of Sphagnum peat and their corresponding humic acids, and implications for understanding past dust depositions. *Quaternary International*, *306*, 80–87. http://doi.org/10.1016/j.quaint.2013.04.017

Zhang, Y., Shotyk, W., Zaccone, C., Noernberg, T., Pelletier, R., Bicalho, B., Froese, D. G., Davies, L., Martin, J. W. (2016). Airborne petcoke dust is a major source of polycyclic aromatic hydrocarbons in the Athabasca oil sands region. *Environmental Science and Technology*, *50* (4), 1711–1720.

APPENDIX 1: Bibliography of papers to which this work has contributed

APPENDIX 2: A copy of "Peat bogs in northern Alberta, Canada reveal decades of declining atmospheric Pb contamination" which was published in geophysical research letters.

APPENDIX 3: Fort McKay furnace filter SEM and EDX analysis

APPENDIX 4: JPH4-W1 SEM images and EDX spectrum. AIA samples were examined for morphology and mineralogy. The number on the SEM image corresponds with the spectrum number.

APPENDIX 5: XRD mineral analysis on 2013-2014 moss samples performed by Steve Hillier of the University of Edinburgh.

APPENDIX 6: UTK-W2 SEM images and EDX spectrum. AIA samples were examined for morphology and mineralogy. The number on the SEM image corresponds with the spectrum number.

APPENDIX 1: Bibliography of papers to which this work has contributed

Shotyk W, Appleby PG, Bicalho B, Davies L, Froese D, Grant-Weaver I, Krachler M, Magnan G, Mullan-Boudreau G, Noernberg T, Pelletier R Shannon B, van Bellen S, and Zaccone C (2016). Peat bogs in northern Alberta, Canada reveal decades of declining atmospheric Pb contamination. Geophysical Research Letters 43(18): 9964-9974.

Groebner, K., Haughland, D., Mullan-Boudreau, G., and Shotyk, W. (####) Comparison of the acid-insoluble ash content of lichens and Sphagnum moss from ombrotrophic bogs: implications for monitoring atmospheric deposition of contaminants. Ecological Indicators (in preparation).

Magnan, G, van Bellen S, Zaccone, C, Mullan-Boudreau G, Davies L, Froese D, Garneau M, Shotyk W. Impact of the Little Ice age and 20th century climate change on peatland vegetation dynamics in northern Alberta using a multi-proxy approach and high-resolution peat chronologies. (to be submitted to Quaternary Science Reviews)

Shotyk W, Appleby PG, Bicalho B, Davies L, Froese D, Grant-Weaver I, Krachler M, Magnan G, Mullan-Boudreau G, Noernberg T, Pelletier R, Shannon B, van Bellen S, and Zaccone C (2016). Peat bogs document decades of declining atmospheric contamination by trace metals in the Athabasca Bituminous Sands region of northern Alberta, Canada. Environmental Science and Technology (in review).

van Bellen S, Magnan G, Davies L, Froese D, Mullan-Boudreau G, Zaccone C, Garneau M, and Shotyk W. (2017) Testate amoebae records indicate widespread and unprecedented late-20th century drying in ombrotrophic peatlands of northern Alberta, Canada. (in preparation)

APPENDIX 2: A copy of "Peat bogs in northern Alberta, Canada reveal decades of declining atmospheric Pb contamination" which was published in geophysical research letters.

AGU PUBLICATIONS

Geophysical Research Letters

RESEARCH LETTER

10.1002/2016GL070952

Key Points:

- There is effectively zero atmospheric Pb contamination in this region today
- Atmospheric Pb contamination has been in decline for decades
- Bogs are excellent archives of atmospheric Pb deposition

Supporting Information:

- Supporting Information S1
- Table S3

Correspondence to:

W. Shotyk,
shotyk@ualberta.ca

Citation:

Shotyk, W., et al. (2016), Peat bogs in northern Alberta, Canada reveal decades of declining atmospheric Pb contamination, Geophys. Res. Lett., 43, 9964–9974, doi:10.1002/2016GL070952.

Received 25 AUG 2016 Accepted 30 AUG 2016 Published online 27 SEP 2016

Peat bogs in northern Alberta, Canada reveal decades of declining atmospheric Pb contamination

William Shotyk[1], Peter G. Appleby[2], Beatriz Bicalho[1], Lauren Davies[3], Duane Froese[3], Iain Grant-Weaver[1], Michael Krachler[4], Gabriel Magnan[1], Gillian Mullan-Boudreau[1], Tommy Noernberg[1], Rick Pelletier[1], Bob Shannon[5], Simon van Bellen[1], and Claudio Zaccone[6]

[1]Department of Renewable Resources, University of Alberta, Edmonton, Alberta, Canada, [2]Department of Mathematical Sciences, University of Liverpool, Liverpool, UK, [3]Department of Earth and Atmospheric Sciences, University of Alberta, Edmonton, Alberta, Canada, [4]European Commission, Joint Research Centre, Directorate Nuclear Safety and Security, Karlsruhe, Germany, [5]Quality Radioanalytical Support, LLC, Grand Marais, Minnesota, USA, [6]Department of the Sciences of Agriculture, Food and Environment, University of Foggia, Foggia, Italy

Abstract Peat cores were collected from six bogs in northern Alberta to reconstruct changes in the atmospheric deposition of Pb, a valuable tracer of human activities. In each profile, the maximum Pb enrichment is found well below the surface. Radiometric age dating using three independent approaches (^{14}C measurements of plant macrofossils combined with the atmospheric bomb pulse curve, plus ^{210}Pb confirmed using the fallout radionuclides ^{137}Cs and ^{241}Am) showed that Pb contamination has been in decline for decades. Today, the surface layers of these bogs are comparable in composition to the "cleanest" peat samples ever found in the Northern Hemisphere, from a Swiss bog ~ 6000 to 9000 years old. The lack of contemporary Pb contamination in the Alberta bogs is testimony to successful international efforts of the past decades to reduce anthropogenic emissions of this potentially toxic metal to the atmosphere.

1. Introduction

Human activities have had a greater impact on the geochemical cycle of Pb than that of any other potentially toxic heavy metal [Nriagu, 1978]. Atmospheric Pb contamination is a global phenomenon [Ng and Patterson, 1981; Boutron et al., 1994], the result of mining, smelting, refining, and metallurgical processing of Pb and other metal sulphides, in addition to the combustion of coal and other fossil fuels [Shotyk and Le Roux, 2005]. During the twentieth century, gasoline Pb additives were the largest single source of anthropogenic Pb to the atmosphere [Wu and Boyle, 1997], but Arctic ice cores provide remarkable records of hemispheric Pb contamination extending back in time more than three millennia [Murozumi et al., 1969; Rosman et al., 1997; Zheng et al., 2007]. An ice core from Devon Island, Nunavut, Canada, for example, has provided a 15,000 year record of atmospheric Pb deposition, with evidence of Pb contamination dating back to the time of the Phoenicians, followed by the Greek and then Roman civilizations, with notable episodes of intense Pb emissions during the Medieval Period from silver mining in central Europe, then the Industrial Revolution, and later, from the introduction of leaded gasoline [Zheng et al., 2007]. The use of gasoline Pb additives, first introduced in the U.S., in 1923 [Nriagu, 1990], peaked in 1970, when global production reached 250,000 tons per year [Wu and Boyle, 1997] and air Pb has been in decline ever since. High-resolution reconstructions of Pb concentrations [McConnell et al., 2002] and stable Pb isotopes [Shotyk et al., 2005] of polar ice representing the 19th and 20th centuries show that the elimination of leaded gasoline played a very important role in the reduction of the global Pb problem, but that other technological changes and improvements were also very important, given that Pb was emitted to the environment from many other sources. Lead in the atmosphere, therefore, is derived from a complex mixture of natural and anthropogenic sources varying in time and space. One of the challenges of environmental geochemistry is to develop ways and means of reconstructing the changing sources of atmospheric Pb and their rates of deposition to terrestrial and aquatic ecosystems [Bindler et al., 2008; Shotyk and Krachler, 2010].

Ombrotrophic (i.e., rain-fed) peat bogs are also excellent archives of atmospheric Pb, providing the first com-plete, long-term record (15,000 years) of atmospheric Pb deposition in Europe: there, anthropogenic inputs have dominated continuously for more than 3000 years [Shotyk et al., 1998; Shotyk et al., 2001]. Detailed his-tories of atmospheric Pb contamination have since been reconstructed using peat cores from bogs across

Geophysical Research Letters 10.1002/2016GL070952

Europe [Bränvall et al., 2001; Klaminder et al., 2003; Novák et al., 2003; Monna et al., 2004; Cloy et al., 2005, 2008; Kylander et al., 2005; Le Roux et al., 2005; Bindler et al., 2008; Farmer et al., 2015]. With appropriate methods for sample collection, handling, preparation, and age dating [Givelet et al., 2004] peat cores have provided extremely detailed reconstructions of atmospheric Pb pollution histories, from Antiquity to the present day. The Lindow Moss near Manchester, for example, showed evidence of atmospheric Pb contamination beginning around 900 B.C., predating the arrival of the Romans in 50 B.C. and resulting from Iron Age Pb mining in England [Le Roux et al., 2004]. Precisely dated peat cores from Denmark and the Faroe Islands showed that atmospheric Pb contamination began its decline 25 years before the introduction of unleaded gasoline [Shotyk et al., 2003, 2005]. Given that rates of atmospheric Pb deposition obtained from living Sphagnum moss collected from bogs agree with data obtained from direct deposition measurements [Kempter et al., 2010], rates of Pb accumulation obtained from peat cores appear to be reasonable reflections of past rates of atmospheric Pb deposition.

In contrast to the detailed reconstructions of atmospheric metal contamination in Europe, much less work has been undertaken in North America. Except for recent studies of atmospheric Hg deposition reconstructed using peat cores from Ontario [Givelet et al., 2003] and Maine [Roos-Barraclough et al., 2006; Norton et al.,

2015] there have been few studies of atmospheric Pb using peat cores from ombrotrophic bogs in North America [Norton et al., 1997; Benoit et al., 1998; Weiss et al., 2002; Kylander et al., 2009; Pratte et al., 2013]. Careful age dating of peat cores from three bogs in southern Ontario showed that atmospheric Pb deposition went into decline toward the end of the 1950s [Givelet et al., 2003], two decades before the introduction of unleaded gasoline in Canada, in 1976. Subsequent work on one of those cores using stable Pb isotopes showed that the predominant anthropogenic source of Pb in southern Ontario today is from the smelting and refining of metallic ores in northern Ontario and Quebec [Shotyk and Krachler, 2010]. In western Canada, there are no published peat bog reconstructions of atmospheric Pb deposition available for comparison.

Based on a recent survey of heavy metals using snowpack sampling, it was claimed that open pit mining and upgrading of the Athabasca Bituminous Sands (ABS) in northeastern Alberta (AB) is a significant source of atmospheric Pb along with many other chalcophile elements such as Ag, Cd, Sb, and Tl [Kelly et al., 2010]. To test this hypothesis, Sphagnum moss was collected at three sites from each of 22 bogs in the vicinity of the ABS and total metal concentrations measured [Shotyk et al., 2014]. Sphagnum fuscum is the dominant hummock-forming moss in peat bogs, and as such, it receives metals exclusively from the air [Crum, 1988]. This species is found in bogs across North America and Europe and has been used for many decades, particularly in Europe, for monitoring atmospheric heavy metal deposition [Shotyk et al., 2015]. After correcting for differences in the abundance of mineral dust particles using Th, no significant contribution of anthropogenic Pb could be found in the moss samples from the ABS region [Shotyk et al., 2014]. A subsequent study con-firmed this result and, further, showed that metal concentrations in these moss samples were comparable to the contemporary "background" values for moss from central and northern Norway [Shotyk et al., 1996a].

While moss samples provide an indication of the extent of contamination in contemporary atmospheric deposition, they provide no indication of the changing rates and sources of contaminants in the past. To fill this knowledge gap, peat cores were collected from five bogs in the vicinity of the open pit mines and bitumen upgraders in the ABS region, as well as a core from a bog 264 km upwind of this increasingly industrialized region. The results obtained from these cores are then compared with peat cores collected from ombrotrophic bogs in Europe to help put the results from the AB bogs into a global perspective.

2. Methods

Peat cores were collected from ombrotrophic (rain-fed) bogs in northern AB (Figure 1 and Figure S1): five sites are in the vicinity of open pit mines and upgrading facilities of ABS, and one site is far removed from this area and serves to provide a regional background signal. We provide the precise location of each coring site along with the distance (in km) from the midpoint to the two central upgraders (supporting information Table S1). Samples and certified reference materials were dissolved and trace metals determined using inductively coupled plasma-mass spectrometry (ICP-MS) in the ultraclean, metal-free SWAMP laboratory (supporting information Table S2). The paleobotanical stratigraphy of each site was reconstructed (supporting information Figure S2) and selected plant macrofossils age dated using ^{14}C. The pH of the pore waters and the ash content of the peats were used to identify the thickness of the ombrotrophic zone in each profile

Geophysical Research Letters 10.1002/2016GL070952

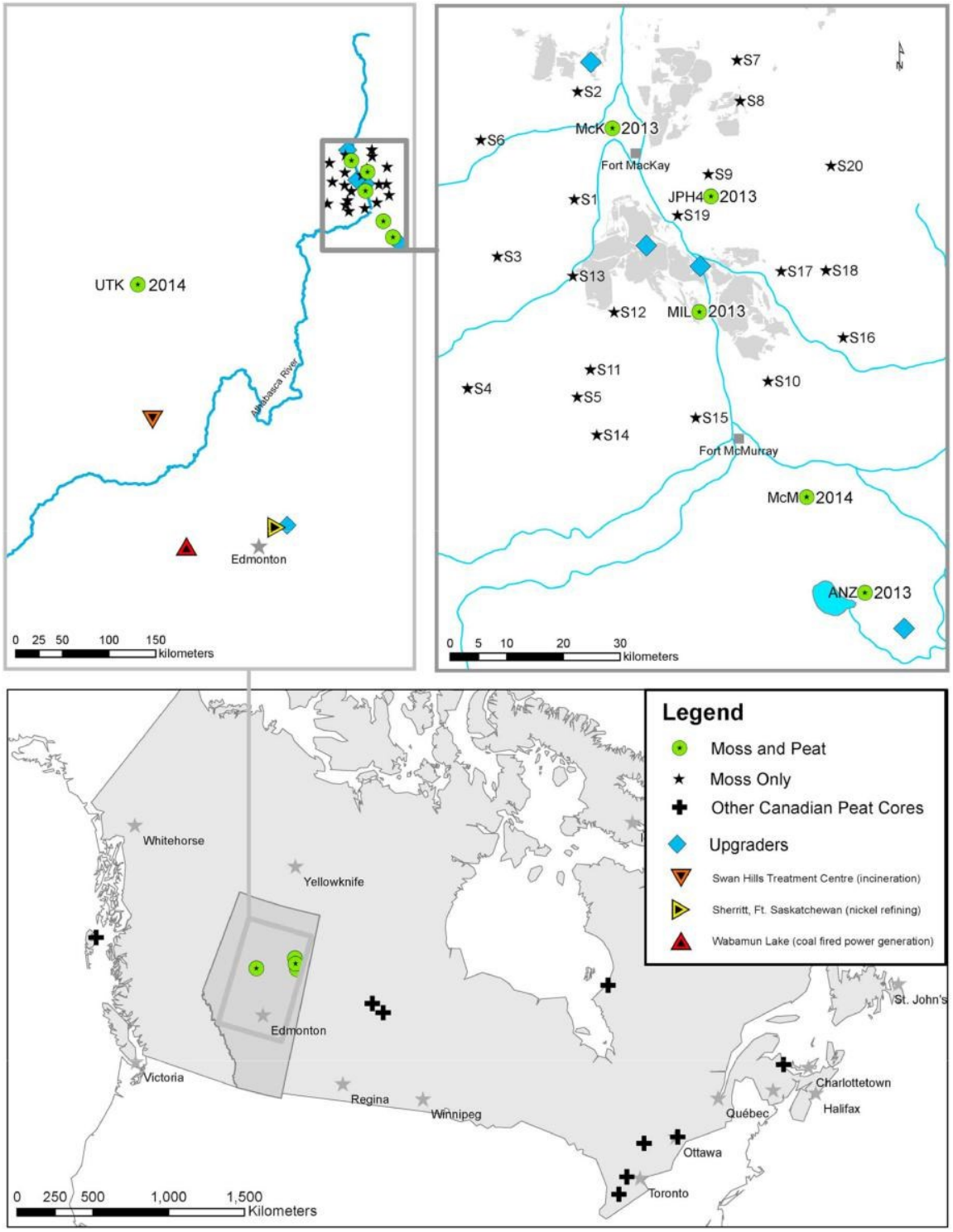

Figure 1. Map showing the locations of the peat cores described in the text (McK, JPH4, MIL, McM, ANZ and UTK) as well as the year of collection. Also shown for comparison, the locations of the moss samples collected from peat bogs of this region which were also measured for trace metals, including Pb and Th (Shotyk et al., 2014). The shaded area in the map shown in the upper right corner refers to the locations of open pit bitumen mines. Also shown are the locations of the bitumen upgraders in the area of the Athabasca Bituminous Sands, namely Suncor, Syncrude, CNRL, and Nexen. The locations of coal-fired electricity generating stations near Lake Wabamun west of Edmonton, the bitumen upgrader east of Edmonton, the Ni refinery at Fort Saskatchewan, and the hazardous waste incinerator at Swan Hills, are also shown. The map of Canada shows the locations of peat cores collected in the past, but recently measured for Pb and Th in their surface layers [Shotyk et al., 2014]

Geophysical Research Letters 10.1002/2016GL070952

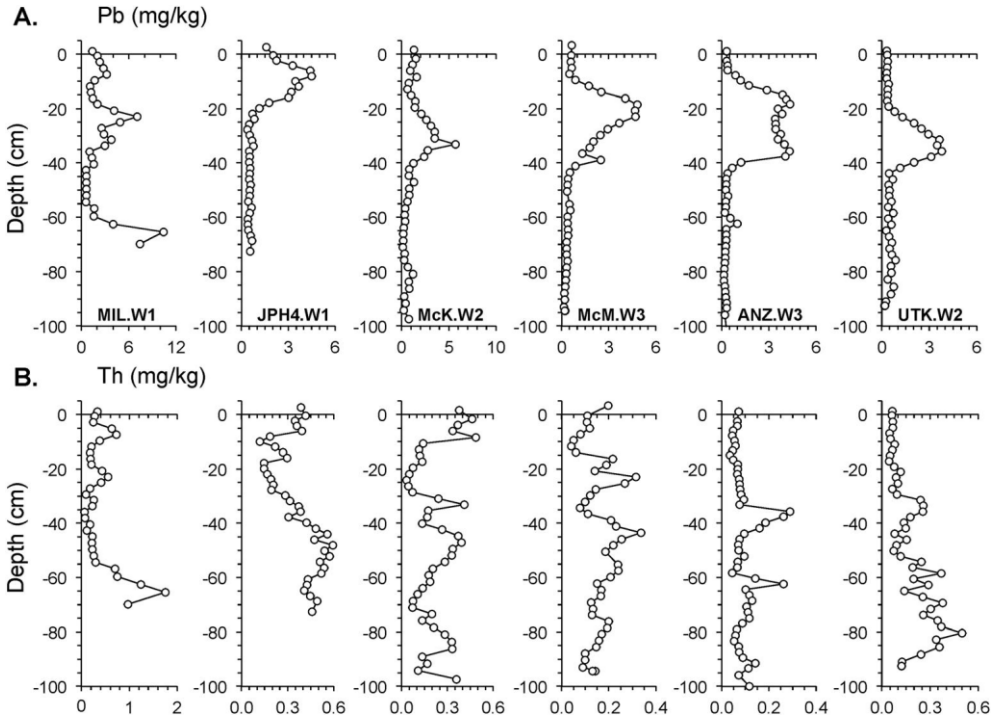

Figure 2. (A) Pb concentrations (mg/kg) in the six peat cores, listed in order of increasing distance from the mid-point between the two central bitumen upgraders. (B) Th concentrations (mg/kg).

(supporting information Figure S3). In addition to ^{14}C (supporting information Tables S3 and S4), all six peat cores were also dated using ^{210}Pb (CRS Model) determined using gamma spectrometry, and the ages confirmed with established chronostratigraphic markers (^{137}Cs and ^{241}Am). The degree of peat humification was evaluated using the main atomic ratios (C/N, H/C and O/C) of selected samples combined with stable isotopes ($\delta^{13}C$ and $\delta^{15}N$) and bulk density (supporting information Table S5). Analytical details are provided in the supporting information.

3. Results and Discussion

The Pb concentrations in the top living layer of each core are very low (Figure 2a): the maximum (1.6 mg/kg at JPH4) is less than corresponding value for the Drizzle Bog (2.0 mg/kg) on Haida Gwai, a large island west of British Columbia (Figure 1). The Pb concentrations in the top layer at ANZ and UTK (0.3 mg/kg) are similar to the corresponding values for the "cleanest" peat samples ever found (0.28 ± 0.05 mg/kg, n = 17) in the Swiss bog "Etang de la Gruère" (EGR) and dating from 5320 to 8030 ^{14}C yr B.P. [Shotyk et al., 1998]. In each bog, the Pb concentration profiles reveal a prominent peak below the surface, ranging in depth from ~ 10 cm at MIL to ~ 35 cm at UTK (Figure 2a). Part of the variation in Pb concentrations seen in any given peat profile will have been caused by anthropogenic, atmospheric deposition, but part may be due to differences in the abundance of mineral matter, reflecting natural variations in atmospheric deposition of mineral dusts, peat decom-position, and humification, or both (supporting information Figure S1). Thorium, a conservative, lithophile element which is easily measured using ICP-MS alongside Pb, can be used as an indicator of the abundance of mineral particles (Figure 2b). To correct the Pb concentrations for these variations, Pb was normalized to Th (Figure 3a). The Pb:Th ratios show maxima which are ~ 10 to 30 cm below the surface of each bog: this is a clear and unambiguous indication that the maximum extent of Pb contamination in atmospheric aerosols has been declining. Moreover, the Pb:Th ratios measured in the topmost layers of peat from these bogs (2.1 to 5.0) are comparable to the corresponding values for the cleanest peat samples ever found (2.3 to 4.6, average 3.4 ± 0.6, n = 18), namely those from the EGR bog in Switzerland [Krachler and Shotyk, 2004] and dating from 5320 to 8030 ^{14}C yr B.P. The crustal enrichment factor (EF) for Pb in the AB profiles was calculated by normalizing the Pb:Th ratio (Figure 3a) to the corresponding ratio for the Upper Continental Crust [Wedepohl, 1995].

Geophysical Research Letters 10.1002/2016GL070952

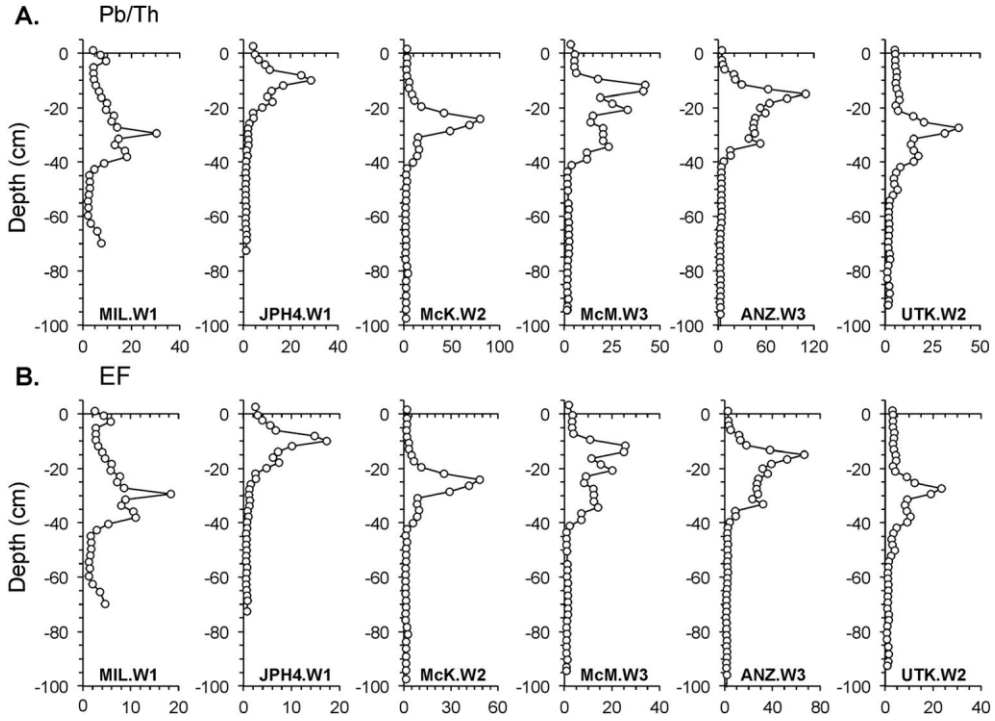

Figure 3. (A) Pb:Th for each of the six peat cores. (B) Pb Enrichment Factor, calculated using the Pb and Th concentrations for the Upper Continental Crust (Wedepohl, 1995).

Remarkably, the Pb EF at the surface of these bogs today ranges from only 1.9 to 2.5 (Figure 3b). A Pb EF = 1 indicates no Pb enrichment, relative to the Pb:Th ratio of crustal rocks, and an EF ≥ 2 may be considered the minimum EF to signal an additional, anthropogenic Pb source, over and above the natural Pb contribution to the atmosphere from soil-derived dust particles [Shotyk et al., 1998; Zheng et al., 2007]. In other words, the extent of Pb contamination in the topmost layers of the AB bogs is so small, and it is difficult to distinguish contemporary Pb to Th ratios from the natural background values. The Th concentrations were also used to calculate the natural concentrations of Pb in these profiles and total Pb to calculate the concentrations of anthropogenic Pb by difference: these calculations show that (i) in the past, natural Pb inputs were tiny, compared to the supply of Pb from human activities, (ii) that anthropogenic inputs have been in decline for decades, and (iii) that today, anthropogenic and natural Pb concentrations have converged (supporting information Figure S4).

3.1. Atmospheric Pb in AB, in Perspective

To put the data for the AB samples into context, the extent of Pb contamination in the top layers of these peat bogs today is no more than that found in the EGR peat bog from Switzerland in the sample dating from 3000 ^{14}C yr B.P. (3710 to 3210 cal yr B.P.): that sample was the first to have a Pb:Sc ratio double the natural back-ground ratio [Shotyk et al., 1998]. In the Swiss bog, the background ratio was defined as the average of peat samples (n = 17) dating from 5320 to 8030 ^{14}C yr B.P. which, in turn, were the lowest Pb:Sc (and Pb:Th) ratios found throughout the Holocene. In other words, the extent of Pb contamination being recorded by the peat bogs of northern AB today is no different than the intensity of atmospheric Pb contamination which occurred during the Iron Age of central Europe. Again, to view the Pb EF values from AB in the context of global atmospheric Pb contamination, the Pb EF in the Swiss peat samples dating from the Roman Period (1520 to 2100 cal yr B.P.) averages 10.3 (n = 7). So atmospheric Pb contamination in northern AB today is approximately 20% of that found in Switzerland during Roman times: this finding has special significance considering that most of the Pb production during Roman times was from mines in Spain and the U.K. [Le Roux et al., 2004] and was therefore supplied to the Swiss bog by long-range atmospheric transport.

Geophysical Research Letters 10.1002/2016GL070952

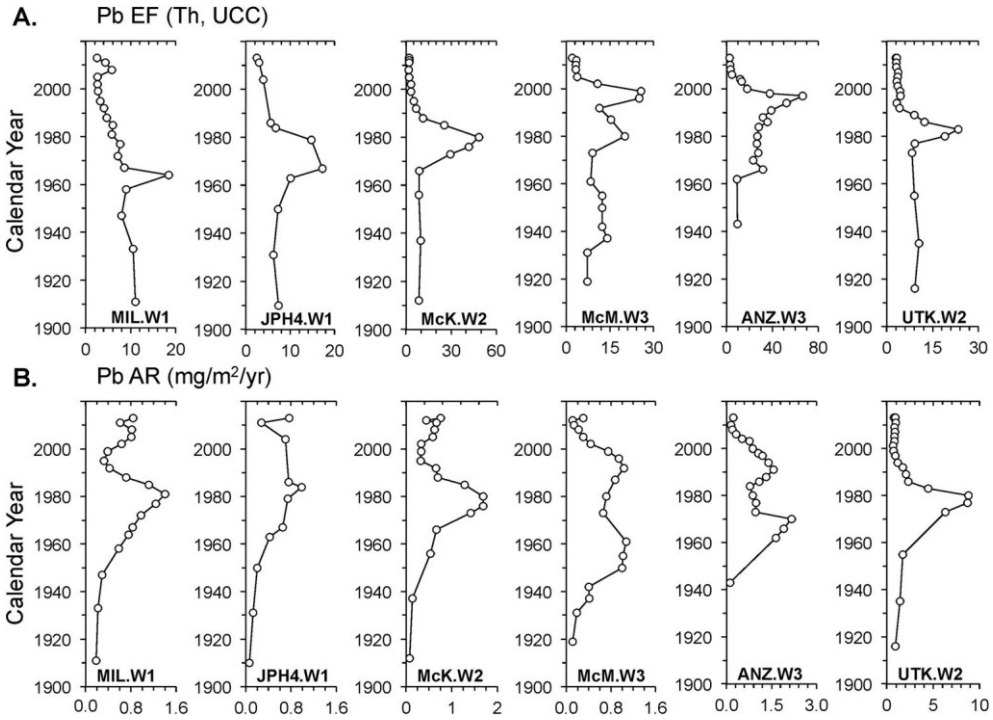

Figure 4. (A) Pb EF versus time. The age-depth models employed ^{210}Pb dating (CRS model, validated using ^{137}Cs and ^{241}Am) along with ^{14}C age dates (supporting information Table S3) including those obtained using the atmospheric bomb pulse curve (B) Pb accumulation rates versus time. Lead accumulation rates were calculated as the product of peat accumulation rates (cm/yr), bulk density (g/cm^3), and Pb concentrations (μg/g).

The cumulative mass of anthropogenic, atmospheric Pb which has been stored in the AB peat cores since industrialization began is approximately 5% of the values reported for the cleanest peat bogs we have studied in Switzerland or the remote Shetland and Faroe Islands, and only 10% of the value from the cleanest peat bogs studied in Europe by our team to date, from eastern Finland (supporting information Table S6). Compared to other peat bogs we have studied in Canada, the AB peat bogs contain no more than 5% of the anthropogenic Pb found in bogs from southern Ontario, 25% of that found in the bog from Point Escuminac National Park on the coast of New Brunswick, and only 70% of the Pb found in our cleanest peat core from northern Quebec. The inventories of anthropogenic Pb in the AB peat cores are within a factor of 4 of the cleanest peat bog we have found in Canada to date, from remote Haida Gwai which is west of the coast of British Columbia (supporting information Table S6). In fact, the average anthropogenic Pb inventory in the AB bogs is within a factor of 7 times the industrial Pb burden (7 mg/m^2) preserved in the past five centuries of ice from Greenland [Hong et al., 1994].

3.2. Pb From the Industrial Development of Bituminous Sands?

Although it had been suggested that open pit mining and upgrading of bitumen in AB is a significant source of Pb and other heavy metals to the environment [Kelly et al., 2010], the AB peat bogs provide no evidence of this. First, the Pb:Th ratio of the topmost peat layers of the bogs in the vicinity of the ABS mines and upgraders is actually slightly less than that of the remote site, UTK (Figure 3). Second, the Pb:Th ratios of the top layers of all of the peat cores are similar to the background values for the mid-Holocene [Krachler and Shotyk, 2004]. Third, the Pb:Th ratios have been in decline for decades. For example, consider the peat core from JPH-4 which is exclusively ombrotrophic and only 12 km from the midpoint between the two central upgraders: the maximum Pb EF value was found in peat dating from 1967, and Pb EF has been in decline ever since (Figure 4a). Thus, according to this peat profile, the extent of Pb contamination in atmospheric aerosols in the ABS region of northern Alberta began its continual decline when the industrial development of the bituminous sands was just beginning in 1967, with the opening of the Great Canadian Oil Sands. This finding is consistent with the results obtained from

Geophysical Research Letters 10.1002/2016GL070952

sediment cores taken in the Peace-Athabasca Delta which yielded a chronology of Pb accumulation which was inversely related to oil production in the ABS region [Wiklund et al., 2012].

To further illustrate the recent declines in atmospheric Pb contamination, the peat accumulation rates, bulk density, and Pb concentrations were used to calculate the Pb accumulation rates (Figure 4b). The maxi-mum Pb accumulation rates (ARs) shown here (~ 1.5 mg/m^2/yr) are one third the maximum value recently reported for the Hietajärvi peat bog, a background site within the Patvinsuo National Park in eastern Finland [Shotyk et al., 2016b], and one tenth the maximum value (15 mg/m^2/yr) reported for peat cores collected from the EGR bog in a rural setting of the Jura Mountains in Switzerland [Shotyk et al., 1998]. Compared to more industrialized regions of Europe, the Pb ARs for the bogs in northern AB are dwarfed by the maximum values (mg/m^2/yr) reported for peat cores from bogs in northern Poland (16 [De Vleeschouwer et al., 2009]), Scotland (60 [Farmer et al., 2006]), Denmark (105 [Shotyk et al., 2003]), England (147 [Rothwell et al., 2010]), Sweden (150 [Bindler, 2011]), Germany (176 [Hettwer et al., 2003]), and the Czech Republic (320 [Mihaljevič et al., 2006]).

3.3. Environmental Significance of Diminishing Atmospheric Pb Contamination

Lead poisoning was known in antiquity, having been described in the earliest writings on papyrus, parchment, copper, and clay [Lessler, 1988; Hernberg, 2000; Needleman, 2004]. This knowledge, however, did not prevent the introduction of Pb additives to gasoline. Since the first discovery of Pb contamination along road-ways in Vancouver, British Columbia by Warren and Delevault [1960], the environmental impacts of gasoline Pb additives have generated a voluminous scientific literature: according to Nriagu [1990], in 1978 alone there were more than 5000 papers and reports on virtually every aspect of Pb in the environment. Despite claims from industry that it was a "gift from God" and "essential to civilization" [Rosner and Markowitz, 1985], the addition of tetraethyl Pb to gasoline was controversial from the start, partly because 15 workers died and 300 became insane, due to occupational exposure when production first began in American factories [Needleman, 1997, 1998, 2000; Nriagu, 1998]. Decades later, an international survey would show strong linear correlations between blood Pb concentrations and gasoline Pb concentrations in cities worldwide, but thankfully blood Pb concentrations began their decline soon after the introduction of unleaded gasoline in 1976 [Thomas, 1995; Thomas et al., 1999].

The environmental history of this fascinating element continues to unfold, with evidence of atmospheric Pb contamination dating from the Bronze Age having been found in peat bogs from central Romania [Grüters, 2010], the Czech Republic [Veron et al., 2014], and most recently from the Iberian Peninsula [Martínez Cortizas et al., 2016]. Environmental Pb contamination in Egypt has an even longer history [Véron et al., 2006, 2013]. Pioneering work on skeletal Pb concentrations of ancient Peruvians by Clair Patterson [Ericson et al., 1979; Settle and Patterson, 1980] suggested that Pb exposure by modern humans dwarfs natural levels and has allowed blood Pb concentrations of unimpacted humans to be estimated [Smith and Flegal, 1992, 1995]. Human dental tooth enamel from archeological sites across Britain and Ireland since the Neolithic illustrate the connection between Pb use and body Pb burdens [Montgomery et al., 2010], with values from the Roman Period up to 10,000 times natural levels; these individuals would have had blood Pb concentrations corresponding to "very severe" poisoning. Although blood Pb concentrations have widely declined [Petit et al., 2015], there is no known safe level and this measure is now "seen by society as evidence of its commitment to its own health" [Amaya et al., 2010].

The report of an additional, new source of Pb to the environment, from the industrial development of ABS in northern AB [Kelly et al., 2010], raised considerable concern among First Nations communities who feared for the safety and security of their indigenous food supply (primarily berries, fish, and meat) and therefore also for their traditional lifestyle. In fact, the declining concentrations and enrichments of Pb seen in the peat bogs of northern AB are consistent with declines found in peat cores from Ontario [Givelet et al., 2003; Shotyk and Krachler, 2010; Pratte et al., 2013] as well as Manitoba [Shotyk et al., 2016c], northern Quebec, and coastal British Columbia (W. Shotyk, unpublished data, 2005 and 2007). Viewed in this light and considering the pronounced declines in the extent of atmospheric Pb contamination found in bogs across Europe [Shotyk et al., 2001, 2003, 2005, and many other authors], it would appear that the battle to end global atmospheric Pb contamination has been largely successful, at least in Europe and North America.

Geophysical Research Letters 10.1002/2016GL070952

Acknowledgments

Thanks from W.S. to Alberta Innovates-Energy and Environment Solutions for funding (special thanks to John Zhou, Brett Purdy, and Dallas Johnson), to the University of Alberta, the Faculty of Agricultural, Life and Environmental Sciences, and Alberta Environment and Parks for munificent start-up support for the SWAMP laboratory, and to the Canada Foundation for Innovation for a generous equipment grant and matching funds from Alberta Enterprise and Advanced Education. The Land Reclamation International Graduate School of the University of Alberta and NSERC CREATE provided Gillian Mullan-Boudreau with financial and logistical support. Sarah Gooding, Tracy Gartner, Claudia Sabrina Soto Farfan, Melanie Bolstler, and Karen Lund provided administrative support. We thank Madeleine Jensen-Fontaine, Ehsanul Hoque, Lucas Arantes Garcia, and Brittney Wipf for their help in the laboratory as well as Pedro Henrique Simões and Cara Albright for their help in the field. Anita Nowinka prepared many of the figures, and Sandor Haas-Neill the bibliography. Special thanks to Melanie Vile, Kelman Wieder, and Kevin Devito for introducing us to the beautiful bogs of this province, and to Peter Outridge for reviewing an early version of the manuscript. We are grateful to the reviewers for helpful comments and suggestions. This paper is dedicated by W.S. to Jerome Nriagu, for decades of illuminating thought on this subject and so much inspiration.

Author contributions: W.S. design of the laboratories (metal-free ultraclean SWAMP, sample preparation, and ultra-low background gamma spectrometry laboratories), grant funding for the laboratories and analytical instruments; design and grant funding for the study; collection of the peat cores, design of the analytical protocol, supervision of staff, interpretation of the results, and writing the paper. P.A. ^{210}Pb age dating using Constant Rate of Supply model. B. B. supervision of acid digestion and trace metal determination using ICP-MS, including QA/QC protocol. L.D. preparation of samples for ^{14}C age dating using accelerator mass spectrometry (AMS) and modeling of ^{14}C age dates. D. F. preparation of samples for ^{14}C age dating using AMS and modeling of ^{14}C age dates. I.G.W. acid digestion and trace metal determination using ICP-MS. M.K. provided Pb and Th data, of ancient Swiss peat samples. G.M. plant macro-fossil stratigraphy and selection/identification of samples for ^{14}C age dating using AMS. G.M.B. pH of pore waters and ash content of peats. T. N. design and construction of peat corer

4. Conclusion

Peat cores from five bogs in northern Alberta show that atmospheric Pb contamination has been in decline for decades and has reached the point where, today, it is difficult to detect any Pb contamination, relative to background levels, in the topmost layers of these ecosystems. Although it had been suggested that the industrial development of the Athabasca Bituminous Sands is a significant source of Pb to the environment, in fact, the extent of atmospheric Pb contamination has been in decline more or less since the industry began and despite its rapid expansion.

References

Amaya, M. A., K. W. Jolly, and N. E. Pingitore Jr. (2010), Blood lead in the 21st Century: The sub-microgram challenge, J. Blood Med., 1, 71–78.

American Geological Institute (1976), Dictionary of Geological Terms, Anchor Press.

Anon (1984), The Pocket Oxford Dictionary of Current English, Oxford Univ. Press.

Appleby, P. G., and F. Oldfield (1978), The calculation of ^{210}Pb dates assuming a constant rate of supply of unsupported ^{210}Pb to the sediment, Catena, 5, 1–8.

Appleby, P. G., W. Shotyk, and A. Fankhauser (1997), Lead-210 age dating of three peat cores in the Jura Mountains, Switzerland, Water Air Soil Pollut., 100(3-4), 223–231, doi:10.1023/A:1018380922280.

Ayotte, G., and L. Rochefort (2006), Les Sphaignes du Québec, Univ. Laval, Quebec City.

Benoit, J. M., W. F. Fitzgerald, and A. W. Damman (1998), The biogeochemistry of an ombrotrophic bog: Evaluation of use as an archive of atmosphere mercury deposition, Environ. Res., 78(2), 118–133, doi:10.1006/enrs.1998.3850.

Bindler, R. (2011), Contaminated lead environments of man: Reviewing the lead isotopic evidence in sediments, peat, and soils for the temporal and spatial patterns of atmospheric lead pollution in Sweden, Environ. Geochem. Health, 33, 311–329.

Bindler, R., I. Renberg, and J. Klaminder (2008), Bridging the gap between ancient metal pollution and contemporary biogeochemistry, J. Paleolimnol., 40(3), 755–770, doi:10.1007/s10933-008-9208-4.

Boutron, C. F., J. P. Candelone, and S. Hong (1994), Past and recent changes in the large-scale tropospheric cycles of lead and other heavy metals as documented in Antarctic and Greenland snow and ice: A review, Geochim. Cosmochim. Acta, 58(15), 3217–3225, doi:10.1016/ 0016-7037(94)90049-3.

Bränvall, M. L., R. Bindler, O. Emteryd, and I. Renberg (2001), Four thousand years of atmospheric lead pollution in northern Europe: A summary from Swedish lake sediments, J. Paleolimnol., 25, 421–435.

Clark, K. A., and S. M. Blair (1927), The Bituminous Sands of Alberta, Edmonton: Sci. and Industrial Res. Council of Alberta. Report No. 18. Cloy, J.

M., J. G. Farmer, M. C. Graham, A. B. MacKenzie, and G. T. Cook (2005), A comparison of antimony and lead profiles over the past 2500 years in Flanders Moss ombrotrophic peat bog, Scotland, J. Environ. Monit., 7(12), 1137–1147, doi:10.1039/b510987f.

Cloy, J. M., J. G. Farmer, M. C. Graham, A. B. MacKenzie, and G. T. Cook (2008), Historical records of atmospheric Pb deposition in four Scottish ombrotrophic peat bogs: An isotopic comparison with other records from western Europe and Greenland, Global Biogeochem. Cycles, 22, GB2016, doi:10.1029/2007GB003059.

Crum, H. (1988), A Focus on Peatlands and Peat Mosses, Univ. of Michigan Press, Ann Arbor.

Crum, H. A., and L. E. Anderson (1981), Mosses of Eastern North America, Columbia Univ. Press, New York.

De Vleeschouwer, F., N. Fagel, A. Cheburkin, A. Pazdur, J. Sikorski, N. Mattielli, V. Renson, B. Fialkiewicz, N. Piotrowska, and G. Le Roux (2009), Anthropogenic impacts in North Poland over the last 1300 years—A record of Pb, Zn, Cu, Ni and S in an ombrotrophic peat bog, Sci. Total Environ., 407, 5674–5684, doi:10.1016/j.scitotenv.2009.07.020.

Ericson, J. E., H. Shirahata, and C. C. Patterson (1979), Skeletal concentrations of lead in ancient Peruvians, New England J. Med., 300(17), 946–951, doi:10.1056/NEJM197904263001703.

Fairbridge, R. W. (1972), in The Encyclopedia of Geochemistry and Environmental Sciences, edited by R. W. Fairbridge, Dowden, Hutchinson, and Ross, Stroudsburg, Pa.

Farmer, J. G., A. B. MacKenzie, M. C. Graham, K. Macgregor, and A. Kirika (2015), Development of recent chronologies and evaluation of temporal variations in Pb fluxes and sources in lake sediment and peat cores in a remote, highly radiogenic environment, Cairngorm Mountains, Scottish Highlands, Geochim. Cosmochim. Acta, 156, 25–49, doi:10.1016/j.gca.2015.02.003.

Farmer, J., M. Graham, C. Yafa, J. Cloy, A. Freeman, and A. MacKenzie (2006), Use of ^{206}Pb/^{207}Pb ratios to investigate the surface integrity of peat cores used to study the recent depositional history and geochemical behaviour of inorganic elements in peat bogs, Global Planet. Change, 53(4), 240–248, doi:10.1016/j.gloplacha.2006.03.006.

Garneau, M. (1995), Reference Collection of Seeds and Other Botanical Macrofossils From Meridional and Boreal Quebec, Geol. Surv. of Canada. Open file 3048, Terrain Sci. Div., Sainte-Foy, Quebec.

Givelet, N., F. Roos-Barraclough, and W. Shotyk (2003), Predominant anthropogenic sources and rates of atmospheric mercury accumulation in southern Ontario recorded by peat cores from three bogs: Comparison with natural "background" values (past 8000 years), J. Environ. Monit., 5(6), 935–949.

Givelet, N., et al. (2004), Suggested protocol for collecting, handling and preparing peat cores and peat samples for physical, chemical, mineralogical and isotopic analyses, J. Environ. Monit., 6(5), 481–492, doi:10.1039/b401601g.

Grüters J. (2010), Geochemical evidence of the onset of the Bronze Age in central Europe from the peat bog 'Taul Negru' [in German], Romania. B.Sc. thesis, Univ. of Heidelberg.

Hernberg, S. (2000), Lead poisoning in a historical perspective, Am. J. Ind. Med., 38(3), 244–254.

Hettwer, K., M. Deicke, and H. Ruppert (2003), Fens in karst sinkholes—Archives for long lasting "immission" chronologies, Water Air Soil Pollut., 149(1/4), 363–384, doi:10.1023/A:1025627218432.

Hong, S., J. P. Candelone, C. C. Patterson, and C. F. Boutron (1994), Greenland ice evidence of hemispheric lead pollution two millennia ago by Greek and Roman civilizations, Science, 265(9), 1841–1843, doi:10.1126/science.265.5180.1841.

Hua, Q., M. Barbetti, and A. Z. Rakowski (2013), Atmospheric radiocarbon for the period 1950–2010, Radiocarbon, 55(4), 2059–2072. Huntley, M. J.,

R. W. Mathewes, and W. Shotyk (2013), High-resolution palynology, climate change and human impact on a late Holocene peat bog on Haida Gwaii, British Columbia, Canada, The Holocene, 23(11), 1572–1583, doi:10.1177/0959683613499051. Hurtig,

M. (1985), Canadian Encyclopedia, Hurtig Publishers, Edmonton.

Geophysical Research Letters 10.1002/2016GL070952

as well as table for precise sectioning of frozen peat cores; sample collection and preparation; preparation and measurement of samples for ^{137}Cs, ^{210}Pb, and ^{241}Am using ultralow background gamma spectrometry, including QA/QC. R.P. creation of maps showing all relevant geographic features and locations of bogs from this and previous studies, including both peat and moss only collection sites. B.S. design of calibration standards for ^{137}Cs, ^{210}Pb, and ^{241}Am using ultralow background gamma spectrometry; design of analytical protocols for these fallout radionuclides in peat including QA/QC program; calibration of these instruments and training of Noernberg. S.vB. responsible for plant macrofossil stratigraphy and selection/identification of samples for ^{14}C age dating using AMS. C.Z. peat core collection and preparation, and peat humification. The authors declare no competing financial interests.

Jones, J. M., and J. Hao (1993), Ombrotrophic peat as a medium for historical monitoring of heavy metal pollution, Environ. Geochem. Health, 15(2-3), 67–74, doi:10.1007/BF02627824.

Kelly, E. N., D. W. Schindler, P. V. Hodson, J. W. Short, R. Radmanovich, and C. C. Nielsen (2010), Oil sands development contributes elements toxic at low concentrations to the Athabasca River and its tributaries, Proc. Natl. Acad. Sci. U.S.A., 107(37), 16,178–16,183, doi:10.1073/ pnas.1008754107.

Kempter, H., M. Krachler, and W. Shotyk (2010), Atmospheric Pb and Ti accumulation rates from Sphagnum moss: Dependence upon plant productivity, Environ. Sci. Technol., 44(14), 5509–5515, doi:10.1021/es100366d.

Klaminder, J., I. Renberg, R. Bindler, and O. Emteryd (2003), Isotopic trends and background fluxes of atmospheric lead in northern Europe: Analyses of three ombrotrophic bogs from south Sweden, Global Biogeochem. Cycles, 17(1), 1019, doi:10.1029/2002GB001921.

Krachler, M., and W. Shotyk (2004), Natural and anthropogenic enrichments of molybdenum, thorium, and uranium in a complete peat bog profile, Jura Mountains, Switzerland, J. Environ. Monit., 6(5), 418–426, doi:10.1039/b313300a.

Kylander, M. E., D. J. Weiss, A. Martínez Cortizas, B. Spiro, R. Garcia-Sanchez, and B. J. Coles (2005), Refining the pre-industrial atmospheric Pb isotope evolution curve in Europe using an 8000 year old peat core from NW Spain, Earth Planet. Sci. Lett., 240(2), 467–485, doi:10.1016/j.epsl.2005.09.024.

Kylander, M. E., D. J. Weiss, and B. Kober (2009), Two high resolution terrestrial records of atmospheric Pb deposition from New Brunswick, Canada, and Loch Laxford, Scotland, Sci. Total Environ., 407, 1644–1657.

Laine, J., P. Harju, T. Timonen, A. Laine, E.-S. Tuittila, K. Minkkinen, and H. Vasander (2009), The Intricate Beauty of Sphagnum Mosses—A Finnish Guide to Identification, Univ. of Helsinki, Dep. of Forest Ecol.

Le Roux, G., D. Weiss, J. Grattan, N. Givelet, M. Krachler, A. Cheburkin, N. Rausch, B. Kober, and W. Shotyk (2004), Identifying the sources and timing of ancient and medieval atmospheric lead pollution in England using a peat profile from Lindow bog, Manchester, J. Environ. Monit., 6(5), 502–510, doi:10.1039/b401500b.

Le Roux, G., D. Aubert, P. Stille, M. Krachler, B. Kober, A. Cheburkin, G. Bonani, and W. Shotyk (2005), Recent atmospheric Pb deposition at a rural site in southern Germany assessed using a peat core and snowpack, and comparison with other archives, Atmos. Environ., 39(36), 6790–6801, doi:10.1016/j.atmosenv.2005.07.026.

Lee, J. A., and J. H. Tallis (1973), Regional and historical aspects of lead pollution in Britain, Nature, 245(5422), 216–218, doi:10.1038/245216a0.

Lessler, M. A. (1988), Lead and lead poisoning from antiquity to modern times, Ohio J. Sci., 88, 78–84.

Lindemann, M. (2010), Titanium and Lead in Peat as Indicators of Natural and Anthropogenic Aerosols (in German), Univ. of Heidelberg. Martínez Cortizas, A., L. López-Merino, R. Bindler, T. Mighall, and M. E. Kylander (2016), Early atmospheric metal pollution provides evidence for Chalcolithic/Bronze Age mining and metallurgy in southwestern Europe, Sci. Total Environ., 545-546, 398–406, doi:10.1016/j.scitotenv.2015.12.078.

McConnell, J. R. J. R., G. W. Lamorey, and M. A. Hutterli (2002), A 250-year high-resolution record of Pb flux and crustal enrichment in central Greenland, Geophys. Res. Lett., 29(23), 2130, doi:10.1029/2002GL016016.

Mihaljevič, M., M. Zuna, V. Ettler, O. Šebek, L. Strnad, and V. Goliáš (2006), Lead fluxes, isotopic and concentration profiles in a peat deposit near a lead smelter (Pribram, Czech Republic), Sci. Total Environ., 372(1), 334–344, doi:10.1016/j.scitotenv.2006.09.019.

Monna, F., C. Petit, J.-P. Guillaumet, I. Jouffroy-Bapicot, C. Blanchot, J. Dominik, R. Losno, H. Richard, J. Lévêque, and C. Chateau (2004), History and environmental impact of mining activity in Celtic Aeduan territory recorded in a peat bog (Morvan, France), Environ. Sci. Technol., 38(3), 665–673, doi:10.1021/es034704v.

Montgomery, J., J. Evans, S. Chenery, V. Pashley, and K. Killgrove (2010), "Gleaming, white and deadly": Using lead to track human exposure and geographic origins in the Roman period in Britain, J. Roman Archaeol., 78, 199–226.

Murozumi, M., T. Chow, and C. Patterson (1969), Chemical concentrations of pollutant lead aerosols, terrestrial dusts and sea salts in Greenland and Antarctic snow strata, Geochim. Cosmochim. Acta, 33, 1247–1294.

Needleman, H. (1997), Clamped in a straitjacket: the insertion of lead into gasoline, Environ. Res., 74(2), 95–103, doi:10.1006/enrs.1997.3767.

Needleman, H. (2004), Lead poisoning, Annu. Rev. Med., 55(1), 209–222, doi:10.1146/annurev.med.55.091902.103653.

Needleman, H. L. (1998), Clair Patterson and Robert Kehoe: Two views of lead toxicity, Environ. Res., 78(2), 79–85, doi:10.1006/enrs.1997.3807.

Needleman, H. L. (2000), The removal of lead from gasoline: Historical and personal reflections, Environ. Res., 84, 20–35, doi:10.1006/enrs.2000.4069.

Ng, A., and C. Patterson (1981), Natural concentrations of lead in ancient Arctic and Antarctic ice, Geochim. Cosmochim. Acta, 45(11), 2109–2121, doi:10.1016/0016-7037(81)90064-8.

Nilsson, M., M. Klarqvist, and G. Possnert (2001), Variation in ^{14}C age of macrofossils and different fractions of minute peat samples dated by AMS, The Holocene, 11(5), 579–586, doi:10.1191/095968301680223521.

Norton, S. A., G. C. Evans, and J. S. Kahl (1997), Comparison of Hg and Pb fluxes to hummocks and hollows of ombrotrophic big heath bog and to nearby Sargent Mt. Pond, Maine, USA, Water Air Soil Pollut., 100(3-4), 271–286, doi:10.1023/A:1018380610893.

Norton, S. A., G. L. Jacobson, J. Kopácek, and T. Navrátil (2015), A comparative study of long-term Hg and Pb sediment archives, Environ. Chem., doi:10.1071/EN15114.

Novák, M., et al. (2003), Origin of lead in eight central European peat bogs determined from isotope ratios, strengths, and operation times of regional pollution sources, Environ. Sci. Technol., 37(3), 437–445, doi:10.1021/es0200387.

Nriagu, J. O. (1978), in Biogeochemistry of Lead in the Environment, edited by J. O. Nriagu, Elsevier Biomedical Press, Amsterdam. Nriagu, J. O. (1990), The rise and fall of leaded gasoline, Sci. Total Environ., 92(C), 13–28, doi:10.1016/0048-9697(90)90318-O.

Nriagu, J. O. (1998), Clair Patterson and Robert Kehoe's paradigm of "show me the data" on environmental lead poisoning, Environ. Res., 78(2), 71–78, doi:10.1006/enrs.1997.3808.

Petit, D., A. Véron, P. Flament, K. Deboudt, and A. Poirier (2015), Review of pollutant lead decline in urban air and human blood: A case study from northwestern Europe, Comptes Rendus Geosci., 347(5-6), 247–256, doi:10.1016/j.crte.2015.02.004.

Pratte, S., A. Mucci, and M. Garneau (2013), Historical records of atmospheric metal deposition along the St. Lawrence Valley (eastern Canada) based on peat bog cores, Atmos. Environ., 79, 831–840, doi:10.1016/j.atmosenv.2013.07.063.

Reimer, P. (2013), IntCal13 and Marine13 radiocarbon age calibration curves 0–50,000 years cal BP, Radiocarbon, 55(4), 1869–1887, doi:10.2458/azu_js_rc.55.16947.

Roos-Barraclough, F., N. Givelet, A. K. Cheburkin, W. Shotyk, and S. A. Norton (2006), A ten thousand year record of atmospheric mercury accumulation in peat from Caribou Bog, Maine, and its correlation to bromine and selenium, Environ. Sci. Technol., 40, 3188–3194.

Rosman, K. J. R., W. Chisholm, S. Hong, J. P. Candelone, and C. F. Boutron (1997), Lead from Carthaginian and Roman Spanish mines isotopically identified in Greenland ice dated from 600 B.C. to 300 A.D, Environ. Sci. Technol., 31(12), 3413–3416, doi:10.1021/es970038k.

Rosner, D., and G. Markowitz (1985), A "gift of God"?: The public health controversy over leaded gasoline during the 1920s, Am. J. Public Health, 75(4), 344–352, doi:10.2105/AJPH.75.4.344.

Geophysical Research Letters 10.1002/2016GL070952

Rothwell, J. J., K. G. Taylor, S. R. N. Chenery, A. B. Cundy, M. G. Evans, and T. E. H. Allott (2010), Storage and behavior of As, Sb, Pb, and Cu in ombrotrophic peat bogs under contrasting water table conditions, Environ. Sci. Technol., 44(22), 8497–8502, doi:10.1021/ es101150w.

Settle, D. M., and C. C. Patterson (1980), Lead in albacore: Guide to lead pollution in Americans, Science, 207(4436), 1167–1176, doi:10.1126/ science.6986654.

Shotyk, W. (1996a), Natural and anthropogenic enrichments of As, Cu, Pb, Sb, and Zn in ombrotrophic versus minerotrophic peat bog profiles, Jura Mountains, Switzerland, Water Air Soil Pollut., 90(3-4), 375–405, doi:10.1007/BF00282657.

Shotyk, W. (1996b), Peat bog archives of atmospheric metal deposition: Geochemical evaluation of peat profiles, natural variations in metal concentrations, and metal enrichment factors, Environ. Rev., 4(2), 149–183, doi:10.1139/a96-010.

Shotyk, W. (2002), The chronology of anthropogenic, atmospheric Pb deposition recorded by peat cores in three minerogenic peat deposits from Switzerland, Sci. Total Environ., 292(1-2), 19–31, doi:10.1016/S0048-9697(02)00030-X.

Shotyk, W., and G. Le Roux (2005), Biochemistry and cycling of lead, in Biogeochemical Cycles of the Elements, edited by A. Sigel, H. Sigel, and R. O. K. Sigel, Marcel Dekker, New York.

Shotyk, W., and M. Krachler (2010), The isotopic evolution of atmospheric Pb in central Ontario since AD 1800, and its impacts on the soils, waters, and sediments of a forested watershed, Kawagama Lake, Geochim. Cosmochim. Acta, 74(7), 1963–1981, doi:10.1016/ j.gca.2010.01.009.

Shotyk, W., H. W. Nesbitt, and W. Fyfe (1990), The behaviour of major and trace elements in complete vertical peat profiles from three Sphagnum bogs, Int. J. Coal Geol., 15, 163–190.

Shotyk, W., H. Wayne Nesbitt, and W. S. Fyfe (1992), Natural and anthropogenic enrichments of trace metals in peat profiles, Int. J. Coal Geol., 20(1-2), 49–84, doi:10.1016/0166-5162(92)90004-G.

Shotyk, W., A. K. Cheburkin, P. G. Appleby, A. Fankhauser, and J. D. Kramers (1997), Lead in three peat bog profiles, Jura Mountains, Switzerland: Enrichment factors, isotopic composition, and chronology of atmospheric deposition, Water Air Soil Pollut., 100(3-4), 297–310, doi:10.1023/A:1018384711802.

Shotyk, W., D. Weiss, P. Appleby, A. Cheburkin, R. Gloor, J. Kramers, S. Reese, and W. O. Van Der Knaap (1998), History of atmospheric lead deposition since 12,370 ^{14}C yr BP from a peat bog, Jura mountains, Switzerland, Science, 281(5383), 1635–1640.

Shotyk, W., P. Blaser, A. Grünig, and A. K. Cheburkin (2000), A new approach for quantifying cumulative, anthropogenic, atmospheric lead deposition using peat cores from bogs: Pb in eight Swiss peat bog profiles, Sci. Total Environ., 249(1-3), 281–295, doi:10.1016/S0048-9697 (99)00523-9.

Shotyk, W., D. Weiss, J. D. Kramers, R. Frei, A. K. Cheburkin, M. Gloor, and S. Reese (2001), Geochemistry of the peat bog at Etang de la Gruère, Jura Mountains, Switzerland, and its record of atmospheric Pb and lithogenic trace metals (Sc, Ti, Y, Zr, and REE) since 12,370 ^{14}C yr BP, Geochim. Cosmochim. Acta, 65(14), 2337–2360, doi:10.1016/S0016-7037(01)00586-5.

Shotyk, W., D. Weiss, M. Heisterkamp, A. K. Cheburkin, P. G. Appleby, and F. C. Adams (2002), New peat bog record of atmospheric lead pollution in Switzerland: Pb concentrations, enrichment factors, isotopic composition, and organolead species, Environ. Sci. Technol., 36(18), 3893–3900.

Shotyk, W., M. E. Goodsite, F. Roos-Barraclough, R. Frei, J. Heinemeier, G. Asmund, C. Lohse, and T. S. Hansen (2003), Anthropogenic contributions to atmospheric Hg, Pb, and As accumulation recorded by peat cores from southern Greenland and Denmark dated using the ^{14}C "bomb pulse curve,", Geochim. Cosmochim. Acta, 67(21), 3991–4011, doi:10.1016/S0016-7037(03)00409-5.

Shotyk, W., et al. (2005a), Accumulation rates and predominant atmospheric sources of natural and anthropogenic Hg and Pb on the Faroe Islands, Geochim. Cosmochim. Acta, 69(1), 1–17, doi:10.1016/j.gca.2004.06.011.

Shotyk, W., J. Zheng, M. Krachler, C. Zdanowicz, R. Koerner, and D. Fisher (2005b), Predominance of industrial Pb in recent snow (1994–2004) and ice (1842–1996) from Devon Island, Arctic Canada, Geophys. Res. Lett., 32, L21814, doi:10.1029/2005GL023860.

Shotyk, W., et al. (2014), Sphagnum mosses from 21 ombrotrophic bogs in the Athabasca bituminous sands region show no significant atmospheric contamination of "heavy metals", Environ. Sci. Technol., 48(21), 12,603–12,611, doi:10.1021/es503751v.

Shotyk, W., H. Kempter, M. Krachler, and C. Zaccone (2015), Stable (^{206}Pb, ^{207}Pb, ^{208}Pb) and radioactive (^{210}Pb) lead isotopes in 1 year of growth of Sphagnum moss from four ombrotrophic bogs in southern Germany: Geochemical significance and environmental implications, Geochim. Cosmochim. Acta, 163, 101–125, doi:10.1016/j.gca.2015.04.026.

Shotyk, W., B. Bicalho, C. W. Cuss, M. J. Duke, T. Noernberg, R. Pelletier, E. Steinnes, and C. Zaccone (2016a), Dust is the dominant source of "heavy metals" to peat moss (Sphagnum fuscum) from the industrial development of the Athabasca Bituminous Sands in northern Alberta, Canada, Environ. Int., 92-93, 494–506, doi:10.1016/j.envint.2016.03.018.

Shotyk, W., N. Rausch, T. Nieminen, L. Ukomaanaho, and M. Krachler (2016b), Isotopic composition of Pb in peat and porewaters from three contrasting ombrotrophic bogs in Finland: Evidence of chemical diagenesis in response to acidification, Environ. Sci. Technol., doi:10.1021/ acs.est.6b01076.

Shotyk, W., N. Rausch, M. Krachler, and P. M. Outridge (2016c), Isotopic evolution of atmospheric Pb from metallurgical processing in Flin Flon, Manitoba: Retrospective analysis using peat cores from bogs, Environ. Pollut., doi:10.1016/j.envpol.2016.07.009.

Smith, D. R., and A. R. Flegal (1992), The public health implications of humans' natural levels of lead, Am. J. Public Health, 82(11), 1565–1566. Smith, D. R., and A. R. Flegal (1995), Lead in the biosphere: Recent trends, Ambio, 24(1), 21–23.

Thomas, V. M. (1995), The elimination of lead in gasoline, Annu. Rev. Energy Environ., 20, 301–324, doi:10.1146/annurev.energy.20.1.301. Thomas, V. M., R. Socolow, J. Fanelli, and T. Spiro (1999), Effects of reducing lead in gasoline: An analysis of the international experience, Environ. Sci. Technol., 33, 3942–3948.

Véron, A. J., C. Flaux, N. Marriner, A. Poirier, S. Rigaud, C. Morhange, and J. Y. Empereur (2013), A 6000-year geochemical record of human activities from Alexandria (Egypt), Quat. Sci. Rev., 81, 138–147, doi:10.1016/j.quascirev.2013.09.029.

Véron, A., J. P. Goiran, C. Morhange, N. Marriner, and J. Y. Empereur (2006), Pollutant lead reveals the pre-Hellenistic occupation and ancient growth of Alexandria, Egypt, Geophys. Res. Lett., 33, L06409, doi:10.1029/2006GL025824.

Veron, A., M. Novak, E. Brizova, and M. Stepanova (2014), Environmental imprints of climate changes and anthropogenic activities in the Ore Mountains of Bohemia (Central Europe) since 13 cal. kyr BP, The Holocene, 24(8), 919–931, doi:10.1177/0959683614534746.

Vile, M. A., R. K. Wieder, S. Berryman, and D. Vitt (2013), Development of Monitoring Protocols for N & S Sensitive Bog Ecosystems, pp. 91 , Wood Buffalo Environmental Association: Fort McMurray, Alberta, Canada.

Wardenaar, E. (1987), A new hand tool for cutting peat profiles, Can. J. Bot., 65, 1772–1773.

Warren, H. V., and R. E. Delevault (1960), Observations on the biogeochemistry of lead in Canada, Trans. R. Soc. Canada, 54, 11–20.

Wedepohl, K. H. (1995), The composition of the continental crust, Geochim. Cosmochim. Acta, 59, 1217–1232.

Weiss, D., W. Shotyk, and O. Kempf (1999a), Archives of atmospheric lead pollution, Naturwissenschaften, 86(6), 262–275, doi:10.1007/ s001140050612.

Geophysical Research Letters 10.1002/2016GL070952

Weiss, D., W. Shotyk, P. G. Appleby, J. D. Kramers, and A. K. Cheburkin (1999b), Atmospheric Pb deposition since the industrial revolution recorded by five Swiss peat profiles: Enrichment factors, fluxes, isotopic composition, and sources, Environ. Sci. Technol., 33(9), 1340–1352, doi:10.1021/es980882q.

Weiss, D., W. Shotyk, M. Gloor, and J. D. Kramers (1999c), Herbarium specimens of Sphagnum moss as archives of recent and past atmospheric Pb deposition in Switzerland: Isotopic composition and source assessment, Atmos. Environ., 33, 3751–3763.

Weiss, D., W. Shotyk, E. A. Boyle, J. D. Kramers, P. G. Appleby, and A. K. Cheburkin (2002), Constraining lead sources to the North Atlantic Ocean: Recent atmospheric lead deposition recorded by two ombrotrophic peat bogs in Scotland and Eastern Canada, Sci. Total Environ., 292, 7–18.

Wiklund, J. A., R. I. Hall, B. B. Wolfe, T. W. D. Edwards, A. J. Farwell, and D. G. Dixon (2012), Has Alberta oil sands development increased far-field delivery of airborne contaminants to the Peace-Athabasca Delta?, Sci. Total Environ., 433, 379–382, doi:10.1016/j.scitotenv.2012.06.074.

Wu, J. F., and E. A. Boyle (1997), Lead in the western North Atlantic Ocean: Completed response to leaded gasoline phase-out, Geochim. Cosmochim. Acta, 61(15), 3279–3283, doi:10.1016/s0016-7037(97)89711-6.

Zheng, J., W. Shotyk, M. Krachler, and D. A. Fisher (2007), A 15,800-year record of atmospheric lead deposition on the Devon Island Ice Cap, Nunavut, Canada: Natural and anthropogenic enrichments, isotopic composition, and predominant sources, Global Biogeochem. Cycles, 21, GB2027, doi:10.1029/2006GB002897.

[Geophysical Research Letters]
Supporting Information for

Back to background: peat bogs in northern Alberta, Canada reveal decades of declining atmospheric Pb contamination

Authors: W. Shotyk[1*], P. Appleby[2], B. Bicalho[1], L. Davies[3], D. Froese[3], I. Grant-Weaver[1], M. Krachler[4], G. Magnan[1], G. Mullan-Boudreau[1], T. Noernberg[1], R. Pelletier[1], B. Shannon[5], S. van Bellen[1], C. Zaccone[6]
[1]Department of Renewable Resources, University of Alberta, 348 South Academic Building, Edmonton, AB CANADA T6G 2H1.
[2]Dept of Mathematical Sciences, University of Liverpool, Liverpool L69 3BX, UNITED KINGDOM.
[3]Department of Earth and Atmospheric Sciences, University of Alberta, Edmonton, AB CANADA T6G 2H.
[4]European Commission, Joint Research Centre, Directorate Nuclear Safety and Security P.O. Box 2340, 76125 Karlsruhe, GERMANY.
[5]Quality Radioanalytical Support, LLC, 123 Cougar Trail, PO Box 774 Grand Marais, MN USA 55604.
[6]Department of the Sciences of Agriculture, Food and Environment, University of Foggia, ITALY.

Contents of this file

Text S1.

Peat bog archives of atmospheric Pb deposition: Until twenty years ago, there had been two schools of thought regarding the possible importance of post-depositional migration of Pb in peat cores from ombrotrophic bogs: one view was that Pb was mobile, and the second that Pb was immobile. Except for the compelling study of atmospheric Pb contamination in the U.K. dating from the Roman period (Lee and Tallis, 1973), neither group provided convincing evidence one way or the other (Shotyk, 1996a,b). Until 1995, therefore, it was not yet known to what extent peat bogs functioned as faithful archives of atmospheric Pb deposition. Since that time, a considerable research effort was invested to help resolve the issue. Using the most sensitive analytical methods available including measurements of both stable and radioactive Pb isotopes, the following ten sets of investigations all failed to detect any measurable post-depositional migration of Pb in peat bog profiles:

i) Peat cores from two bogs in the Jura Mountains of Switzerland were age dated using ^{210}Pb, and the age-depth relationships were found to be in good agreement with the presence of radionuclide (^{241}Am) and botanical (*Cannabis* pollen) chronostratigraphic markers (Appleby et al., 1997).

ii) Using high-precision TIMS analyses of the isotopic composition of Pb in a peat profile which had been aged dated using ^{210}Pb, it was possible to show that there had been no significant post-depositional migration of Pb in the peat bog profile because there were two peaks in Pb concentration and Pb enrichment, and these were isotopically different (Shotyk et al., 1997). The older peak in Pb dating from AD 1936 ± 3 (^{206}Pb/^{207}Pb = 1.1631 ± 0.0002) could not be explained by vertical downward Pb migration from the

more recent peak in Pb dating from AD 1967 ± 2 ($^{206}Pb/^{207}Pb = 1.1492 \pm 0.0002$) because they are separated by a zone which is much less enriched in Pb.

iii) The isotopic composition of Pb was measured in peat cores from three other bogs in Switzerland which also were dated using ^{210}Pb. These results (Weiss et al., 1999a) showed remarkably similar temporal trends in the isotopic evolution of atmospheric Pb reported for the two peat bogs studied earlier (Shotyk et al., 1997).

iv) The isotopic composition of Pb (^{204}Pb, ^{206}Pb, ^{207}Pb, ^{208}Pb) was also measured in herbarium samples of *Sphagnum* moss which had been collected since AD 1867. The agreement between the temporal trends in the isotopic evolution of atmospheric Pb revealed by the peat cores (dated using ^{210}Pb) and by the herbarium specimens of *Sphagnum* moss (whose date of sample collection is known exactly) is remarkable (Weiss et al., 1999b).

v) A replicate core collected from Etang de la Gruère in Switzerland in 1993 (Shotyk et al., 2002) yielded essentially the same chronology and intensity of atmospheric Pb deposition as the first core from the same bog which had been collected in 1991 (Shotyk et al., 1997).

vi) Measurements of alkyl lead compounds in age-dated peat cores yielded a chronology of organolead deposition which matched the history of leaded gasoline use in Europe (Shotyk et al., 2002).

vii) Peat cores from minerotrophic (groundwater-fed) peatlands in Switzerland (Shotyk, 2002) yielded chronologies of atmospheric Pb deposition which matched those obtained using peat cores from ombrotrophic bogs.

viii) A peat core collected from a bog in the Black Forest of Germany (Le Roux et al., 2005) yielded a chronology of atmospheric Pb deposition virtually identical to that obtained from the Swiss bogs (Weiss et al., 1999a).

ix) Peat cores from three bogs in southern Ontario yielded very different Pb concentration-depth profiles, but precise age dating using ^{210}Pb and the bomb pulse curve of ^{14}C yielded identical chronologies of Pb accumulation (Givelet et al., 2003).

x) Despite the input of marine aerosols and the potential of elevated chloride ion concentrations to mobilize Pb via complexation, a pronounced peak in Pb dating from the Roman period was perfectly preserved in a peat core collected from blanket bog on the Faroe Islands (Shotyk et al., 2005a).

In the intervening period, there have been numerous papers published by other groups working independently, showing that peat cores from ombrotrophic bogs are faithful archives of atmospheric Pb deposition; many of these studies have been reviewed elsewhere (Shotyk et al., 1990, 1992, 1998, 2015; Jones and Hao, 1993; Shotyk, 1996a,b; Weiss et al, 1999c;).

Terminology: We use the geological term “bituminous sand” to describe these deposits which consist of approximately 85 % sand,10 % bitumen and 5 % water found mainly in the Athabasca, Cold Lake, and Peace River and Wabasca regions of Alberta (Canadian Encyclopedia 1985). The historical precedence for this term was established by Clark and Blair (Clark and Blair, 1927). This is also the term used by the American Geological Institute (1976), Oxford English Dictionary (1984), as well as the Encyclopedia of Geochemistry which provides data for V, Ni, and Mo concentrations in bitumen deposits worldwide (Fairbridge, 1972). The use of “bituminous sand” is the English language

equivalent of the French “les sables bitumineux” which provides consistence in both official languages of Canada. The term “oil sand” has come to be used in the popular press by those generally in favour of the industrial development of these resources for the recovery of their hydrocarbons, and “tar sand” by those opposed; we avoid the use of potentially polarizing terminology and prefer to use the geological term.

Peat core collection: Three peat cores were collected from each bog, ca. 3 m apart, using a modified Wardenaar monolith sampler (Wardenaar, 1987): our custom-built corer removes a monolith 15 x 15 x ca. 100 cm, includes serrated cutting edges and was constructed entirely using a Ti-Al-Mn alloy. The top of the corer is reinforced to allow it to be driven into the bog surface using a nylon sledgehammer: this minimizes compression of the peat core. The peat cores were extracted, photographed, wrapped in polyethylene cling film, then packed into wooden boxes in the field. In the lab, the cores were frozen at -18^{o}C. The living (green) layer at the top of the peat core is removed first: although this material represents the first sample in each peat bog profile, this is living plant material and not peat: this distinction may be relevant to the distribution of trace metals which are essential to plants such as Cu or Zn and may be enriched in this layer due to bioaccumulation, but it is not relevant to potentially toxic heavy metals such as Pb. The remainder of each core was then cut precisely into 1 cm slices, while frozen, using a stainless steel band saw and polypropylene cutting table. The edges (1 cm) were trimmed away from each slice and the porewaters extracted for pH and electrical conductivity; these pieces were then dried and combusted to determine ash content. One half of each remaining sample was reserved for a separate study of organic contaminants, with the rest dried at 105^{o}C for 36 h in polypropylene jars. Grinding was done using a Retsch agate

ball mill (PM 400, Haan, Germany) with 250 mL jars containing three 30 mm balls at 300 rpm for four x 2.3 minutes (first forward, then reverse, then forward, then reverse).

Trace metal analyses: Trace metal analyses of the powders (living layer and all odd numbered samples from each core) were carried out in the new, metal-free, ultraclean SWAMP lab for Soil, Water, Air, Manure and Plant analysis. Sample aliquots of 200 to 230 mg were weighed into PTFE vessels and then dissolved in a mixture of 3 mL concentrated nitric acid (distilled twice in a Milestone DuoPur high purity quartz still) and 0.1 mL tetrafluoroboric acid within a Milestone UltraClave high pressure reaction system. The UltraClave reaction chamber was pressurized to 50 bar with argon gas before the microwave heating program began. The heating program includes these steps: from room temperature to 60 °C in 9 minutes; 60 to 125°C in 25 minutes; 125 to 160°C in 12 minutes; 160 to 240°C in 14 minutes; remaining at 240°C for 20 minutes. At the end of the microwave heating steps, the reaction chamber was cooled by the circulated cooling water and the chamber was depressurized when the interior temperature of the chamber was below 80°C. 11.9 mL of 18 MΩ water was added to the digestion vessels. The diluted digests were then quantitatively transferred to 15 mL Fisher-Brand centrifuge tubes. The digestion solutions were diluted 6000-6500 times with 2% nitric acid before they were measured for trace metals using a Thermo Scientific iCAP Qc ICP-MS. The multi-element concentrations were measured against the diluted calibration standard solutions with concentrations of 0.05, 1 and 10 µg/kg of the elements derived from the Spex CertiPrep (Metuchen, NJ, USA) multielement standards CLMS-2AN, and 0.05, 0.5 and 5 µg/kg from the Spex CertiPrep CLMS-1 and CLMS-4.

For quality control purposes, Certified standard Reference Materials were also dissolved and measured along with each batch of samples (table SI2). The Spex CertiPrep indium standard was individually added to all the sample solutions as the internal standard. All the elements were measured using the iCAP Qc's Kinetic Energy Discrimination mode, with 0.01 second of dwell time and 20 sweeps and the element concentration values were the averages of the three runs during the data acquisition.

Peat stratigraphy: Plant macrofossils were analyzed from 2-cm^3 subsamples at 2-cm intervals along the peat cores (figure SI2). Each subsample represented 1-cm of vertical peat accumulation. Subsamples were gently boiled for 5 minutes in 5% KOH to dissolve humic and fulvic acids and rinsed over 125-µm sieves to retain the larger fraction. The identification and estimation of the abundance (volume percentage or absolute numbers) of peat-forming vegetation was performed in a petri dish using a binocular microscope at 10-16x magnification. The identification of taxa was based on a plant macrofossil reference collection (Garneau, 1995) and identification guides for mosses (Crum and Anderson, 1981) and *Sphagnum* (Ayotte and Rochefort, 2006; Laine et. al 2009). S*phagnum* spp. and other bryophyte leaves were identified to species level using a microscope at 40–100x magnification.

Material for AMS radiocarbon dating was selected from the plant macrofossil subsamples. *Sphagnum* remains were preferred, including stems, branches and leaves as they tend to provide the most reliable ^{14}C dates (Nilsson et al., 2001). For some samples, other aboveground plant remains (twigs, needles, leaves) and parts of sedges were used to attain the minimum mass required for dating.

Characterization of the peat cores: The pH of pore water and ash content of peat (figure SI3) was measured in every odd-numbered slice, the living layer and the last layer of each core. Each frozen sample was warmed to room temperature over 24 hours. The pore water was extracted from the samples using luer-slip plastic syringes (10 mL) into microcentrifuge tubes (1.5 mL graduated tube with flat cap) through a syringe filter (Teflon 0.45 microns, 30mm) to be analyzed for pH (Mettler Toledo Seven Excellence pH/ORP/Ion/Conductivity/DO Meter). The meter was calibrated before each core was analyzed (about every 40 samples) using standards. Once all the water was extracted, the remaining peat was placed in 120 ml PP containers and dried at 105°C for 24 hours, then ashed in ceramic crucibles at 550°C for 18 hours. The samples were then placed into a desiccator for 24 hours to prevent moisture uptake. The weights of the samples after ashing were compared to the weights before to determine ash content.

^{14}C age dating: Between 5 and 12 samples from each peat core were analyzed for radiocarbon. The description of plant macrofossil specimens analyzed for ^{14}C dating by accelerator mass spectrometry (AMS) are provided in table SI3. All samples were pre-treated at the University of Alberta following standard acid-base-acid procedures: solutions were heated to 70°C: 30 min in 1M HCl, 60 minutes in 1M NaOH with solution changed until clear, 30 min 1M HCl, and rinsed with room-temperature ultrapure water until pH neutral. Secondary standards were also pre-treated concurrently: non-finite-age wood (AVR-PAL-07) and, latest Pleistocene and middle Holocene wood (FIRI-F standard) material (table SI4); all values were within the normal range. Pre-treated samples were graphitized and all samples were analysed at the Keck-Carbon Cycle AMS facility (University of California, Irvine). The resulting ^{14}C ages were calibrated using

Bomb13NH1 (Hua et al., 2013) and IntCal13 (Reimer et al., 2013) calibration curves (as appropriate) within Oxcal v4.2 (Bronk Ramsey, 2009).

Gamma spectrometry: Lead-210 activities were measured using one of three ultralow background gamma spectrometers (ORTEC, Oak Ridge, TN, USA): each instrument is equipped with an ORTEC GWL-250-15 HPGe well detector (with OFHC Cu endcap and high purity Al well tube) in an ultralow background J-type cryostat surrounded by a virgin lead shield (15 cm thick) with nitrogen purge port. Dried and milled peat samples were placed in polypropylene plastic tubes (Sarstedt, Hildesheim, Germany) 15.3 mm OD and 93 mm high: these are filled to a height of 50 mm to align with the geometry of the crystal, closed with a PP septum, sealed with epoxy glue (Devcon, Danvers, MA, USA) and left for 29 days at room temperature to allow any Rn to decay. The mass of sample used ranged from 1.6-3.5 g (average 2.2 g), depending on peat density. After a 30-day period for equilibration of ^{222}Rn and decay progeny, the sample containers were placed in the well of the detector and ^{210}Pb determined using its gamma-ray emission at 46.5 keV line; ^{226}Ra was determined based on gamma emissions of ingrown decay progeny at 352 (^{214}Pb) and 609 (^{214}Bi) keV; ^{137}Cs and ^{241}Am were determined simultaneously based on their respective photopeaks at 662 and 59.5 keV. The spectrometers were calibrated for measurement of ^{210}Pb, ^{226}Ra, ^{241}Am, and ^{137}Cs in peat using six, custom-made calibration standards (Eckert and Ziegler Analytics, Atlanta, GA, USA): two low-density (gas-equivalent) standards containing either a nine-nuclide mixture (including ^{137}Cs, ^{241}Am, and ^{210}Pb), or a mixture of ^{210}Pb and ^{226}Ra; and four with the same two radionuclide mixtures homogenously distributed in ancient peat from a Swiss bog spanning the range of densities of the calibration standards (0.02 to 0.41

g/cm^3) All calibration standards are traceable to the National Institute of Standards and Technology (NIST). Spectra were processed using ORTEC DSPEC Jr. 2.0 Digital Gamma Spectrometer with GammaVision 7 software. Acquisition times of 24, 48, or 72 hours varied depending on the ^{210}Pb activity of the sample. For quality assurance, a check standard of known nuclide activity was measured on each detector between each peat sample. Each successive 1-cm peat slice is measured until ^{210}Pb is observed in equilibrium with its decay-chain parent ^{226}Ra. Lead-210 dates were calculated using the Constant Rate of Supply Model (Appleby and Oldfield, 1978).

Peat humification: To assess the degree of peat humification, the elemental composition (CHNS-O) was measured in every second peat sample and the isotopic composition (δ^{13}C, δ^{15}N) in every fourth peat samples from all six peat profiles (G.G. Hatch Stable Isotope Lab, Department of Earth Sciences, University of Ottawa, Ottawa, ONT, Canada).

Peat and Pb accumulation rates: The ^{210}Pb age dates were combined with the ^{14}C age dates to create robust age-depth models for each peat core, for the period since AD 1900, using the P_Sequence function in OxCal 4.2. These models yield peat accumulation rates (cm/yr) and this information, combined with the dry bulk density (g/cm^3) and Pb concentrations (µg/g) of individual samples allows the Pb accumulation rates (mg/m^2/yr) to be calculated for each profile (figure SI4a). Determining the dry matter accumulation rate for the top slice of the core (the living layer) is challenging because of the difficulty in visually estimating where the living layer ends and the top of the peat core begins; this is currently done in the lab, when the core is frozen, before slicing. To calculate the Pb accumulation rate (mg/m^2/yr) for the living layer for each core, we use the average value

of the dry matter accumulation rate (1086 g/m^2/yr) obtained from the living layers of twelve peat cores: the primary cores from each of these six peat bogs, plus the first replicate core from each bog.

For the ABS region, the Pb accumulation rates for the living layer range from 0.34 mg/m^2/yr (ANZ) to 1.53 mg/m^2/yr (MIL). An independent assessment of these values can be obtained using the Pb concentrations reported for *Sphagnum* moss from these same bogs (Shotyk et al., 2014; 2016a) which range from ca. 0.5 to 1.2 μg/g, and the growth rate of *Sphagnum fuscum* in this area which has been measured and ranges from 120 to 160 g/m^2/yr (Vile et al., 2010). Using these values, the Pb accumulation rates obtained from *Sphagnum* moss are in the range 0.06 to 0.19 mg/m^2/yr. The following *caveat* must be considered when comparing Pb accumulation rates obtained using these two approaches: the *Sphagnum* moss samples (Shotyk et al., 2014; 2016a) were hand-picked to remove all foreign matter; in contrast, the living layer found at the top of each peat core consists of a complex milieu of plant materials (Vile et al., 2010), including not only *Sphagnum (S. fuscum, S. magellanicum, S. angustifolium, S. capillifolium)*, but also the leaves and stems of shrubs (*Vaccinium oxycoccos, V. vitis-idaea, Ledum groenlandicum, Rubus chamaemorus, Smilacina trifolia*), needles and bark from conifers (*Picea mariana*) as well as lichens (*Cladina mitis, Evernia mesomorpha*). Whereas the
Sphagnum moss specimens harvested for Pb analyses (Shotyk et al., 2014; 2016a) were sectioned to allow only living plant matter to be studied (and represent atmospheric inputs corresponding to the year of sample collection), the age of the other plant materials that make up the living layer, and the duration of atmospheric inputs they represent, are

unknown. The Pb accumulation rates presented here (figure SI4b), especially for the living layer, are conservative estimates. Moreover, they are not corrected for dust deposition, to allow them to be directly compared with Pb accumulation rates in published studies from other regions.

Figure SI1. Photos of the six peat cores showing variations in peat stratigraphy reflecting changes in botanical composition and degree of humification. The monoliths vary from ca. 70 cm (MIL, JPH4, both shallow peatlands) to ca. 100 cm (McK, McM, ANZ, UTK).

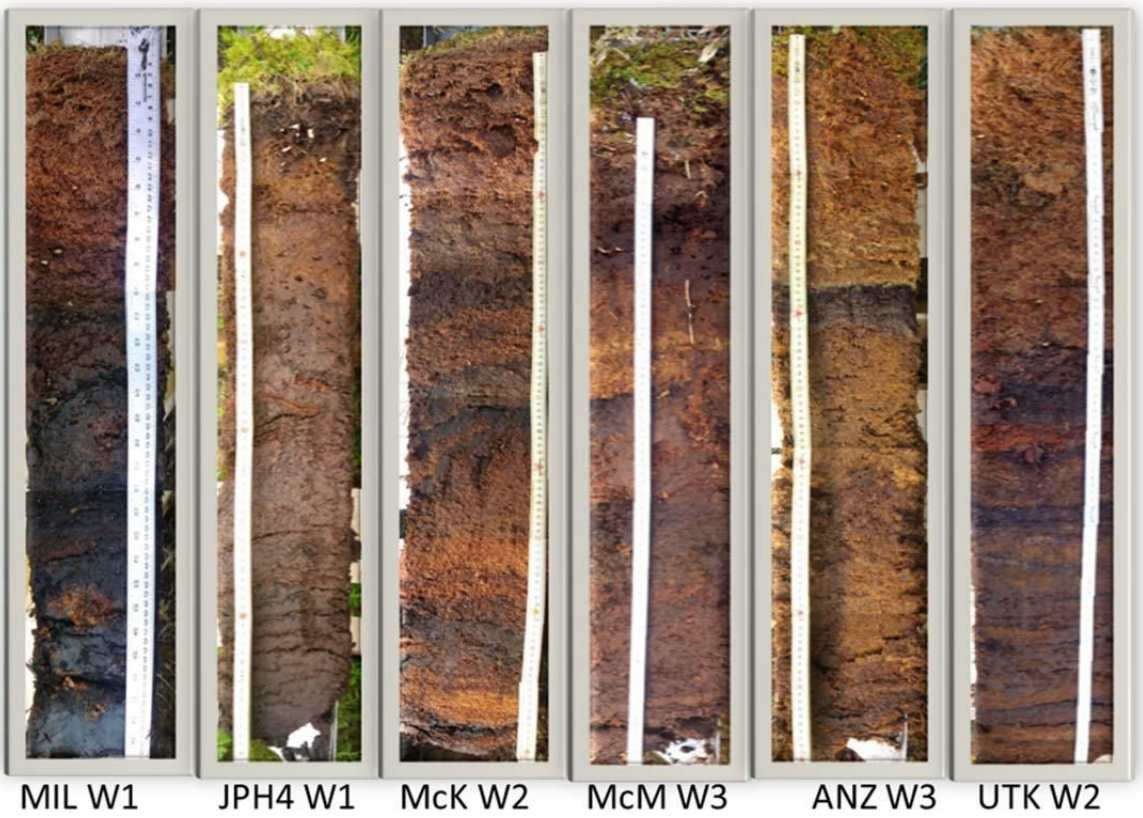

Figure SI2. Summary of plant macrofossil stratigraphy for the six peat cores.

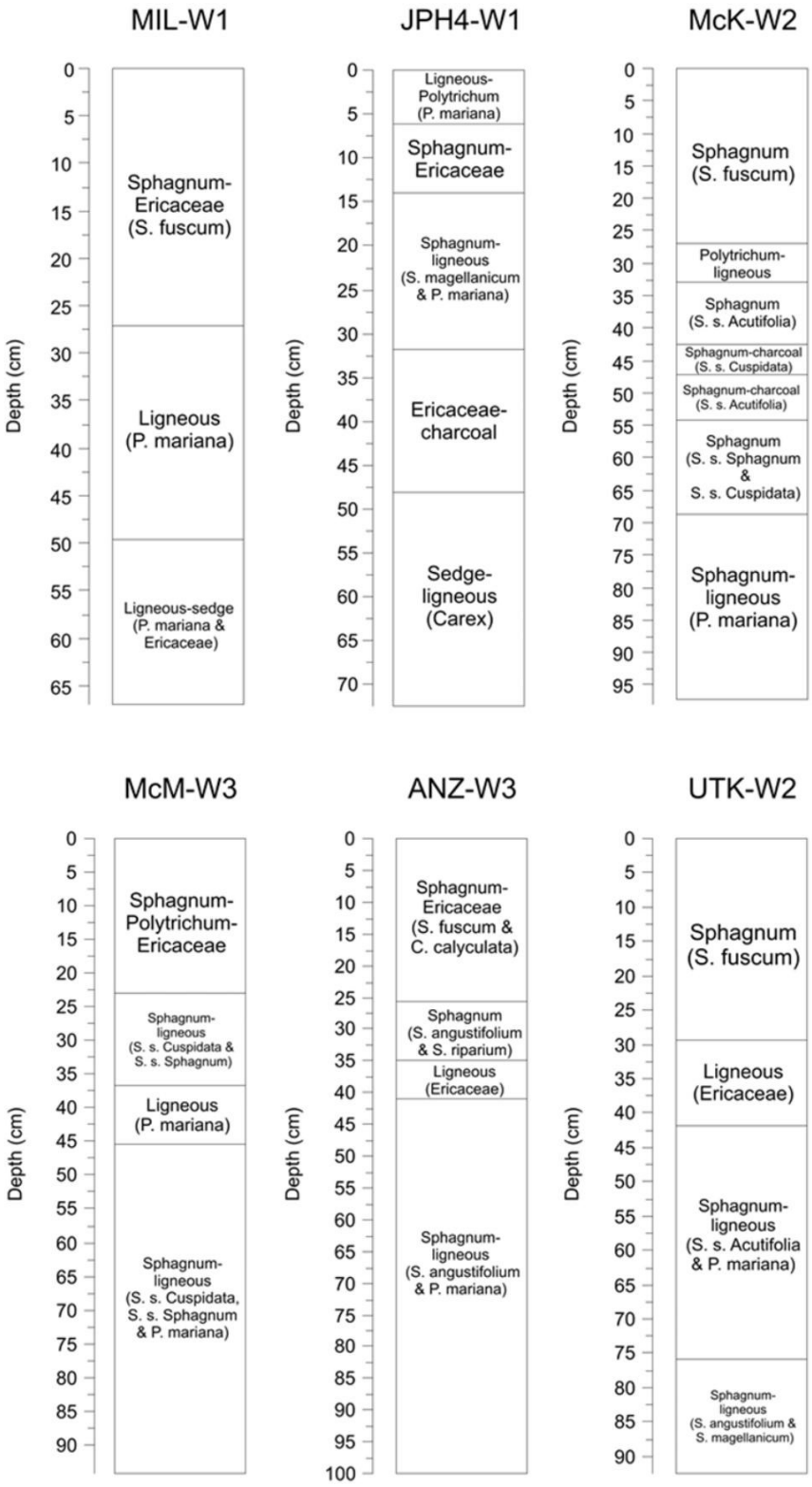

Figure SI3. (**A**) The pH of expressed porewaters and the (**B**) ash content of the peats (every second sample) of the six bogs. Only the top 20 cm of the MIL core is ombrotrophic, the remainder minerotrophic. The other five cores are ombrotrophic throughout.

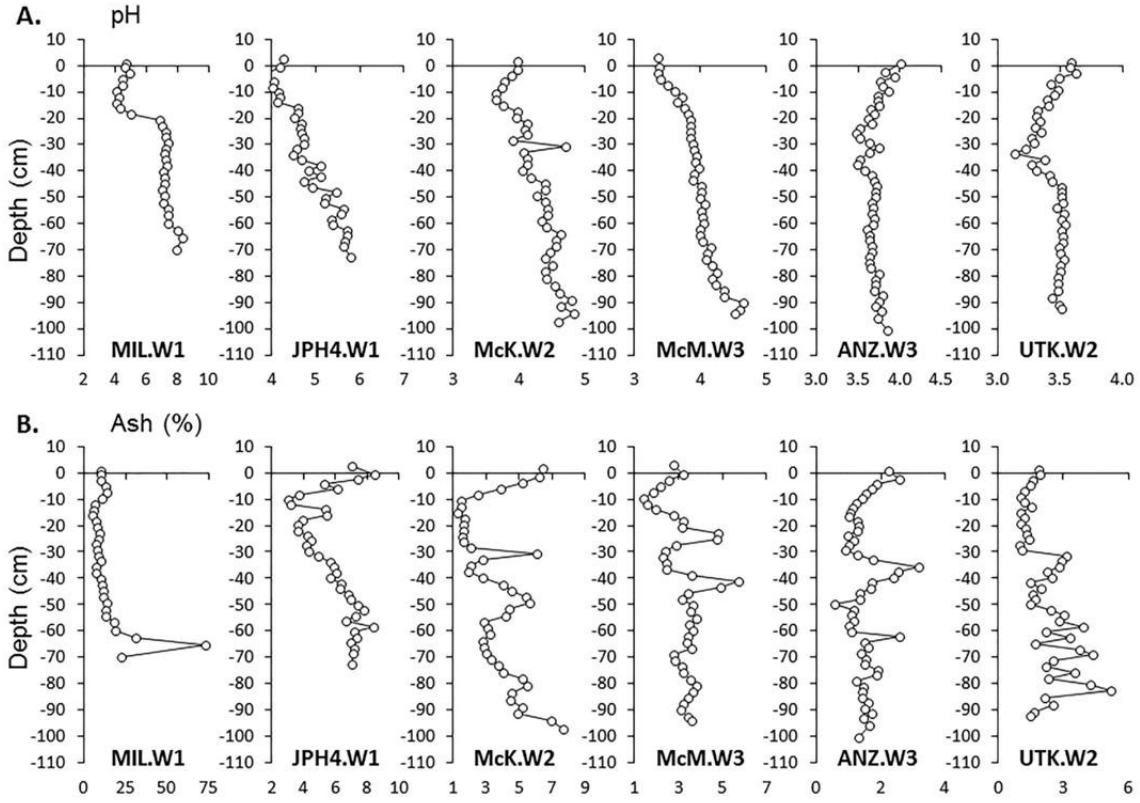

Figure SI4. (A) Anthropogenic Pb (solid line) and natural Pb (dashed line) concentrations calculated using the measured concentrations of Pb and Th, and the Pb/Th ratio of the Upper Continental Crust (Wedephol, 1995) and (B) the same information, shown as a function of age dating since the start of the 20th century.

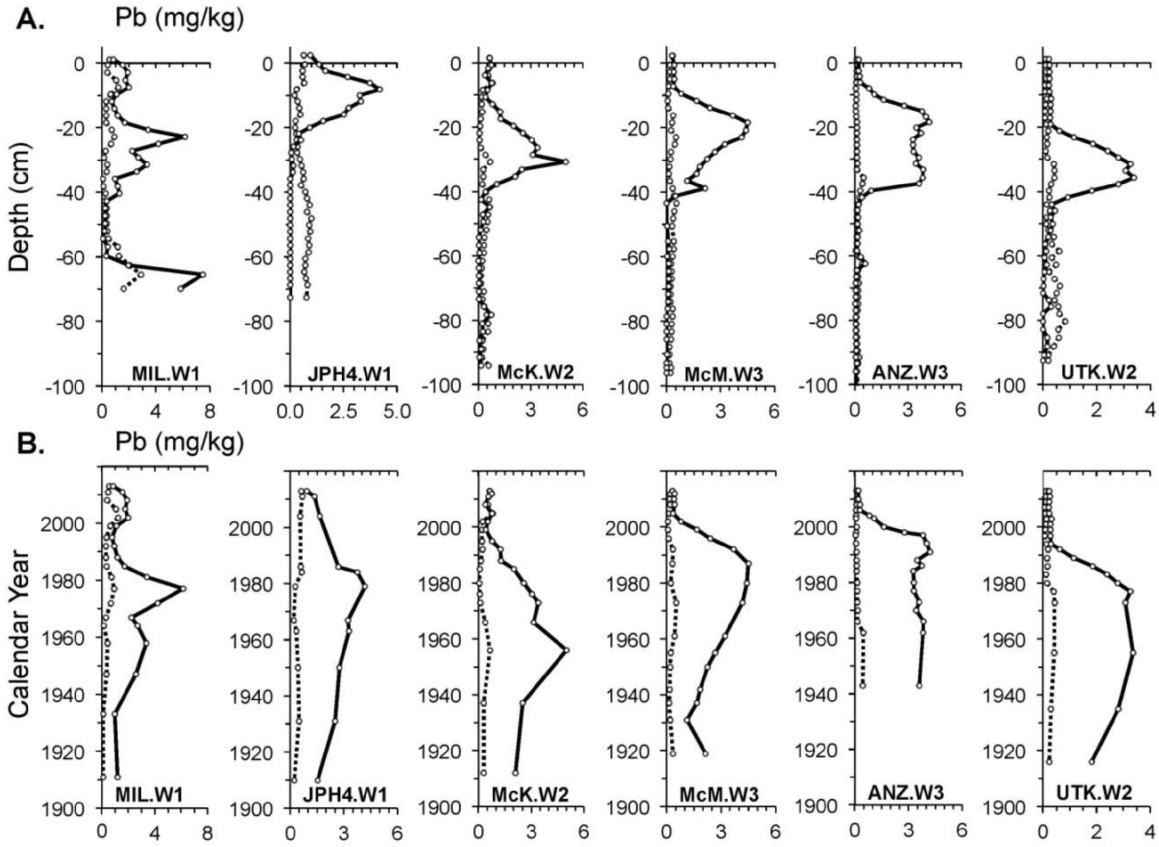

Table SI1. Locations of peat cores collected, with GPS coordinates and distance from the mid-point between Syncrude and Suncor upgraders.

		Latitude	Longitude	Distance from midpoint (km)
Moss and peat cores collected	MIL	56° 55'50.4" N	111° 28'30.3" W	11.0
	JPH-4	57° 6'44.10" N	111° 25'24.42" W	12.4
	McK	57° 13'42.4" N	111° 42'00.8" W	24.9
	McM	56° 37'40.4" N	111° 11'39.1" W	48.7
	ANZ	56° 28'19.08" N	111° 2'33.66" W	68.4
	UTK	56° 04'34.6" N	115° 28'31.2" W	263.8
	Syncrude stack	57° 2'49.61" N	111° 37'5.09" W	5.0
	Suncor stack	57° 00'8.36" N	111° 28'36.44" W	5.0
	CNRL stack	57° 20'16" N	111° 45'18.88" W	37.2
	Nexen stack	56° 24' 42.12" N	110° 56' 15.36" W	77.4
	Midpoint	57° 1'29" N	111° 32'51" W	0

Table SI2. Accuracy of Pb and Th determinations obtained using Certified Reference Materials.

Certified Reference Materials (Values in bold indicate informational values)	Pb mg/kg	Th mg/kg
NIST 1575a - Trace Elements in Pine Needles		
Certified value	0.167 ± 0.015	
Average measured value (n = 24)	0.147	0.013
Std. Dev.	0.015	0.002
% Accuracy	88	
Average measured value (n = 11)	10.5	0.037
Std. Dev.	0.5	0.005
% Accuracy	97	99
NIST 1547 - Trace Elements in Peach Leaves		
Certified value	0.87 ± 0.03	**0.05**
Average measured value (n = 28)	0.81	0.049
Std. Dev.	0.06	0.003
RSD	7	7
% Accuracy	93	98
NIST 1515 - Trace Elements in Apple Leaves		
Certified value	0.47 ± 0.024	**0.03**
Average measured value (n = 28)	0.44	0.026
Std. Dev.	0.03	0.004
RSD	7	15
% Accuracy	93	87
IAEA-336 - Trace and Minor Elements in Lichen		
Certified value	**4.9 ± 0.6**	0.14 ± 0.02
Average measured value (n = 8)	4.6	0.123
Std. Dev.	0.2	0.004
RSD	4	3
% Accuracy	94	88
IAEA-V-10 - Trace Elements in Hay (Powder)		
Certified value	1.60	
Average measured value (n = 7)	1.46	0.009
Std. Dev.	0.07	0.000
RSD	5	5
% Accuracy	91	
OGS 1878P - Trace Elements in Peat		
Certified value	78.8 ± 2.9	
Average measured value (n = 17)	69.1	0.373
Std. Dev.	7.3	0.051
RSD	11	14
% Accuracy	88	

Table SI3. Radiocarbon age dates of plant macrofossils from selected samples taken from the six peat cores.
Table SI3 is a large data table provided separately as a supporting Excel file, titled: Table SI3

Table SI4 Associated secondary standard radiocarbon dates.

Sample ID	Laboratory code	Descriptions	^{14}C age (BP)	Error	Consensus age
FIRI-F	142046	Wood shavings	4525	20	ca. 4515
AVR-07-PAL-37	142035	Wood shavings	48900	470	Non-finite
FIRI-F	142075	Wood shavings	4530	20	ca. 4515
AVR-07-PAL-37	142076	Wood shavings	50330	300	Non-finite
FIRI-F	152372	Wood shavings	4540	20	ca. 4515
AVR-07-PAL-37	152353	Wood shavings	48820	240	Non-finite
FIRI-F	154003	Wood shavings	4560	20	ca. 4515
AVR-07-PAL-37	154010	Wood shavings	44950	180	Non-finite
FIRI-F	154019	Wood shavings	4500	20	ca. 4515
AVR-07-PAL-37	154029	Wood shavings	8820	180	Non-finite
FIRI F	170655	Wood shavings	4530	15	ca. 4515
AVR-07-PAL-37	170657	Wood shavings	48460	330	Non-finite

Table SI5. Linear correlation coefficients between Pb concentration and humification proxies. Significant ($p<0.05$) correlations are shown in red. An increase in peat humification is generally associated with a decrease in C/N, H/C and O/C ratios, as well as an increase in density. We found that the Pb concentration profile is independent of peat humification in all 5 peat cores of the ABS region, and that the greatest Pb concentrations were generally found in less humified peat (higher values of atomic ratios and lower bulk density).

	C/N	H/C	O/C	Density	$\delta^{13}C$	$\delta^{15}N$
MIL	-0.2283 $p = 0.217$ ($n = 31$)	0.5915 $p = 0.000$ ($n = 31$)	0.4369 $p = 0.014$ ($n = 31$)	0.5891 $p = 0.000$ ($n = 31$)	0.3359 $p = 0.221$ ($n = 15$)	0.2571 $p = 0.355$ ($n = 15$)
JPH4	0.7798 $p = 0.000$ ($n = 37$)	-0.0888 $p = 0.601$ ($n = 37$)	0.6877 $p = 0.000$ ($n = 37$)	-0.7892 $p = 0.000$ ($n = 37$)	-0.0579 $p = 0.820$ ($n = 18$)	0.2624 $p = 0.239$ ($n = 18$)
McK	-0.0709 $p = 0.660$ ($n = 41$)	-0.0849 $p = 0.597$ ($n = 41$)	0.0863 $p = 0.592$ ($n = 41$)	-0.3170 $p = 0.043$ ($n = 41$)	-0.4229 $p = 0.063$ ($n = 20$)	-0.1000 $p = 0.675$ ($n = 20$)
McM	0.1798 $p = 0.254$ ($n = 42$)	0.4732 $p = 0.002$ ($n = 42$)	0.4259 $p = 0.005$ ($n = 42$)	-0.4768 $p = 0.001$ ($n = 42$)	0.1023 $p = 0.642$ ($n = 23$)	0.1670 $p = 0.446$ ($n = 23$)
ANZ	0.1972 $p = 0.170$ ($n = 50$)	-0.1966 $p = 0.171$ ($n = 50$)	0.0124 $p = 0.932$ ($n = 50$)	-0.3841 $p = 0.006$ ($n = 50$)	-0.1600 $p = 0.445$ ($n = 25$)	0.1903 $p = 0.362$ ($n = 25$)

Table SI6. Cumulative Anthropogenic, Atmospheric Pb (CAAPb) for peat cores studied by W.S. to date. For the peat cores from New Brunswick, Quebec, and Ontario, we used existing data for Pb and Ti concentrations (obtained in solid samples using X-ray fluorescence spectroscopy) and the ratio of Pb to Ti in the Upper Continental Crust[43]. For the peat cores from Finland and Manitoba, we used existing Pb and Sc data (from sector-field ICP mass spectrometry of acid digests) and the corresponding ratio for the UCC. Finally, for the AB peat cores, namely ANZ-W3, MIL-W1, McM-W3, UTK-W2, JPH4-W1, and McK-W2, we used Pb and Th concentrations (quadruopole ICP-MS of acid digests, this study) and the ratio of Pb to Th in the UCC. The calculation of CAAPb has been found to be largely unaffected by the choice of the lithophile reference element (Sc, Th, Ti or even Zr), simply because recent layers of peat bogs from Europe as well as northeastern North America are overwhelmingly dominated by anthropogenic Pb (Shotyk et al, 2000) which renders the natural component insignificant.

Name	Location	CAAPb (g/m2)	Reference
UNITED KINGDOM			
Lindow Bog	Manchester, England, UK	4.25	Le Roux et al. (2004)
Fleck's Loch	Foula, Shetland Islands, Scotland, UK	1.89	Weiss et al. (2002)
Loch Laxford	Scotland, UK	0.91	Weiss et al. (2002)
DENMARK			
Stoby Mose	Denmark	3.06	Shotyk, unpublished data
Myrarnar	Faroe Islands	1.90	Shotyk et al. (2005)
FINLAND			
Hietajaervi	Patvinsuo National Park, eastern Finland	0.44	Shotyk et al. (2016b)
Outokumpu	8 km southwest of Outokumpu Cu-Ni mine	0.49	Shotyk et al. (2016b)
Harjavalta	6 km northeast of Cu-Ni smelter	0.89	Shotyk et al. (2016b)
UKRAINE			
Bagno	Irshavsky District, Transcarpathia	4.64	Shotyk, unpublished data
Nebuga	250 km NW of Kiev, Ukraine	0.94	Shotyk, unpublished data
Babyn Moh	350 km NW of Kiev, Ukraine	0.93	Shotyk, unpublished data
SWITZERLAND			
Etang de la Gruere	Canton Jura	1.87	Shotyk et al. (2000)
Tourbiere des Genevez	Canton Jura	2.16	Shotyk et al. (2000)
Praz Rodet	Canton Vaud	1.95	Shotyk et al. (2000)
Schoepfenwaldmoor	Canton Berne	0.98	Shotyk et al. (2000)
Hagenmoos	Canton Zurich	1.89	Shotyk et al. (2000)
Suossa	Canton Grisons	3.15	Shotyk et al. (2000)
Mauntschas	Canton Grisons	1.11	Shotyk et al. (2000)
Gola di Lago	Canton Ticino	9.70	Shotyk et al. (2000)
GERMANY			
Wildseemoor	Northern Black Forest, Baden-Wurtemberg	1.57	Lindemann (2010)

NEW BRUNSWICK, CANADA			
Point Escuminac	Point Escuminac National Park	0.19	Weiss et al. (2002)
QUEBEC			
Kuujjuarapik (NQT04 core)	Great Whale River, Hudson Bay	0.07	Shotyk, unpublished data
ONTARIO, CANADA			
Sifton Bog	London	2.38	Givelet et al. (2003)
Luther Bog	Grand Valley	1.16	Givelet et al. (2003)
Spruce Bog	Algonquin Provincial Park	0.98	Givelet et al. (2003)
Mer Bleue Bog (MBB01 core)	Ottawa	1.29	Shotyk, unpublished data
Mer Bleue Bog (MBB02 core)	Ottawa	1.59	Shotyk, unpublished data
MANITOBA, CANADA			
Kotyk Lake (KOL27-1 core)	27 km NE of Zn smelter at Flin Flon	1.62	Shotyk et al. (2016c)
Sask Lake (SL4-1 core)	88 km NE of Zn smelter at Flin Flon	0.29	Shotyk et al. (2016c)
ALBERTA, CANADA			
Mildred	Alberta	0.043	this study
JPH4	Alberta	0.049	this study
McKay	Alberta	0.043	this study
McMurray	Alberta	0.035	this study
Anzac	Alberta	0.067	this study
Utikuma	Alberta	0.042	this study
BRITISH COLUMBIA, CANADA			
Drizzle Bog	Haida Gwai	**0.012**	Huntley et al. (2013)

REFERENCES

American Geological Institute (1976), *Dictionary of geological terms*, Anchor Press, New York.

Anon (1984), *The Pocket Oxford Dictionary of Current English*, Oxford University Press, Oxford, United Kingdom.

Appleby, P. G., and F. Oldfield (1978), The calculation of 210Pb dates assuming a constant rate of supply of unsupported 210Pb to the sediment. *Catena*, (5), 1-8.

Appleby, P. G., W. Shotyk, and A. Fankhauser (1997), Lead-210 age dating of three peat cores in the Jura Mountains, Switzerland. *Water Air Soil Pollut., 100*(3-4), 223–231, doi:10.1023/A:1018380922280.

Ayotte, G., and L. Rochefort (2006), *Les sphaignes du Québec*, Université Laval, Quebec City.

Bronk Ramsey, C. (2009), Bayesian analysis of radiocarbon dates. *Radiocarbon, 51*(1), 337-360.

Clark, K. A., and S. M. Blair (1927), *The Bituminous Sands of Alberta*, Edmonton: Scientific and Industrial Research Council of Alberta. Report No. 18.

Crum, H. A., and L. E. Anderson (1981), *Mosses of Eastern North America*, Columbia University Press, New York.

Fairbridge, R. W. (1972), The Encyclopedia of Geochemistry and Environmental Sciences, edited by R. W. Fairbridge, Dowden, Hutchinson, and Ross, Stroudsburg, Pennsylvania.

Garneau, M. (1995), *Reference Collection of Seeds and Other Botanical Macrofossils from Meridional and Boreal Quebec*. Geological Survey of Canada, Terrain sciences division, Sainte-Foy, Quebec. Open file 3048.

Givelet, N., F. Roos-Barraclough, and W. Shotyk (2003), Predominant anthropogenic sources and rates of atmospheric mercury accumulation in southern Ontario recorded by peat cores from three bogs: comparison with natural "background" values (past 8000 years). *J. Environ. Monit., 5*(6), 935–49.

Hua, Q., M. Barbetti, and a Z. Rakowski (2013), Atmospheric radiocarbon for the period 1950-2010. *Radiocarbon*, *55*(4), 2059–2072.

Huntley, M. J., R. W. Mathewes, and W. Shotyk (2013), High-resolution palynology, climate change and human impact on a late Holocene peat bog on Haida Gwaii, British Columbia, Canada. *The Holocene*, *23*(11), 1572–1583, doi:10.1177/0959683613499051.

Hurtig, M. (1985), *Canadian Encyclopedia*, Hurtig Publishers, Edmonton.

Jones, J. M., and J. Hao (1993), Ombrotrophic peat as a medium for historical monitoring of heavy metal pollution. Environ. *Geochem. Health, 15*(2-3), 67–74, doi:10.1007/BF02627824.

Laine, J., P. Harju, T. Timonen, A. Laine, E.-S. Tuittila, K. Minkkinen, and H. Vasander (2009), The Intricate Beauty of Sphagnum Mosses - a Finnish Guide to Identification. University of Helsinki, Department of Forest Ecology, Helsinki, Finland.

Lee, J. A., and J. H. Tallis (1973), Regional and historical aspects of lead pollution in Britain. *Nature*, *245*(5422), 216–218, doi:10.1038/245216a0.

Lindemann, M. (2010), Titanium and Lead in peat as indicators of natural and anthropogenic aerosols (in German), University of Heidelberg, Heidelberg, Germany.

Nilsson, M., M. Klarqvist, and G. Possnert (2001), Variation in ^{14}C age of macrofossils and different fractions of minute peat samples dated by AMS. *The Holocene*, *11*(5), 579–586, doi:10.1191/095968301680223521.

Reimer, P. (2013), IntCal13 and Marine13 Radiocarbon Age Calibration Curves 0– 50,000 Years cal BP. *Radiocarbon*, *55*(4), 1869–1887, doi:10.2458/azu_js_rc.55.16947.

Le Roux, G., D. Aubert, P. Stille, M. Krachler, B. Kober, A. Cheburkin, G. Bonani, and W. Shotyk (2005), Recent atmospheric Pb deposition at a rural site in southern Germany assessed using a peat core and snowpack, and comparison with other archives. *Atmos. Environ., 39*(36), 6790–6801, doi:10.1016/j.atmosenv.2005.07.026.

Shotyk, W. (1996a), Natural and anthropogenic enrichments of As, Cu, Pb, Sb, and Zn in ombrotrophic versus minerotrophic peat bog profiles, Jura Mountains, Switzerland. *Water Air Soil Pollut.*, *90*(3-4), 375–405, doi:10.1007/BF00282657.

Shotyk, W. (1996b), Peat bog archives of atmospheric metal deposition: geochemical evaluation of peat profiles, natural variations in metal concentrations, and metal enrichment factors. *Environ. Rev.*, *4*(2), 149–183, doi:10.1139/a96-010.

Shotyk, W. (2002), The chronology of anthropogenic, atmospheric Pb deposition recorded by peat cores in three minerogenic peat deposits from Switzerland. *Sci. Total Environ.*, *292*(1-2), 19–31, doi:10.1016/S0048-9697(02)00030-X.

Shotyk, W., H. W. Nesbitt, and W. Fyfe (1990), The behaviour of major and trace elements in complete vertical peat profiles from three *Sphagnum* bogs. *Int. J. Coal. Geol.*, *15*, 163–190.

Shotyk, W., H. Wayne Nesbitt, and W. S. Fyfe (1992), Natural and anthropogenic enrichments of trace metals in peat profile. *Int. J. Coal Geol.,* *20*(1-2), 49–84, doi:10.1016/0166-5162(92)90004-G.

Shotyk, W., A. K. Cheburkin, P. G. Appleby, A. Fankhauser, and J. D. Kramers (1997), Lead in three peat bog profiles, Jura Mountains, Switzerland: Enrichment factors, isotopic composition, and chronology of atmospheric deposition. *Water Air Soil Pollut.*, *100*(3-4), 297–310, doi:10.1023/A:1018384711802.

Shotyk, W., D. Weiss, P. Appleby, A. Cheburkin, R. Gloor, J. Kramers, S. Reese, and Van Der Knaap WO (1998), History of atmospheric lead deposition since 12,370 ^{14}C yr BP from a peat bog, Jura mountains, Switzerland. *Science*, *281*(5383), 1635–40.

Shotyk, W., P. Blaser, A. Grünig, and A. K. Cheburkin (2000), A new approach for quantifying cumulative, anthropogenic, atmospheric lead deposition using peat cores from bogs: Pb in eight Swiss peat bog profiles. *Sci. Total Environ.*, *249*(1-3), 281–295, doi:10.1016/S0048-9697(99)00523-9.

Shotyk, W., D. Weiss, M. Heisterkamp, A. K. Cheburkin, P. G. Appleby, and F. C. Adams (2002), New peat bog record of atmospheric lead pollution in Switzerland: Pb concentrations, enrichment factors, isotopic composition, and organolead species. *Environ. Sci. Technol.*, *36*(18), 3893–900.

Shotyk, W., M. E. Goodsite, F. Roos-Barraclough, N. Givelet, G. Le Roux, D. Weiss, A. K. Cheburkin, K. Knudsen, J. Heinemeier, W. O. van Der Knaap, S. A. Norton, C. (2005a), Accumulation rates and predominant atmospheric sources of natural and anthropogenic Hg and Pb on the Faroe Islands. *Geochim. Cosmochim. Acta*, *69*(1), 1–17, doi:10.1016/j.gca.2004.06.011.

Shotyk, W., J. Zheng, M. Krachler, C. Zdanowicz, R. Koerner, and D. Fisher (2005b), Predominance of industrial Pb in recent snow (1994-2004) and ice (1842-1996) from Devon Island, Arctic Canada. *Geophys. Res. Lett.*, *32*(21), 1–4, doi:10.1029/2005GL023860.

Shotyk, W., R. Belland, M. J. Duke, H. Kempter, M. Krachler, T. Noernberg, R. Pelletier, M.A. Vile, K. Wieder, C. Zaccone, S. Zhang (2014), *Sphagnum* mosses from 21 ombrotrophic bogs in the Athabasca bituminous sands region show no significant atmospheric contamination of "heavy metals". *Environ. Sci. Technol.*, *48*(21), 12603–11, doi:10.1021/es503751v.

Shotyk, W., H. Kempter, M. Krachler, and C. Zaccone (2015), Stable (^{206}Pb, ^{20}7Pb, ^{208}Pb) and radioactive (^{210}Pb) lead isotopes in 1 year of growth of *Sphagnum* moss from four ombrotrophic bogs in southern Germany: Geochemical significance and environmental implications. *Geochim. Cosmochim. Acta*, *163*, 101–125, doi:10.1016/j.gca.2015.04.026.

Shotyk, W., B. Bicalho, C.W. Cuss, M.J. Duke, T. Noernberg, R. Pelletier, E. Steinnes, and C. Zaccone (2016a), Dust is the dominant source of "heavy metals" to peat moss (*Sphagnum fuscum*) from the industrial development of the Athabasca Bituminous Sands in northern Alberta, Canada. *Environ. Int.92-93*: 494-506 (doi: 10.1016/j.envint.2016.03.018)

Shotyk, W., N. Rausch, T. Nieminen, L. Ukomaanaho, and M. Krachler (2016b), Isotopic composition of Pb in peat and porewaters from three contrasting ombrotrophic bogs in Finland: evidence of chemical diagenesis in response to acidification. *Environ. Sci. Technol*. (published online 18 August, 2016) doi: 10.1021/acs.est.6b01076

Shotyk, W., N. Rausch, M. Krachler, and P.M. Outridge (2016c), Isotopic evolution of atmospheric Pb from metallurgical processing in Flin Flon, Manitoba: retrospective analysis using peat cores from bogs. *Environ. Poll.* (published online 16 July, 2016). doi:10.1016/j.envpol.2016.07.009

Vile, M. A., R. K. Wieder, S. Berryman, D. Vitt (2010), *Development of Monitoring Protocols for N & S Sensitive Bog Ecosystems,* Wood Buffalo Environmental Association: Fort McMurray, Alberta, Canada, pp 91.

Wardenaar, E. (1987), A new hand tool for cutting peat profiles. *Can. J. Bot.*, *65*, 1772–1773.

Weiss, D., W. Shotyk, and O. Kempf (1999a), Archives of atmospheric lead pollution. *Naturwissenschaften*, *86*(6), 262–275, doi:10.1007/s001140050612.

Weiss, D., W. Shotyk, P. G. Appleby, J. D. Kramers, and A. K. Cheburkin (1999b), Atmospheric Pb deposition since the industrial revolution recorded by five Swiss peat profiles: Enrichment factors, fluxes, isotopic composition, and sources. *Environ. Sci. Technol.*, *33*(9), 1340–1352, doi:10.1021/es980882q.

Weiss, D., W. Shotyk, M. Gloor, and J. D. Kramers (1999c), Herbarium specimens of *Sphagnum* moss as archives of recent and past atmospheric Pb deposition in Switzerland: isotopic composition and source assessment. *Atmos. Environ.*, *33*, 3751–3763.

Sample ID	UCIAMS #	Depth (cm)	Description	Weight (mgC)	Fraction modern	±	14C age (BP)	±	Calibrated age (cal BC/AD) 68.2% range	95.4% range	Modelled age (cal BC/AD) 68.2% range	Median	Range width	
ANZ-W3 #05	170621	-5.99	*Sphagnum* stems	---	1.0634	0.0017	---	---	2005-2006	2005-2008	1956-1957	2006-2008	2007	2	
ANZ-W3 #10	170623	-10.62	*Sphagnum* stems	---	1.0675	0.0019	---	---	2004-2006	2003-2007	1956-1957	2004-2006	2005	2	
ANZ-W3 #15	154027	-14.98	*Sphagnum* stems	15.1	1.1521	0.0023	---	---	1990-1991	1957-1958	1989-1991	1990-1991	1990	1	
ANZ-W3 #20	154026	-19.2	*Sphagnum* stems	11.8	1.2131	0.0022	---	---	1960-1961	1984-1985	1959-1961	1983-1985	1984-1985	1985	1
ANZ-W3 #25	154025	-23.75	*Sphagnum* stems	11.2	1.3133	0.0025	---	---	1978-1979	---	1962	1977-1979	1977-1979	1978	2
ANZ-W3 #30	154024	-28.45	*Sphagnum*, *Ericaceae* leaves	9.9	1.4155	0.0025	---	---	1962	1974	1962-1963	1973-1974	1973-1975	1974	2
ANZ-W3 #40	142039	-38.62	Twig material	---	---	---	170	20	1669-1682; 1736-1780; 1799-1805	1935-1944	1665-1693; 1727-1785; 1793-1813	1919-	1925-1951; 1798-1805	1765	153
ANZ-W3 #50	152367	-49.01	*Sphagnum* stems, *Picea* needles	9.9	---	---	330	15	1514-1528	1553-1599; 1617-1633	1490-1603	1613-1637	1615-1639; 1587-1599	1621	52
ANZ-W3 #60	142038	-59.31	*Sphagnum* stems	---	---	---	325	20	1516-1530; 1539-1596	1618-1635	1490-1603	1612-1642	1484-1527	1502	43
ANZ-W3 #70	152362	-69.62	*Sphagnum* stems and branches, *Picea* needles, *Chamaedaphne calyculata* seed	6.1	---	---	910	15	1049-1085	1124-1137; 1150-1160	1041-1108	1116-1165	1051-1084; 1123-1138; 1149-1160	1097	109
ANZ-W3 #80	142043	-80.15	*Sphagnum* stems and leaves	---	---	---	1245	25	689-751	760-775	682-779	790-869	695-750; 760-776; 793-801; 841-863	765	175
JPH4-W1 #5	154012	-4.31	*Sphagnum*, *Picea* needles	1.5	1.2789	0.0023	---	---	1979-1980	---	1959; 1961-1962	1979-1980; 1981	1979-1981	1980	2
JPH4-W1 #10	154011	-9.08	*Sphagnum* stems	4.3	1.7993	0.0033	---	---	1965	---	1963-1965	---	1964-1965	1964	1
JPH4-W1 #14	154009	-12.89	*Sphagnum* stems	6.4	1.2479	0.0023	---	---	1981-1982	---	1959; 1961-1962	1980-1982	1959-1962	1961	3
JPH4-W1 #20	154008	-18.93	*Sphagnum* stems, *V. oxycoccos* charred leaves, *Picea* charred needles	4.2	---	---	95	15	1698-1724	1815-1835; 1878-1395; 1903-1917	1694-1728	1812-1919	1695-1725; 1815-1835; 1875-1920	1845	225
JPH4-W1 #30	142066	-28.65	*Sphagnum* stems, *Conifer/Ericaceae* bark, *Carex* seeds, *Picea* charred needles	---	---	---	490	40	1411-1445	---	1324-1346	1393-1464	1415-1445	1430	30
JPH4-W1 #39-40	152359	-38.3	Bark	4.1	---	---	605	20	1306-1329; 1341-1363	1385-1396	1299-1370	1380-1404	1300-1330; 1340-1365; 1385-1395	1340	95
JPH4-W1 #50	142037	-49.13	*Carex* seeds, Conifer bark, *Ericaceae* stems	---	---	---	955	20	1029-1047	1091-1121; 1140-1148	1022-1059	1069-1155	1025-1050; 1085-1125; 1135-1150	1095	125
JPH4-W1 #59	152360	-58.47	Stem and fragments (ligneous)	5.7	---	---	1290	15	678-710	746-764	670-723	740-768	675-710; 745-765	710	90
JPH4-W1 #70	142045	-70.07	*Sphagnum* stems	---	---	---	2405	20	*448-409*	---	*703-696*	*541-402*	*510-400*	*470*	110
McK-W2 #10	154007	-11.76	*Sphagnum* stems	12.2	1.1453	0.0025	---	---	1990-1992	---	1957-1958	1990-1992	1990-1992	1991	2
McK-W2 #15	154006	-17.39	*Sphagnum* stems	8.7	1.2336	0.0022	---	---	1960	1982-1983	1959-1960; 1961-1962	1982-1983	1982-1984	1983	2
McK-W2 #20	154005	-22.96	*Sphagnum* stems	10.0	1.5258	0.0033	---	---	1970	1971	1969-1971	---	1969-1971	1970	2
McK-W2 #25	154004	-28.58	*Sphagnum* , Rhododendron leaves	5.2	1.7272	0.0031	---	---	1966	---	1965-1966	---	1965-1966	1965	1
McK-W2 #40	142064	-45.92	*Sphagnum* stems and leaves	---	---	---	280	20	1528-1551	1634-1651	1521-1576; 1584-1591	1626-1662	1525-1555; 1630-1650	1560	125
McK-W2 #50	152365	-57.90	*Picea* charred needles, *Sphagnum* stems	8.0	---	---	1135	15	889-901	921-953	882-972	---	885-900; 920-965	930	80
McK-W2 #60	142065	-69.77	*Sphagnum* stems and leaves	---	---	---	1220	20	728-737; 768-779	790-829; 838-865	713-744	765-885	725-740; 765-780; 785-830; 835-860	805	135
McK-W2 #70	152366	-82.29	*Picea* charred needles, Ericaceae charred leaves, *Sphagnum* stems	3.3	---	---	1575	15	429-436; 446-472	487-498; 505-535	426-538	---	425-475; 485-500; 505-535	480	110
McK-W2 #77	142068	-91.60	*Sphagnum* stems and leaves	---	---	---	1920	45	25-130	---	*21-11*	*2* -216	25-135; 200-210	99	185
MCM W3 #05	170644	-5.02	*Sphagnum* stems	---	1.0901	0.0017	---	---	2000-2001	---	1999-2002	1957	1998-2003	2001	5
McM-W3 #11	170627	-11.74	*Sphagnum* stems	---	1.1318	0.0017	---	---	1993	---	1992-1994	1957-1958	1991-1998	1994	7
McM-W3 #17	170634	-18.48	*Sphagnum* stems	---	1.1621	0.0017	---	---	1989-1990	---	1988-1990	1957-1958	1987-1993	1988	6
McM-W3 #23	170629	-25.27	*Sphagnum* stems	---	1.0004	0.0015	---	---	1954-1955	---	1954-1955	1956-1957	1948-1955	1950	7
MCM W3 #29	170639	-32.06	*Sphagnum* stems	---	---	---	95	15	1698-1724; 1815-1835	1878-1895; 1903-1917	1812-1919	1694-1728	1879-1896; 1903-1916	1892	37
McM-W3 #35	170626	-38.83	*Sphagnum* stems	---	---	---	120	15	1833-1880; 1915-1926	1688-1706; 1720-1730; 1809-1819	1806-1893	1683-1735; 1907-1930	1807-1849	1831	42
McM-W3 #38	154002	-42.29	Charred *Picea* and *Larix* leaves	2.7	---	---	210	20	1655-1670; 1779-1799	1943-	1648-1682; 1739-1744; 1752-1803	1937-	1784-1800	1792	16
McM-W3 #42	163396	-47.02	*Sphagnum* stems and charred *Larix* leaves	---	---	---	985	15	1018-1039	---	1016-1047	1092-1122;1140-1148	1103-1120; 1140-1148	1114	45
McM-W3 #52	163398	-53.96	*Sphagnum* stems	---	---	---	950	20	1030-1049	1085-1124; 1137-1150	1025-1059	1065-1155	1024-1056	1044	32
McM-W3 #60	154001	-68.03	*Sphagnum stems*	6.2	---	---	1220	20	728-737	768-779; 790-829; 838-865	713-744	765-885	721-740; 767-782; 787-829; 844-849	792	128
McM-W3 #80	154000	-91.50	*Larix leaves, Picea leaves*	2.2	---	---	1905	15	76-91	99-124	65-130	---	78-90; 99-125	102	47
MIL-W1 #10	154023	-10.82	*Sphagnum* stems	6.5	1.1235	0.002	---	---	1993-1995	---	1957-1958	1993-1995	1994-1995	1994	1
MIL-W1 #15	154022	-16.24	Sphagnum, Ericaceae leaves	5.3	1.1843	0.0021	---	---	1958-1959	1986-1988	1958-1959	1986-1988	1987-1988	1987	1
MIL-W1 #20	154021	-21.78	*Sphagnum* stems	5.5	1.3382	0.0024	---	---	1977	---	1976-1977	1978	1976-1978	1977	2
MIL-W1 #25	154018	-27.17	*Sphagnum* stems	3.6	1.2256	0.0022	---	---	1959-1960; 1961	1983-1984	1959-1962	1982-1985	1959-1961	1960	2
MIL-W1 #30	154017	-32.56	*Sphagnum* stems	2.5	1.0587	0.0021	---	---	2006-2008	2009-2014	1956	2005-2014	1956-1957	1957	1
MIL-W1 #35	154016	-38.1	*Sphagnum* stems	2.4	---	---	25	15	1896-1904	---	1891-1907	---	1895-1905	1900	10
MIL-W1 #40	142040	-43.77	Bark of twigs, twig, woody fragments, seeds	---	---	---	110	20	1694-1710; 1718-1727	1813-1890; 1910-1917	1685-1733	1807-1896; 1903-1928	1690-1730; 1810-1885	1825	195
MIL-W1 #44	152363	-48.44	Charred *Picea* , *Larix* needles and Ericaceae leaves	3.0	---	---	675	15	1282-1299	1372-1378	1278-1305	1365-1385	1280-1300; 1370-1380	1295	100	
MIL-W1 #50	142041	-55.56	Stems	---	1.3667	0.0029	---	---	1975-1976	---	1974-1976	---				Anomalously young
MIL-W1 #50-51	152364	-55.56	Coniferous bark (peridermis)	3.4	---	---	990	15	1018-1035	---	1012-1045	1095-1121	1015-1035	1025	20	
MIL-W1 #55	152361	-62.60	Charred *Picea* needles	10.0	---	---	1135	15	889-901	921-953	882-972	---	885-905; 915-955	925	70	
MIL-W1 #58	142042	-66.98	Charcoal particles	---	---	---	1500	20	551-593	---	478-482	536-620	555-600	575	45	
UTK W2 #05	170646	-4.87	*Sphagnum stems*	---	1.0489	0.0017	---	---	2007-2009	---	2007-2009	1956-1957	2008-2009	2008	1	
UTK W2 #11	170641	-11.06	*Sphagnum stems*	---	1.0846	0.0018	---	---	2001-2002	---	2000-2003	1957	2001-2002	2002	1	
UTK-W2 #17	170630	-17.10	*Sphagnum stems*	---	1.1349	0.0018	---	---	1992-1993	---	1991-1994	1957-1958	1992-1994	1993	2	
UTK W2 #23	170642	-23.18	*Sphagnum stems*	---	1.2225	0.0021	---	---	1983-1984	1959-1960	1983-1985	1959-1962	1983-1985	1984	2	
UTK-W2 #29	170624	-29.36	*Sphagnum stems*	---	1.3755	0.0023	---	---	1974-1976	---	1974-1976	1962	1975-1976	1975	1	
UTK-W2 #32	163401	-32.50	Sphagnum stems	---	1.5449	0.0025	---	---	1969-1970	---	1968-1970	1971	1969-1970	1969	1	
UTK-W2 #42	154015	-42.85	*Sphagnum stems*	10.1	---	---	55	20	1710-1718	1828-1832; 1890-1910	1697-1725	1814-1835; 1877-1918	1710-1717; 1826-1832; 1890-1910	1894	200	
UTK-W2 #48	163397	-49.07	*Sphagnum stems*	---	---	---	220	15	1660-1666	1784-1796	1648-1670; 1780-1800	1943-	1657-1667; 1784-1795	1667	138	
UTK-W2 #54	163402	-55.22	*Sphagnum stems*	---	---	---	320	15	1522-1530; 1539-1591	1620-1635	1497-1506; 1512-1601	1616-1643	1521-1529; 1540-1577; 1582-1591; 1620-1637	1567	116	
UTK-W2 #62	154014	-63.83	*Sphagnum*	3.8	---	---	1100	15	901-921	950-980	895-929	939-988	901-920; 950-980	949	79	
UTK-W2 #84	154013	-89.53	*Sphagnum stems*	8.6	---	---	2485	15	*594-546*	*648-610; 670-663; 689-681; 754-735*	*696-540*	*721-702; 766-727*	*544-596; 607-648; 663-669; 682-688; 743-749*	*619*	*205*	

Note
Modelled ages are reported to 1 year for post bomb & 5 years for ^{14}C
BC dates are in *italic*
Dates are calibrated using OxCal v 4.2 with IntCal13 and Bomb13NH1 as appropriate
Dates are modelled using a P_Sequence depositional model in OxCal v 4.2 with the above calibration curves

APPENDIX 3: Fort McKay furnace filter SEM and EDX analysis

During a conversation with a local resident of Fort McKay, the Athabasca River project field team (Shotyk, Noernberg, Donner) learned that furnace air filters in homes had to be change twice per month, because of the 'dust from the coke piles'. At that time we requested, and received, a used furnace filter from the resident's home. Examples of the dust particles found using the SEM are presented in this Appendix.

Furnace Filter SEM images

Note: Cu and Zn are artifacts of the plate the samples were on in the SEM

The numbers on the images correlate to the number of the following spectrum

C based furnace filter
Cu is background noise from plate

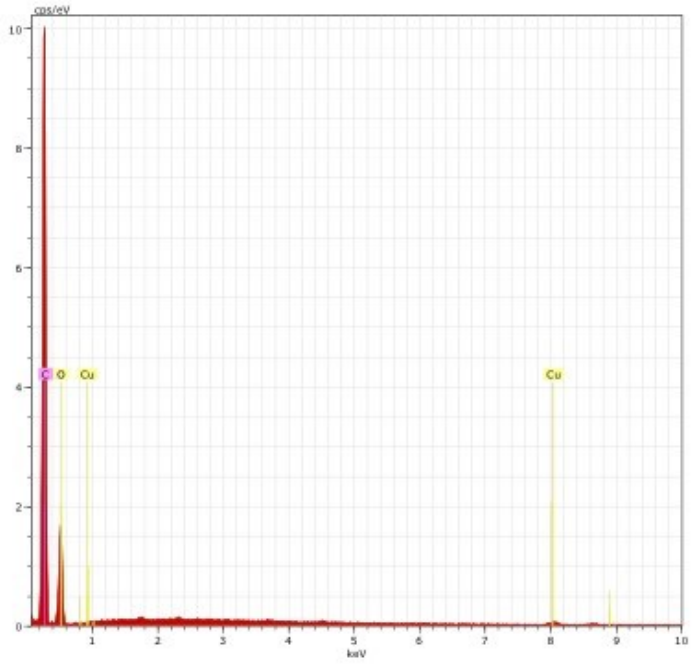

Fur_Clean 1 Date:3/17/2016 1:36:41 PM HV:25.0kV

El	AN	Series	unn. C [wt.%]	norm. C [wt.%]	Atom. C [at.%]	Error (1 Sigma) [wt.%]
O	8	K-series	6.12	89.20	97.04	1.23
Cu	29	K-series	0.74	10.80	2.96	0.09
C	6	K-series	0.00	0.00	0.00	0.00
		Total:	6.86	100.00	100.00	

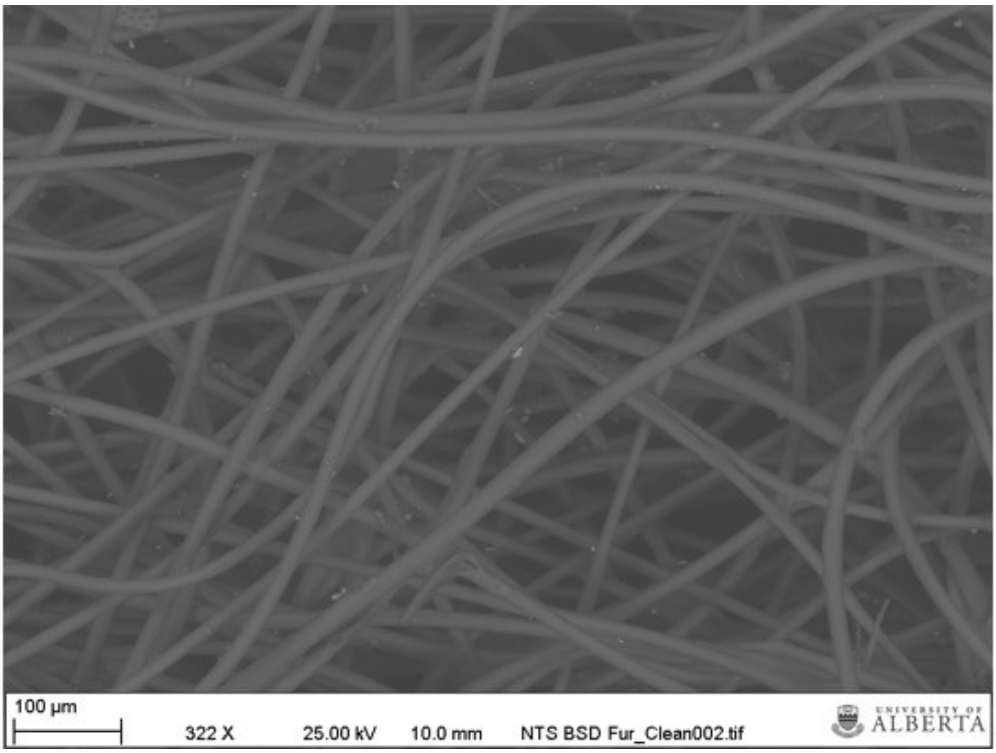

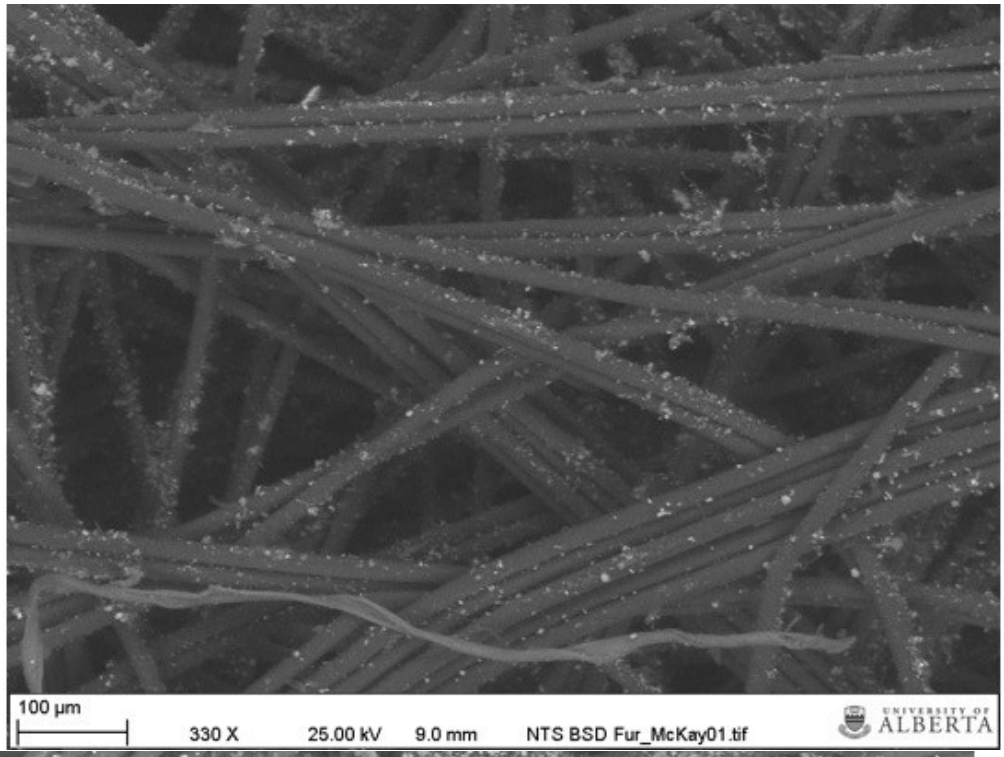
100 µm
330 X
25.00 kV
9.0 mm
NTS BSD Fur_McKay01.tif
UNIVERSITY OF ALBERTA

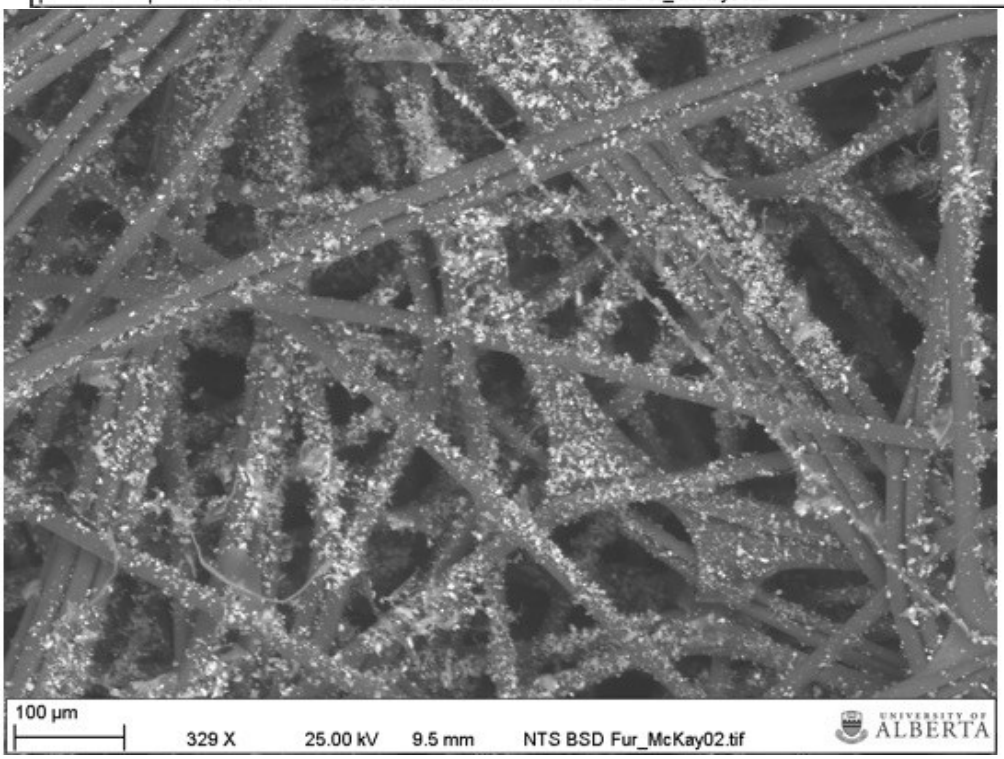
100 µm
329 X
25.00 kV
9.5 mm
NTS BSD Fur_McKay02.tif
UNIVERSITY OF ALBERTA

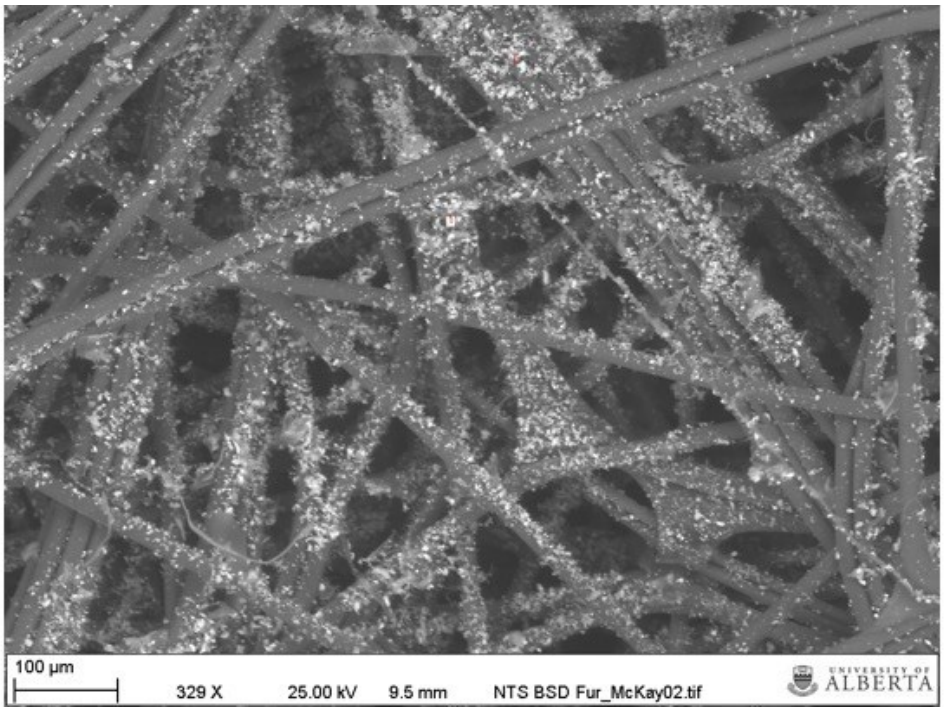

Fine particle Aluminosilicate (probably biotite) mixed with calcite

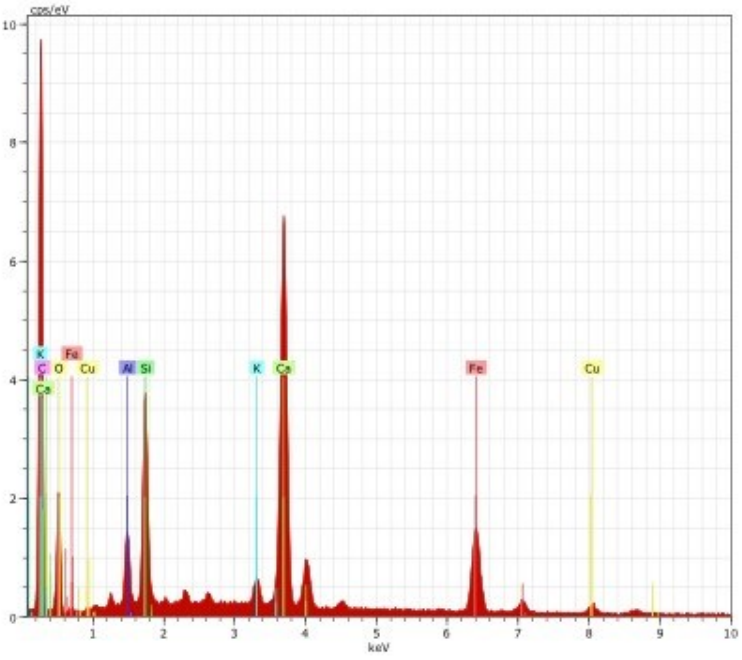

Fur_McKay 1Date:3/17/2016 1:51:12 PM HV:25.0kV

El	AN	Series	unn. C [wt.%]	norm. C [wt.%]	Atom. C [at.%]	Error (1 Sigma) [wt.%]
Ca	20	K-series	18.39	35.21	23.29	0.61
Si	14	K-series	4.66	8.93	8.43	0.26
Fe	26	K-series	6.99	13.38	6.35	0.26
Al	13	K-series	2.61	5.01	4.92	0.19
K	19	K-series	1.08	2.07	1.41	0.08
Cu	29	K-series	1.28	2.46	1.03	0.11
O	8	K-series	17.20	32.94	54.58	3.59
C	6	K-series	0.00	0.00	0.00	0.00
		Total:	52.22	100.00	100.00	

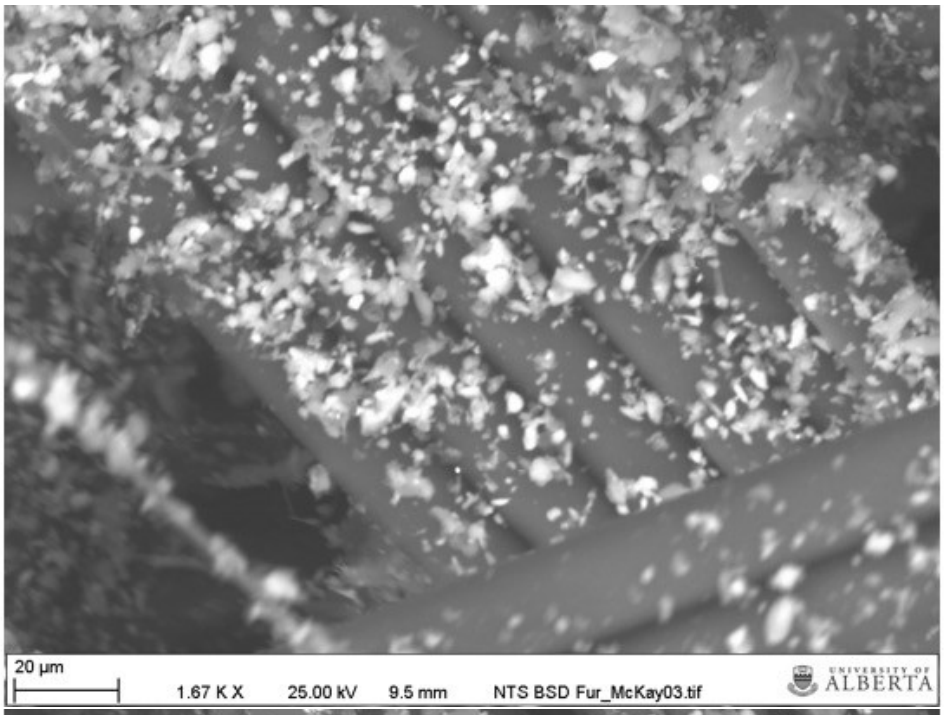
20 µm
1.67 K X
25.00 kV
9.5 mm
NTS BSD Fur_McKay03.tif
UNIVERSITY OF ALBERTA

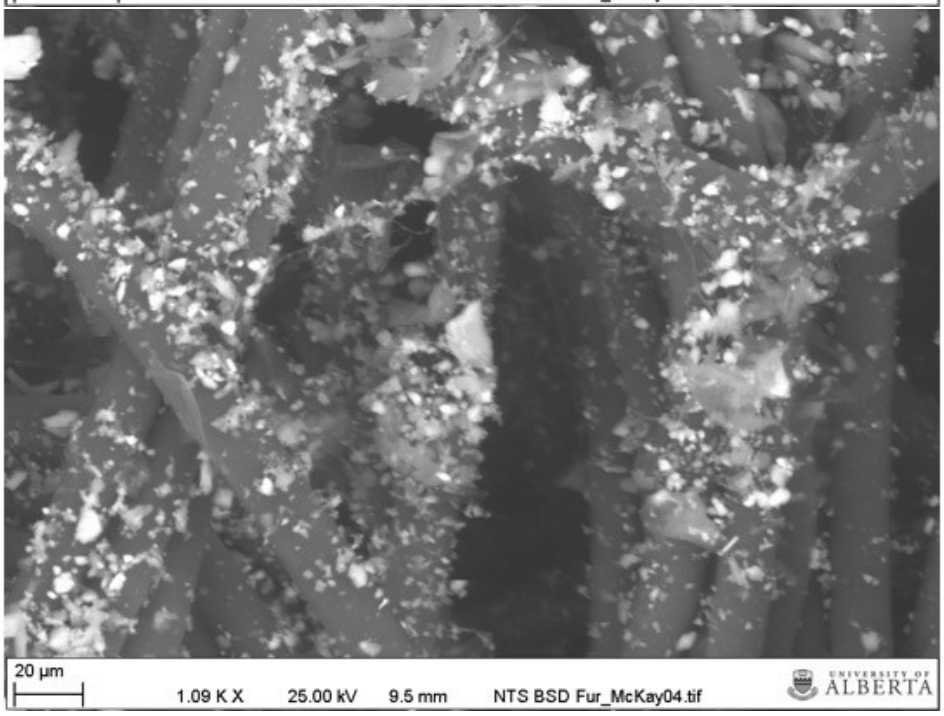
20 µm
1.09 K X
25.00 kV
9.5 mm
NTS BSD Fur_McKay04.tif
UNIVERSITY OF ALBERTA

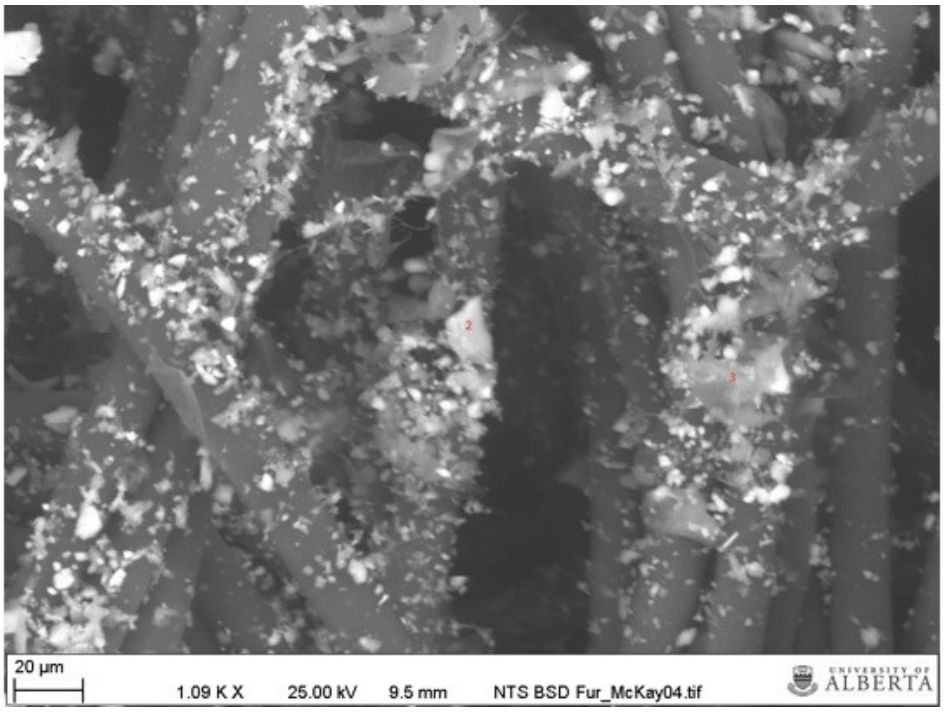

Quartz particle

Fur_McKay 2 Date:3/17/2016 1:55:07 PM HV:25.0kV

El	AN	Series	unn. C [wt.%]	norm. C [wt.%]	Atom. C [at.%]	Error (1 Sigma) [wt.%]
Si	14	K-series	17.48	38.88	29.11	0.85
Al	13	K-series	1.06	2.35	1.83	0.14
Ca	20	K-series	1.28	2.84	1.49	0.10
Cu	29	K-series	1.28	2.84	0.94	0.12
Fe	26	K-series	0.92	2.05	0.77	0.09
S	16	K-series	0.27	0.60	0.39	0.06
K	19	K-series	0.44	0.98	0.53	0.06
P	15	K-series	0.05	0.12	0.08	0.04
O	8	K-series	22.19	49.35	64.86	8.94
C	6	K-series	0.00	0.00	0.00	0.00
		Total:	44.96	100.00	100.00	

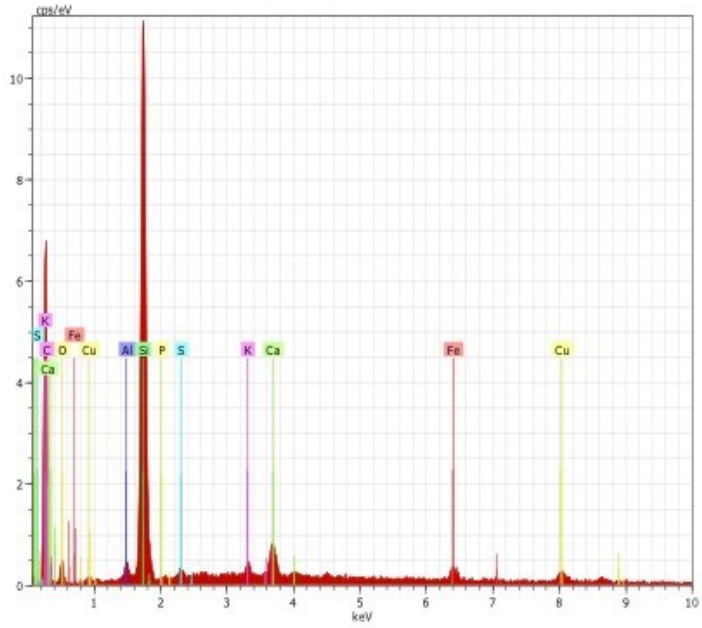

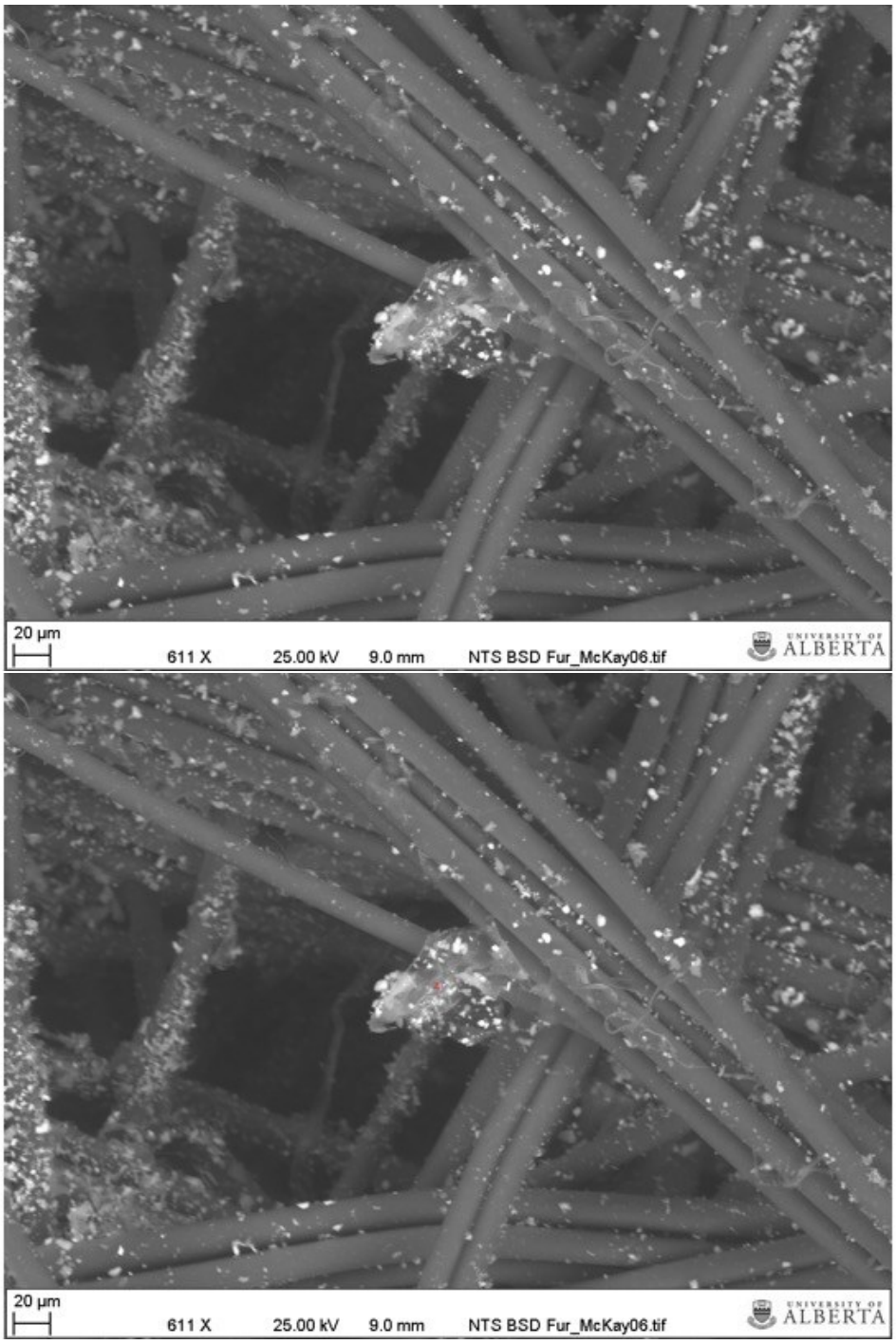
20 µm
611 X
25.00 kV
9.0 mm
NTS BSD Fur_McKay06.tif
UNIVERSITY OF ALBERTA
20 µm
611 X
25.00 kV
9.0 mm
NTS BSD Fur_McKay06.tif
UNIVERSITY OF ALBERTA

Levels too low to be sure... probably an aggregate
Interesting that the Cl is present

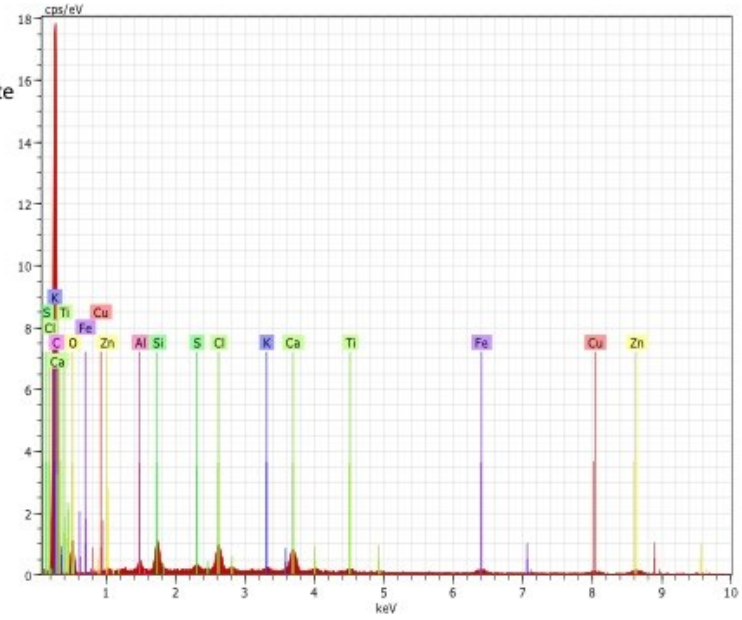

Fur_McKay 4 Date:3/17/2016 2:03:28 PM HV:25.0kV

El	AN	Series	unn. C [wt.%]	norm. C [wt.%]	Atom. C [at.%]	Error (1 Sigma) [wt.%]
Si	14	K-series	2.11	10.33	10.06	0.16
Ca	20	K-series	2.63	12.86	8.78	0.15
Zn	30	K-series	2.33	11.35	4.75	0.20
Cl	17	K-series	1.93	9.44	7.29	0.13
Fe	26	K-series	1.37	6.67	3.27	0.13
Al	13	K-series	0.88	4.30	4.36	0.11
Ti	22	K-series	0.80	3.92	2.24	0.09
Cu	29	K-series	1.23	6.01	2.59	0.14
S	16	K-series	0.42	2.05	1.75	0.07
K	19	K-series	0.33	1.62	1.14	0.06
O	8	K-series	6.44	31.44	53.77	1.66
C	6	K-series	0.00	0.00	0.00	0.00
		Total:	20.48	100.00	100.00	

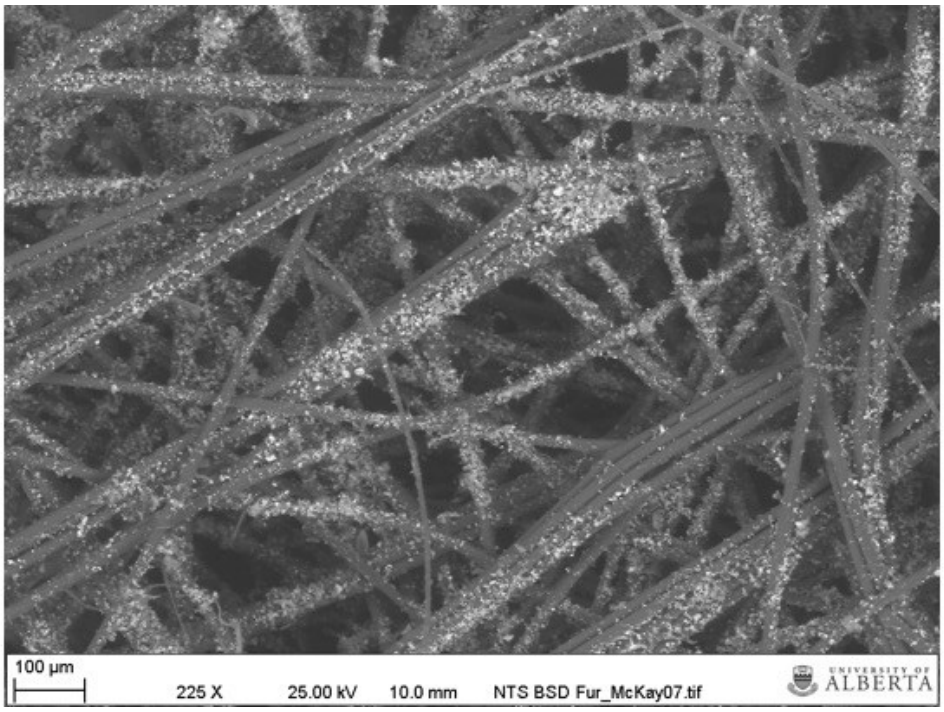

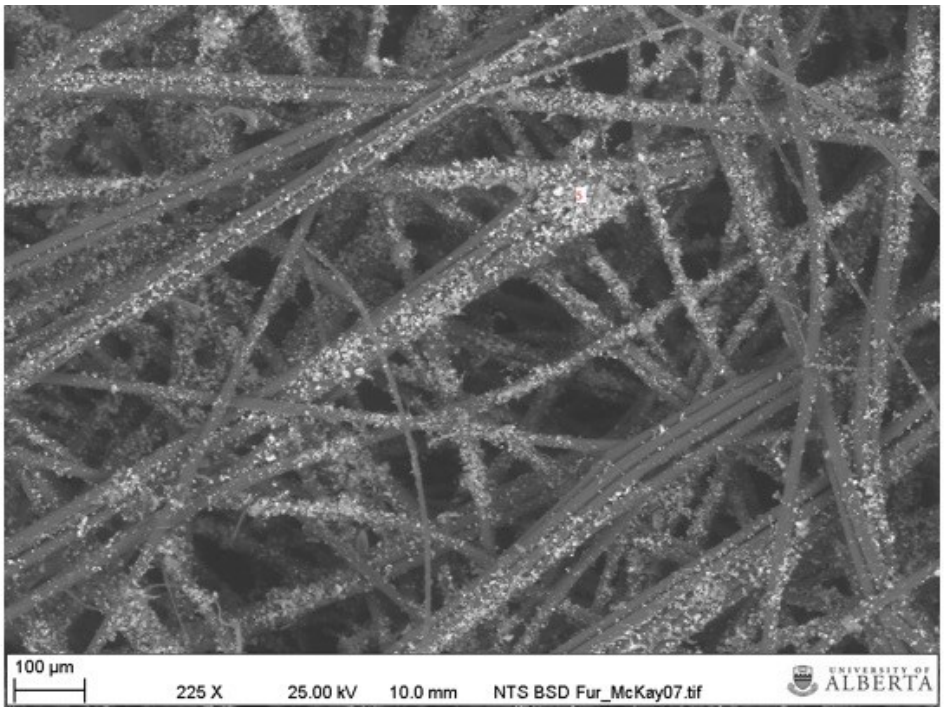

Aluminosilicates (possibly heulandite) present
Again a lot of calcium present

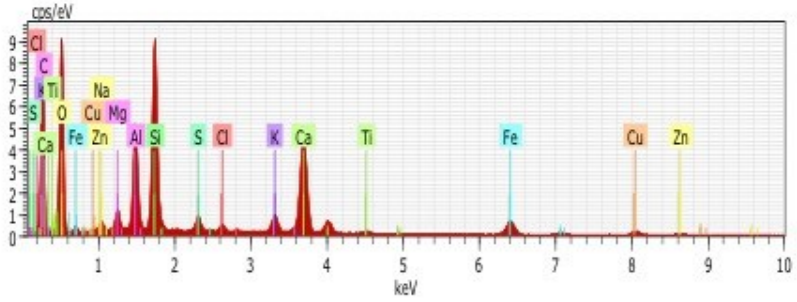

Fur_McKay 5Date:3/17/2016 2:17:38 PM HV:25.0kV

El	AN	Series	unn. C [wt.%]	norm. C [wt.%]	Atom. C [at.%]	Compound	Comp. C [wt.%]	norm. Comp. C [wt.%]	Error (1 Sigma) [wt.%]
Ca	20	K-series	11.94	21.48	13.04	CaO	30.05	16.71	0.38
Si	14	K-series	7.01	12.61	10.92	SiO2	26.97	15.00	0.33
Al	13	K-series	4.51	8.11	7.31	Al2O3	15.32	8.52	0.25
Fe	26	K-series	3.84	6.90	3.01	FeO	8.88	4.94	0.14
S	16	K-series	1.02	1.84	1.40	SO3	4.60	2.56	0.07
K	19	K-series	1.62	2.90	1.81	K2O	3.50	1.95	0.08
Cu	29	K-series	1.58	2.84	1.09		2.84	1.58	0.09
Mg	12	K-series	0.88	1.59	1.59	MgO	2.64	1.47	0.08
Zn	30	K-series	0.97	1.75	0.65	ZnO	2.18	1.21	0.07
Na	11	K-series	0.56	1.01	1.07	Na2O	1.36	0.76	0.07
Ti	22	K-series	0.32	0.57	0.29	TiO2	0.96	0.53	0.04
Cl	17	K-series	0.40	0.71	0.49		0.71	0.40	0.04
C	6	K-series	0.00	0.00	0.00		0.00	0.00	0.00
O	8	K-series	20.96	37.68	57.33		0.00	0.00	2.63
		Total:	55.61	100.00	100.00				

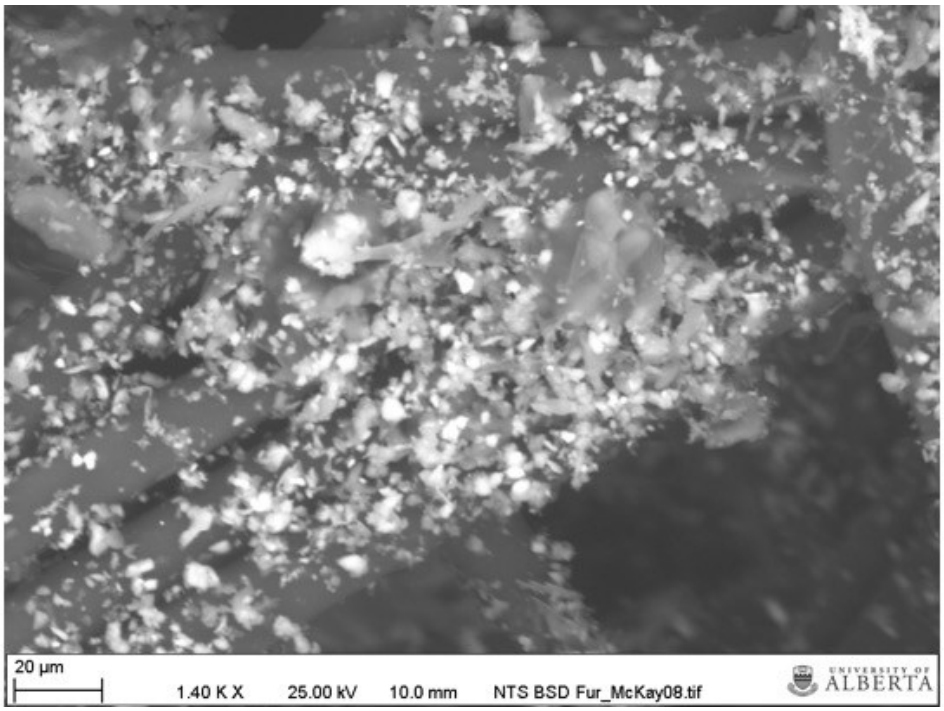
20 µm
1.40 K X
25.00 kV
10.0 mm
NTS BSD Fur_McKay08.tif
UNIVERSITY OF ALBERTA

APPENDIX 4: JPH4-W1 SEM images and EDX spectrum. AIA samples were examined for morphology and mineralogy. The number on the SEM image corresponds with the spectrum number.

JPH4-W1 LL (2013)

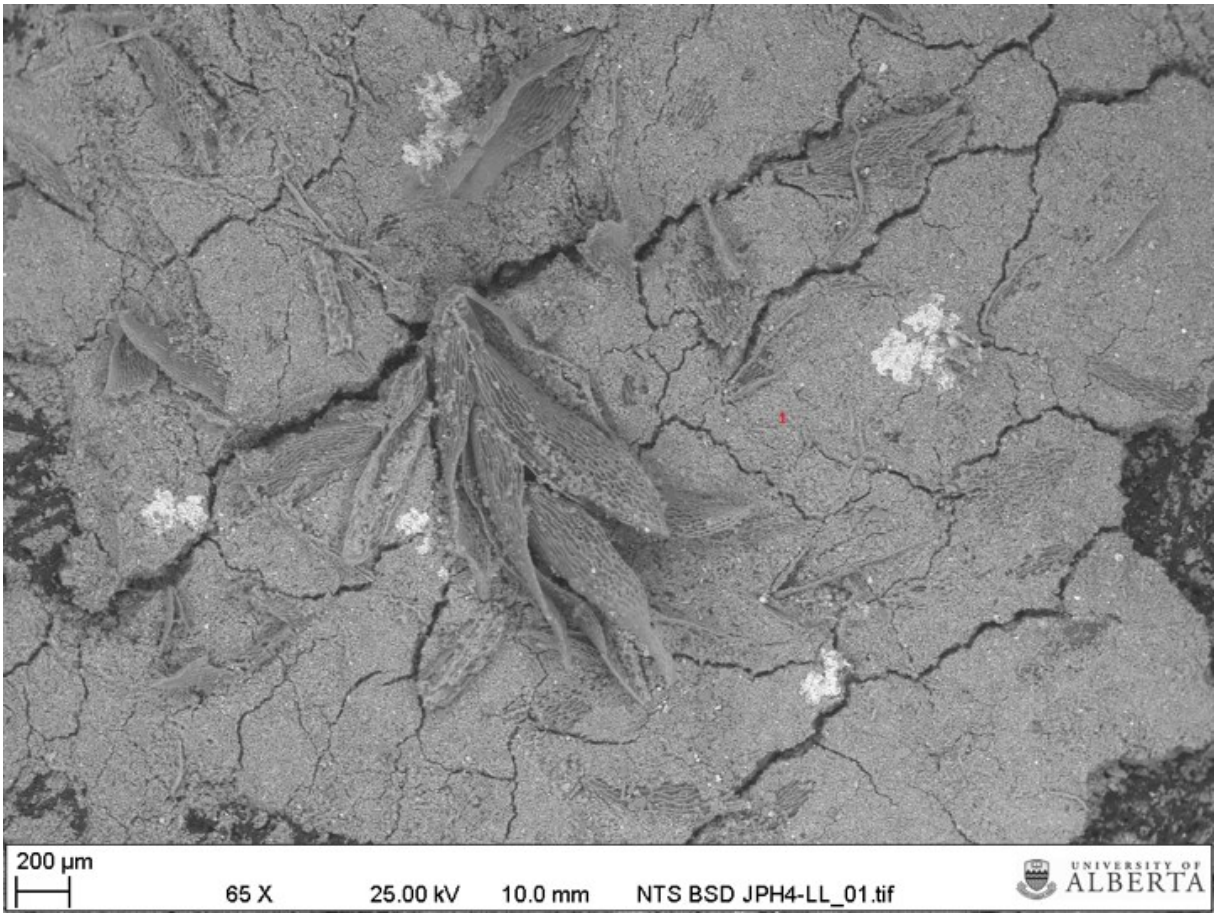
200 µm
65 X
25.00 kV
10.0 mm
NTS BSD JPH4-LL_01.tif
UNIVERSITY OF ALBERTA

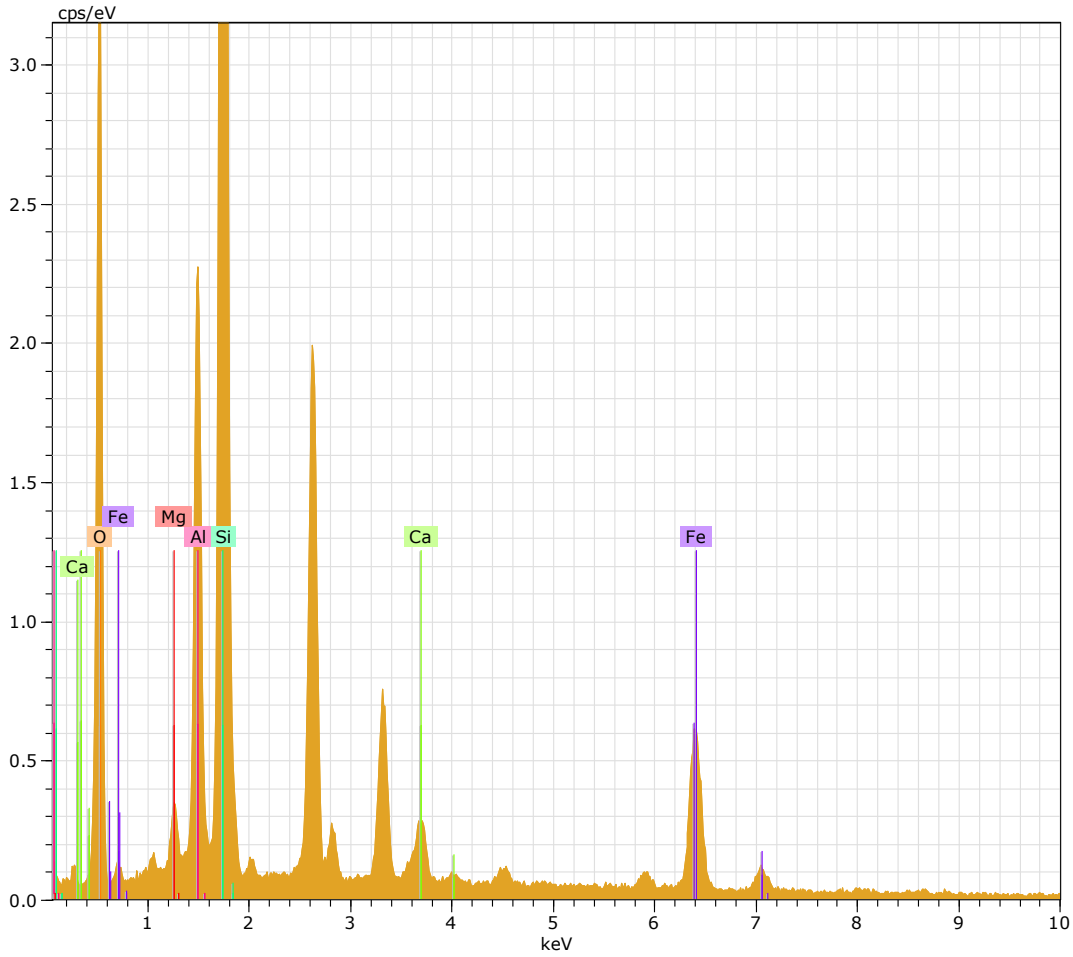

JPH-LL_ 1 Date:7/8/2016 9:46:35 AM HV:25.0kV Puls th.:2.54kcps

El	AN	Series	unn. C [wt.%]	norm. C [wt.%]	Atom. C [at.%]	Error (1 Sigma) [wt.%]
O	8	K-series	27.25	48.43	64.82	4.41
Si	14	K-series	16.04	28.51	21.73	0.75
Fe	26	K-series	6.19	11.00	4.22	0.24
Al	13	K-series	5.20	9.24	7.33	0.31
Ca	20	K-series	0.95	1.69	0.90	0.08
Mg	12	K-series	0.64	1.14	1.00	0.08
		Total:	56.28	100.00	100.00	

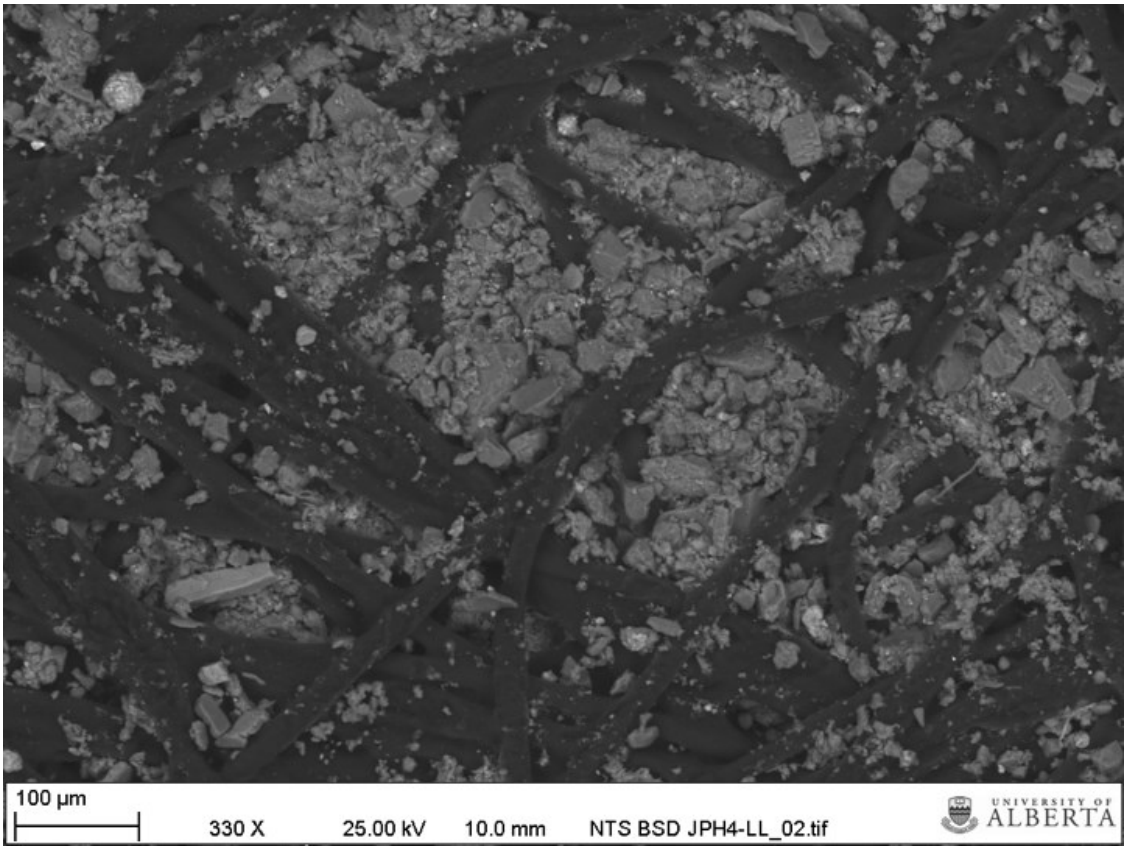
100 µm
330 X
25.00 kV
10.0 mm
NTS BSD JPH4-LL_02.tif
UNIVERSITY OF ALBERTA

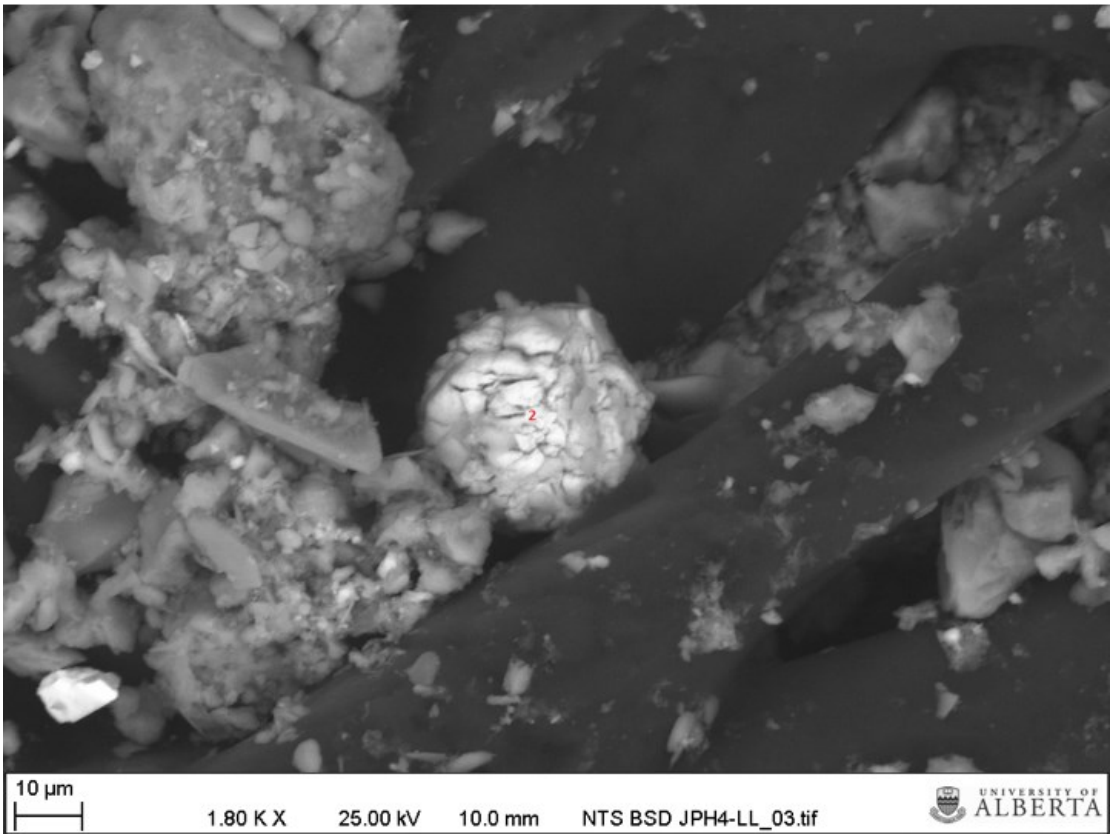
2
10 µm
1.80 K X
25.00 kV
10.0 mm
NTS BSD JPH4-LL_03.tif
UNIVERSITY OF ALBERTA

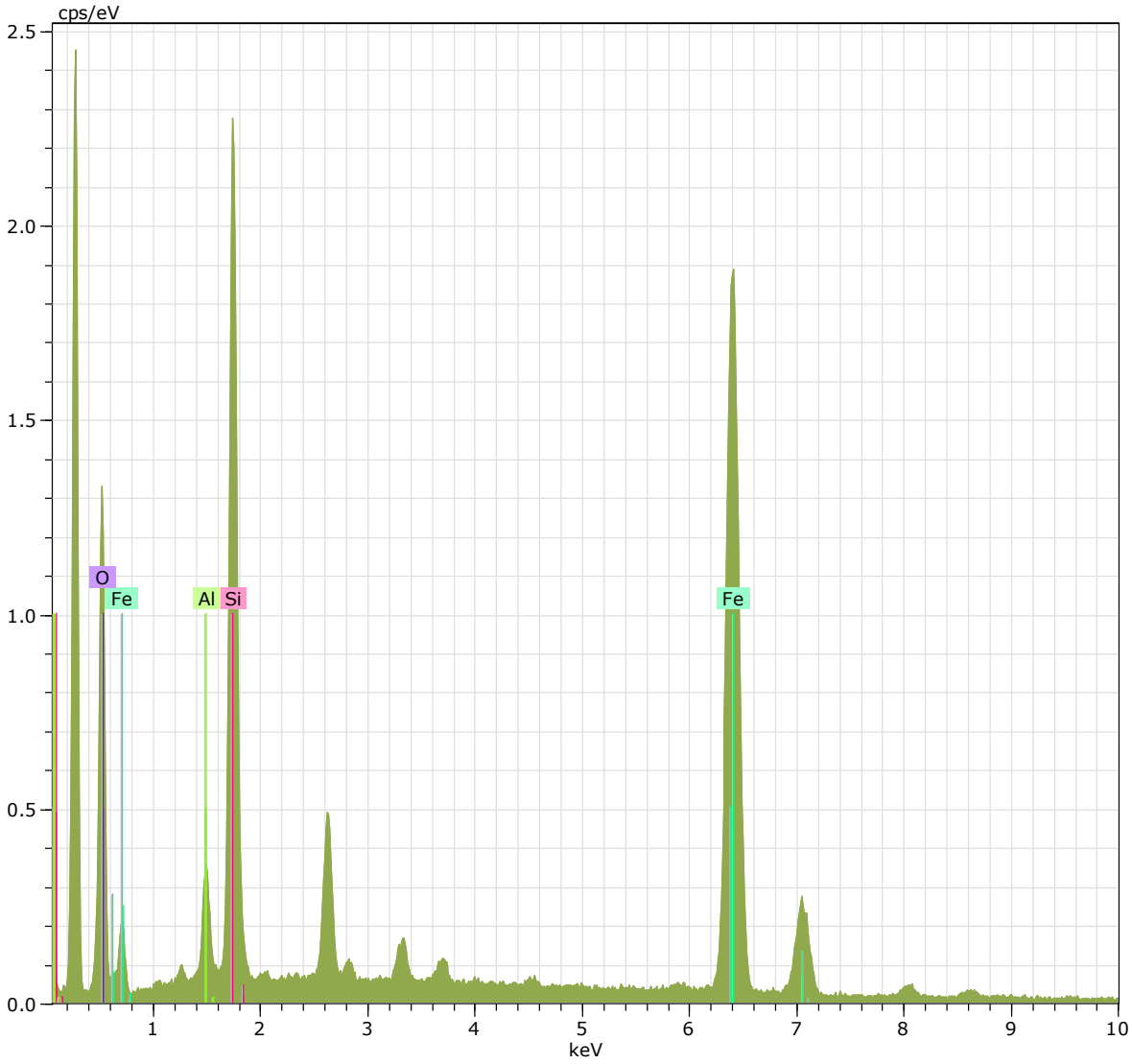

JPH-LL_ 2 Date:7/8/2016 9:52:32 AM HV:25.0kV Puls th.:1.54kcps

El	AN	Series	unn. C [wt.%]	norm. C [wt.%]	Atom. C [at.%]	Error (1 Sigma) [wt.%]
Fe	26	K-series	54.44	69.19	41.55	1.49
O	8	K-series	18.84	23.94	50.17	3.43
Si	14	K-series	4.36	5.55	6.62	0.26
Al	13	K-series	1.05	1.33	1.65	0.12
		Total:	78.69	100.00	100.00	

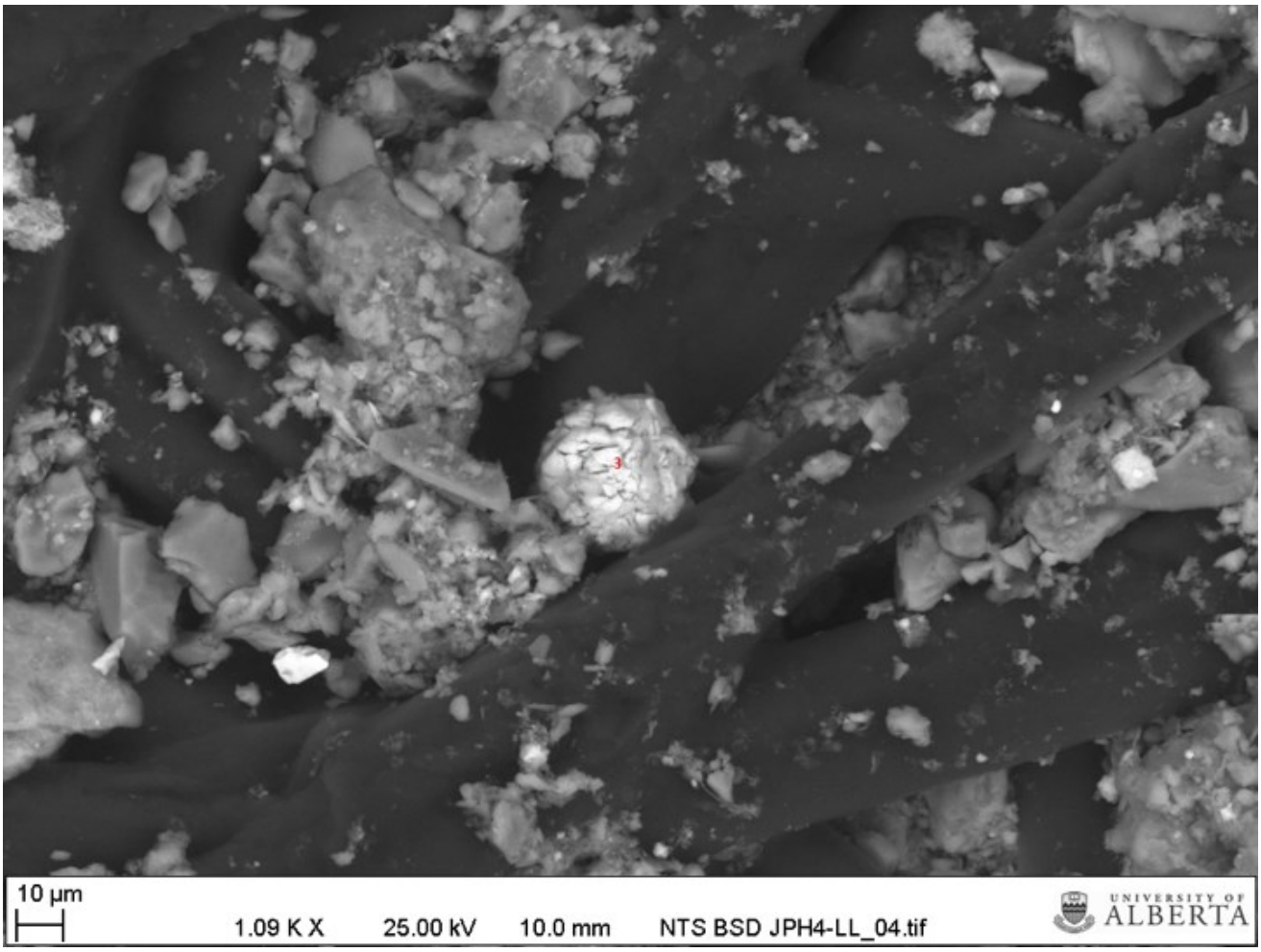
3
10 µm
1.09 K X
25.00 kV
10.0 mm
NTS BSD JPH4-LL_04.tif
UNIVERSITY OF ALBERTA

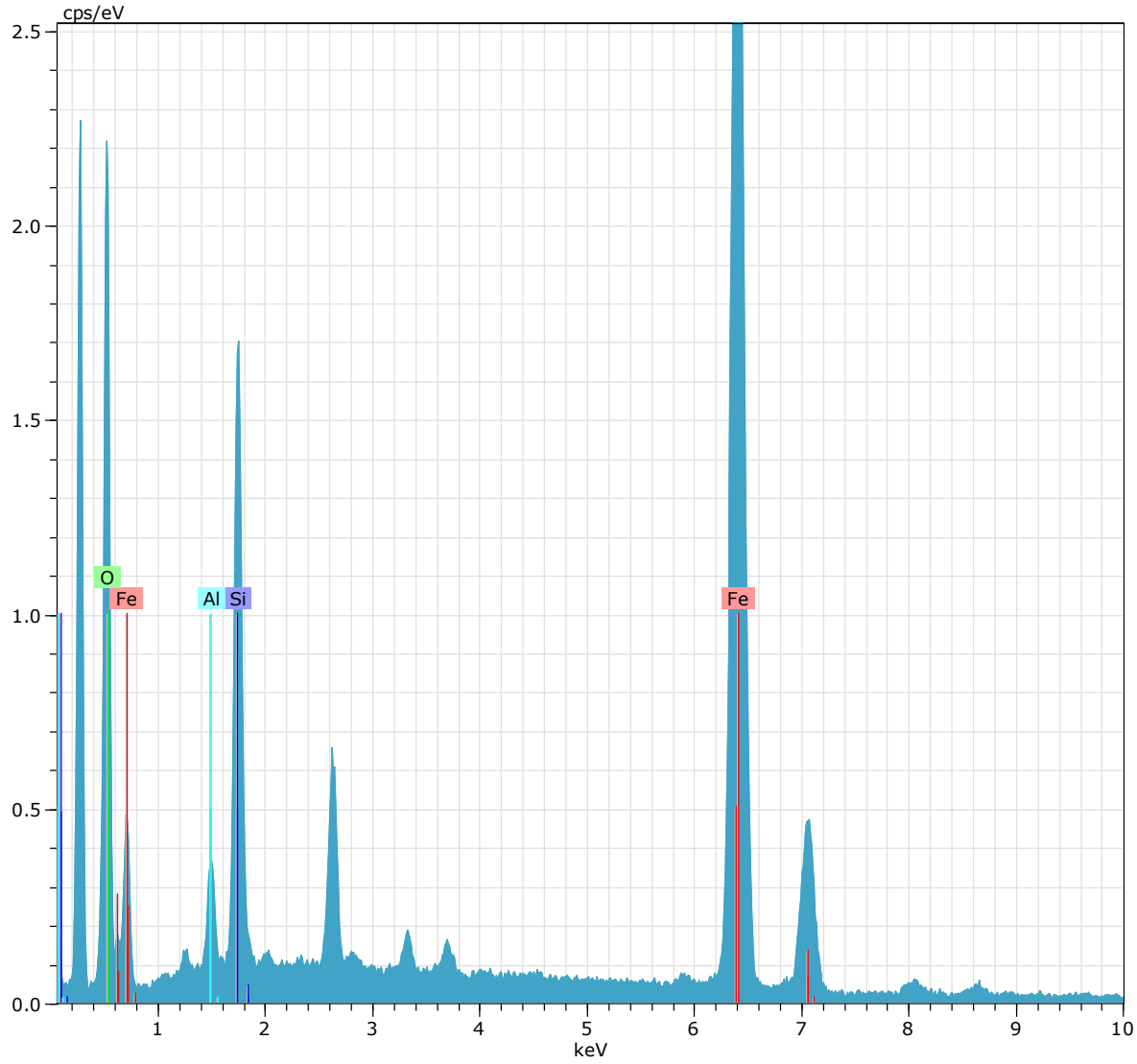

JPH-LL_ 3 Date:7/8/2016 9:59:23 AM HV:25.0kV Puls th.:2.04kcps

El	AN	Series	unn. C [wt.%]	norm. C [wt.%]	Atom. C [at.%]	Error (1 Sigma) [wt.%]
Fe	26	K-series	51.92	63.65	35.33	1.41
O	8	K-series	23.96	29.37	56.90	3.89
Si	14	K-series	4.37	5.36	5.92	0.24
Al	13	K-series	1.31	1.61	1.85	0.12
		Total:	81.56	100.00	100.00	

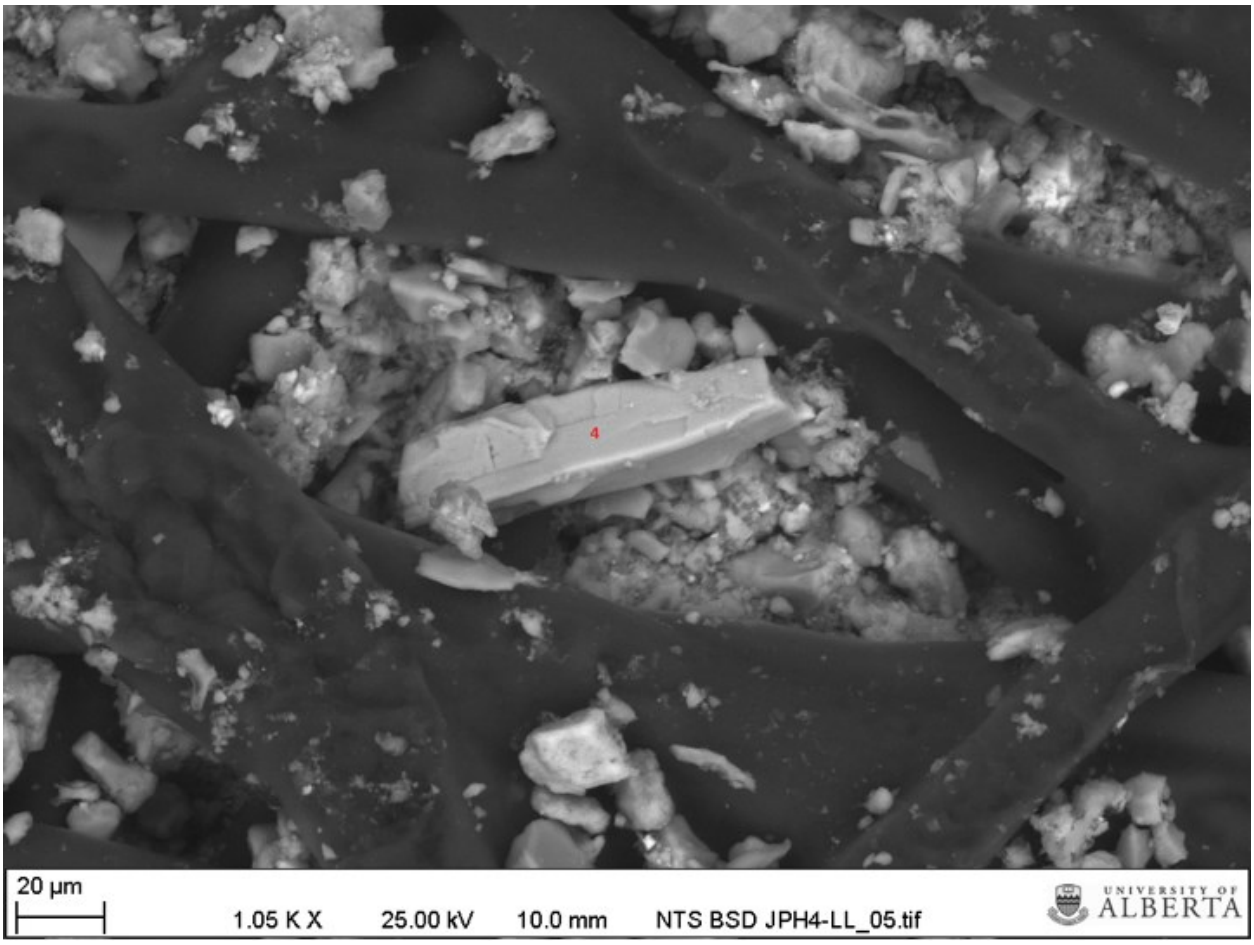
4
20 µm
1.05 K X
25.00 kV
10.0 mm
NTS BSD JPH4-LL_05.tif
UNIVERSITY OF ALBERTA

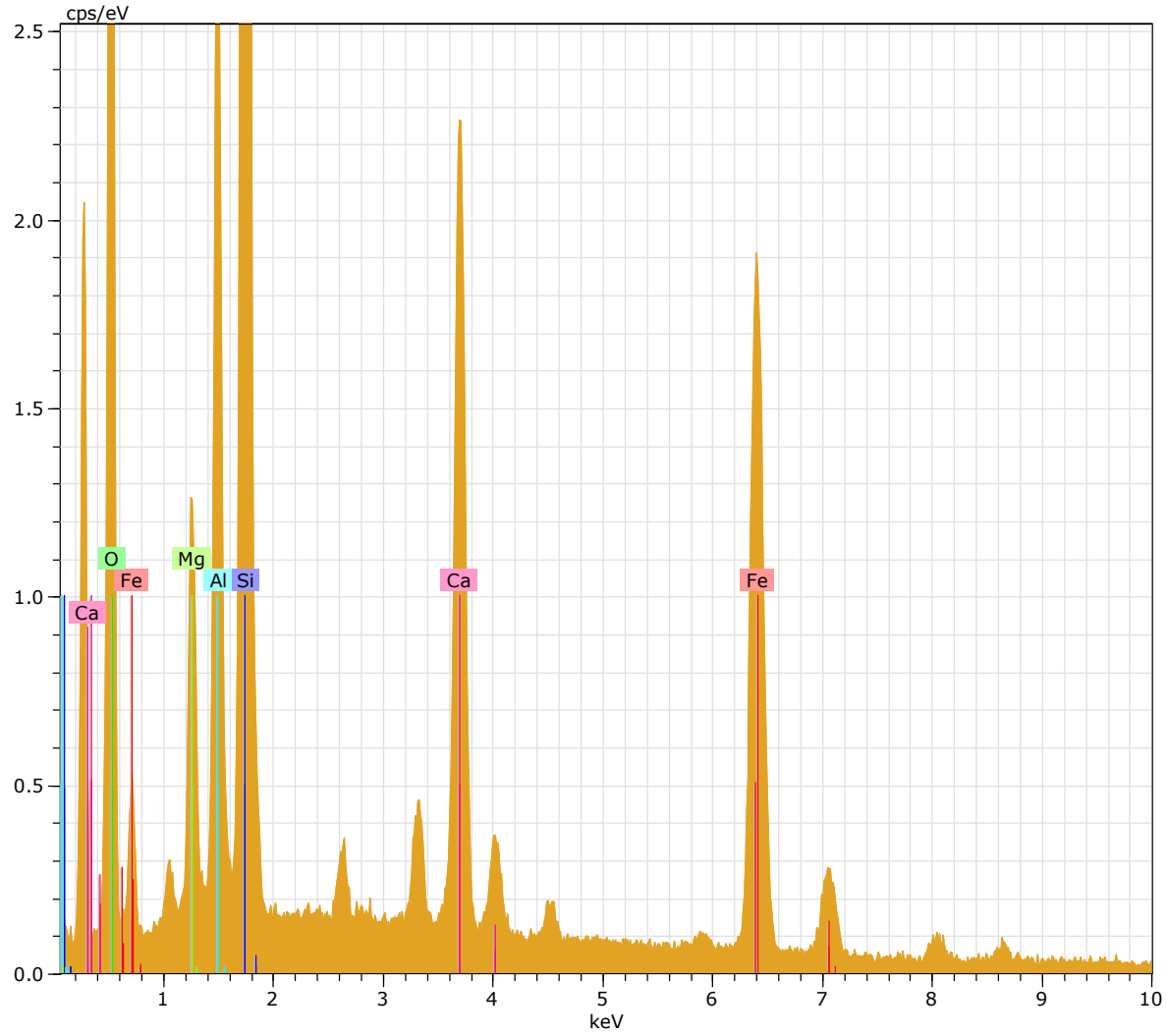

JPH-LL_ 4 Date:7/8/2016 10:05:12 AM HV:25.0kV Puls th.:3.69kcps

El	AN	Series	unn. C [wt.%]	norm. C [wt.%]	Atom. C [at.%]	Error (1 Sigma) [wt.%]
O	8	K-series	36.29	45.86	64.97	4.65
Si	14	K-series	13.56	17.14	13.83	0.62
Fe	26	K-series	13.55	17.13	6.95	0.39
Ca	20	K-series	7.89	9.98	5.64	0.26
Al	13	K-series	5.31	6.71	5.64	0.29
Mg	12	K-series	2.52	3.18	2.97	0.18
		Total:	79.14	100.00	100.00	

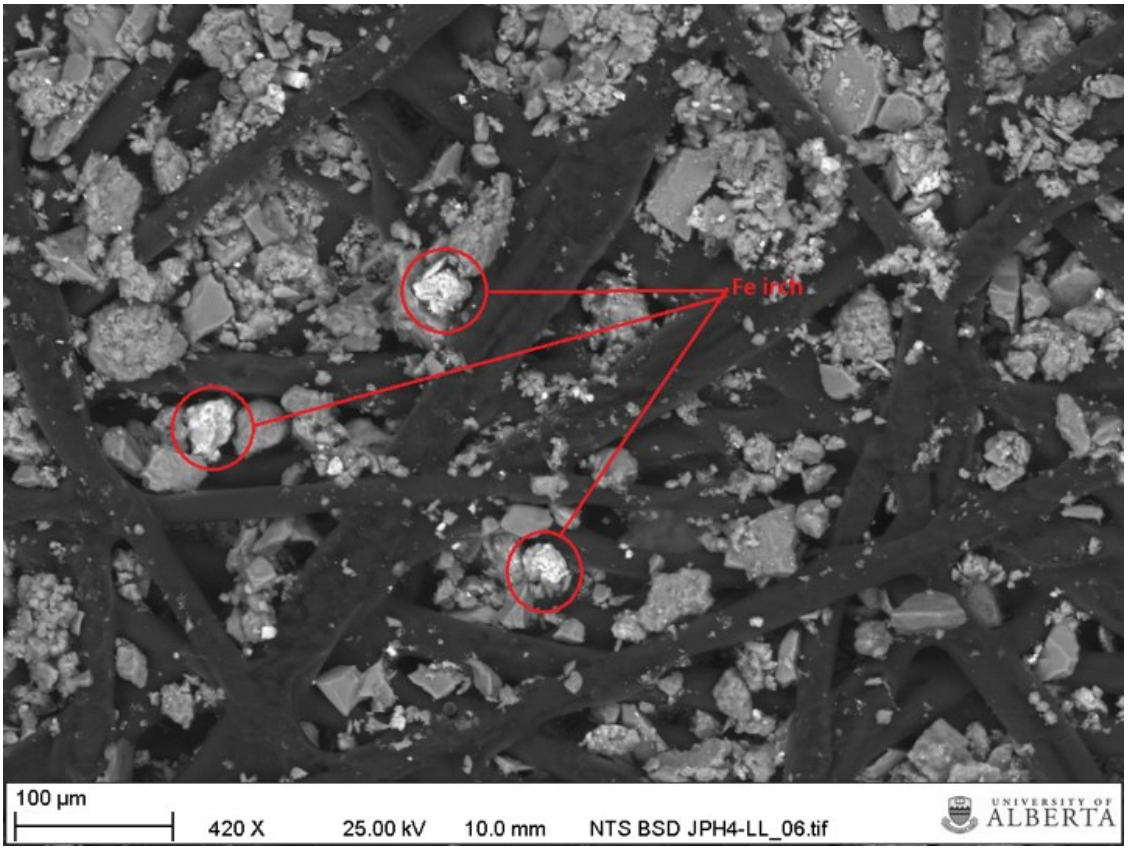
Fe inch
100 µm
420 X
25.00 kV
10.0 mm
NTS BSD JPH4-LL_06.tif
UNIVERSITY OF ALBERTA

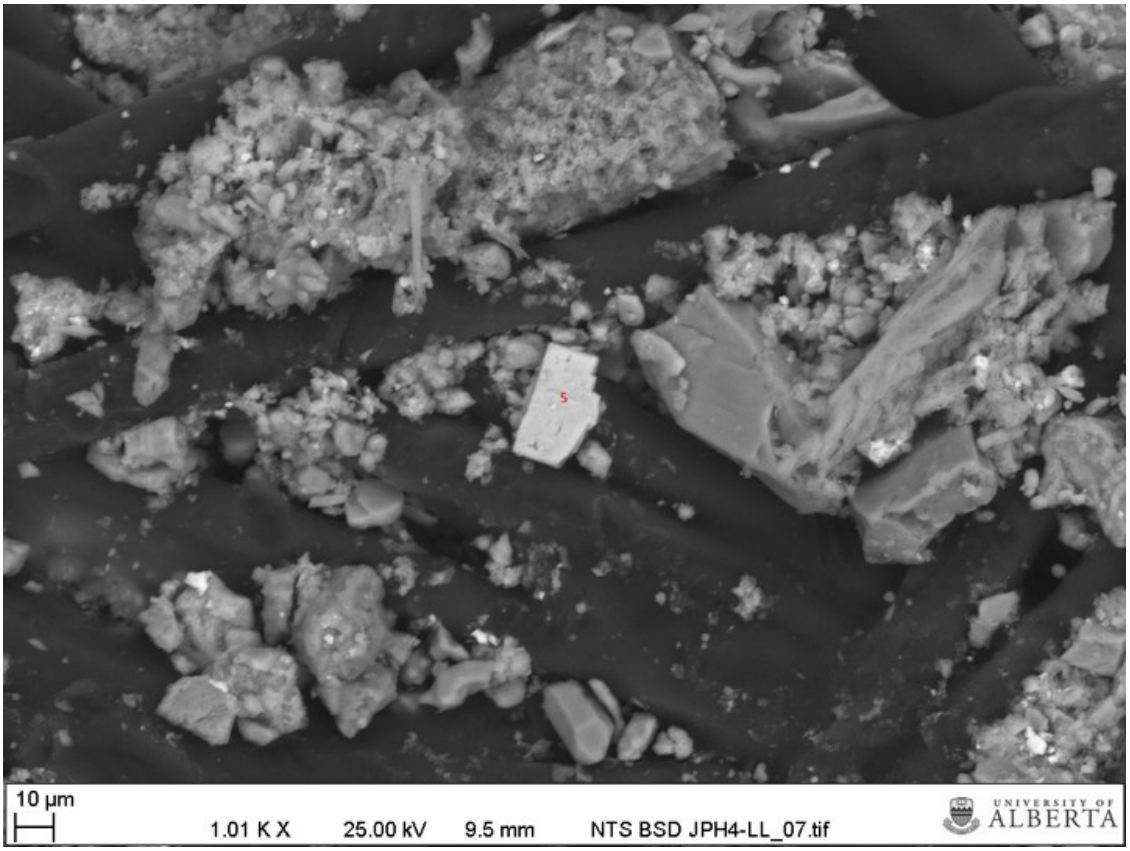
5
10 µm
1.01 K X
25.00 kV
9.5 mm
NTS BSD JPH4-LL_07.tif
UNIVERSITY OF ALBERTA

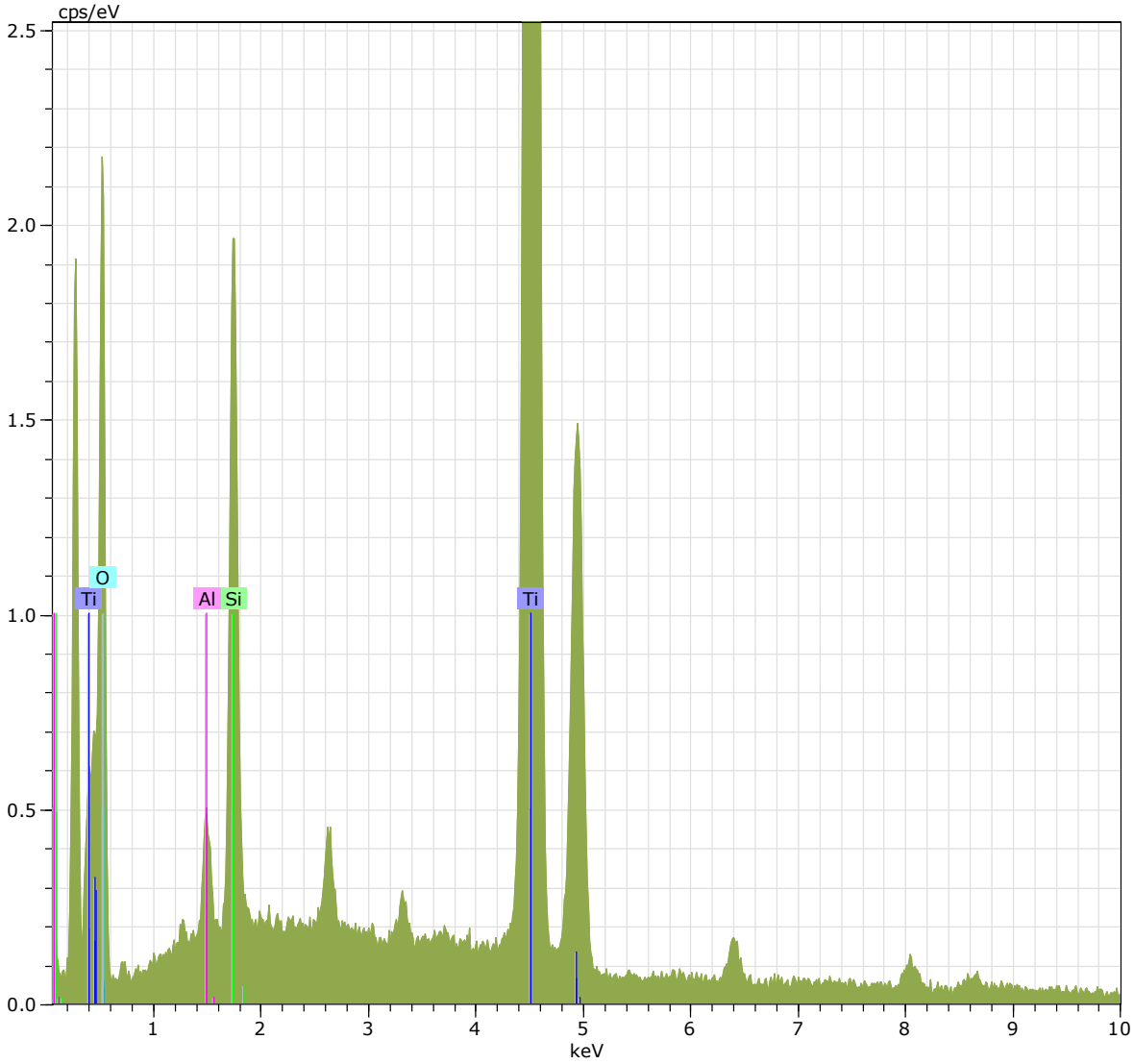

JPH-LL_ 5 Date:7/8/2016 10:16:34 AM HV:25.0kV Puls th.:3.73kcps

El	AN	Series	unn. C [wt.%]	norm. C [wt.%]	Atom. C [at.%]	Error (1 Sigma) [wt.%]
Ti	22	K-series	45.03	48.59	24.58	1.27
O	8	K-series	44.19	47.67	72.17	6.86
Si	14	K-series	2.75	2.96	2.55	0.15
Al	13	K-series	0.72	0.78	0.70	0.07
		Total:	92.69	100.00	100.00	

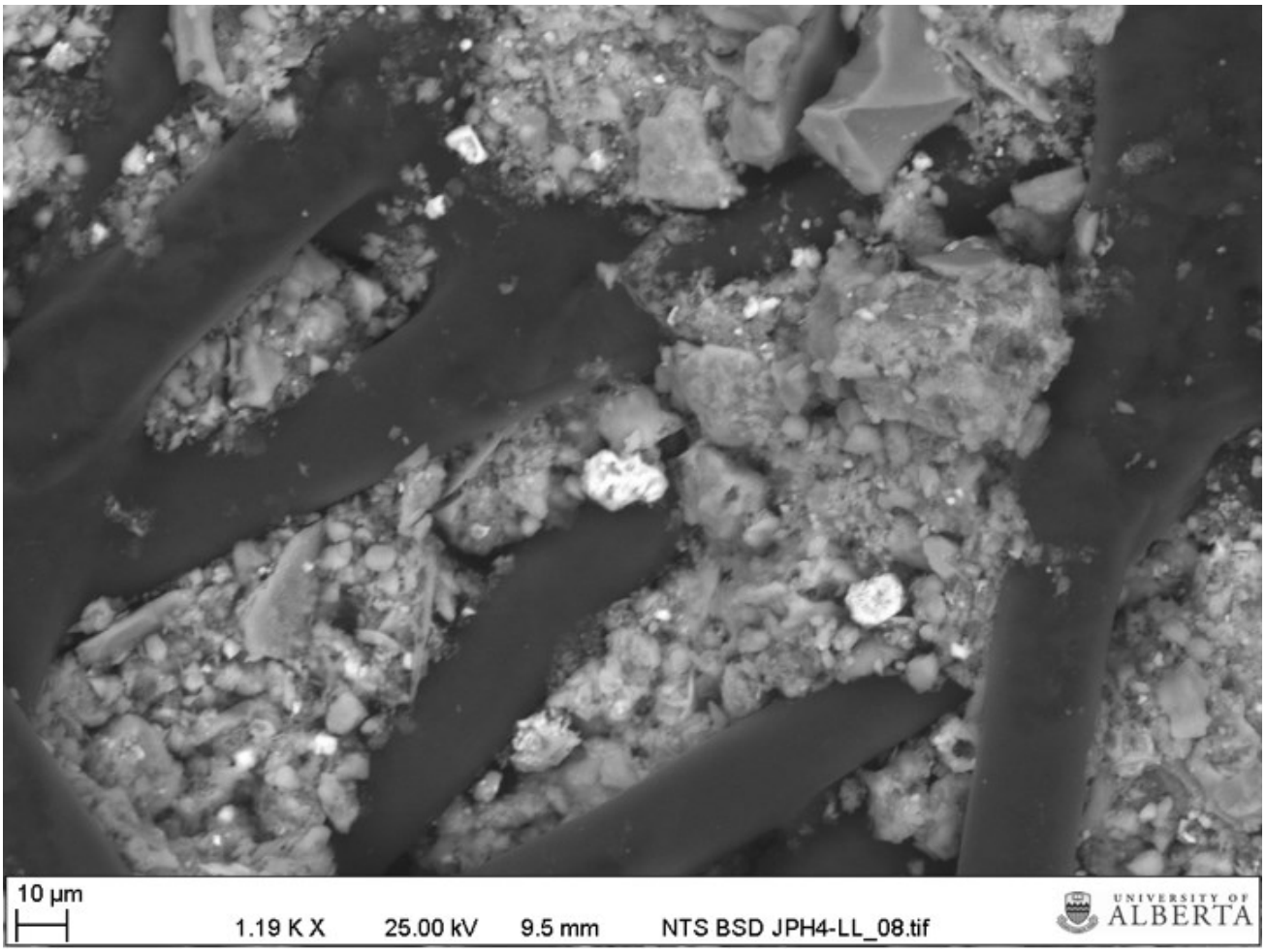
10 µm
1.19 K X
25.00 kV
9.5 mm
NTS BSD JPH4-LL_08.tif
UNIVERSITY OF ALBERTA

JPH4-W1 01 (2011)

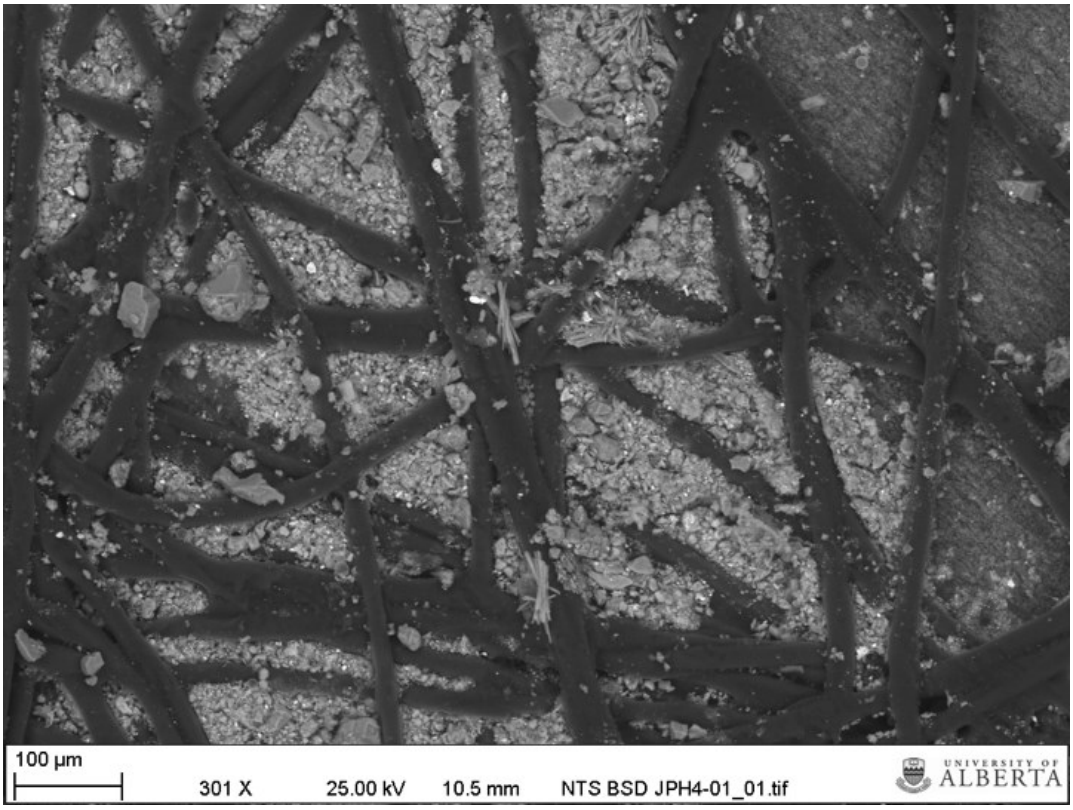
100 µm
301 X
25.00 kV
10.5 mm
NTS BSD JPH4-01_01.tif
UNIVERSITY OF ALBERTA

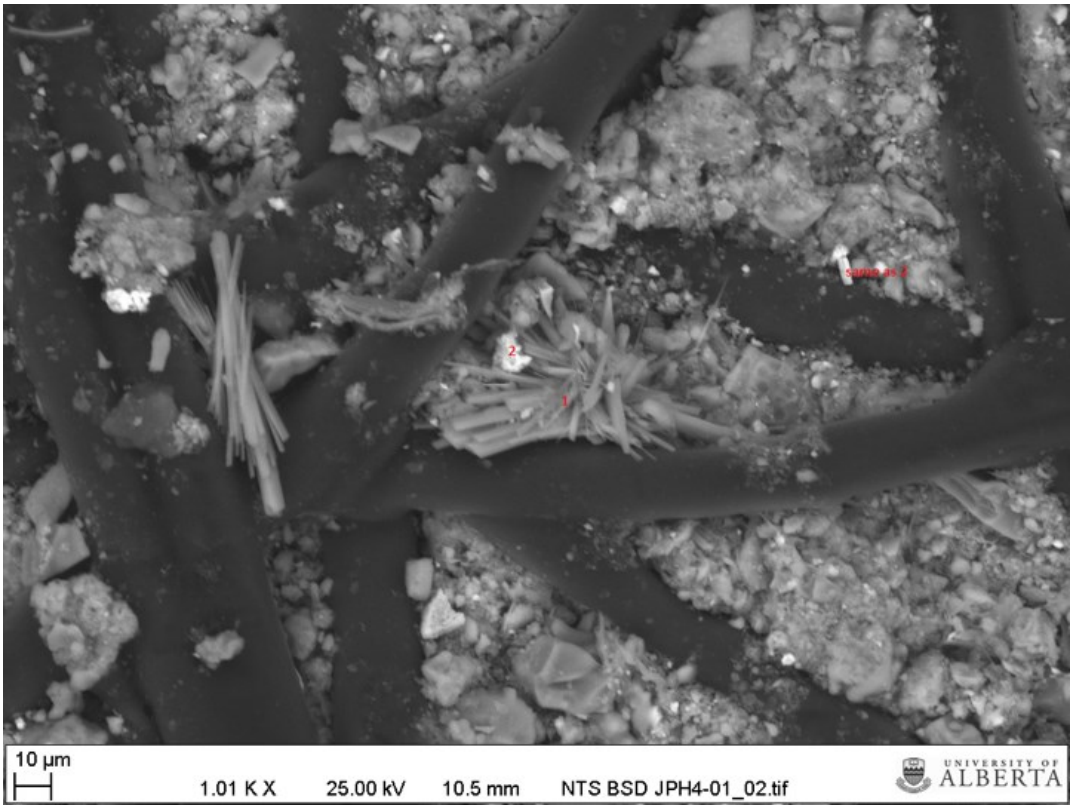
2
1
10 µm
1.01 K X
25.00 kV
10.5 mm
NTS BSD JPH4-01_02.tif
UNIVERSITY OF ALBERTA

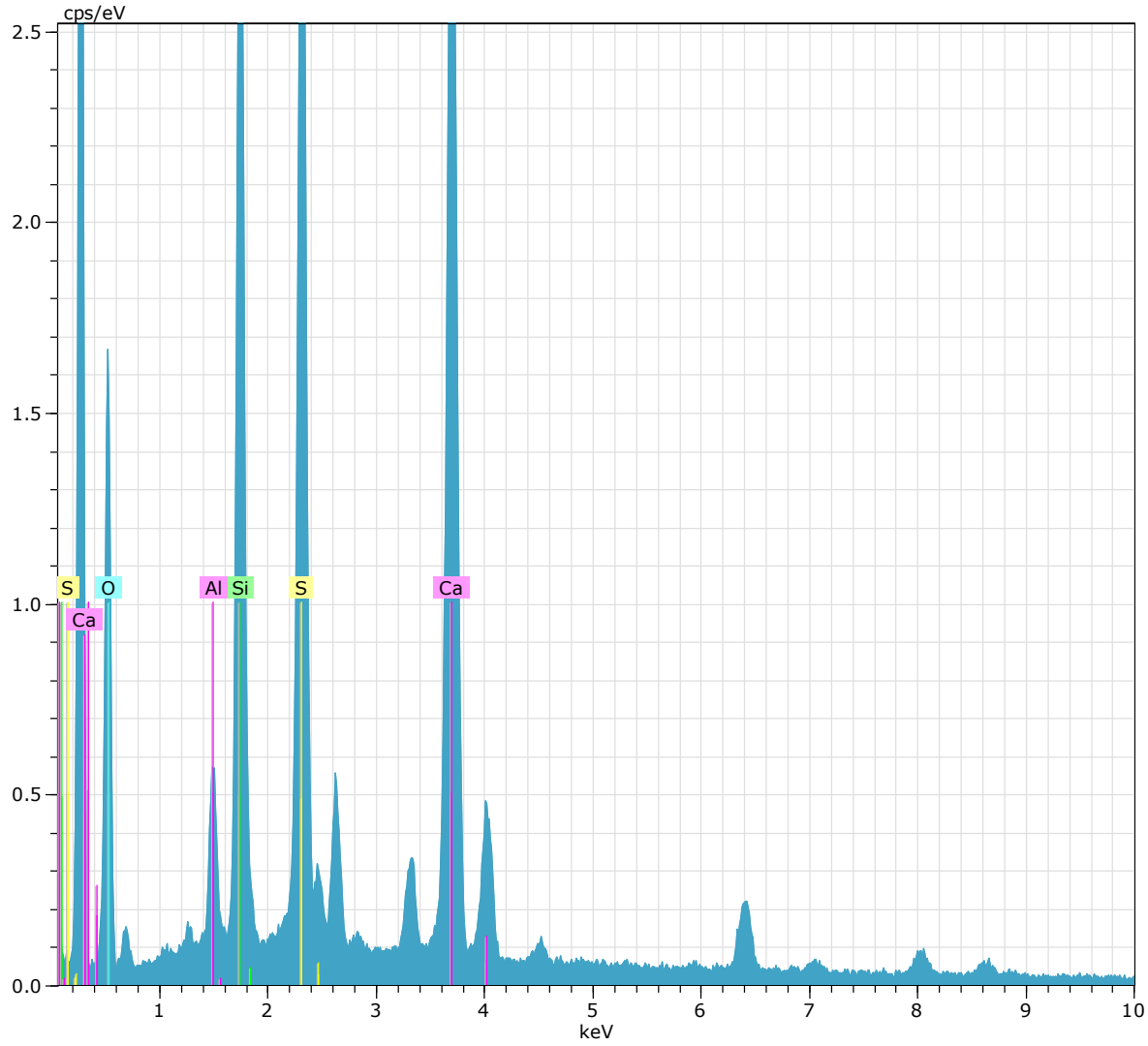

JPH-01_ 1 Date:7/8/2016 10:31:45 AM HV:25.0kV Puls th.:2.51kcps

El	AN	Series	unn. C [wt.%]	norm. C [wt.%]	Atom. C [at.%]	Error (1 Sigma) [wt.%]
O	8	K-series	34.10	46.92	66.06	6.40
Ca	20	K-series	21.63	29.76	16.73	0.69
S	16	K-series	11.21	15.43	10.84	0.46
Si	14	K-series	4.67	6.43	5.16	0.26
Al	13	K-series	1.06	1.46	1.22	0.10
		Total:	72.69	100.00	100.00	

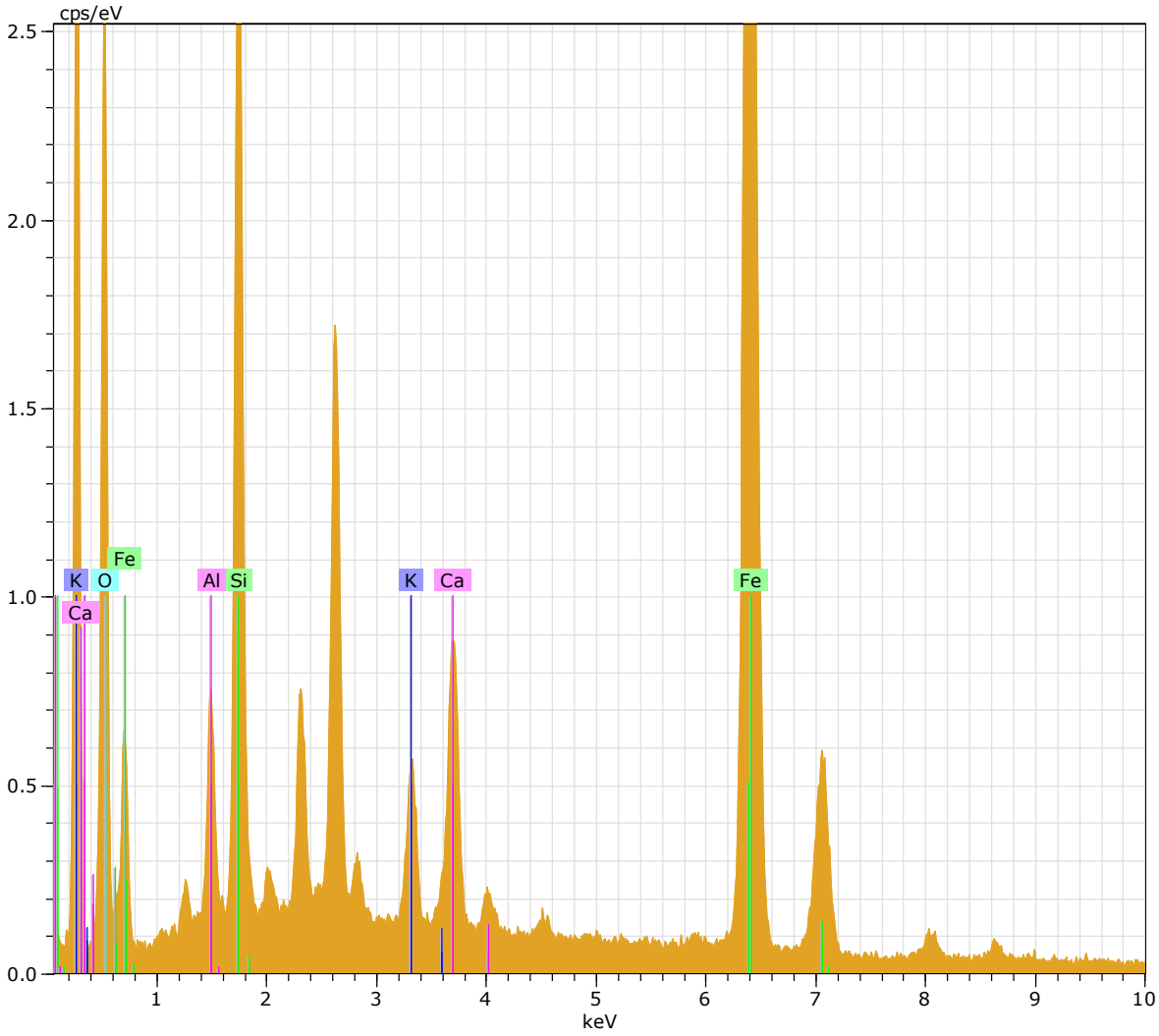

JPH-01_ 2 Date:7/8/2016 10:34:49 AM HV:25.0kV Puls th.:3.26kcps

El	AN	Series	unn. C [wt.%]	norm. C [wt.%]	Atom. C [at.%]	Error (1 Sigma) [wt.%]
Fe	26	K-series	39.98	56.01	30.53	1.09
O	8	K-series	20.58	28.83	54.86	3.35
Si	14	K-series	4.65	6.51	7.06	0.25
Ca	20	K-series	2.74	3.84	2.91	0.13
Al	13	K-series	1.81	2.53	2.86	0.14
K	19	K-series	1.63	2.28	1.77	0.09
		Total:	71.39	100.00	100.00	

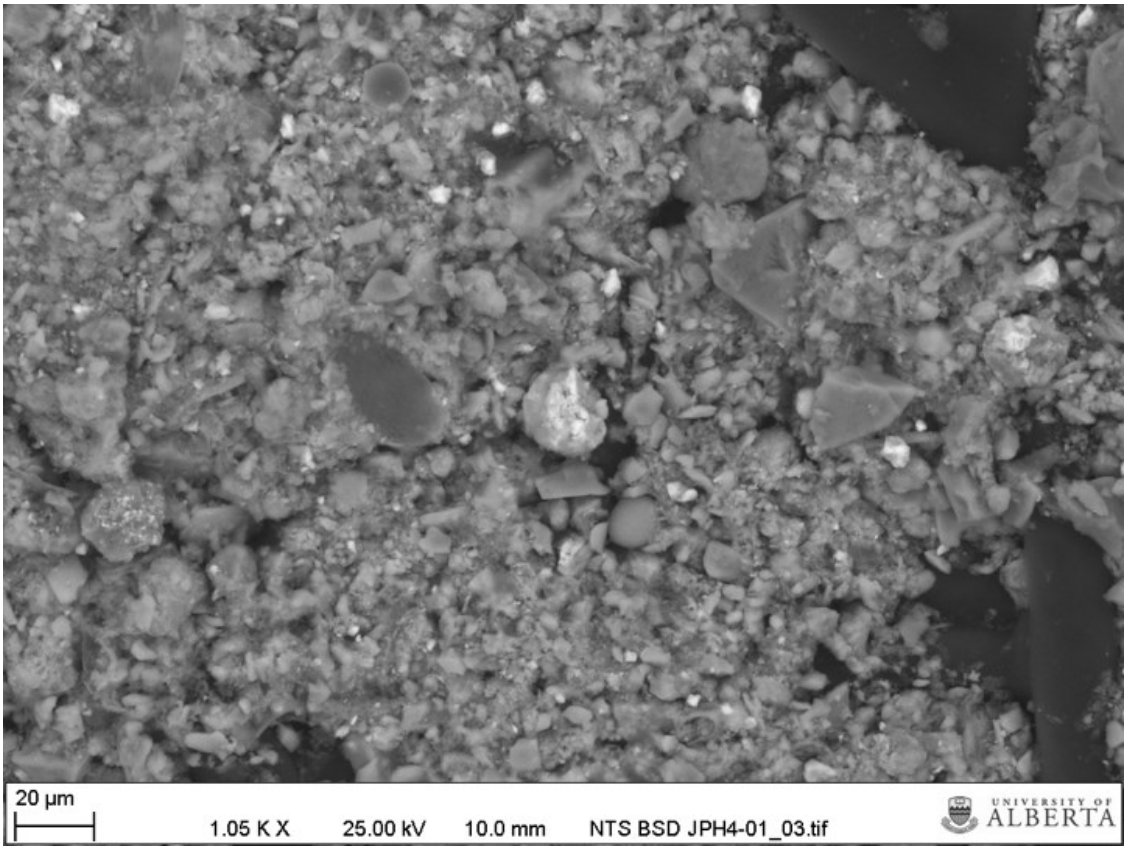
20 µm
1.05 K X
25.00 kV
10.0 mm
NTS BSD JPH4-01_03.tif
UNIVERSITY OF ALBERTA

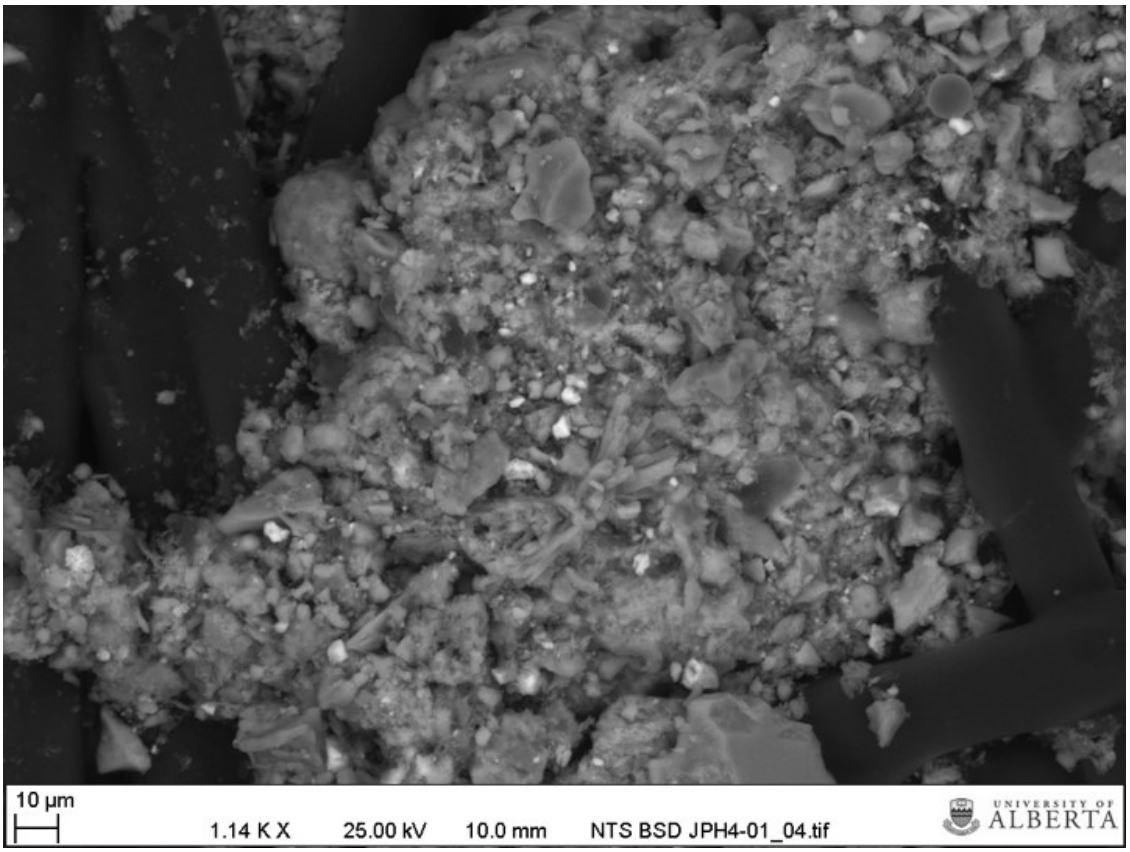
10 µm
1.14 K X
25.00 kV
10.0 mm
NTS BSD JPH4-01_04.tif
UNIVERSITY OF ALBERTA

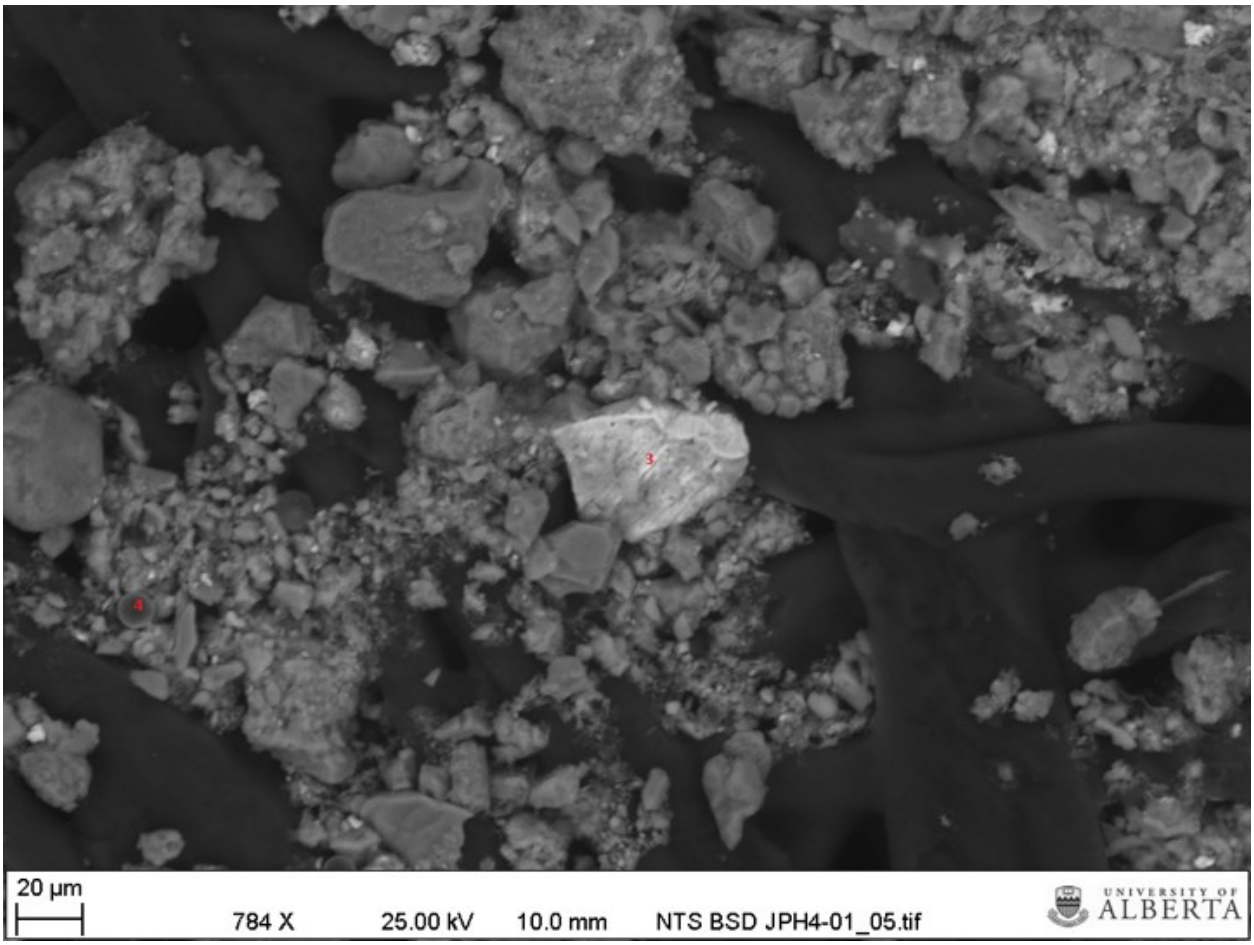
20 µm
784 X
25.00 kV
10.0 mm
NTS BSD JPH4-01_05.tif
UNIVERSITY OF ALBERTA

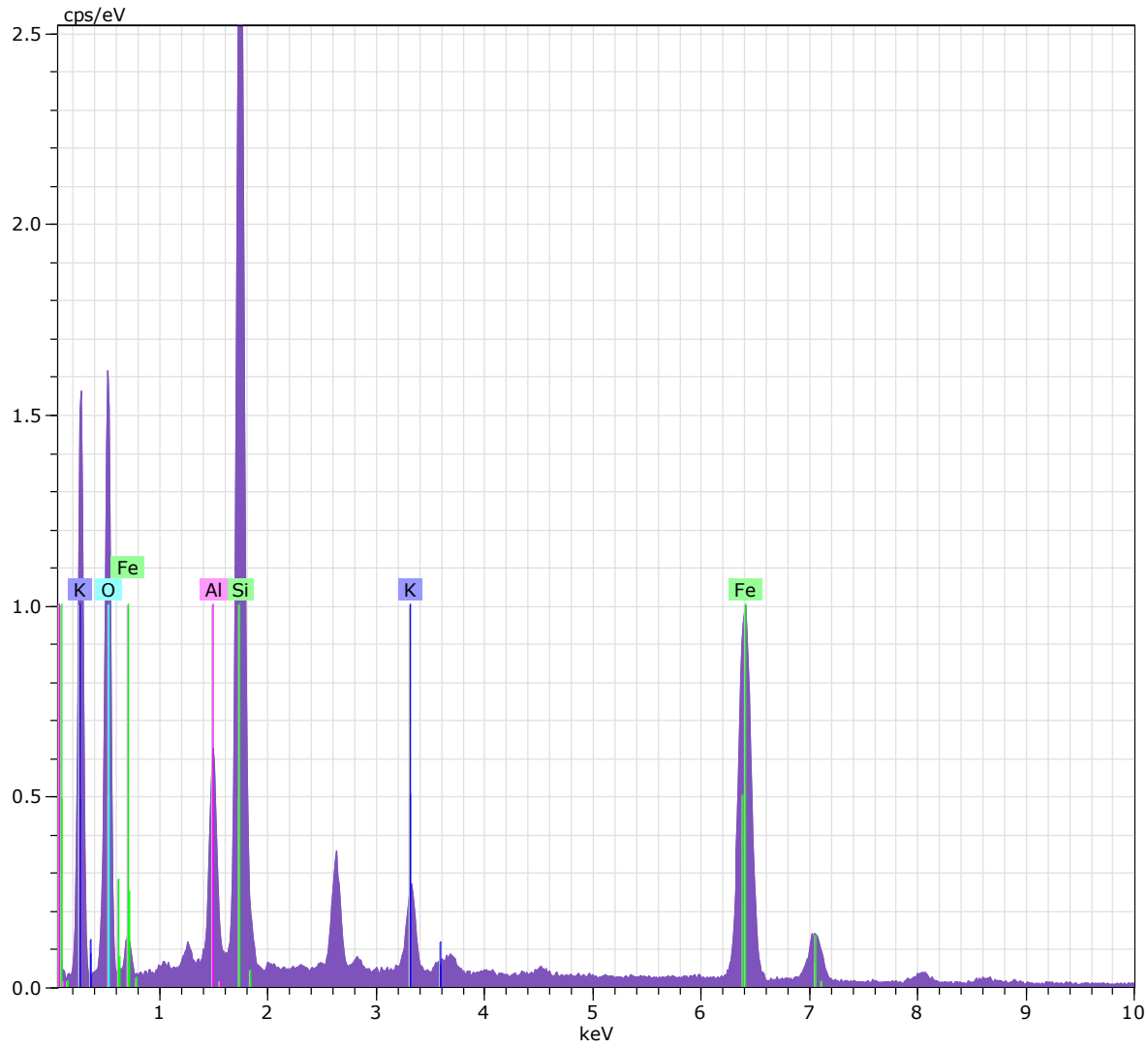

JPH-01_ 3 Date:7/8/2016 10:45:38 AM HV:25.0kV Puls th.:1.53kcps

El	AN	Series	unn. C [wt.%]	norm. C [wt.%]	Atom. C [at.%]	Error (1 Sigma) [wt.%]
Fe	26	K-series	31.58	39.83	18.30	0.87
O	8	K-series	31.35	39.54	63.42	4.56
Si	14	K-series	10.76	13.58	12.40	0.51
Al	13	K-series	3.36	4.23	4.03	0.21
K	19	K-series	2.23	2.82	1.85	0.11
		Total:	79.29	100.00	100.00	

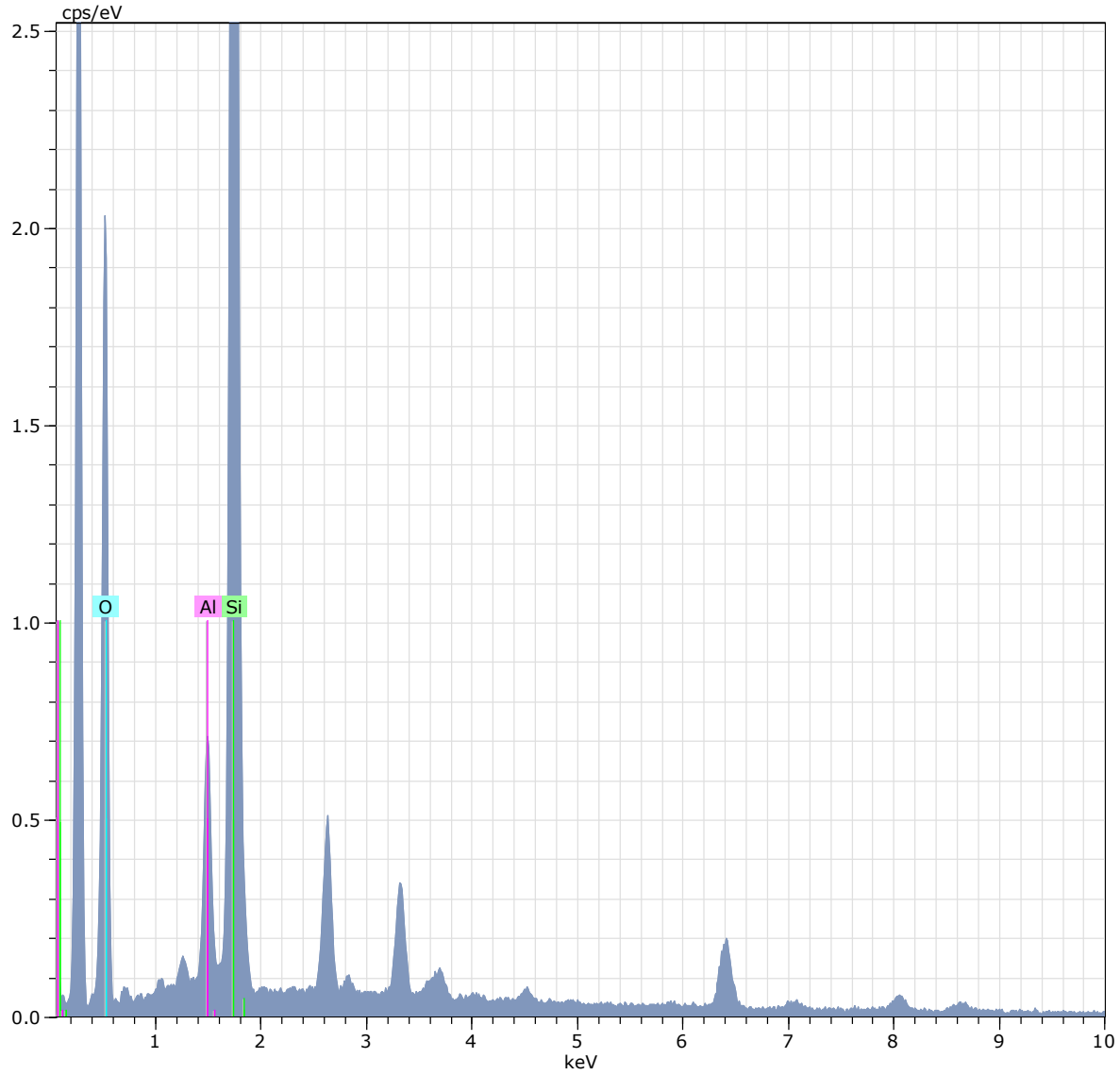

JPH-01_ 4 Date:7/8/2016 10:50:10 AM HV:25.0kV Puls th.:1.56kcps

El	AN	Series	unn. C [wt.%]	norm. C [wt.%]	Atom. C [at.%]	Error (1 Sigma) [wt.%]
O	8	K-series	20.98	57.11	69.94	3.23
Si	14	K-series	14.11	38.41	26.80	0.65
Al	13	K-series	1.65	4.49	3.26	0.12
		Total:	36.74	100.00	100.00	

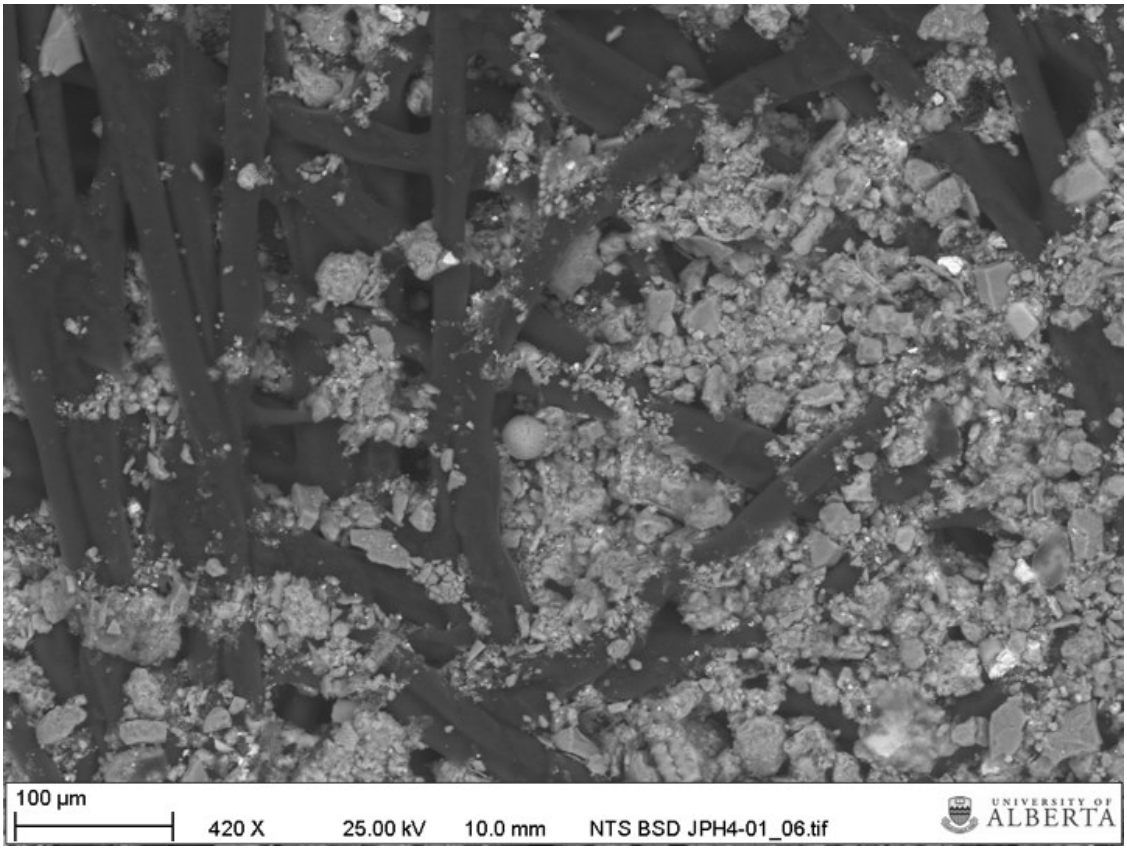
100 µm
420 X
25.00 kV
10.0 mm
NTS BSD JPH4-01_06.tif
UNIVERSITY OF ALBERTA

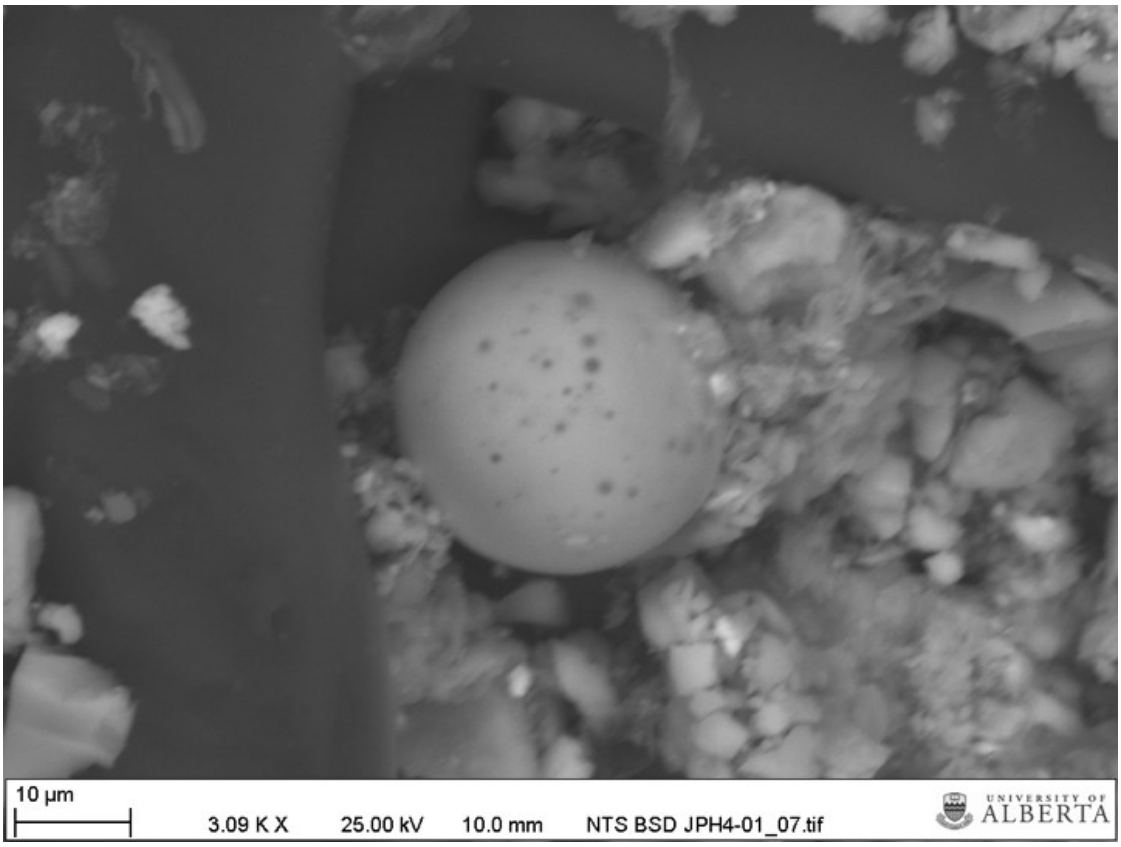
10 µm
3.09 K X
25.00 kV
10.0 mm
NTS BSD JPH4-01_07.tif
UNIVERSITY OF ALBERTA

JPH4-W1 07 (1984)

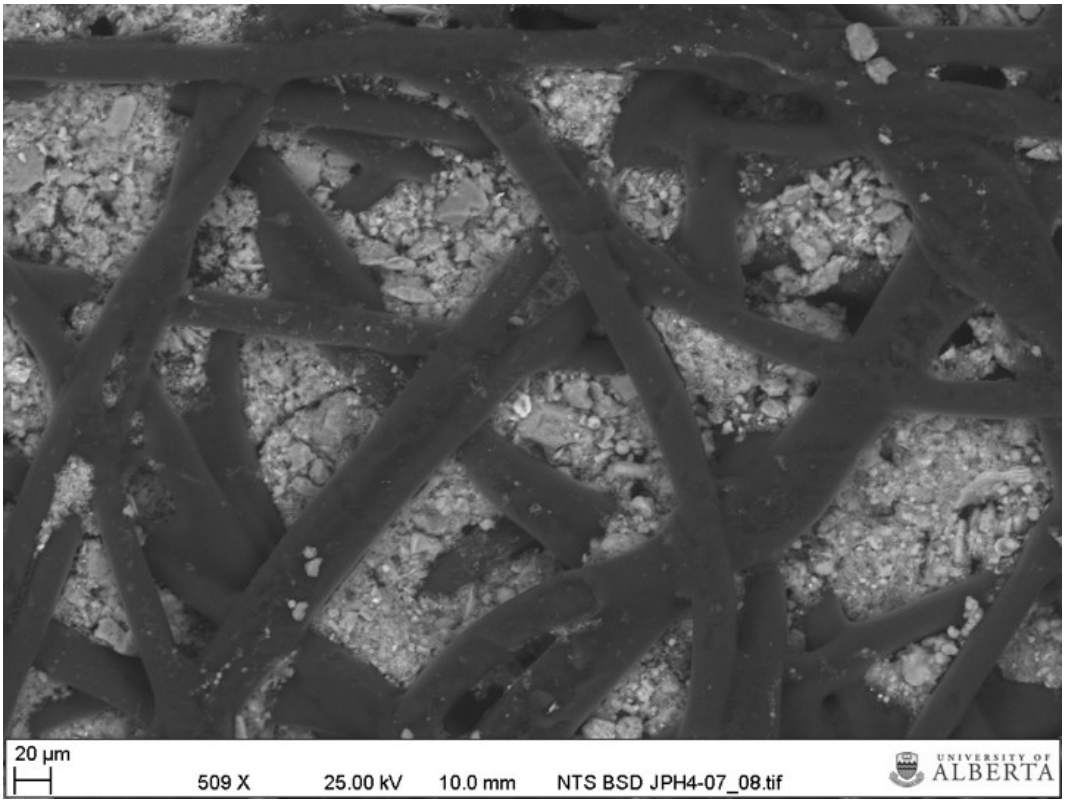
20 µm
509 X
25.00 kV
10.0 mm
NTS BSD JPH4-07_08.tif
UNIVERSITY OF ALBERTA

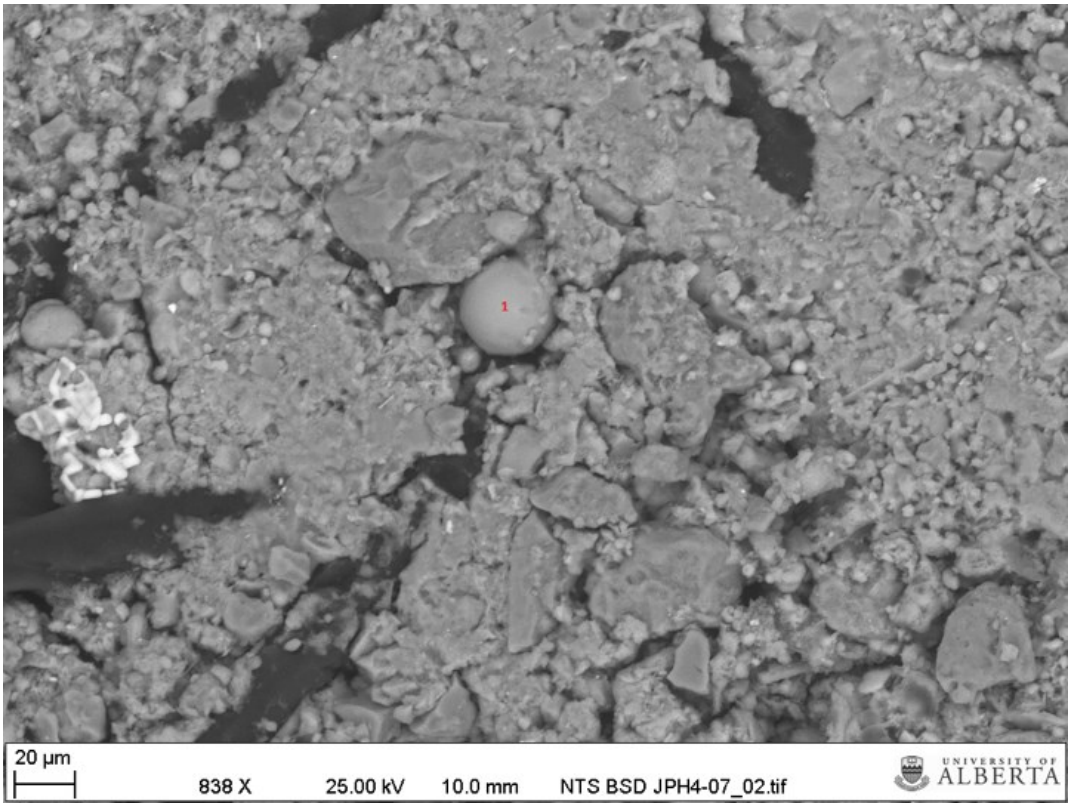
1
20 µm
838 X
25.00 kV
10.0 mm
NTS BSD JPH4-07_02.tif
UNIVERSITY OF ALBERTA

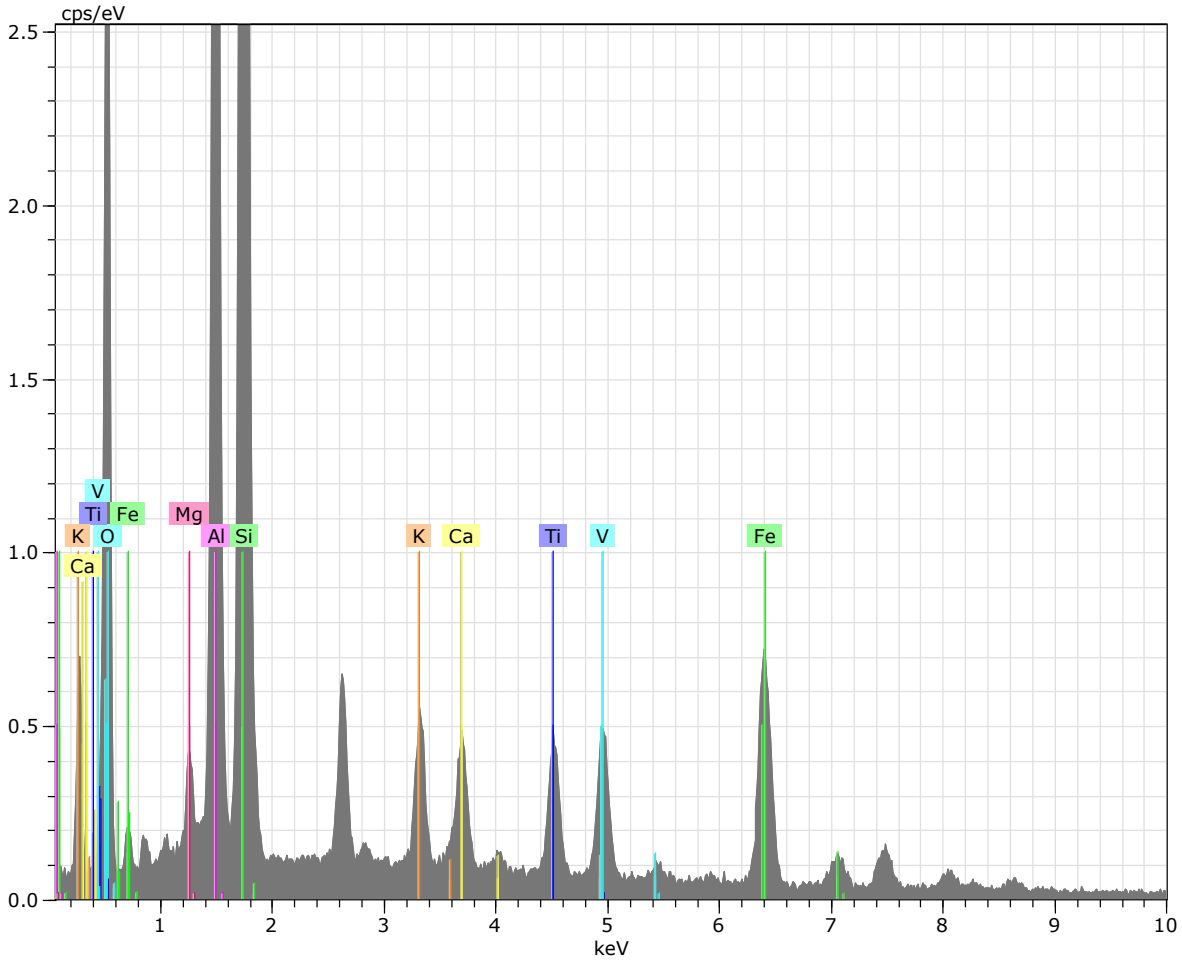

JPH-07_ 1 Date:7/8/2016 11:34:25 AM HV:25.0kV Puls th.:2.91kcps

El	AN	Series	unn. C [wt.%]	norm. C [wt.%]	Atom. C [at.%]	Error (1 Sigma) [wt.%]
O	8	K-series	30.78	41.32	58.85	4.17
Si	14	K-series	15.79	21.20	17.20	0.72
Al	13	K-series	11.68	15.68	13.25	0.61
Fe	26	K-series	6.91	9.28	3.78	0.22
Ti	22	K-series	2.41	3.23	1.54	0.10
V	23	K-series	2.31	3.10	1.39	0.10
Ca	20	K-series	1.88	2.52	1.43	0.09
K	19	K-series	1.85	2.49	1.45	0.09
Mg	12	K-series	0.88	1.18	1.11	0.08
		Total:	74.49	100.00	100.00	

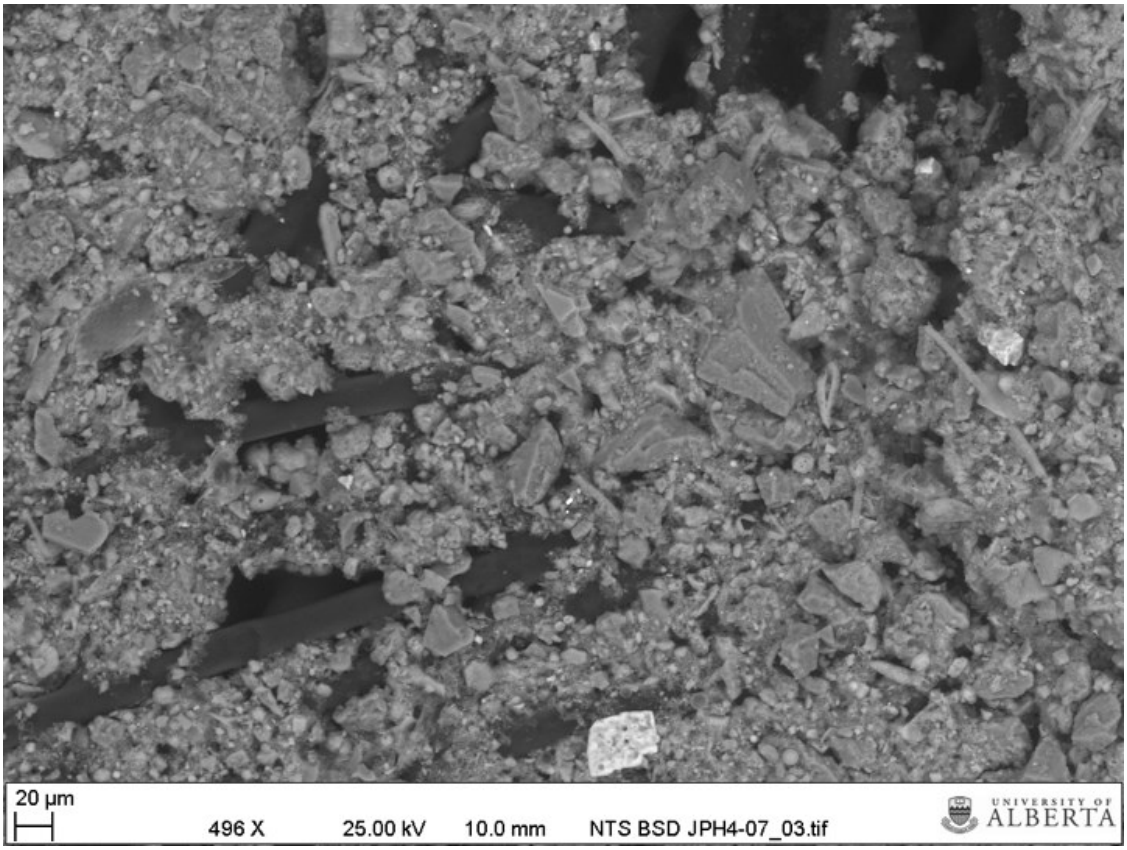
20 µm
496 X
25.00 kV
10.0 mm
NTS BSD JPH4-07_03.tif
UNIVERSITY OF ALBERTA

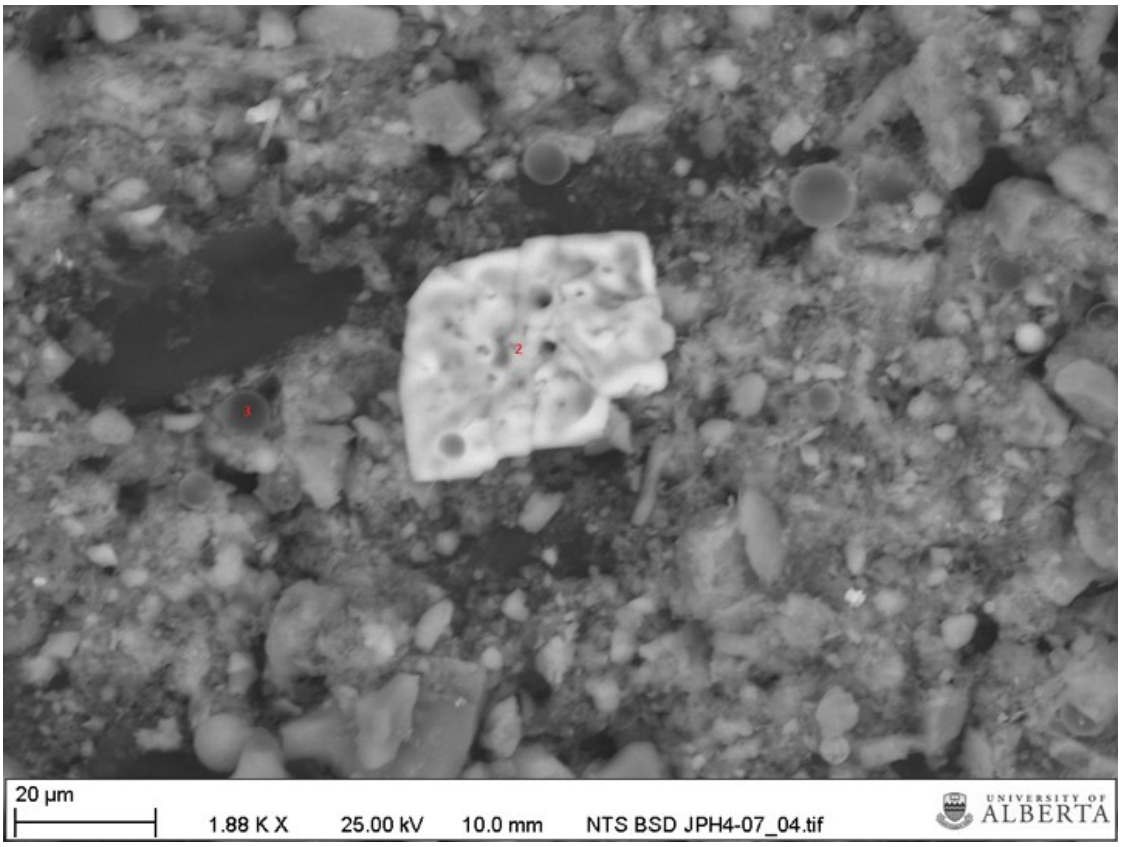
2
3
20 µm
1.88 K X
25.00 kV
10.0 mm
NTS BSD JPH4-07_04.tif
UNIVERSITY OF ALBERTA

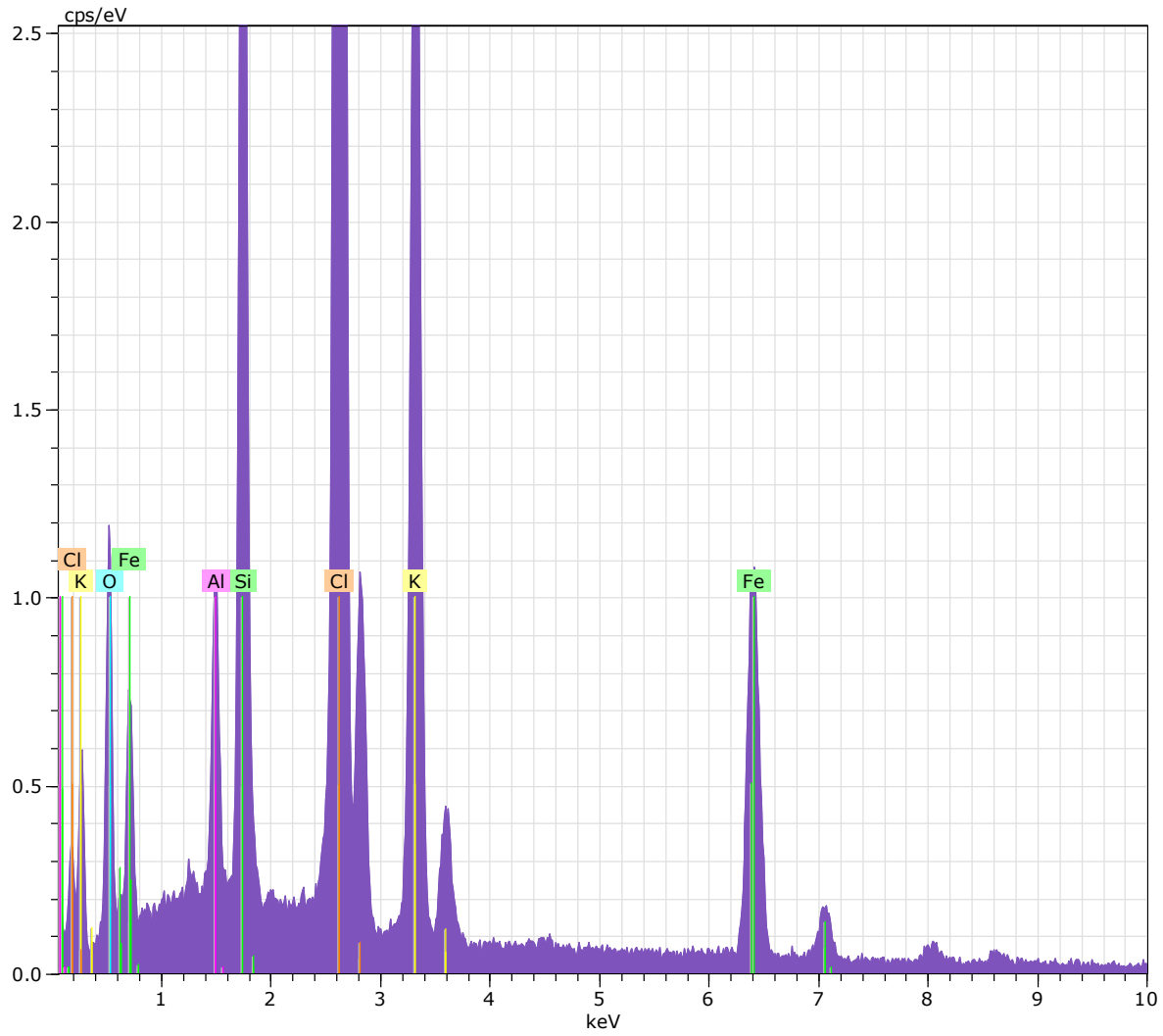

JPH-07_ 2 Date:7/8/2016 11:41:55 AM HV:25.0kV Puls th.:3.84kcps

El	AN	Series	unn. C [wt.%]	norm. C [wt.%]	Atom. C [at.%]	Error (1 Sigma) [wt.%]
Cl	17	K-series	26.62	32.78	25.45	0.94
O	8	K-series	22.03	27.13	46.69	4.13
K	19	K-series	13.38	16.48	11.60	0.46
Fe	26	K-series	11.62	14.31	7.05	0.37
Si	14	K-series	5.94	7.31	7.17	0.30
Al	13	K-series	1.62	1.99	2.03	0.12
		Total:	81.20	100.00	100.00	

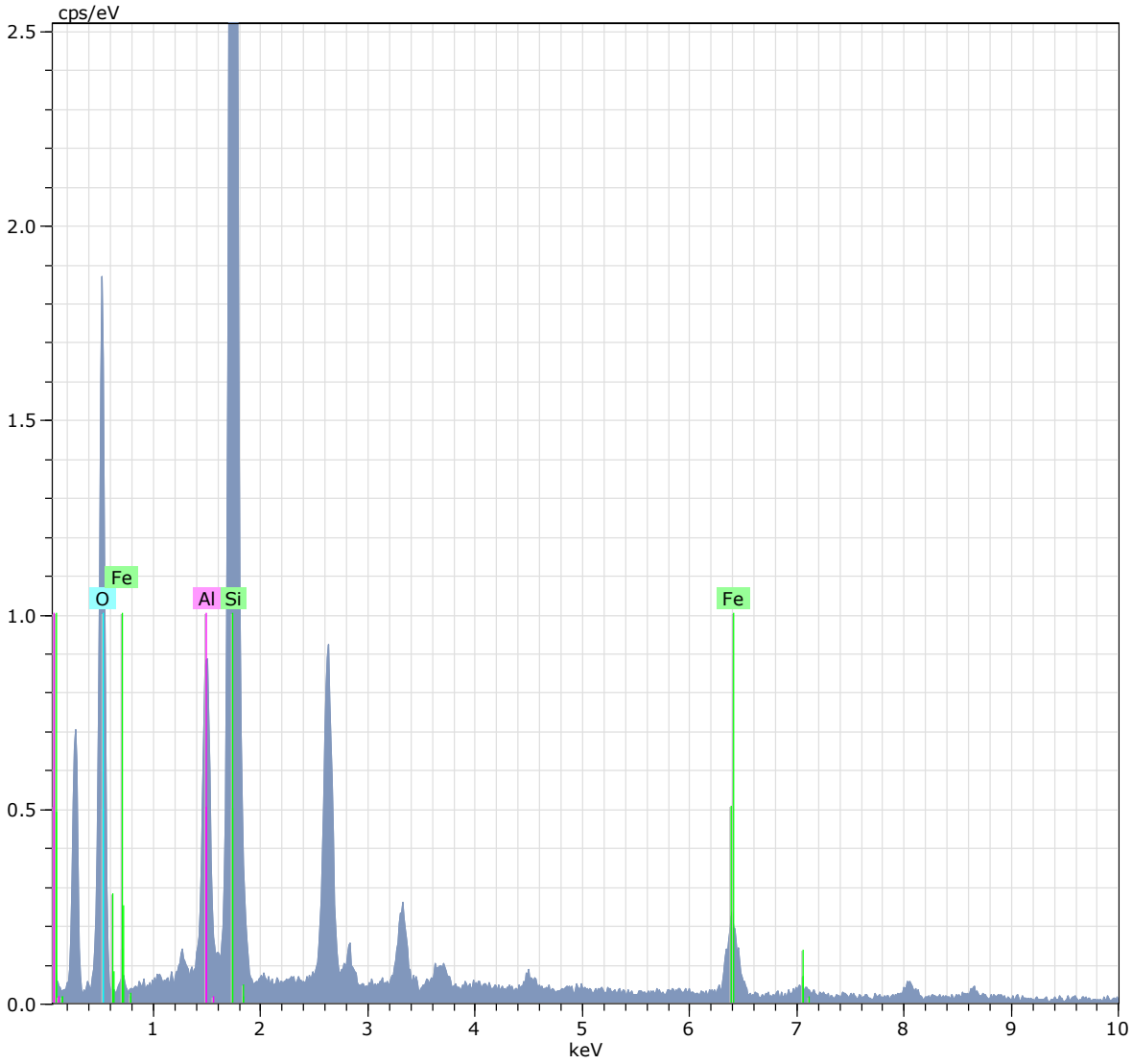

JPH-07_ 3 Date:7/8/2016 11:43:53 AM HV:25.0kV Puls th.:1.46kcps

El	AN	Series	unn. C [wt.%]	norm. C [wt.%]	Atom. C [at.%]	Error (1 Sigma) [wt.%]
O	8	K-series	24.05	49.41	64.19	4.14
Si	14	K-series	18.49	37.97	28.10	0.86
Al	13	K-series	3.68	7.55	5.82	0.24
Fe	26	K-series	2.47	5.07	1.89	0.14
		Total:	48.69	100.00	100.00	

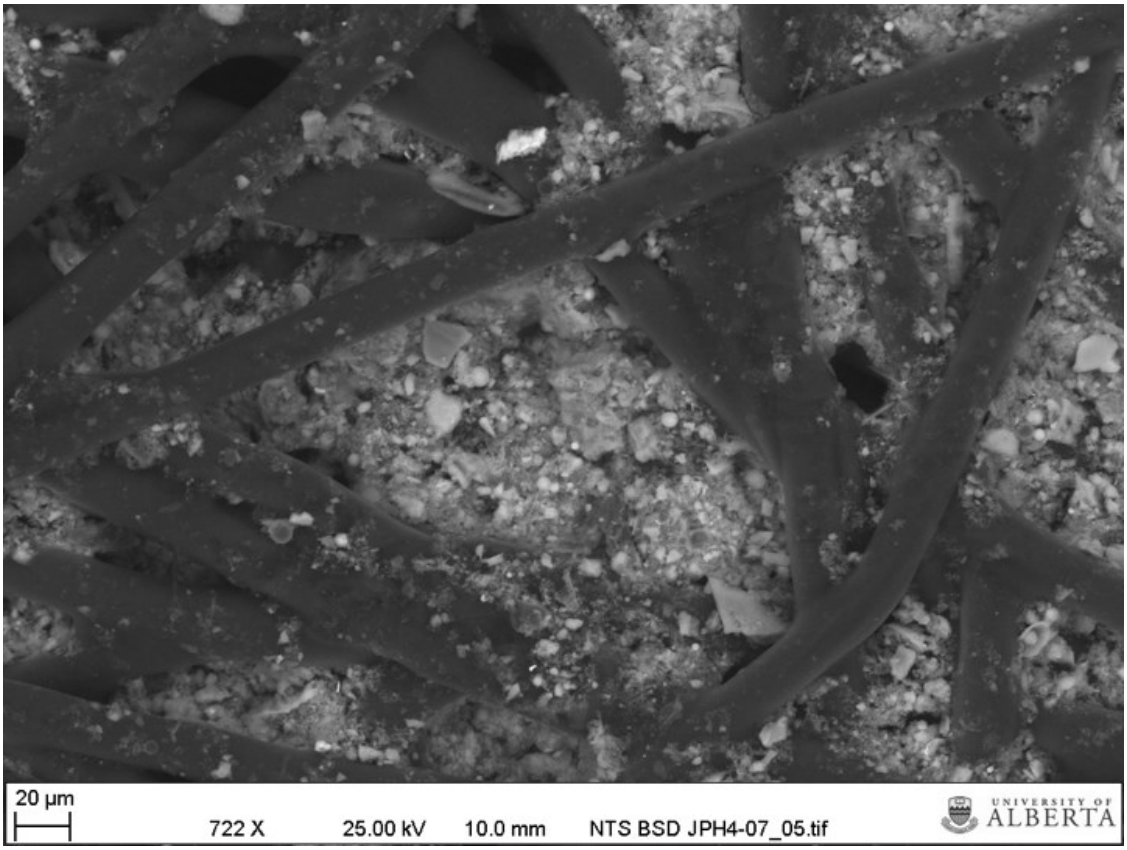
20 µm
722 X
25.00 kV
10.0 mm
NTS BSD JPH4-07_05.tif
UNIVERSITY OF ALBERTA

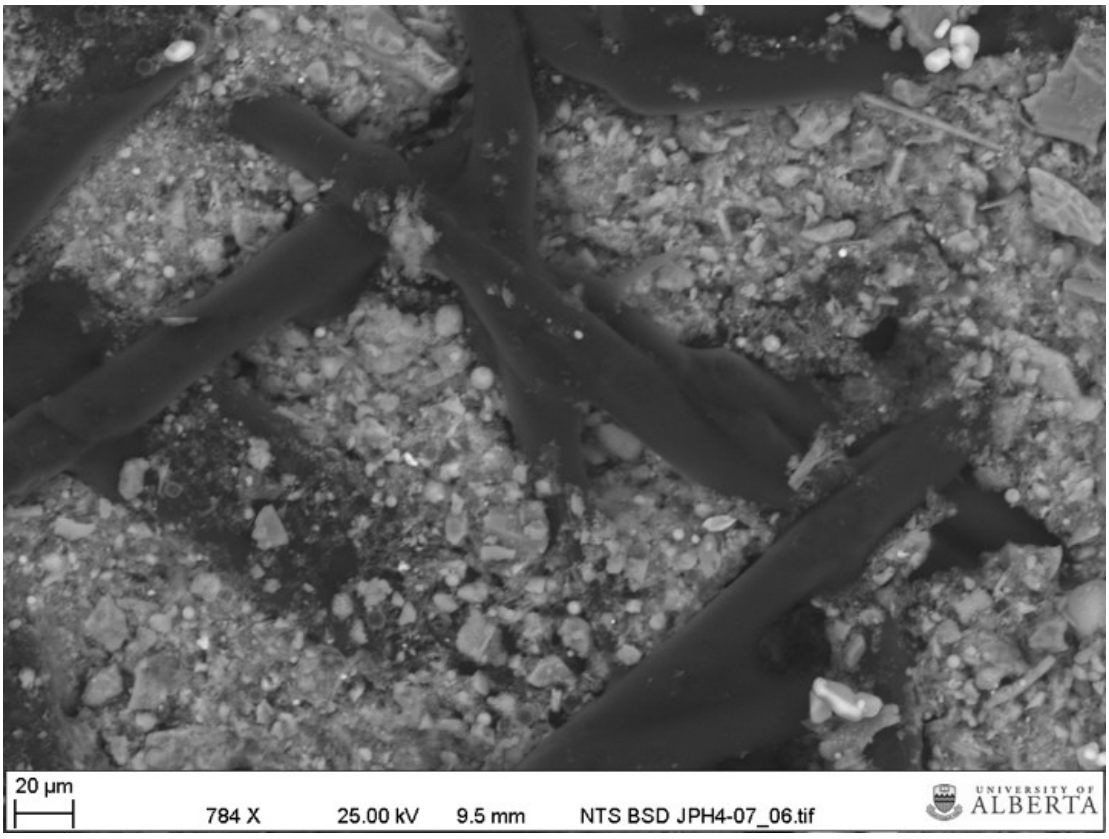
20 µm
784 X
25.00 kV
9.5 mm
NTS BSD JPH4-07_06.tif
UNIVERSITY OF ALBERTA

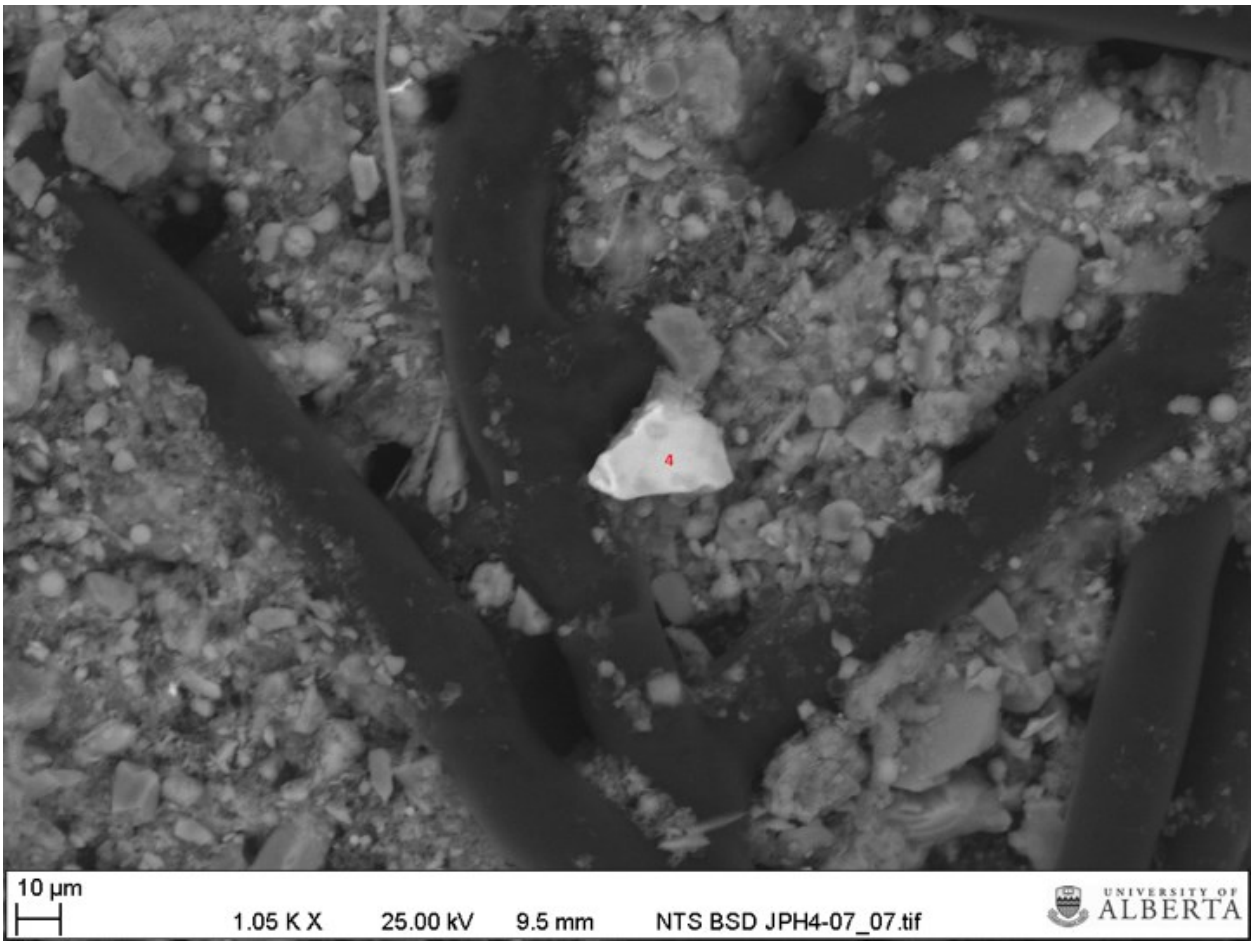
4
10 µm
1.05 K X
25.00 kV
9.5 mm
NTS BSD JPH4-07_07.tif
UNIVERSITY OF ALBERTA

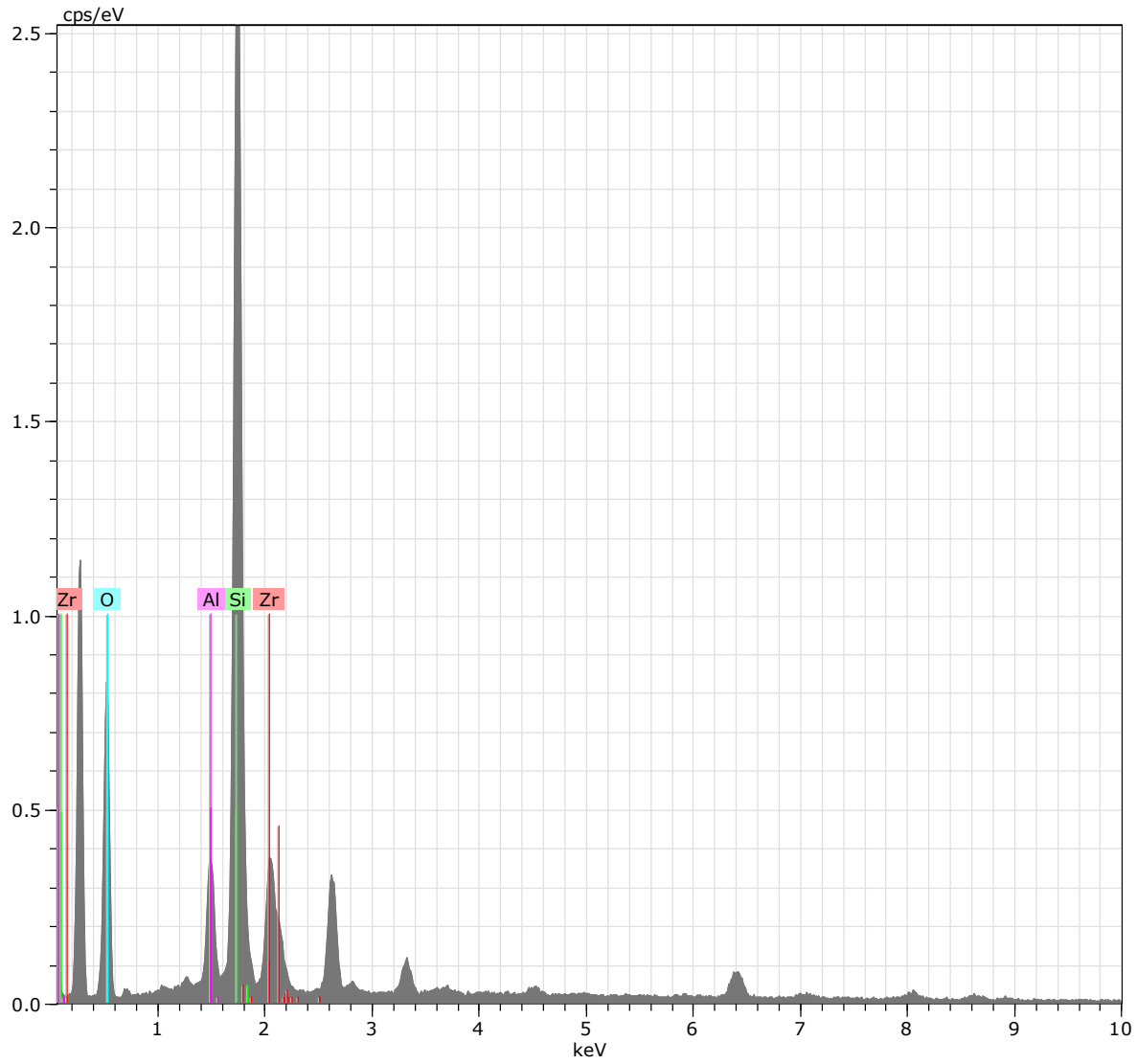

JPH-07_ 4 Date:7/8/2016 11:55:59 AM HV:25.0kV Puls th.:1.02kcps

El	AN	Series	unn. C [wt.%]	norm. C [wt.%]	Atom. C [at.%]	Error (1 Sigma) [wt.%]
Zr	40	L-series	33.62	44.75	14.60	1.40
O	8	K-series	25.08	33.39	62.12	5.02
Si	14	K-series	14.77	19.66	20.84	0.70
Al	13	K-series	1.65	2.20	2.43	0.14
		Total:	75.12	100.00	100.00	

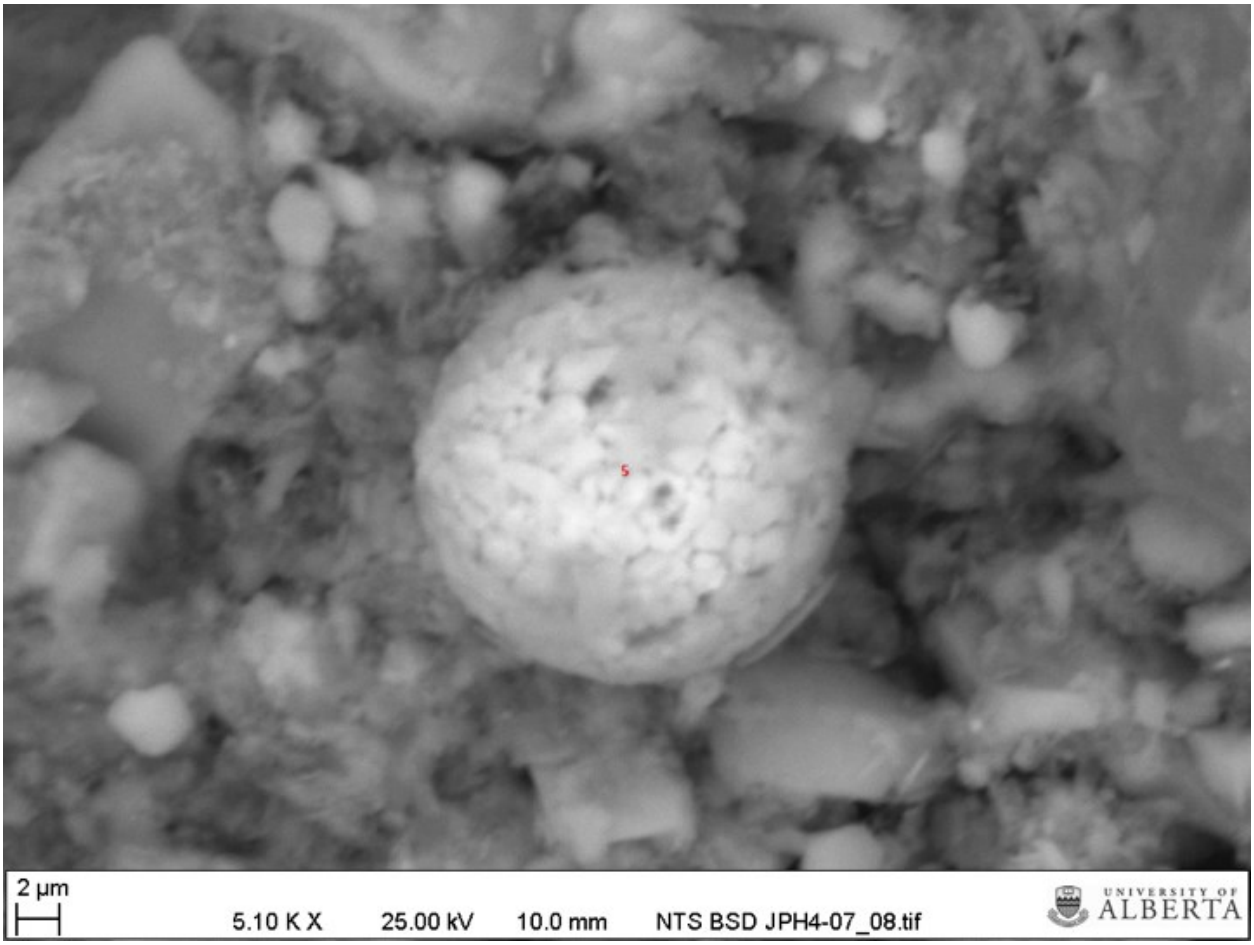
5
2 µm
5.10 K X
25.00 kV
10.0 mm
NTS BSD JPH4-07_08.tif
UNIVERSITY OF ALBERTA

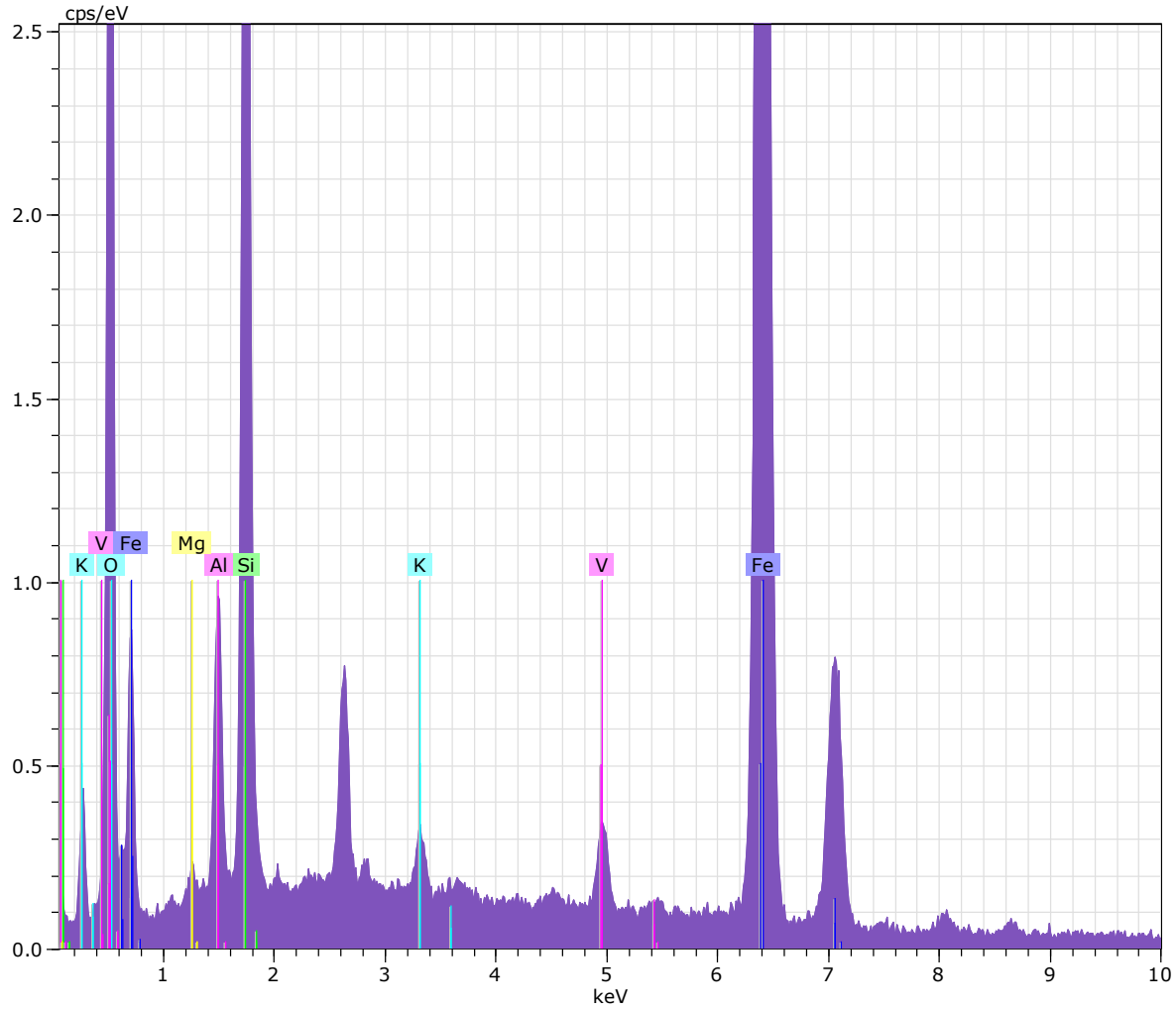

JPH-07_ 5 Date:7/8/2016 12:02:22 PM HV:25.0kV Puls th.:3.50kcps

El	AN	Series	unn. C [wt.%]	norm. C [wt.%]	Atom. C [at.%]	Error (1 Sigma) [wt.%]
Fe	26	K-series	40.50	53.58	27.97	1.07
O	8	K-series	23.60	31.23	56.91	3.09
Si	14	K-series	7.71	10.20	10.59	0.37
Al	13	K-series	2.10	2.78	3.00	0.14
V	23	K-series	1.08	1.44	0.82	0.06
K	19	K-series	0.38	0.50	0.37	0.04
Mg	12	K-series	0.20	0.27	0.32	0.04
		Total:	75.58	100.00	100.00	

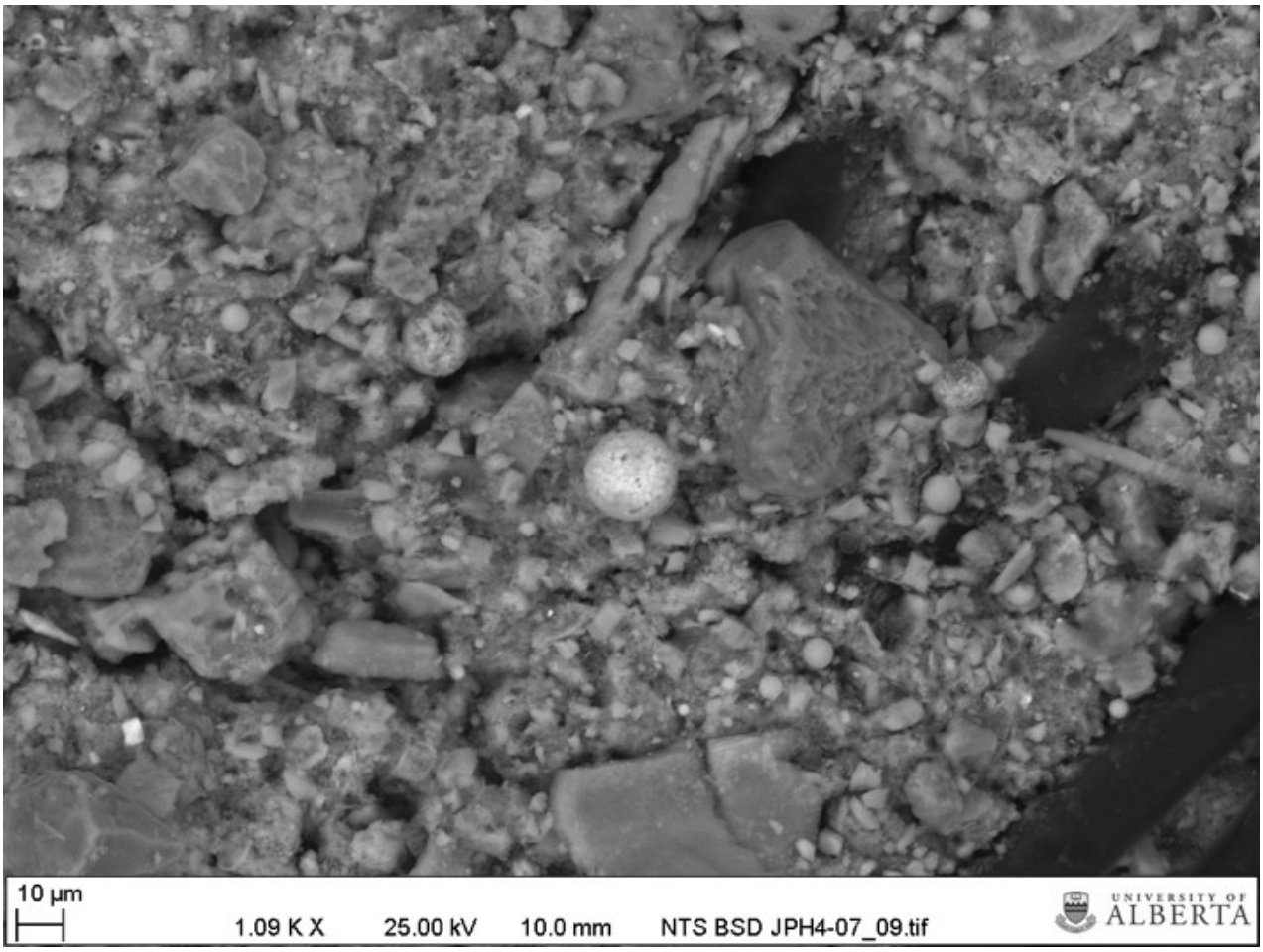
10 µm
1.09 K X
25.00 kV
10.0 mm
NTS BSD JPH4-07_09.tif
UNIVERSITY OF ALBERTA

JPH4-W1 11 (1967)

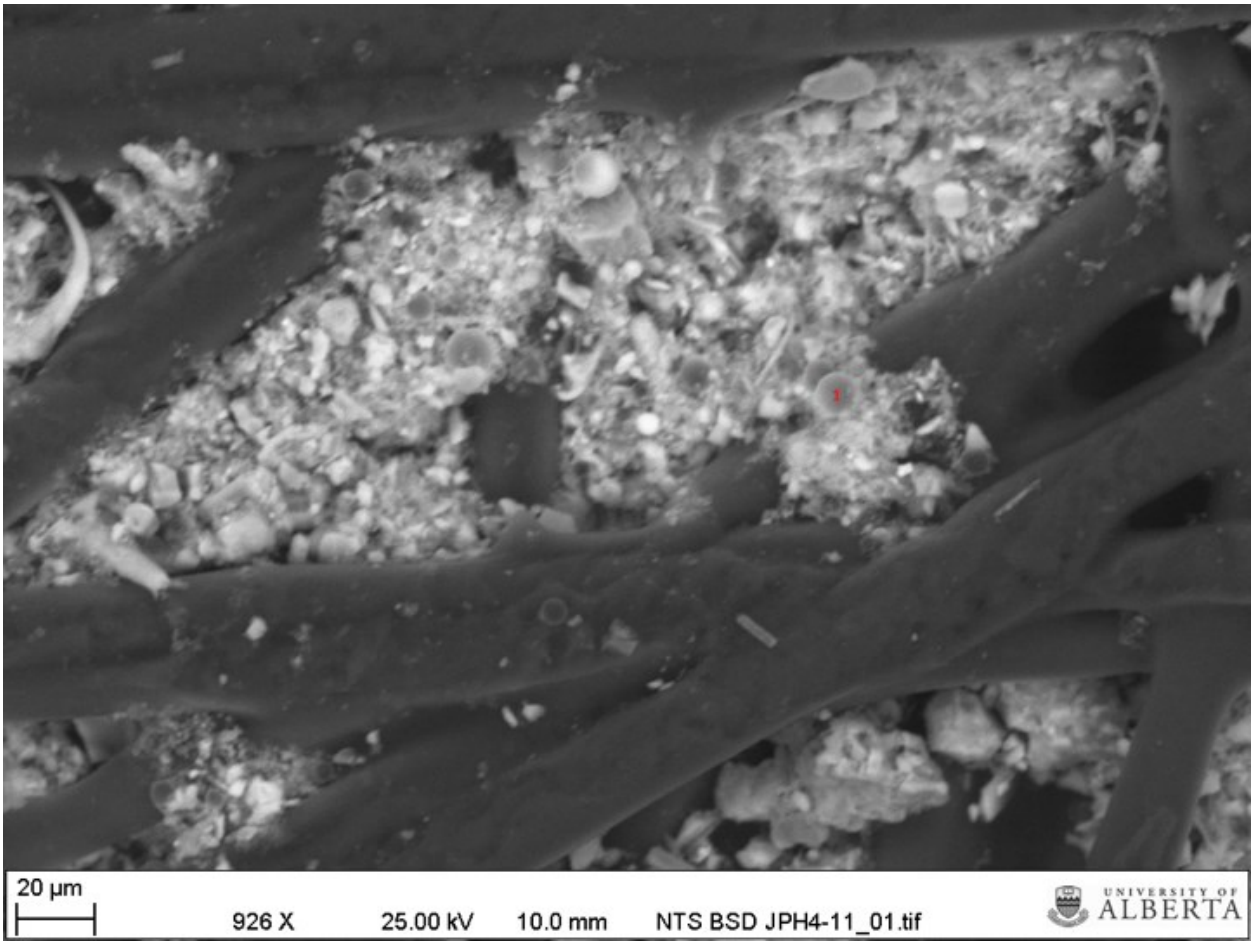
20 µm
926 X
25.00 kV
10.0 mm
NTS BSD JPH4-11_01.tif
UNIVERSITY OF ALBERTA

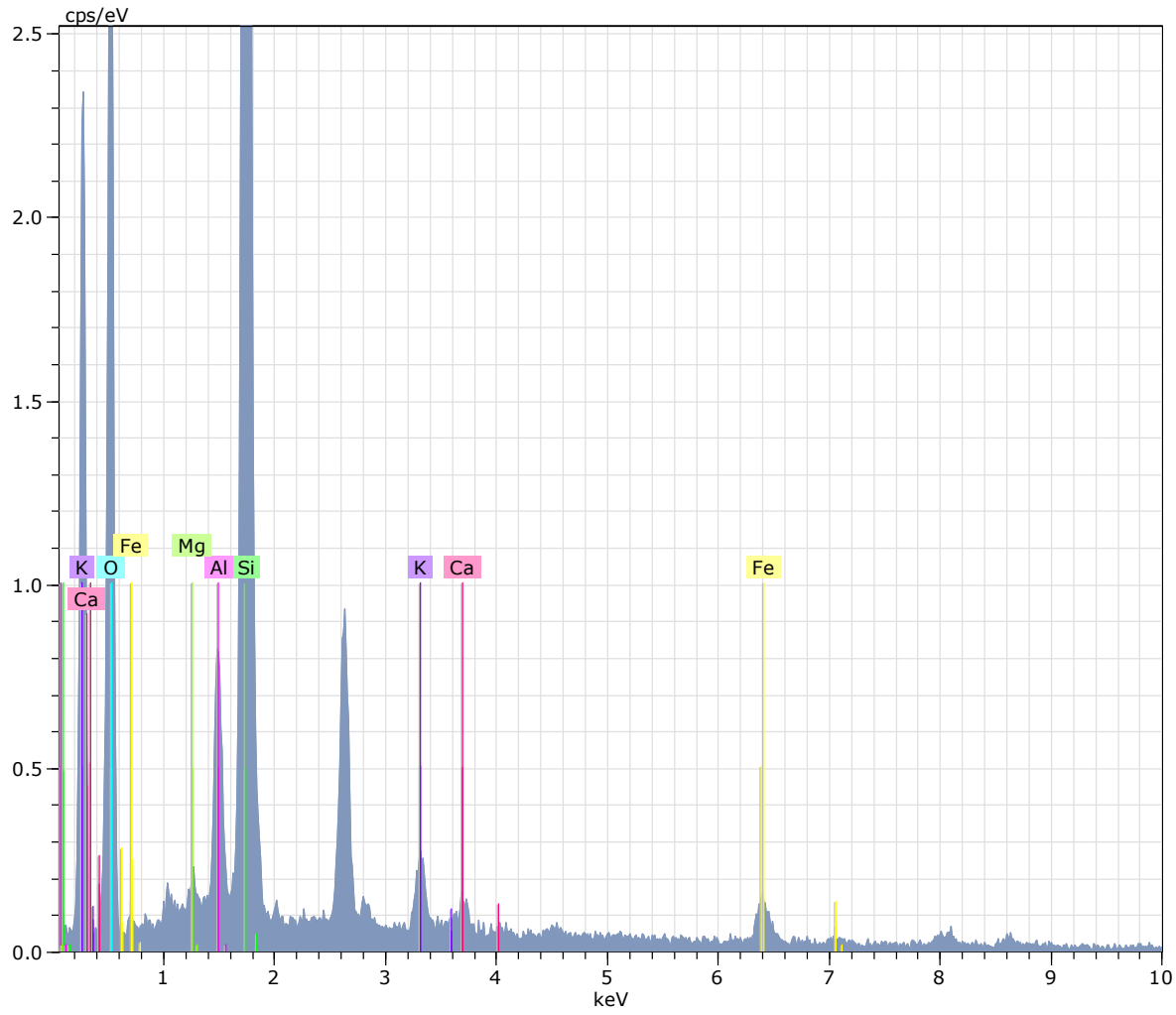

JPH-11_ 1 Date:7/8/2016 12:14:22 PM HV:25.0kV Puls th.:1.96kcps

El	AN	Series	unn. C [wt.%]	norm. C [wt.%]	Atom. C [at.%]	Error (1 Sigma) [wt.%]
O	8	K-series	27.36	56.59	70.83	4.36
Si	14	K-series	15.44	31.94	22.77	0.72
Al	13	K-series	1.90	3.93	2.92	0.14
Fe	26	K-series	1.63	3.38	1.21	0.11
K	19	K-series	1.27	2.62	1.34	0.09
Ca	20	K-series	0.52	1.07	0.54	0.06
Mg	12	K-series	0.23	0.47	0.39	0.05
		Total:	48.36	100.00	100.00	

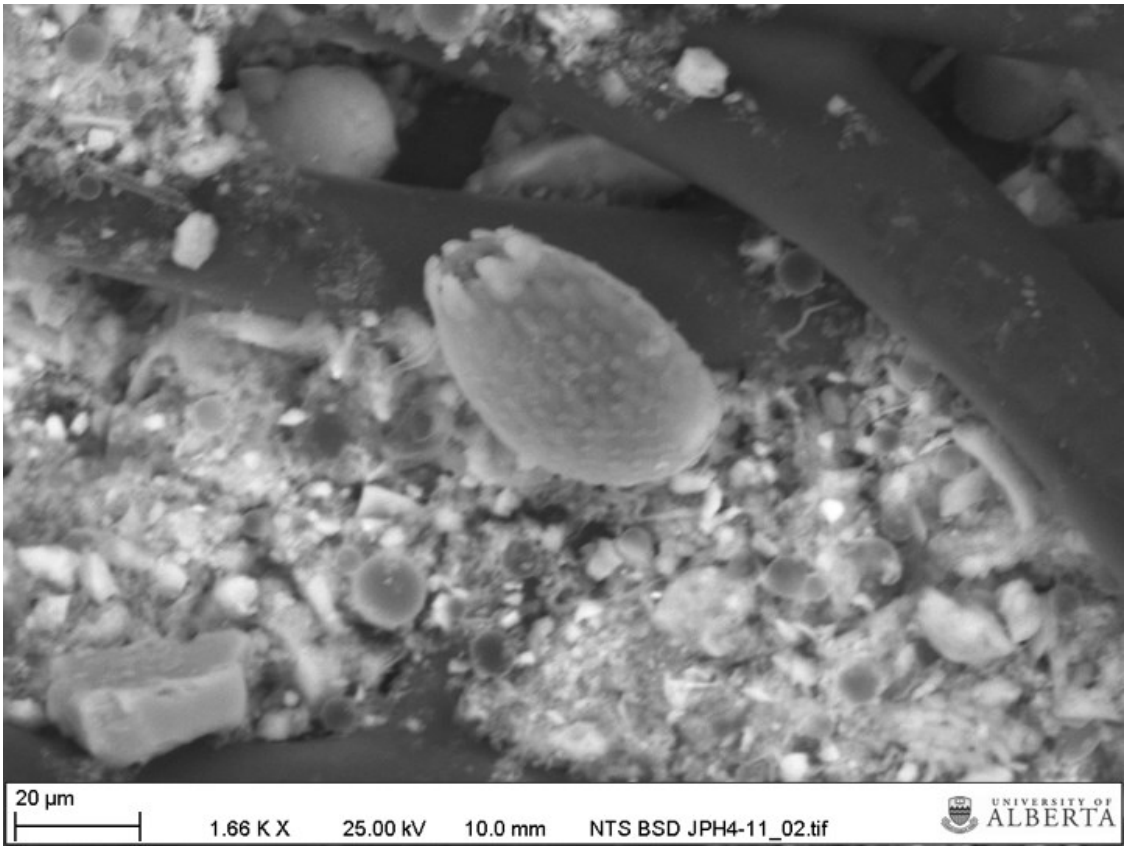
20 µm
1.66 K X
25.00 kV
10.0 mm
NTS BSD JPH4-11_02.tif
UNIVERSITY OF ALBERTA

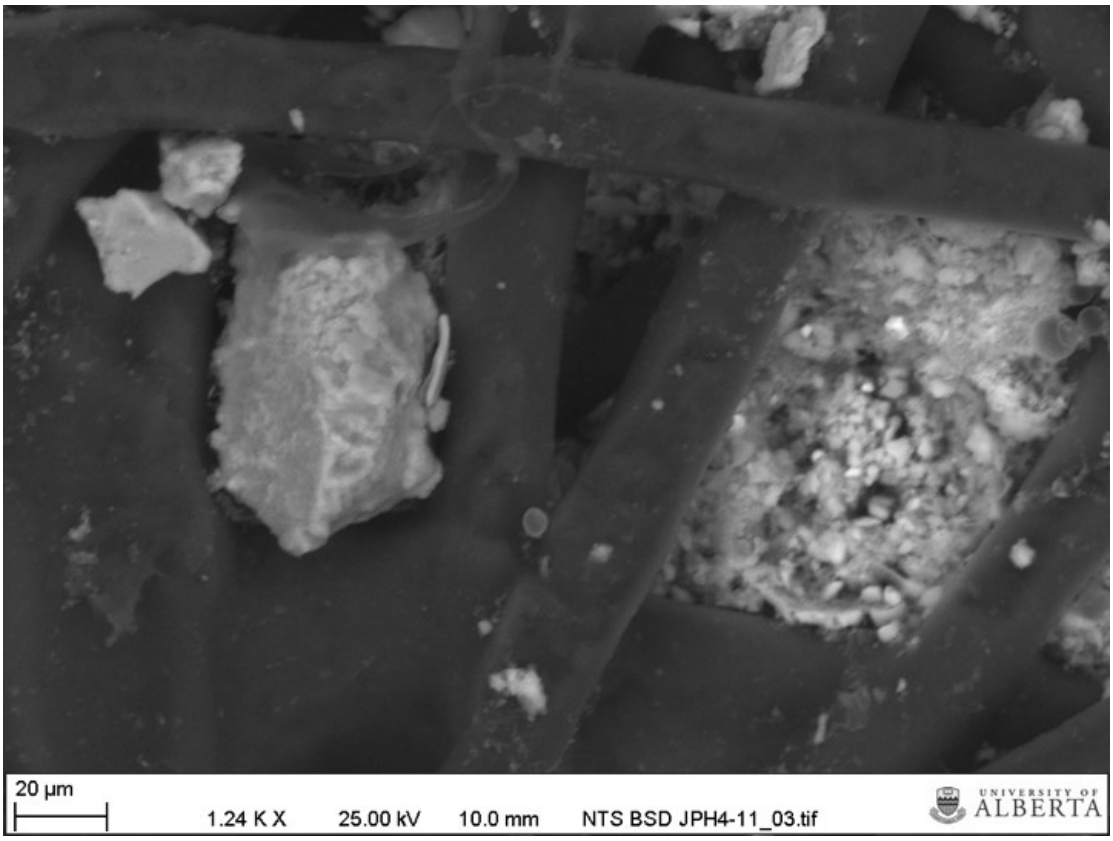
20 µm
1.24 K X
25.00 kV
10.0 mm
NTS BSD JPH4-11_03.tif
UNIVERSITY OF ALBERTA

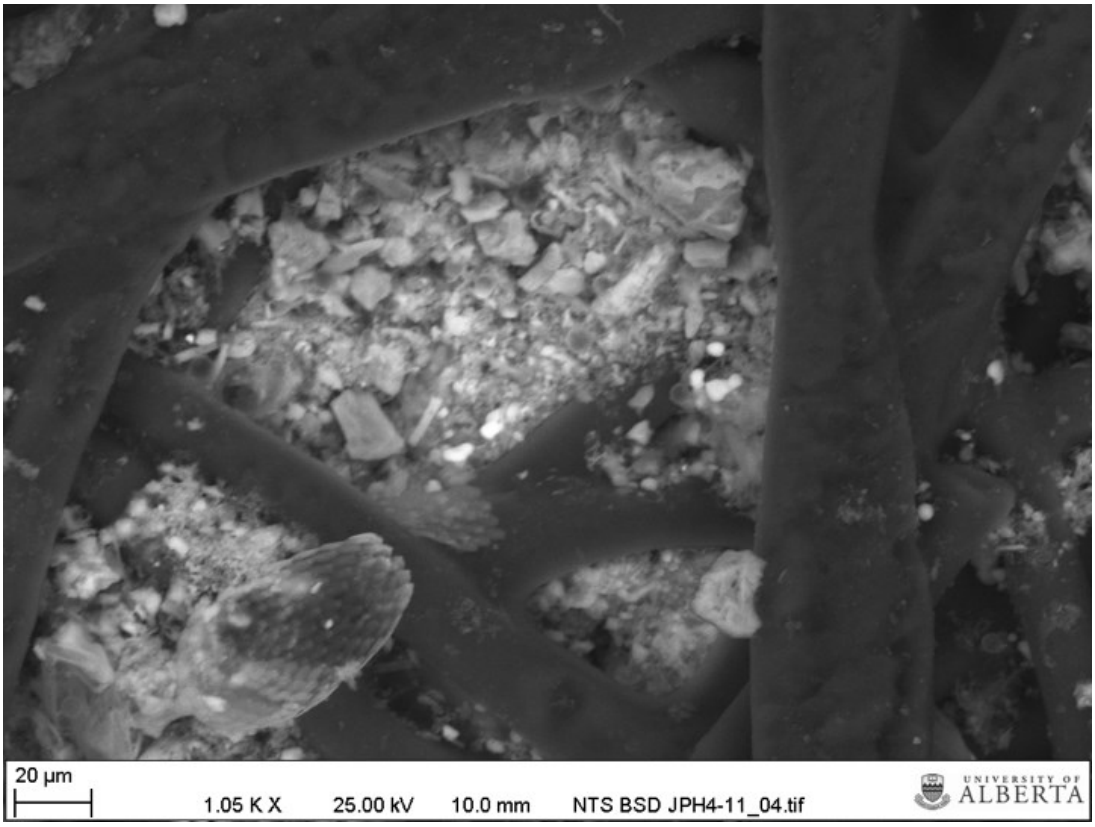
20 µm
1.05 K X
25.00 kV
10.0 mm
NTS BSD JPH4-11_04.tif
UNIVERSITY OF ALBERTA

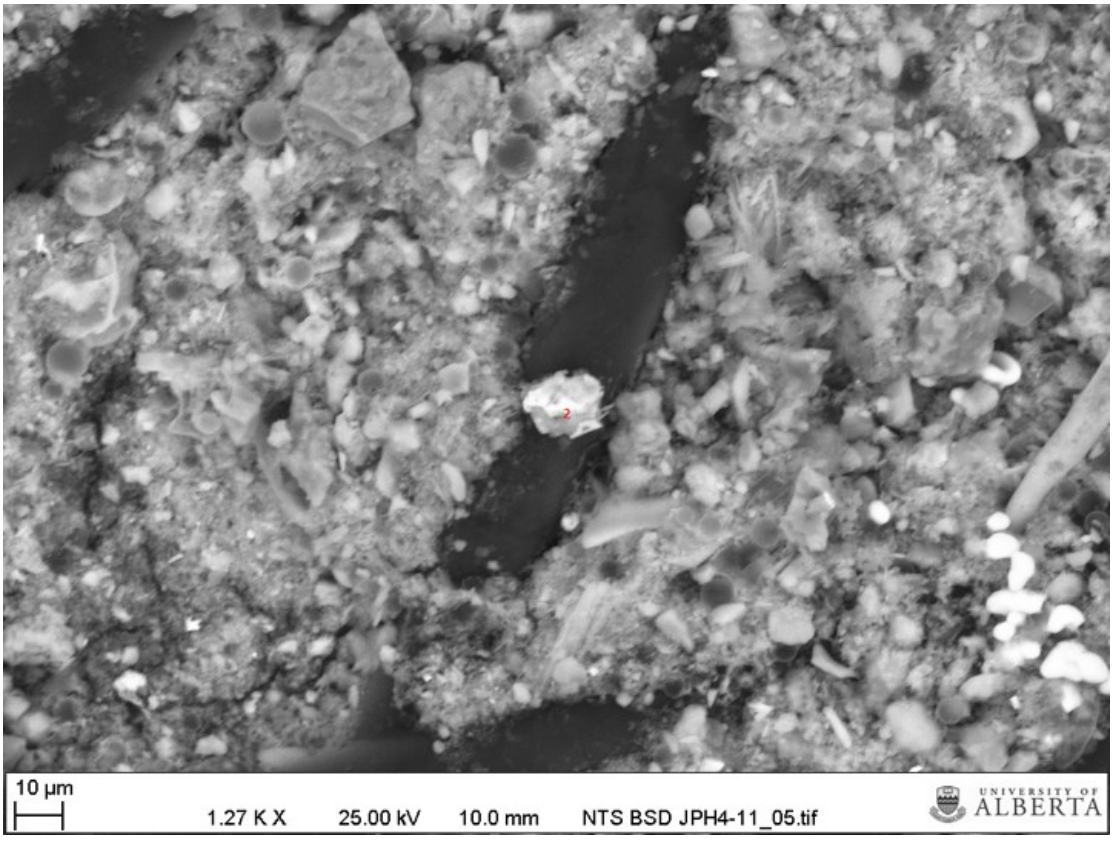
10 µm
1.27 K X
25.00 kV
10.0 mm
NTS BSD JPH4-11_05.tif
UNIVERSITY OF ALBERTA

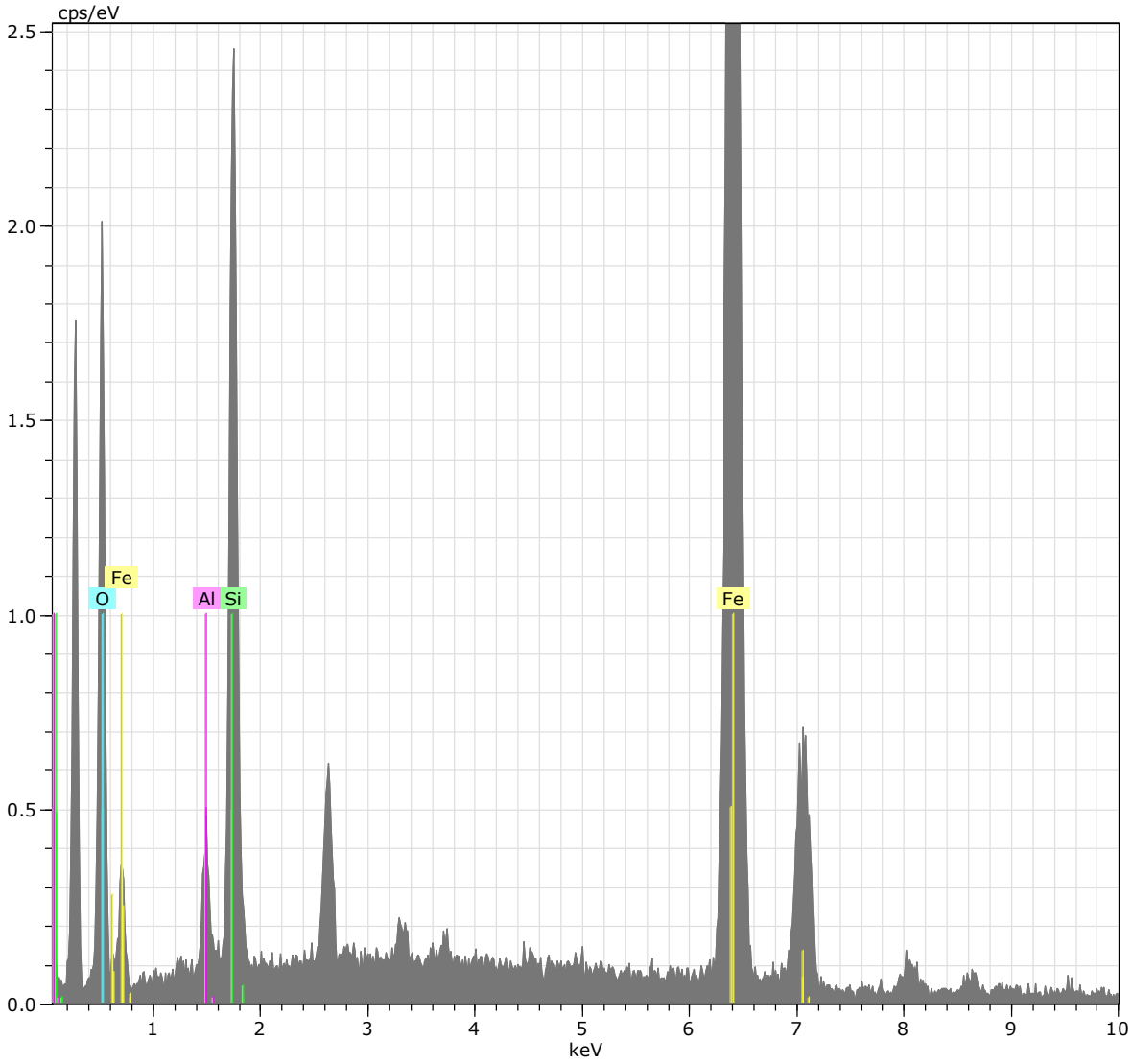

JPH-11_ 2 Date:7/8/2016 12:24:22 PM HV:25.0kV Puls th.:2.53kcps

El	AN	Series	unn. C [wt.%]	norm. C [wt.%]	Atom. C [at.%]	Error (1 Sigma) [wt.%]
Fe	26	K-series	56.85	66.35	40.37	1.56
O	8	K-series	17.62	20.57	43.68	3.39
Si	14	K-series	9.31	10.87	13.15	0.48
Al	13	K-series	1.90	2.22	2.80	0.18
		Total:	85.69	100.00	100.00	


20 µm
722 X
25.00 kV
10.0 mm
NTS BSD JPH4-11_06.tif
UNIVERSITY OF ALBERTA

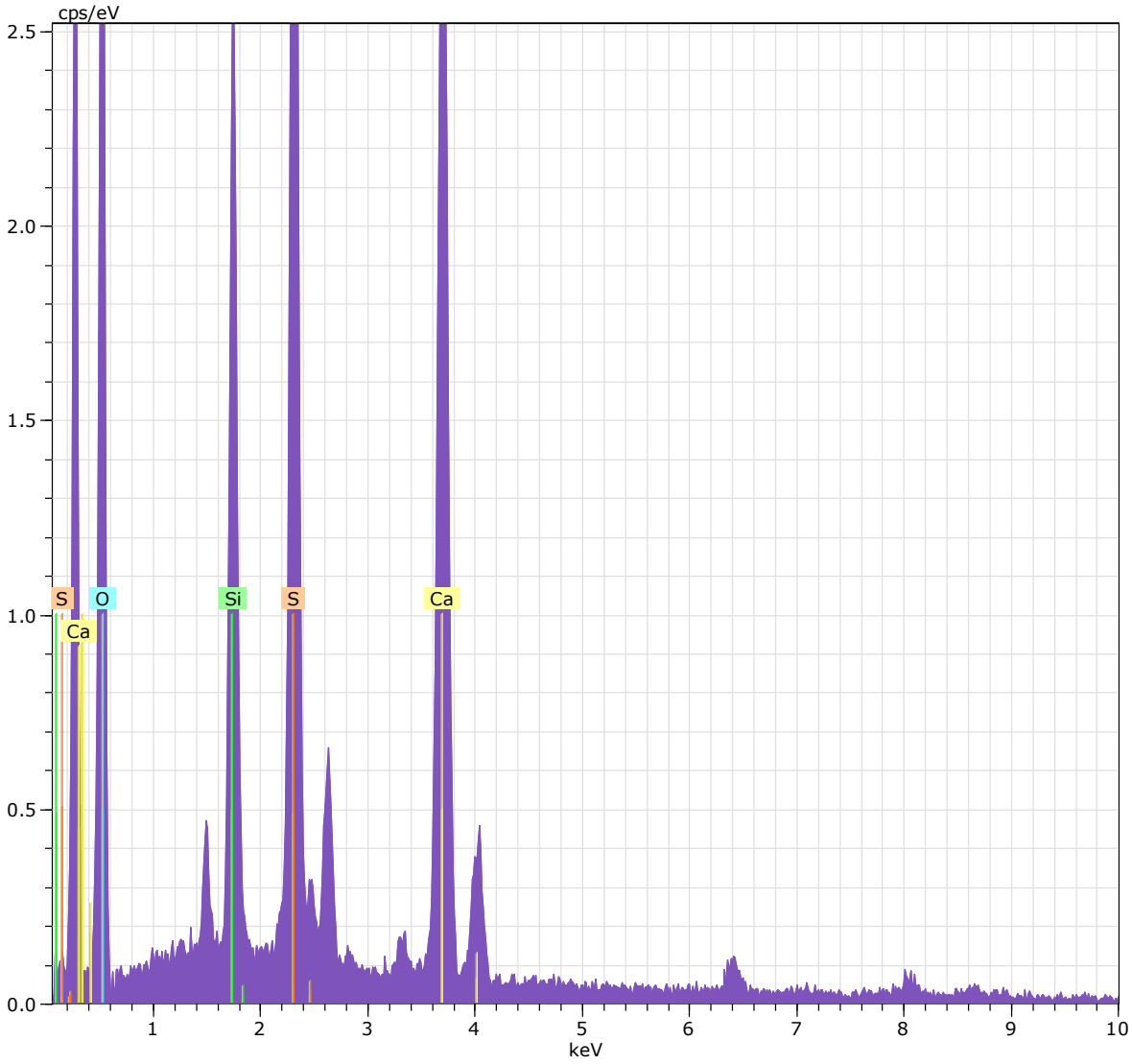

JPH-11_ 3 Date:7/8/2016 12:37:48 PM HV:25.0kV Puls th.:2.45kcps

El	AN	Series	unn. C [wt.%]	norm. C [wt.%]	Atom. C [at.%]	Error (1 Sigma) [wt.%]
O	8	K-series	57.57	64.96	80.24	8.72
Ca	20	K-series	16.47	18.58	9.16	0.54
S	16	K-series	10.03	11.32	6.98	0.41
Si	14	K-series	4.55	5.14	3.61	0.24
		Total:	88.63	100.00	100.00	

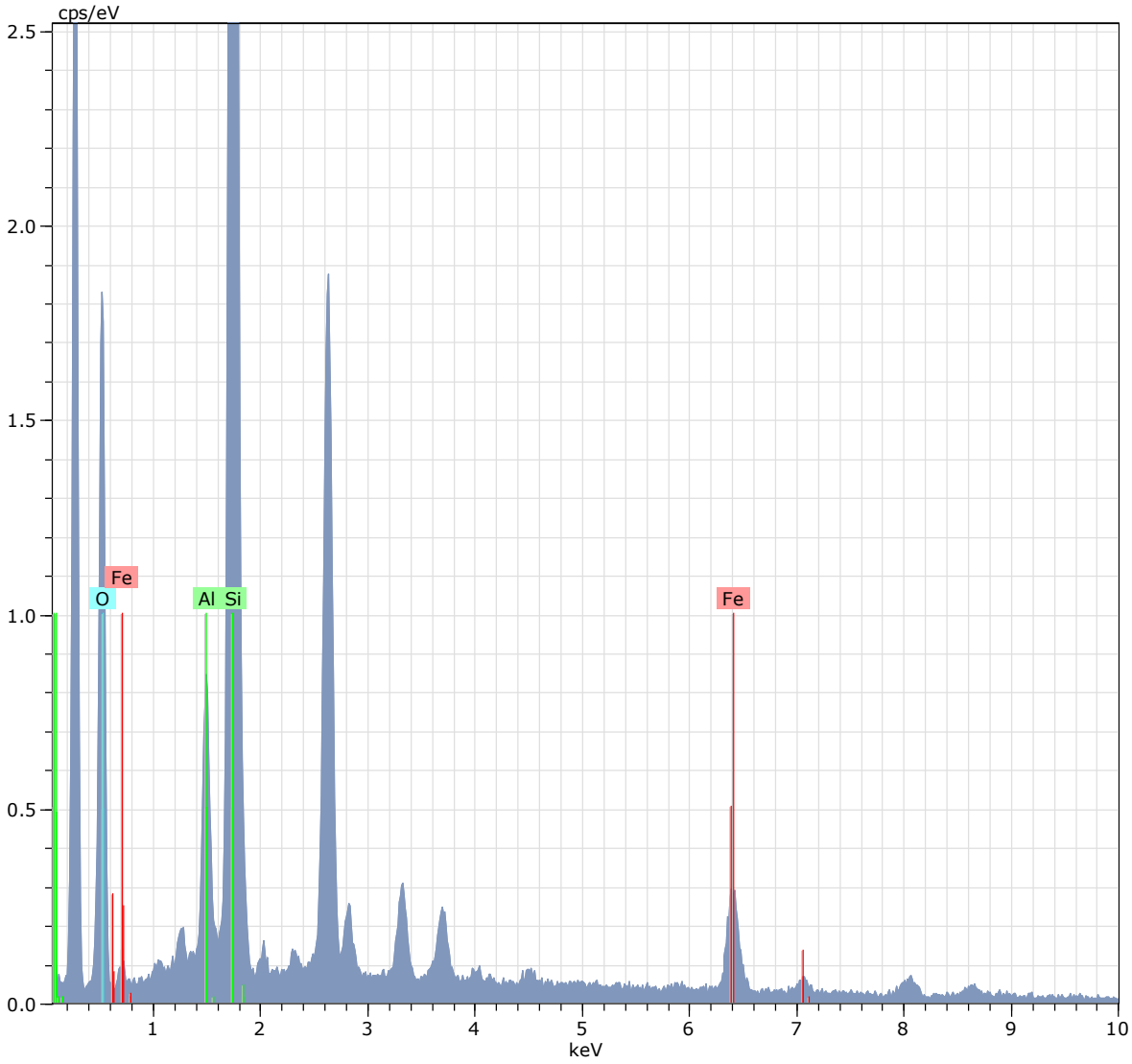

JPH-11_ 4 Date:7/8/2016 12:39:16 PM HV:25.0kV Puls th.:2.19kcps

El	AN	Series	unn. C [wt.%]	norm. C [wt.%]	Atom. C [at.%]	Error (1 Sigma) [wt.%]
O	8	K-series	20.13	44.40	59.69	3.42
Si	14	K-series	19.92	43.93	33.65	0.91
Fe	26	K-series	2.92	6.44	2.48	0.14
Al	13	K-series	2.38	5.24	4.18	0.17
		Total:	45.34	100.00	100.00	

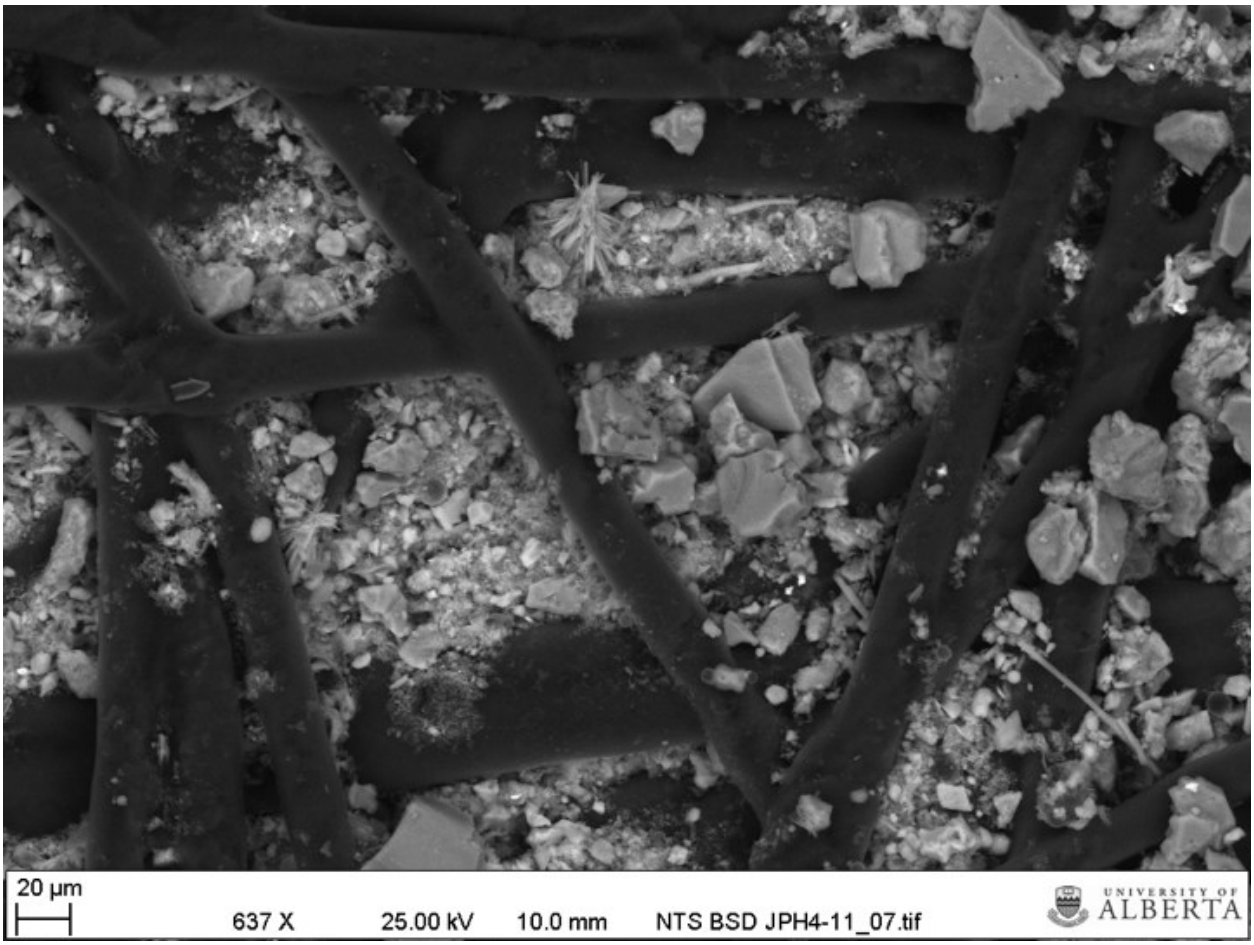
20 µm
637 X
25.00 kV
10.0 mm
NTS BSD JPH4-11_07.tif
UNIVERSITY OF ALBERTA

JPH4-W1 15 (1950)

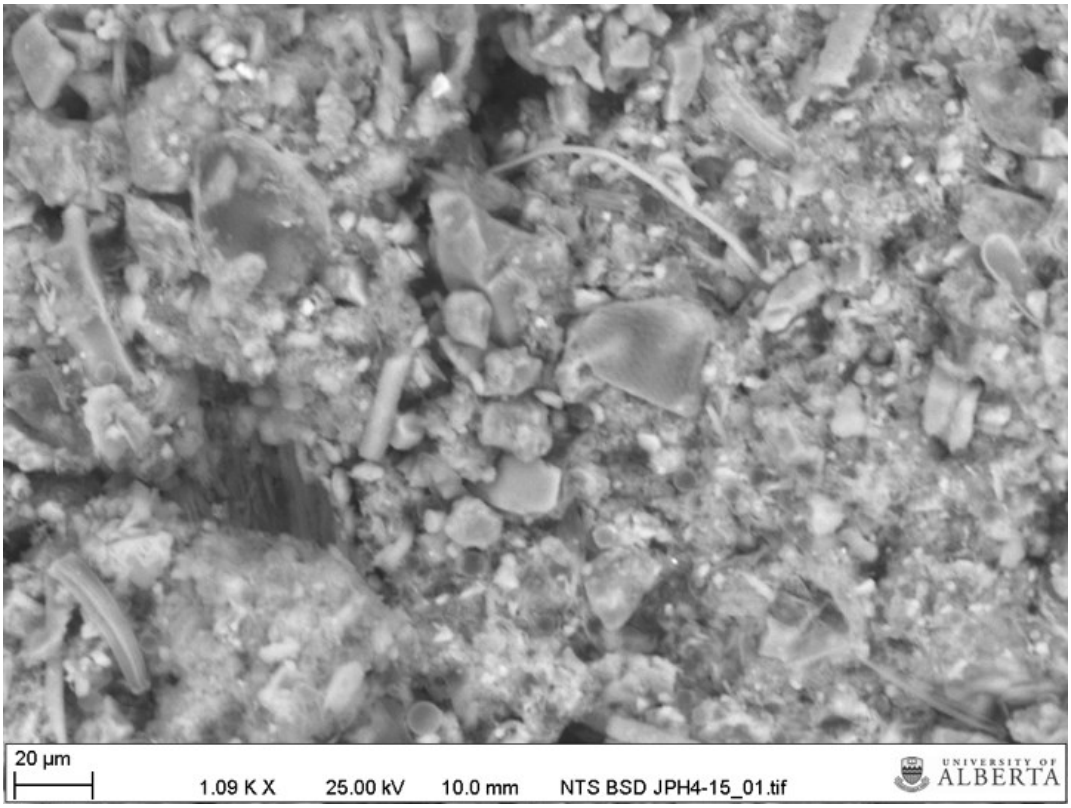
20 µm
1.09 K X
25.00 kV
10.0 mm
NTS BSD JPH4-15_01.tif
UNIVERSITY OF ALBERTA

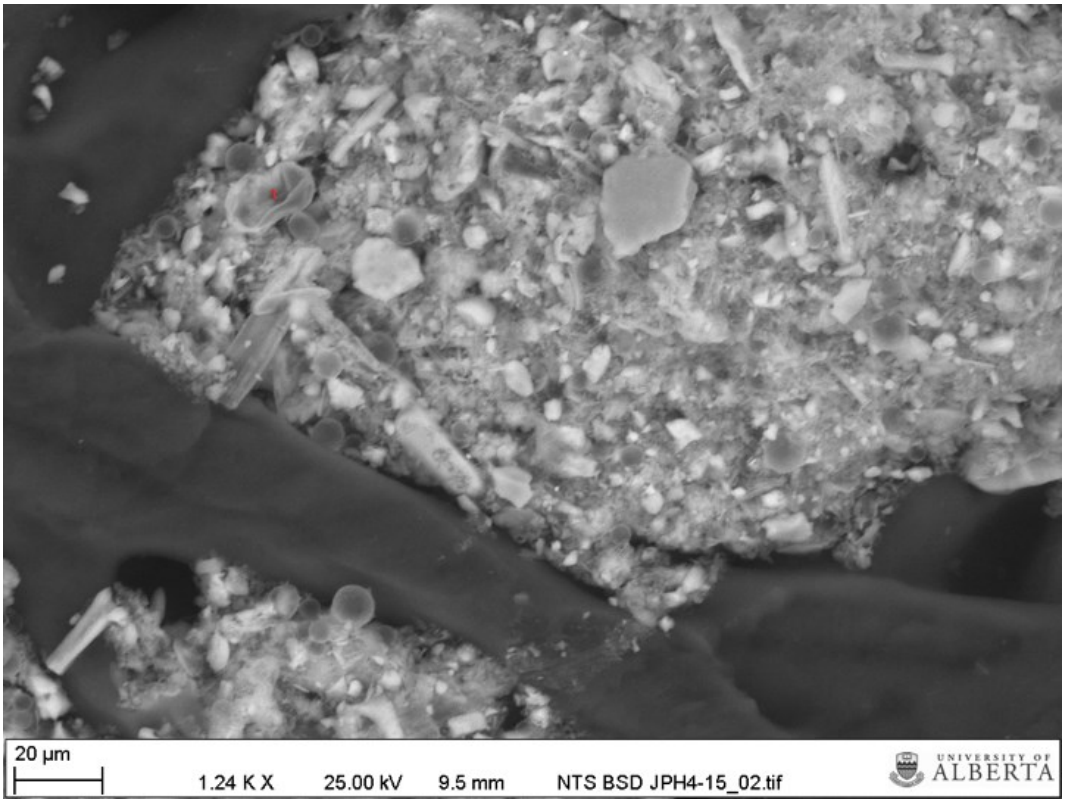
20 µm
1.24 K X
25.00 kV
9.5 mm
NTS BSD JPH4-15_02.tif
UNIVERSITY OF ALBERTA

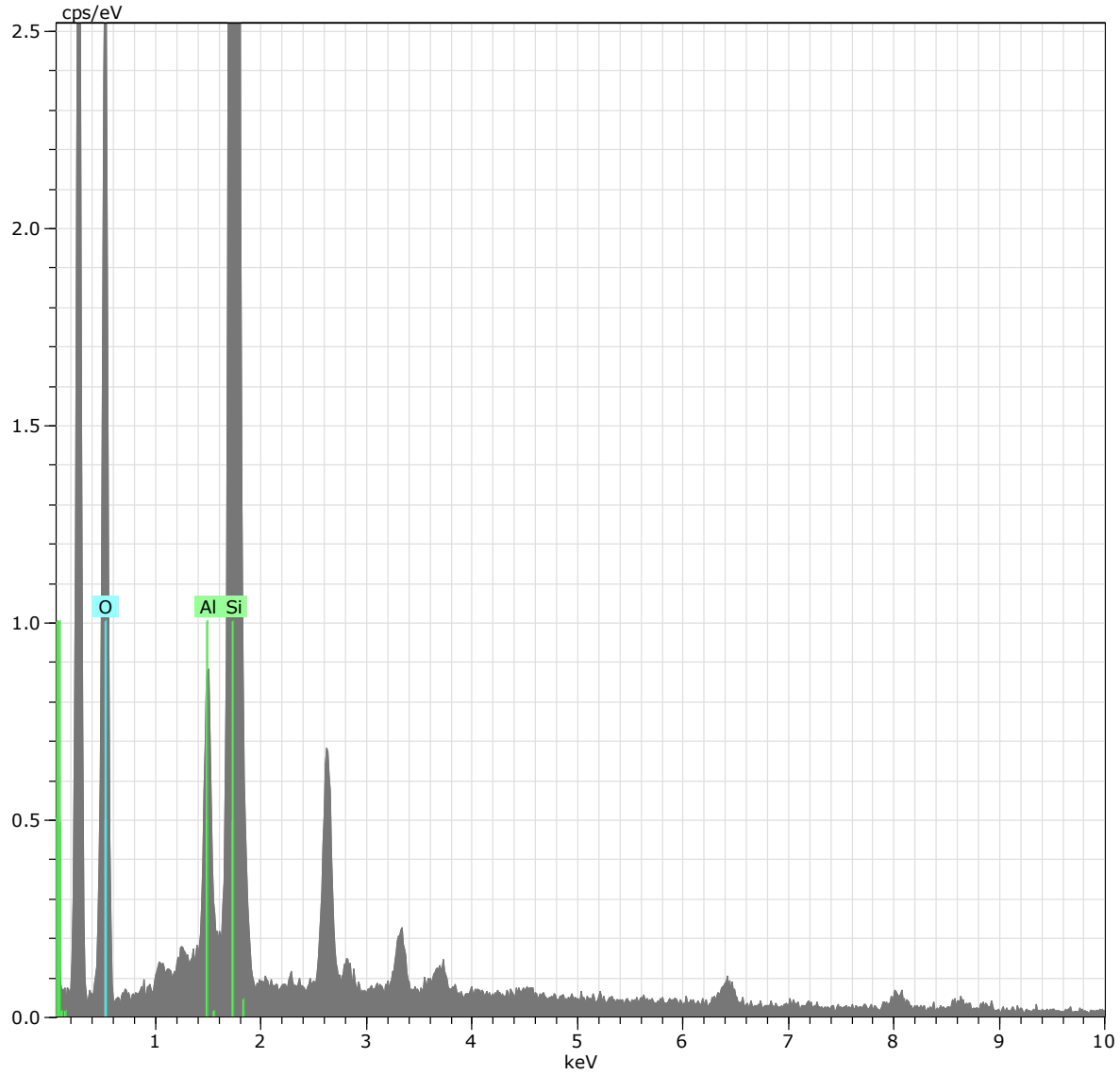

JPH-15_ 1 Date:7/8/2016 1:08:28 PM HV:25.0kV Puls th.:2.39kcps

El	AN	Series	unn. C [wt.%]	norm. C [wt.%]	Atom. C [at.%]	Error (1 Sigma) [wt.%]
O	8	K-series	27.02	48.13	61.88	5.08
Si	14	K-series	26.70	47.55	34.82	1.23
Al	13	K-series	2.43	4.32	3.30	0.19
		Total:	56.15	100.00	100.00	

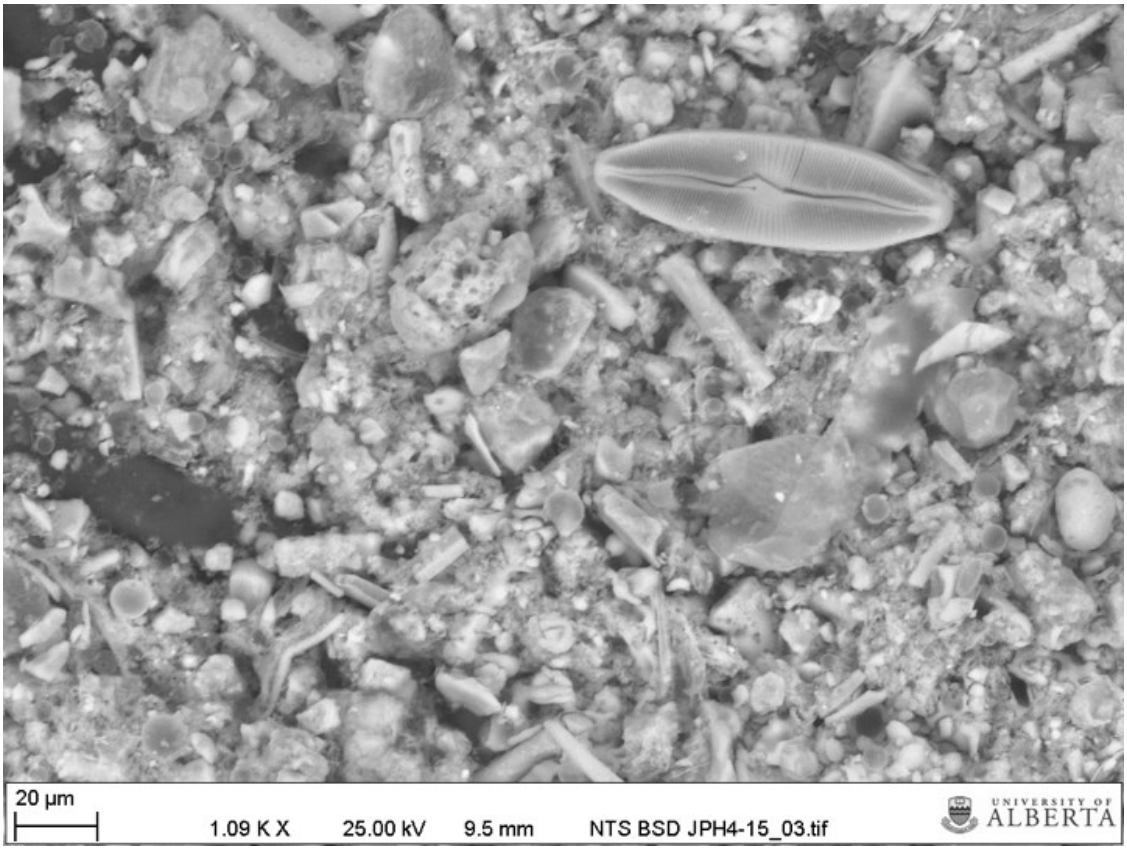
20 µm
1.09 K X
25.00 kV
9.5 mm
NTS BSD JPH4-15_03.tif
UNIVERSITY OF ALBERTA

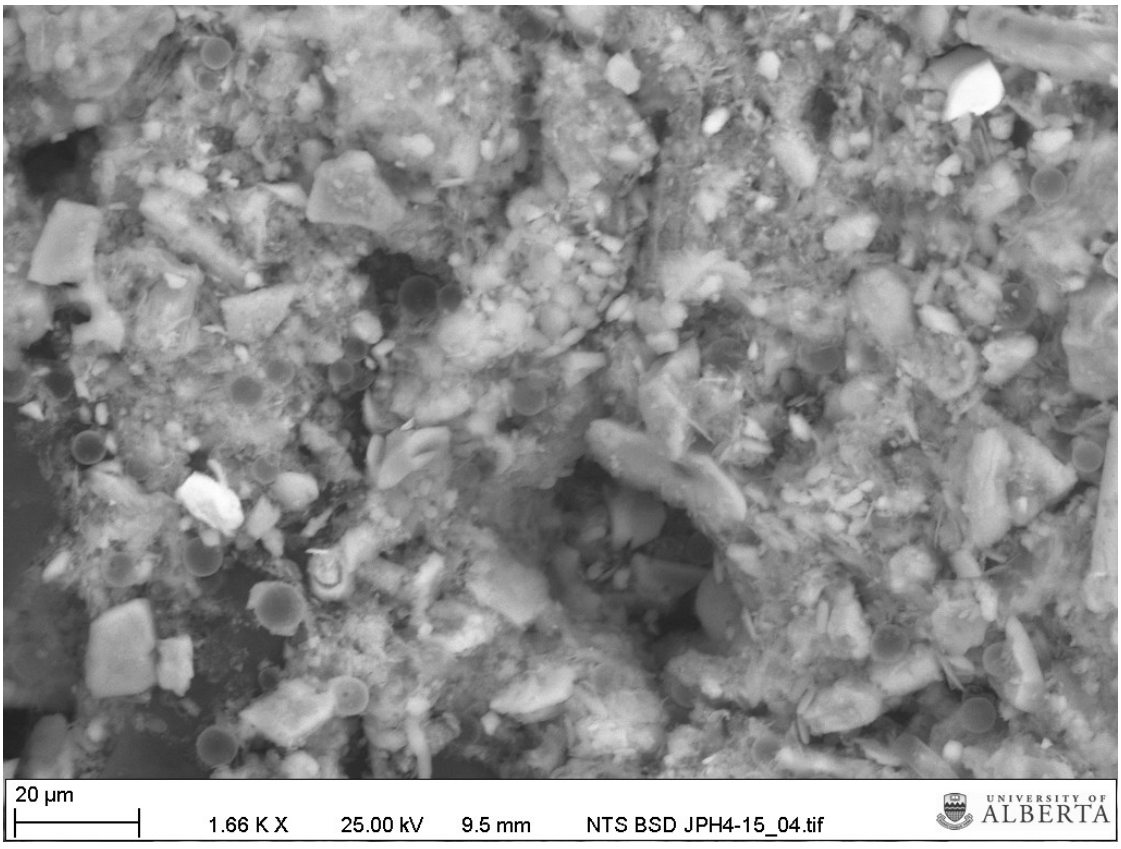
20 µm
1.66 K X
25.00 kV
9.5 mm
NTS BSD JPH4-15_04.tif
UNIVERSITY OF ALBERTA

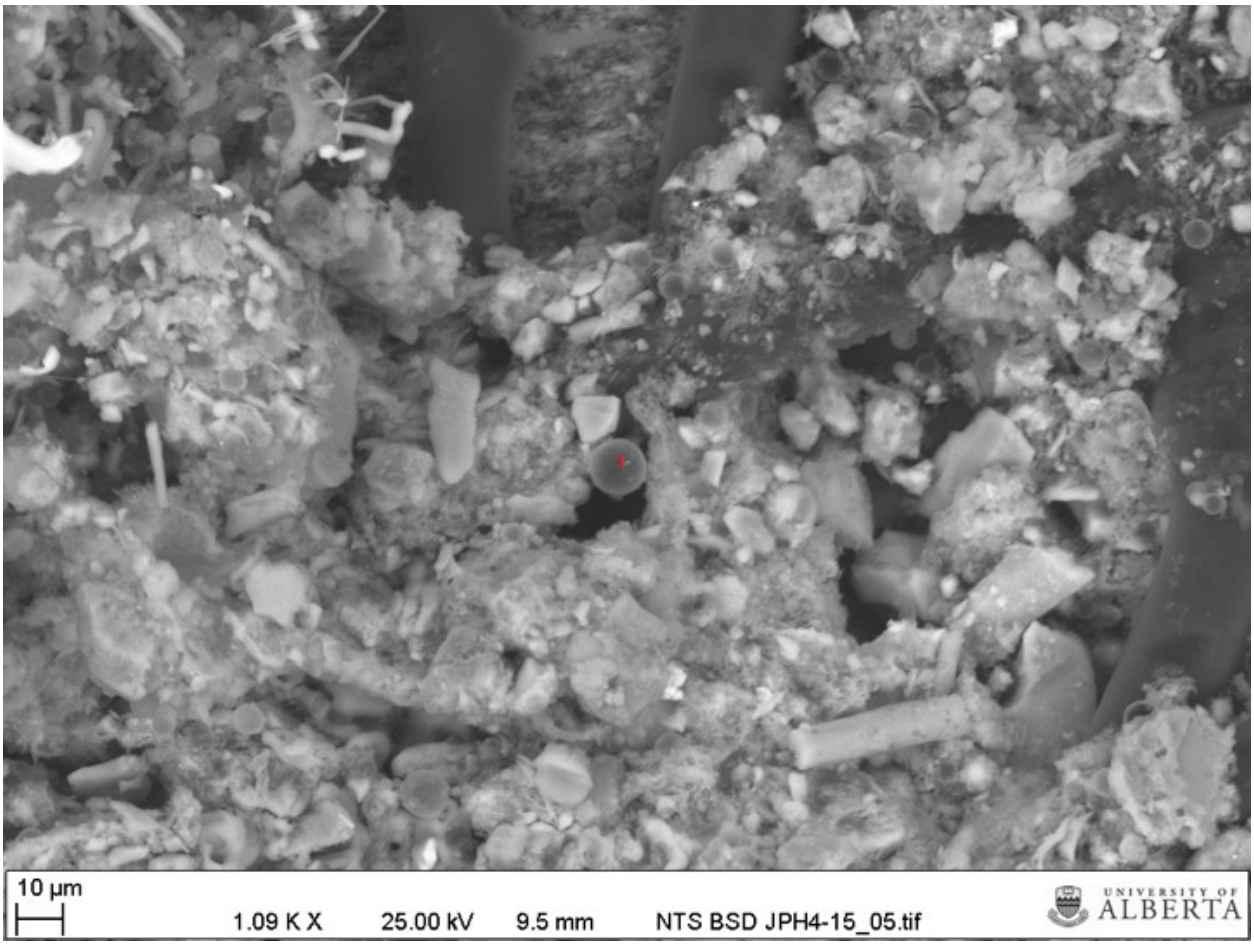
10 µm
1.09 K X
25.00 kV
9.5 mm
NTS BSD JPH4-15_05.tif
UNIVERSITY OF ALBERTA

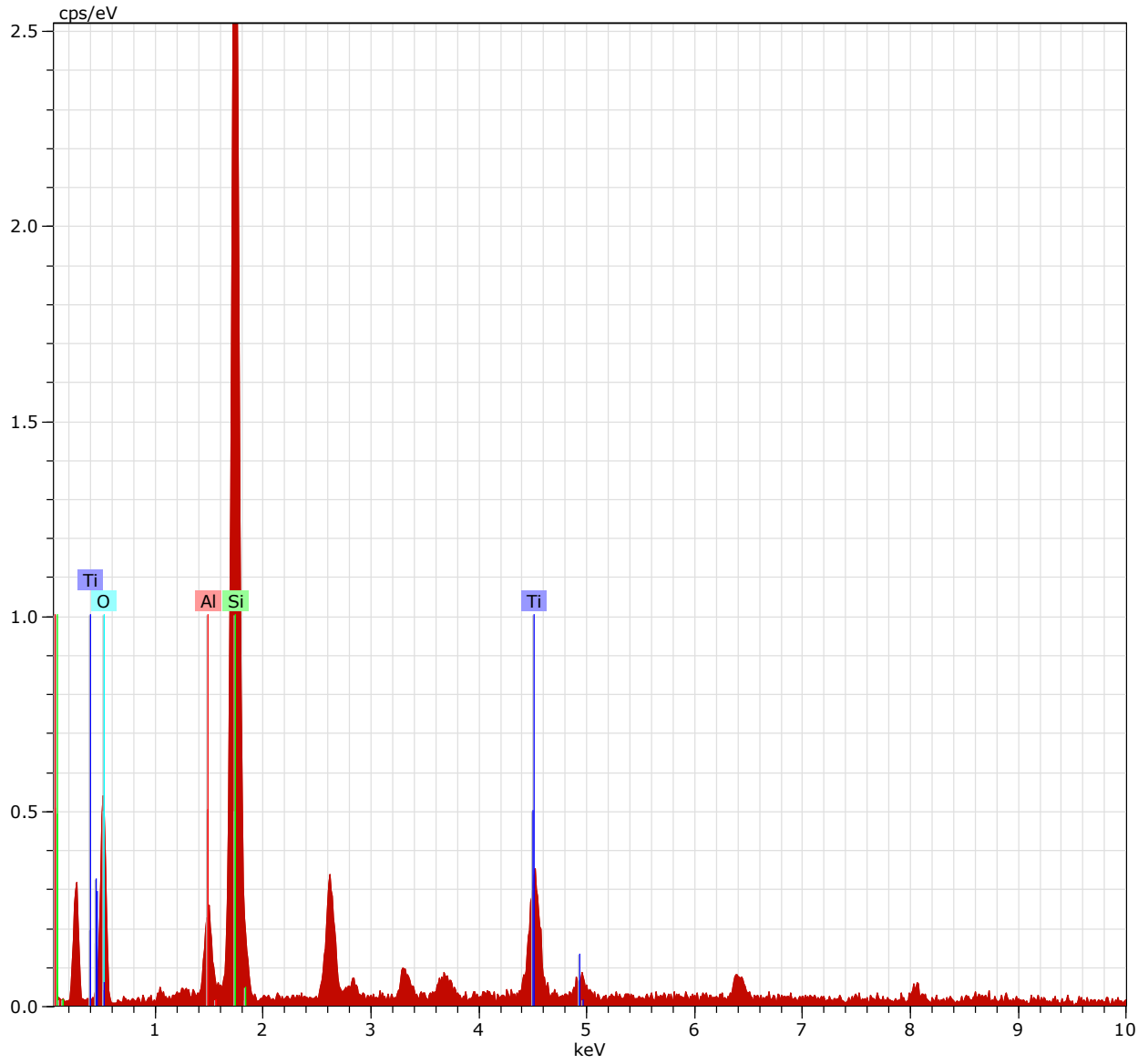

JPH-15_ 3 Date:7/8/2016 1:20:56 PM HV:25.0kV Puls th.:0.85kcps

El	AN	Series	unn. C [wt.%]	norm. C [wt.%]	Atom. C [at.%]	Error (1 Sigma) [wt.%]
Si	14	K-series	21.48	44.16	34.31	1.13
O	8	K-series	20.83	42.84	58.42	7.03
Ti	22	K-series	4.46	9.17	4.18	0.29
Al	13	K-series	1.86	3.83	3.10	0.23
		Total:	48.63	100.00	100.00	

APPENDIX 5: XRD mineral analysis on 2013-2014 moss samples performed by Steve Hillier of the University of Edinburgh.

Sample set

1235689-Blank--F
1235690-A2-NO-11-Test-F
1235691-A2-NO-12-Test-F
1235692-6B-A1A Filter-F
1235693-3C-A1A Filter-F
1235694-19A-A1A Filter-F
1235695-2B-A1A Filter-F
1235696-MCK SF-1B-A1A Filter-F
1235697-JPH4-3-A1A Filter-F
1235698-MIL SF-1C-A1A Filter-F
1235699-ANZ-2-A1A Filter-F
1235700-McM-2--F
1235701-UTK-3--F
1235702-SEB-2--F

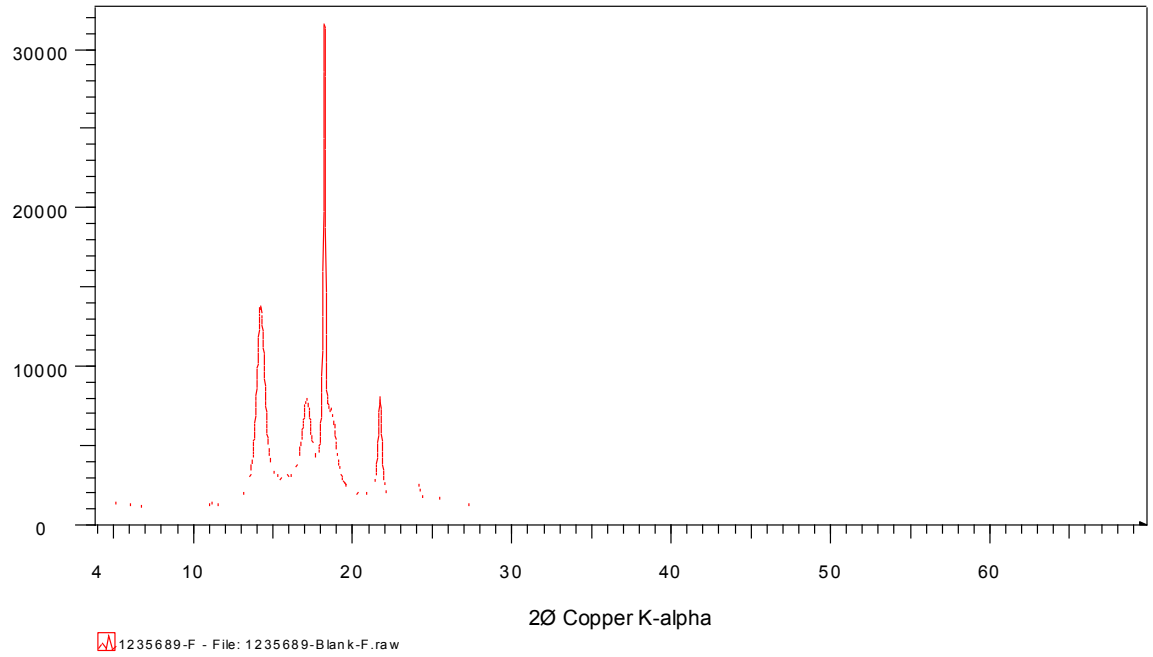

Blank filter looks to be exactly same type as used in previous set. Again I have included the pattern of the black filter in all the figures to help show the peaks that are not due to the filter material itself.

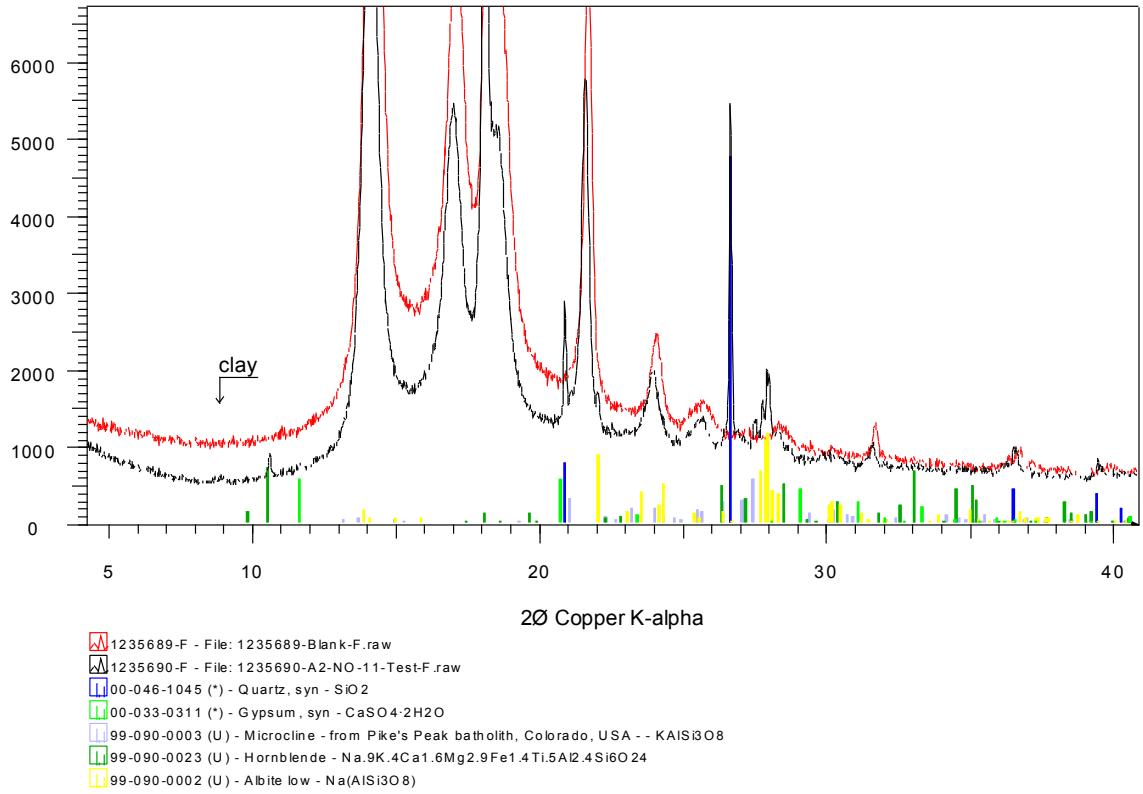

Obvious quartz, along with what look to be feldspars, probably a mixture of plagioclase and K-feldspars, but mainly plagioclase. A small peak at low angle also suggests some amphibole, shown here as hornblende (but amphibole is better ID as can't identify the specific type). A tiny peak also suggests a trace a gypsum, but not sure about this. And a peak near 8.85 2theat indicates a trace of mica/illite labelled clay.

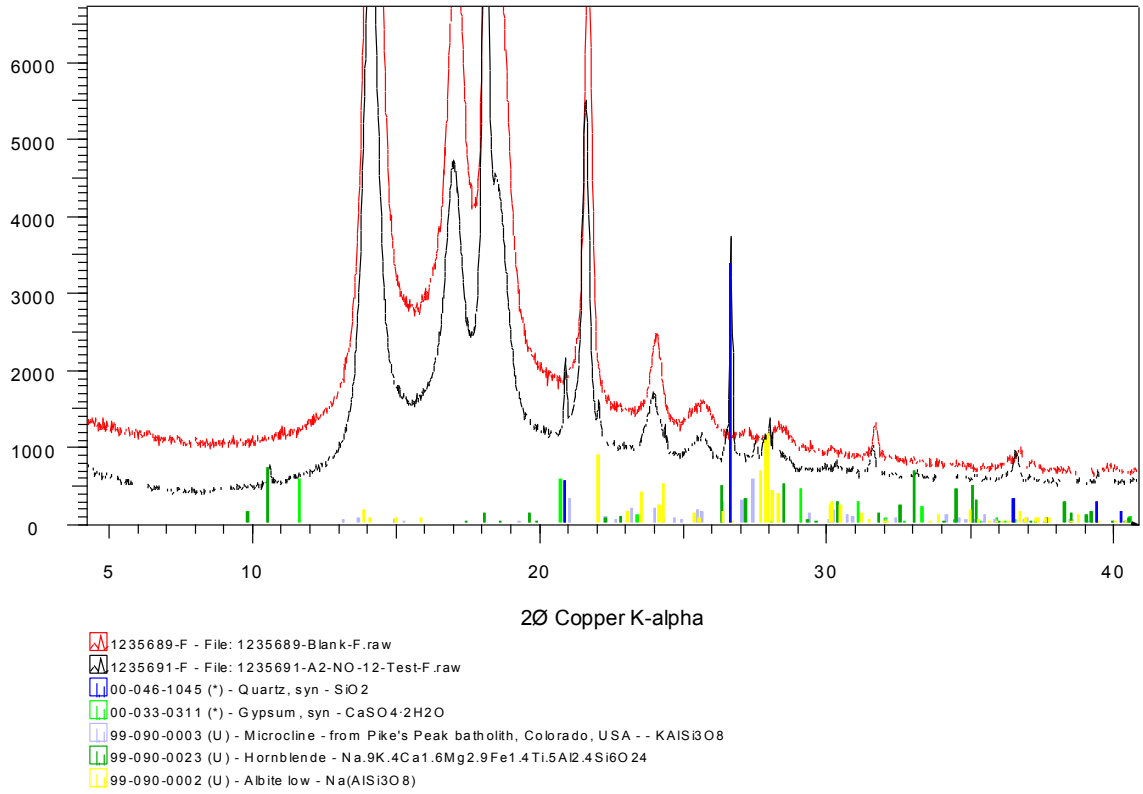

Similar to previous though smaller peaks (less on filter presumably), though mica peak not evident.

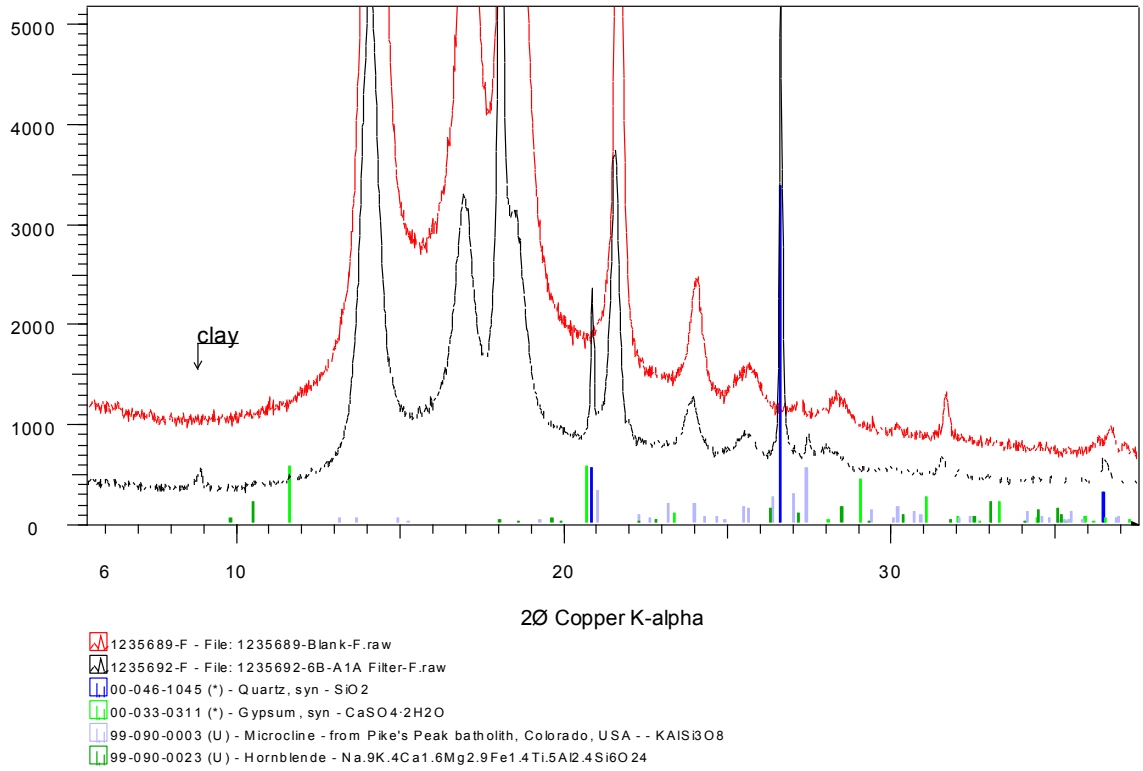

Again quartz but unlike previous one the feldspar looks to be predominantly K-feldspar in this one, mica quite also more obvious. Trace of gypsum again?

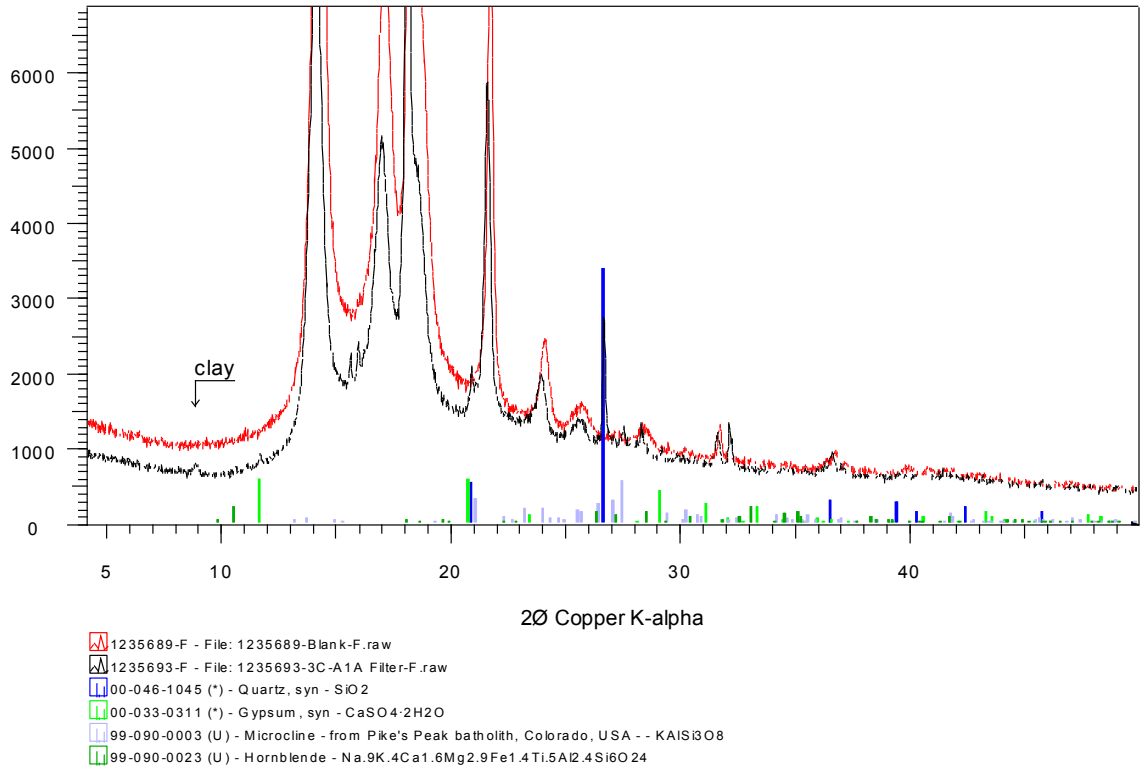

This one mica/ilite, traces amphibole, gypsum? quartz and k-feldspar, but in addition has some peaks that I'm not sure about. You can see two of them inter first filter 'peak valley' region between about 15-16 2theta. One possibility is a hydrated Fe-sulphate but this is not a definite, another that would explain one of the peaks and another at higher angle is dawsonite, a hydrated sodium carbonate, again this is just me putting down some possible phases, no definite ID. The two peaks in the 'valley' region look like they occur together or individually in some other samples so I'll come back to this.

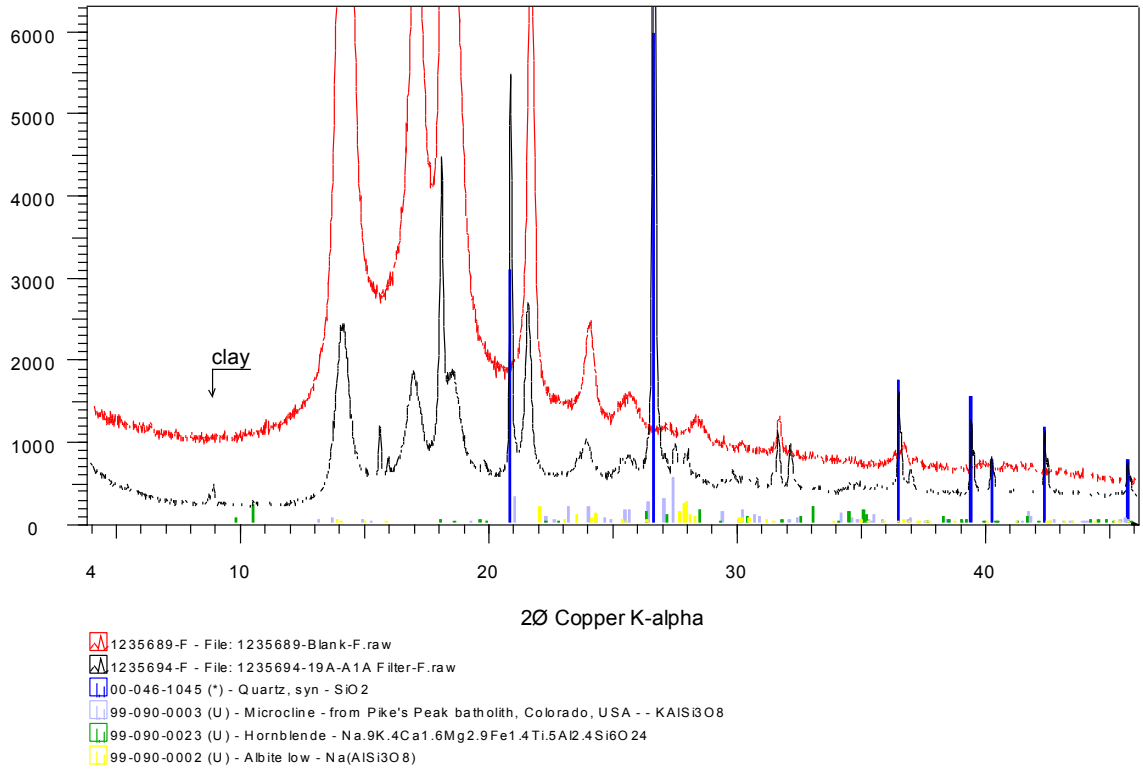

Prominent quartz on this one, along with some feldspar, mica illite and trace amphibole. Reading the unidentified 'valley' peaks, one is more prominent in this sample than the other which may suggest they come from different minerals, i.e. we are looking for two minerals not just one. In this sample they are more consistent with dawsonite than siderotil, but still neither is a definite ID.

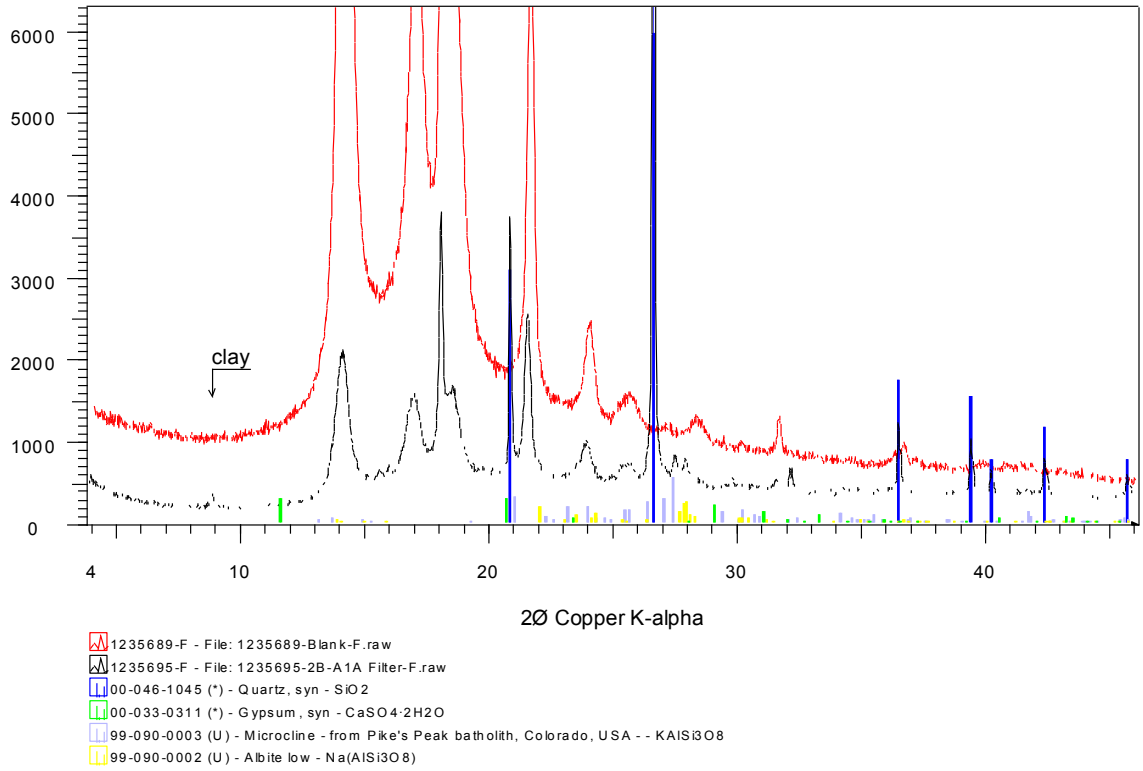

Trace of gypsum is back, two valley peaks are present but lower intensity in this one, quartz, feldspars, mica/illite are all present.

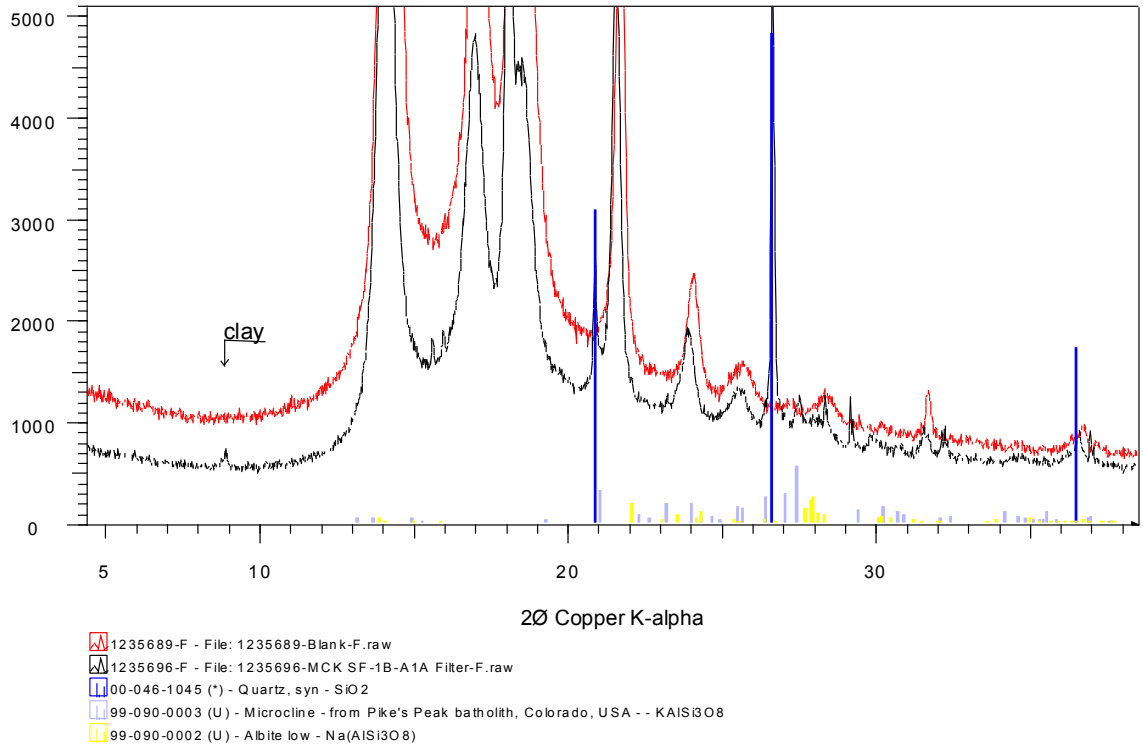

Similar to above sample.

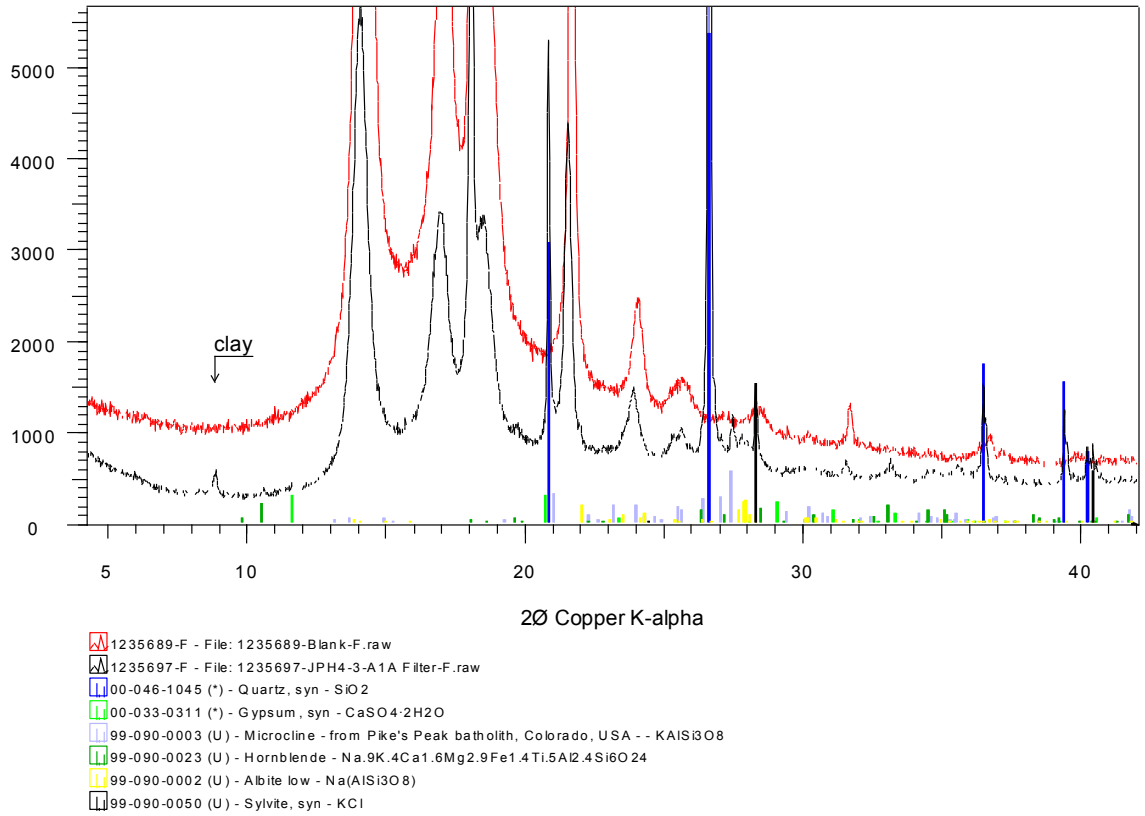

Trace gypsum and trace amphibole are back, along with prominent quartz, minor feldspars, illite/mica, and in this sample looks like there is possibly some sylvite present (KCl).

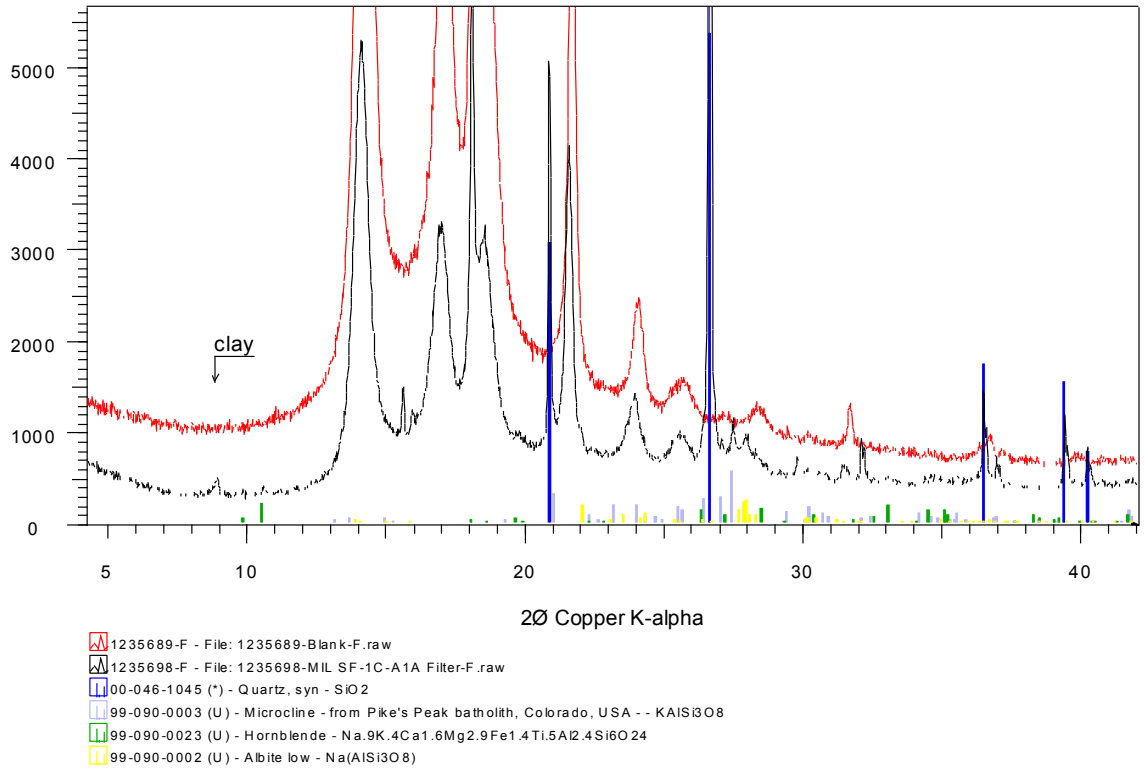

'valley' peaks are back, one more prominent than the other. Sample contains quartz, feldspars, trace amphibole and some mica/ilite.

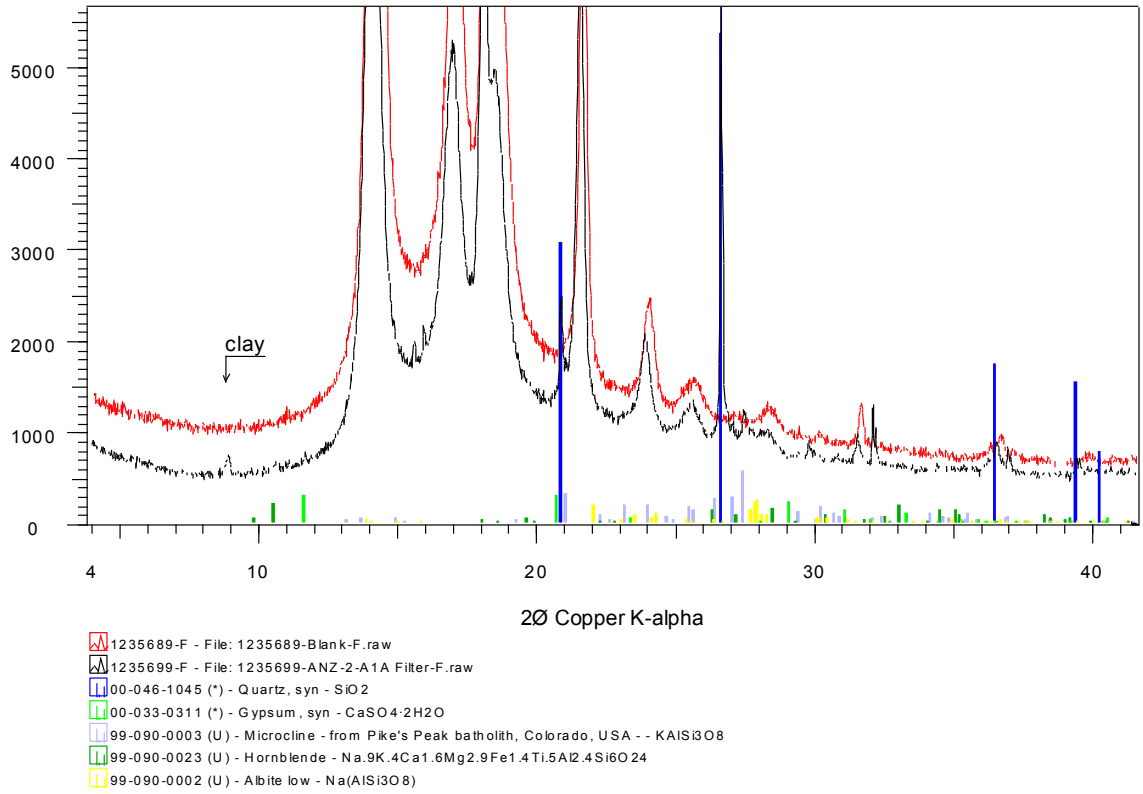

Quartz, feldspars, trace amphibole and illite/mica and the two ‘valley’ peaks.

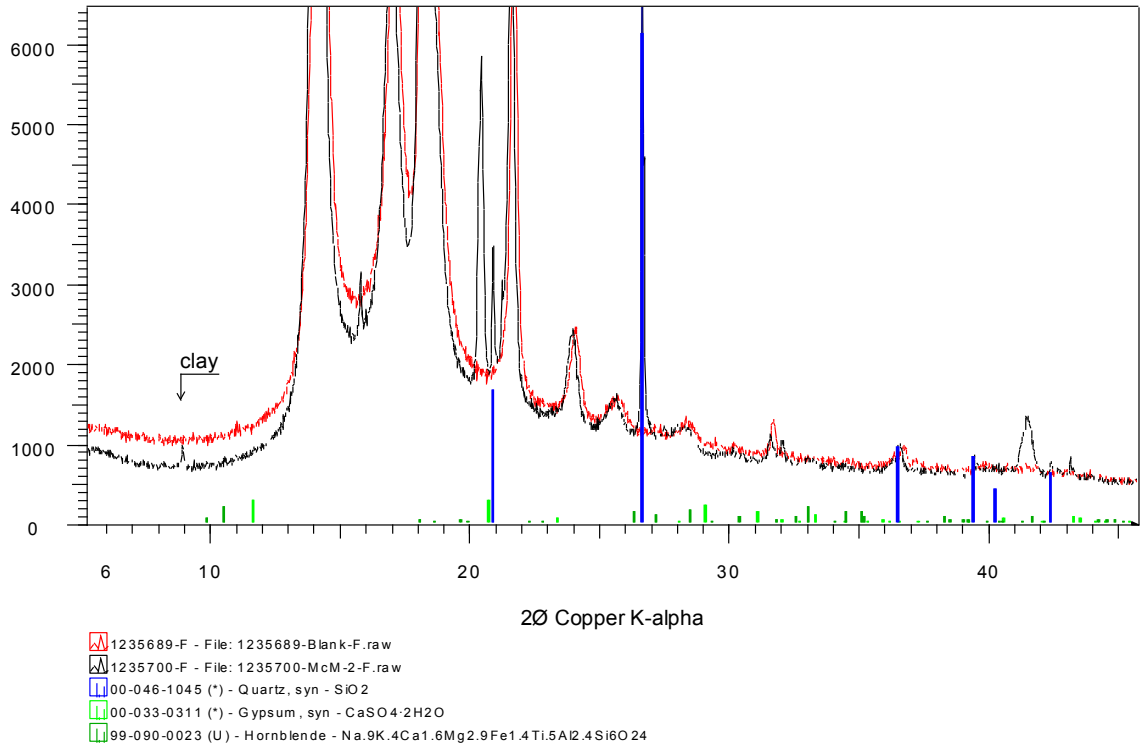

Trace mica/illite, some quartz, possible trace gypsum, one of the 'valley' peaks. Additionally this sample has two relatively broad peaks that I can't identify, they look like they ought to be associated with the polymer filter, but have not be observed in any of the previous filters?!

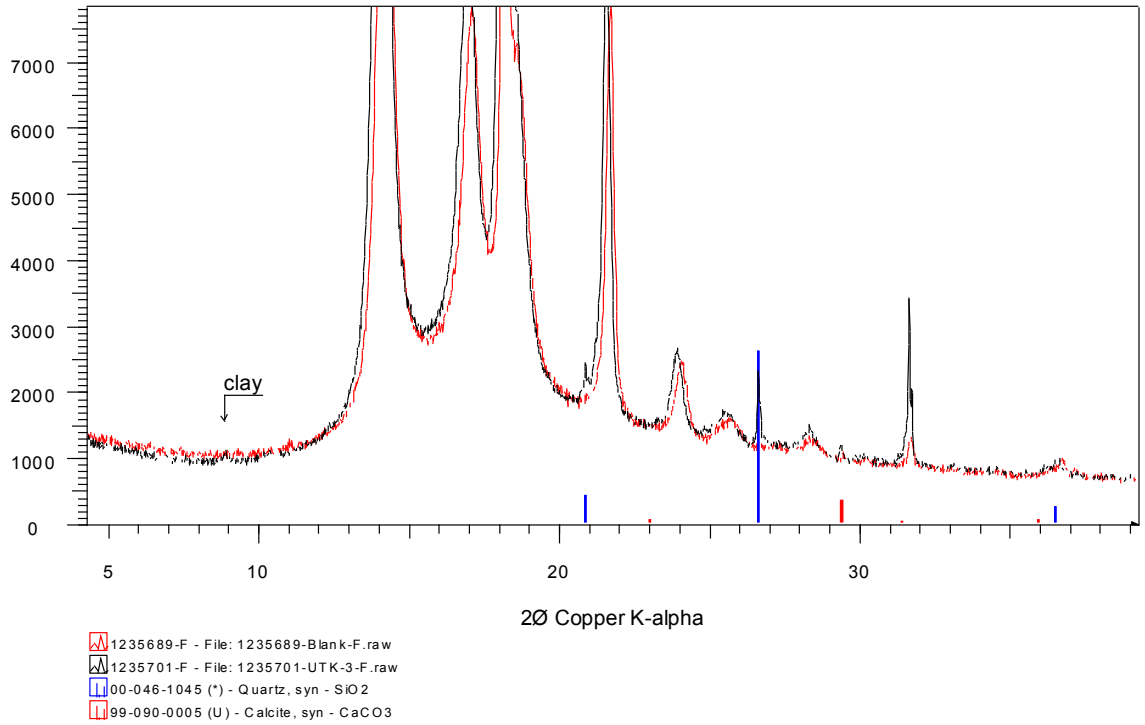

Trace quartz, trace mica/illite, trace calcite? Also an enhanced peak near 32 2theta suggests this filter may have halite (NaCl) though the corresponding higher angle peaks for more robust ID are missing.

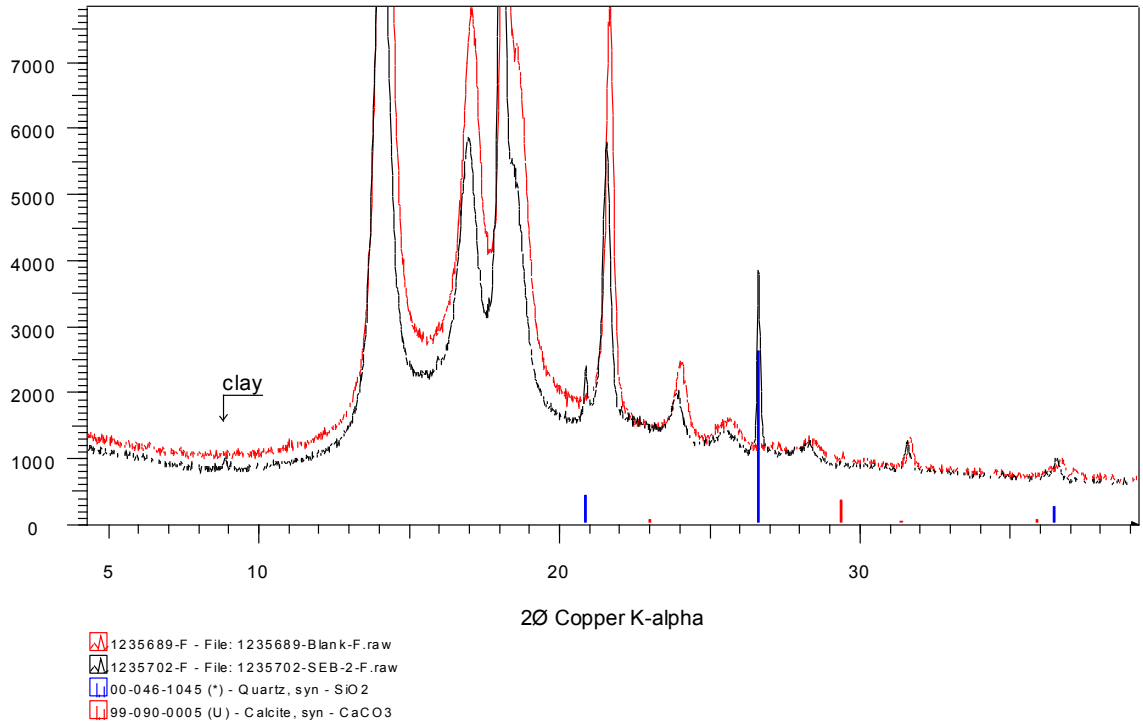

Trace quartz, trace mica/illite trace of one of the ‘valley’ peaks.

Final thoughts on the two 'valley' peaks.

Taken a closer look at this in two samples where the phase or phases responsible for these peaks are best developed, and together with some higher angle peaks that are also not accounted for.

I don't think my two previous suggestions when commenting on above traces i.e. dawsonite and or siderotil are that likely.

The two peaks are quite closely matched by plumbogummite (this is a group so there are related similar minerals).

However, a match that also accounts for two other high angle peaks is Erythrosiderite, a potassium iron chloride hydrate. The match is shown below, think this would require further confirmation and might it make any sense etc., but it is my best guess at what the peaks indicate.

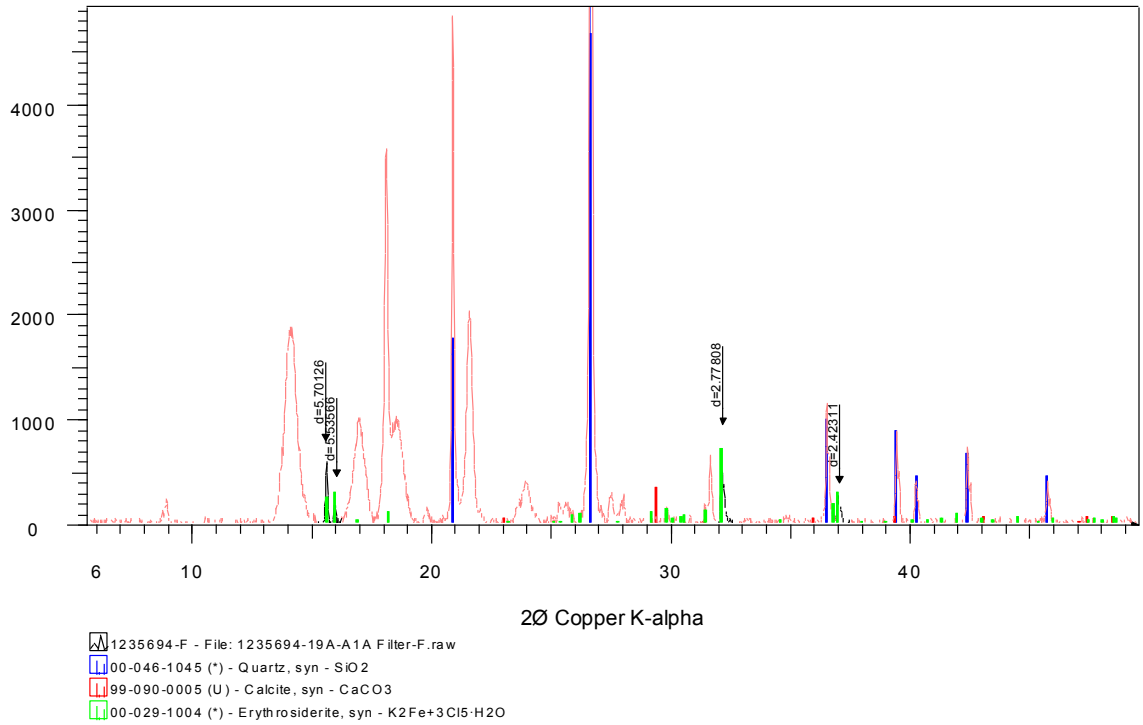

Above shows a background subtracted pattern of one of the traces where the "valley" peaks are prominent and the 4 peaks that are all well accounted for by this phase.

Steve Hillier Aug 2016

APPENDIX 6: UTK-W2 SEM images and EDX spectrum. AIA samples were examined for morphology and mineralogy. The number on the SEM image corresponds with the spectrum number.

UTK-W2 11 (2003)

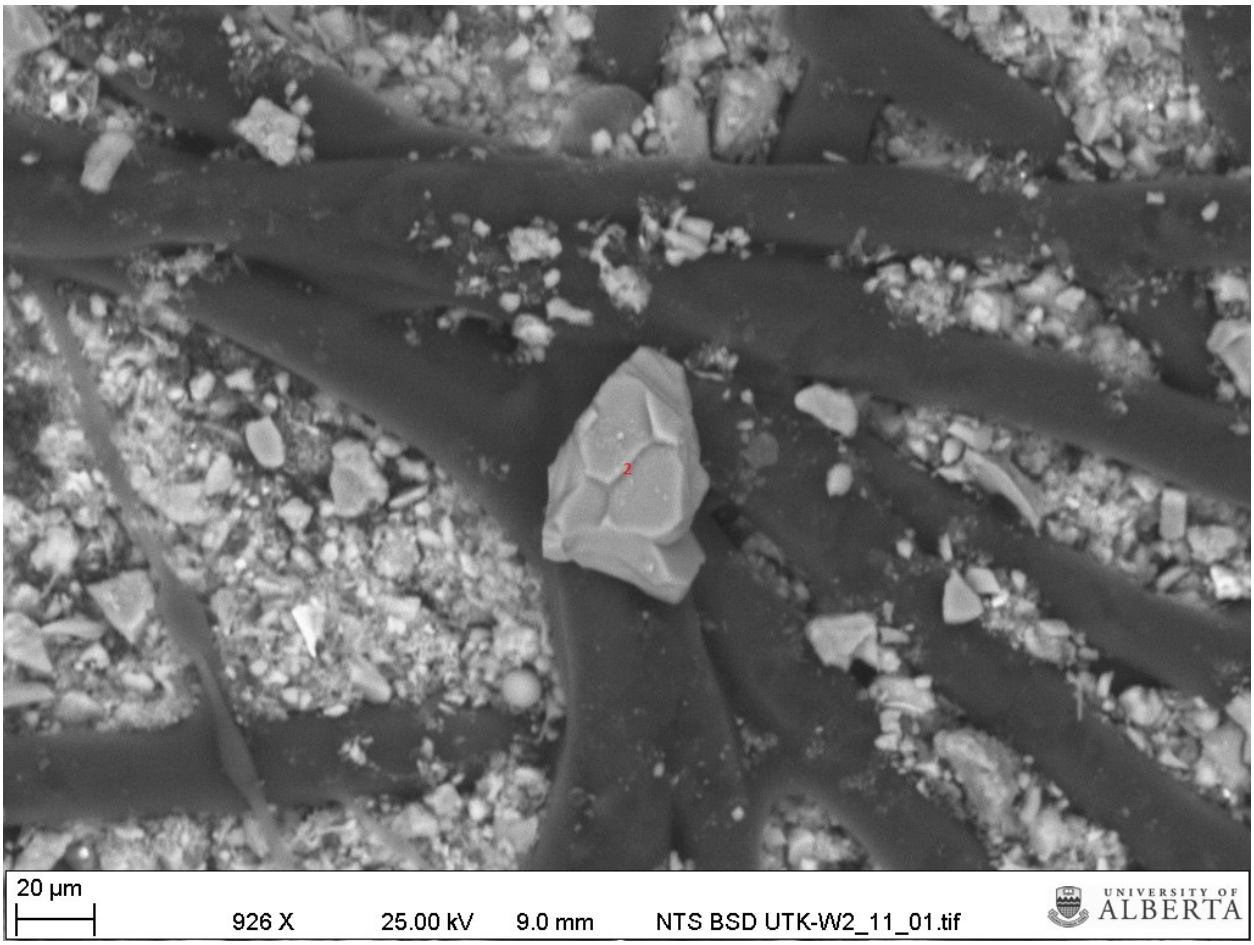
2
20 µm
926 X
25.00 kV
9.0 mm
NTS BSD UTK-W2_11_01.tif
UNIVERSITY OF ALBERTA

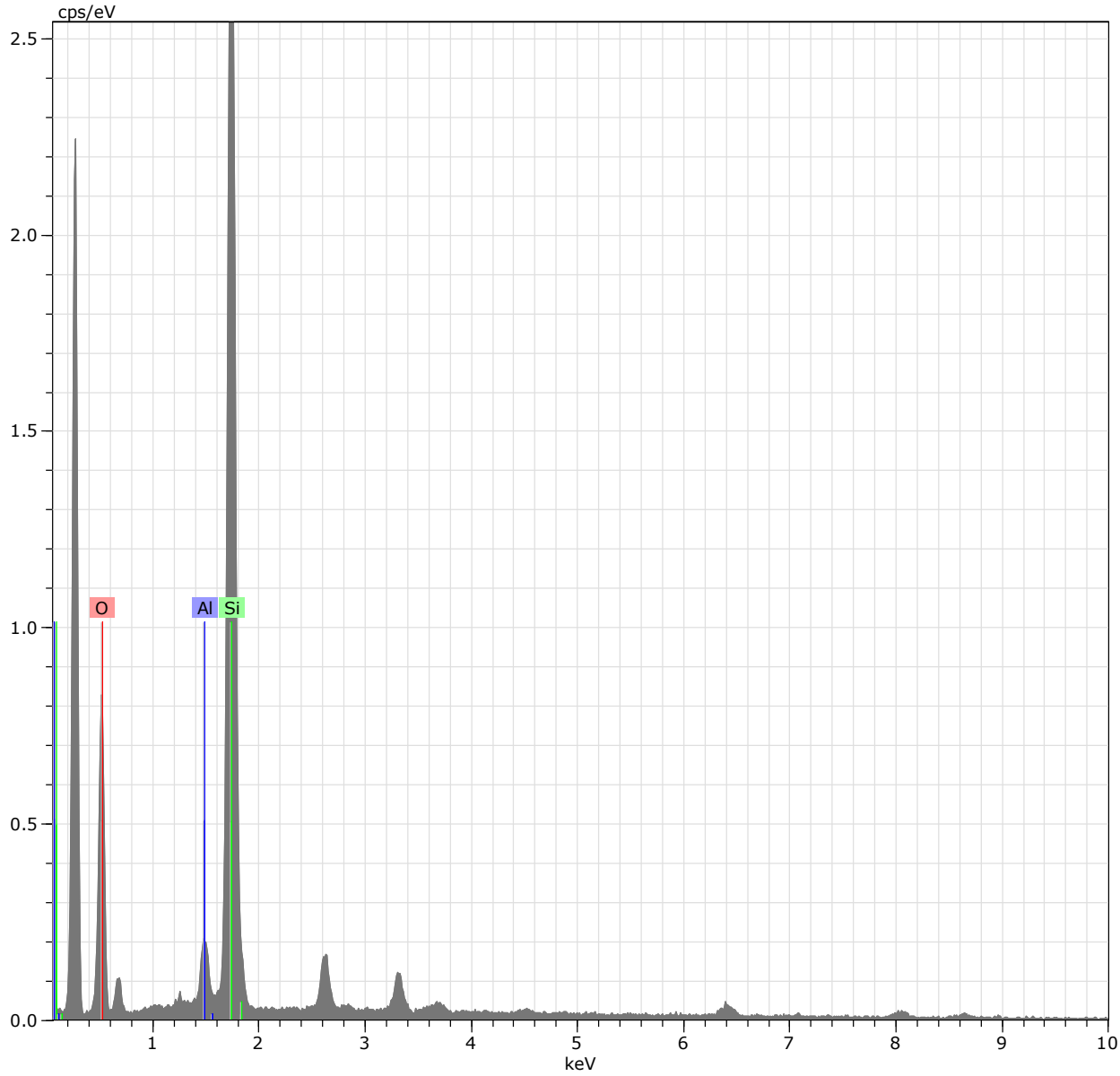

UTK-W2_11_ 2 Date:8/15/2016 10:01:57 AM HV:25.0kV Puls th.:0.99kcps

El	AN	Series	unn. C [wt.%]	norm. C [wt.%]	Atom. C [at.%]	Error (1 Sigma) [wt.%]
O	8	K-series	25.84	49.87	63.56	6.38
Si	14	K-series	25.39	48.99	35.57	1.24
Al	13	K-series	0.59	1.14	0.86	0.11
		Total:	51.83	100.00	100.00	

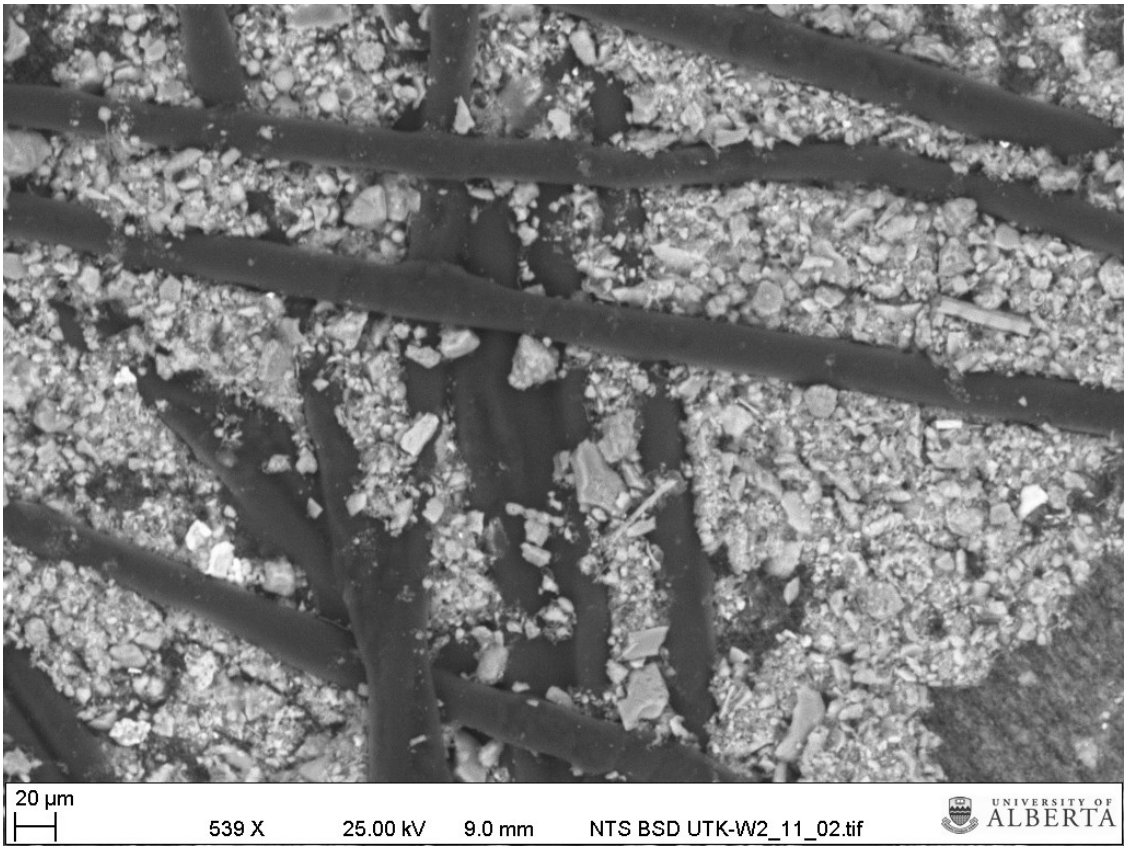
20 µm
539 X
25.00 kV
9.0 mm
NTS BSD UTK-W2_11_02.tif
UNIVERSITY OF ALBERTA

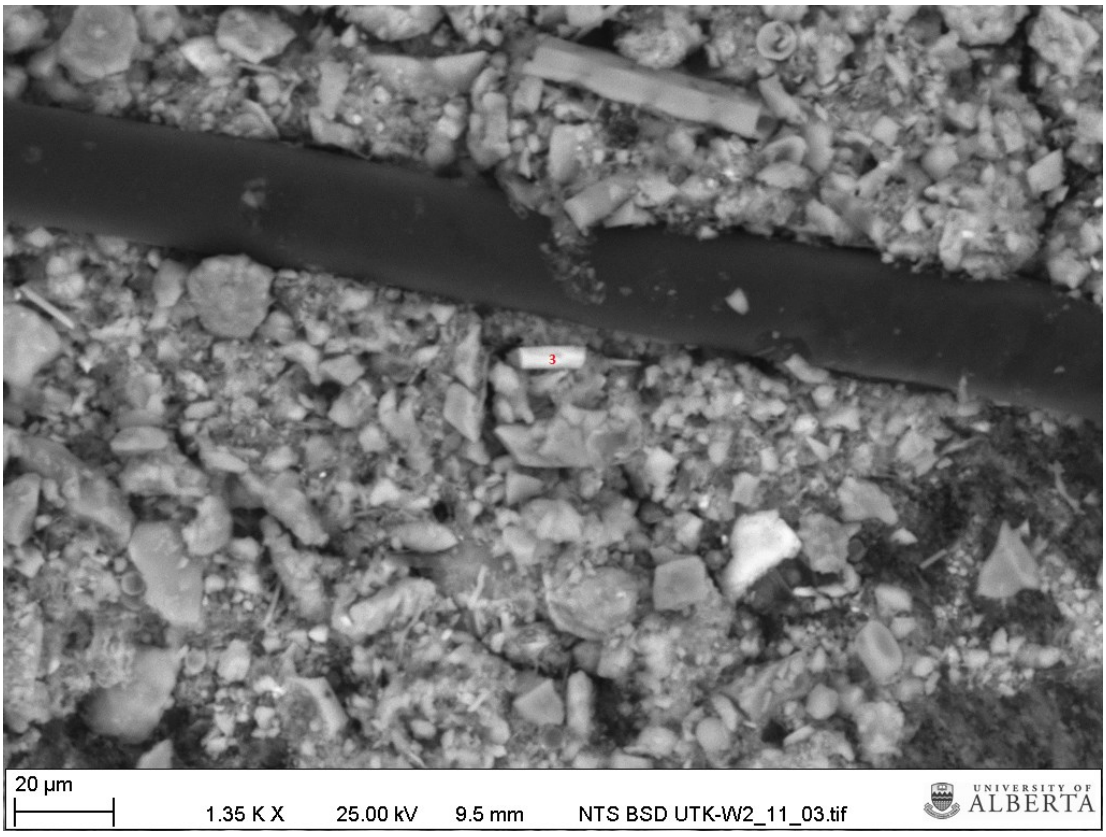
3
20 µm
1.35 K X
25.00 kV
9.5 mm
NTS BSD UTK-W2_11_03.tif
UNIVERSITY OF ALBERTA

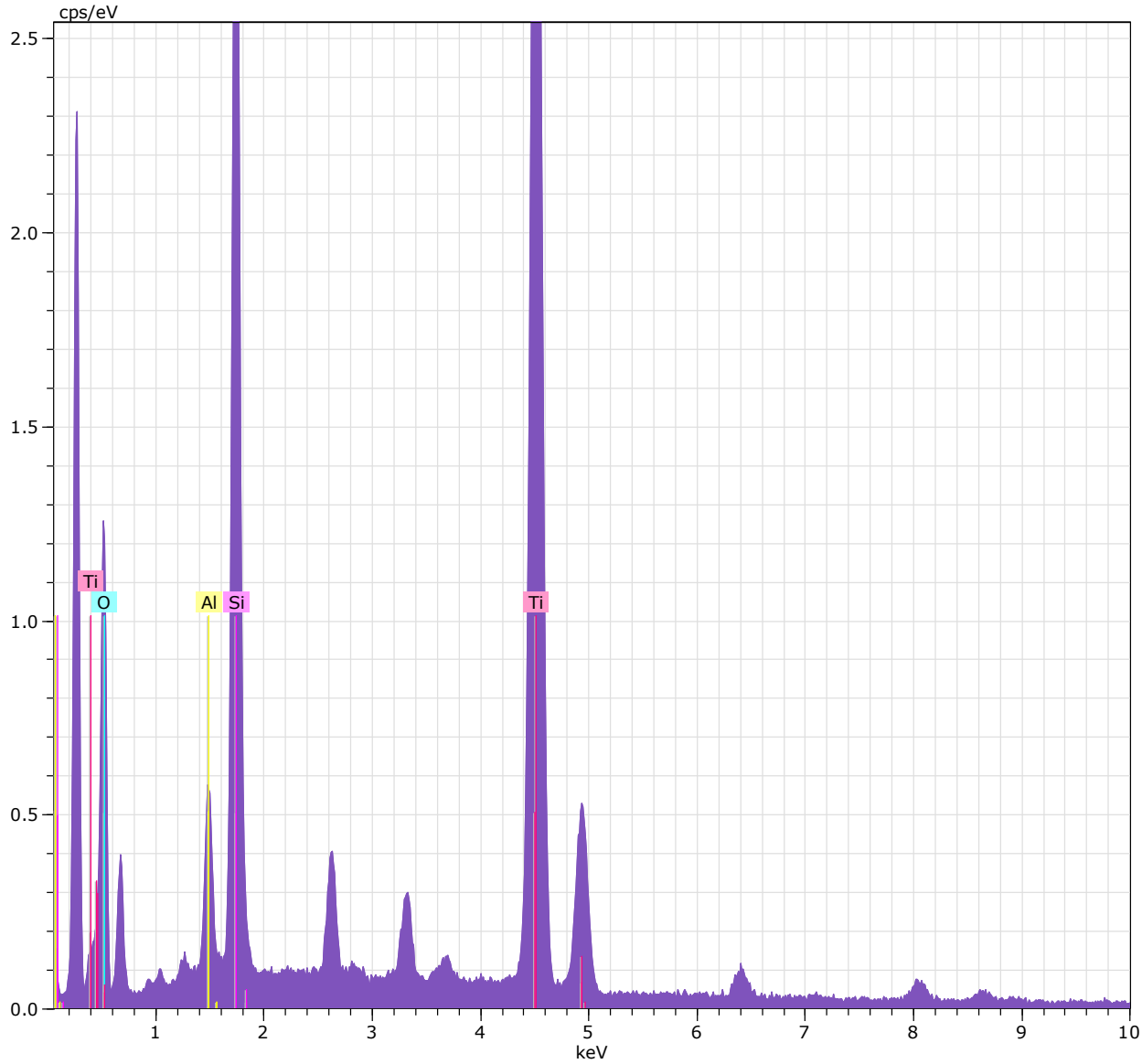

UTK-W2_11_ 3 Date:8/15/2016 10:09:56 AM HV:25.0kV Puls th.:2.07kcps

El	AN	Series	unn. C [wt.%]	norm. C [wt.%]	Atom. C [at.%]	Error (1 Sigma) [wt.%]
Ti	22	K-series	44.63	50.88	26.99	1.63
O	8	K-series	36.63	41.75	66.29	15.64
Si	14	K-series	5.25	5.99	5.42	0.42
Al	13	K-series	1.22	1.39	1.30	0.21
		Total:	87.73	100.00	100.00	

UTK-W2 33 (1973)

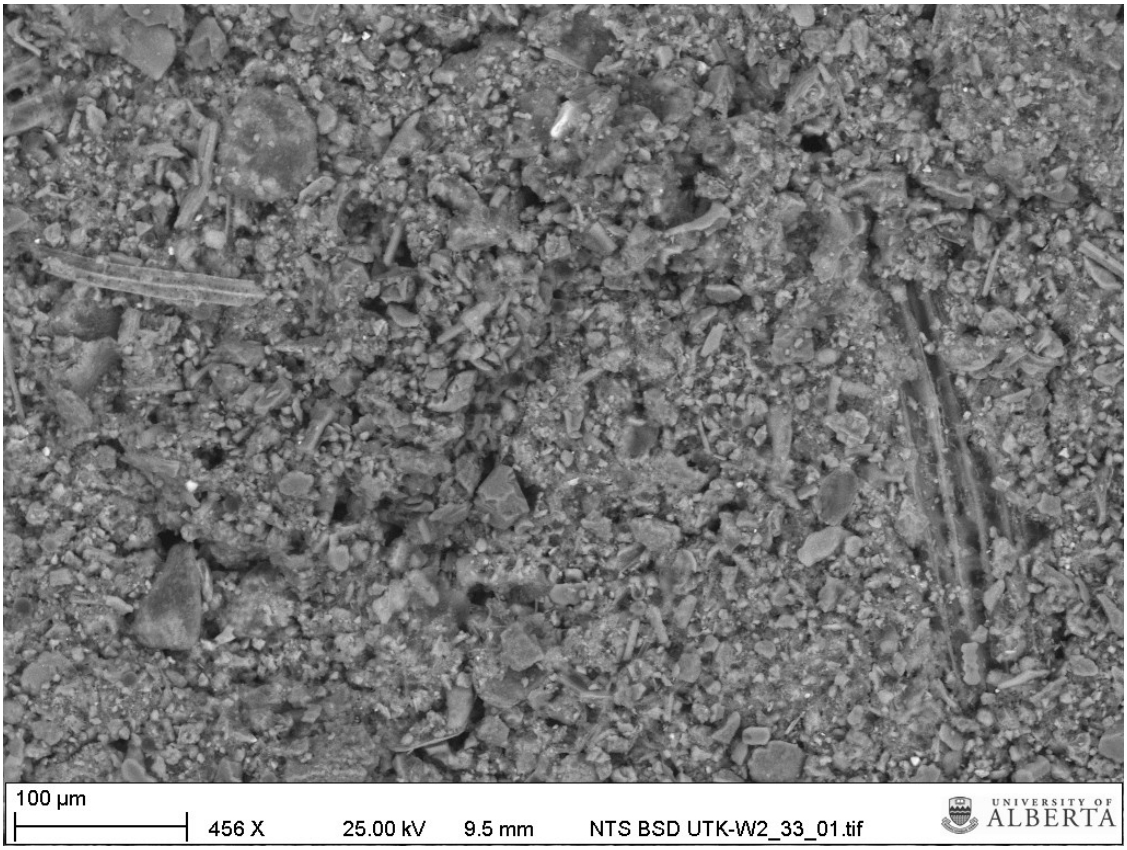
100 µm
456 X
25.00 kV
9.5 mm
NTS BSD UTK-W2_33_01.tif
UNIVERSITY OF ALBERTA

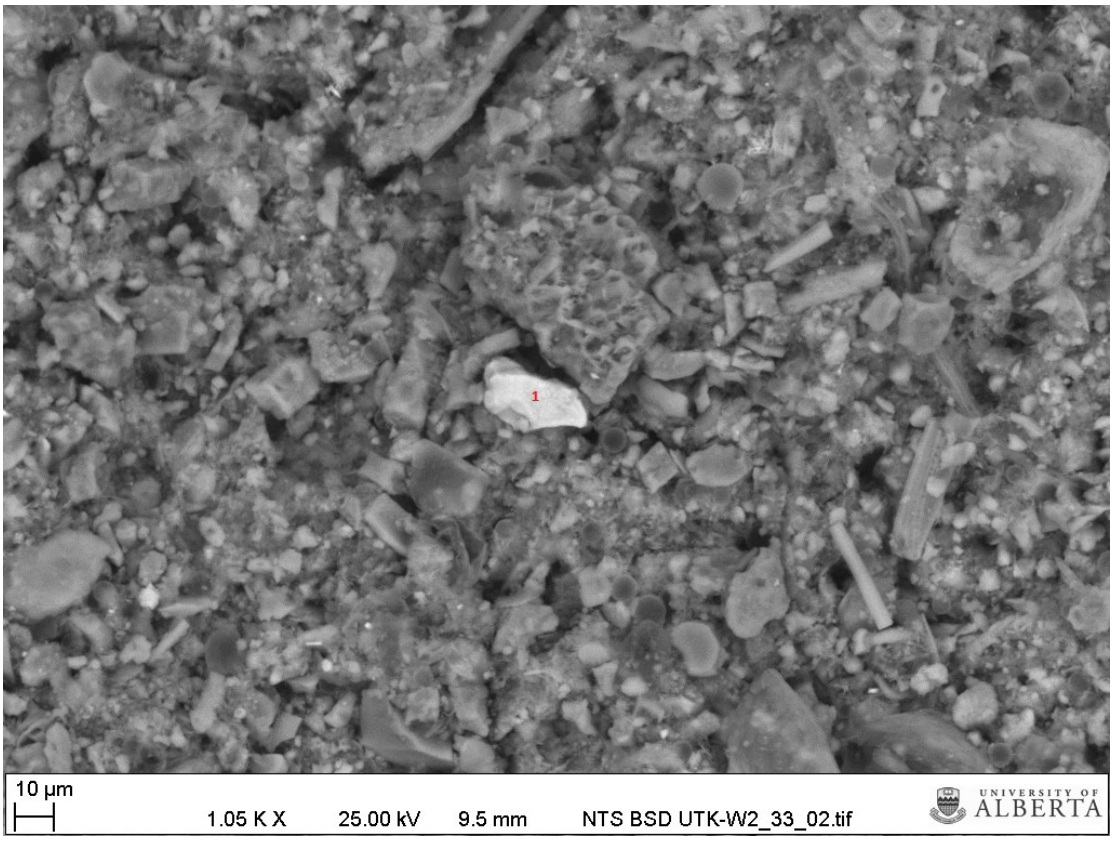
1
10 µm
1.05 K X
25.00 kV
9.5 mm
NTS BSD UTK-W2_33_02.tif
UNIVERSITY OF ALBERTA

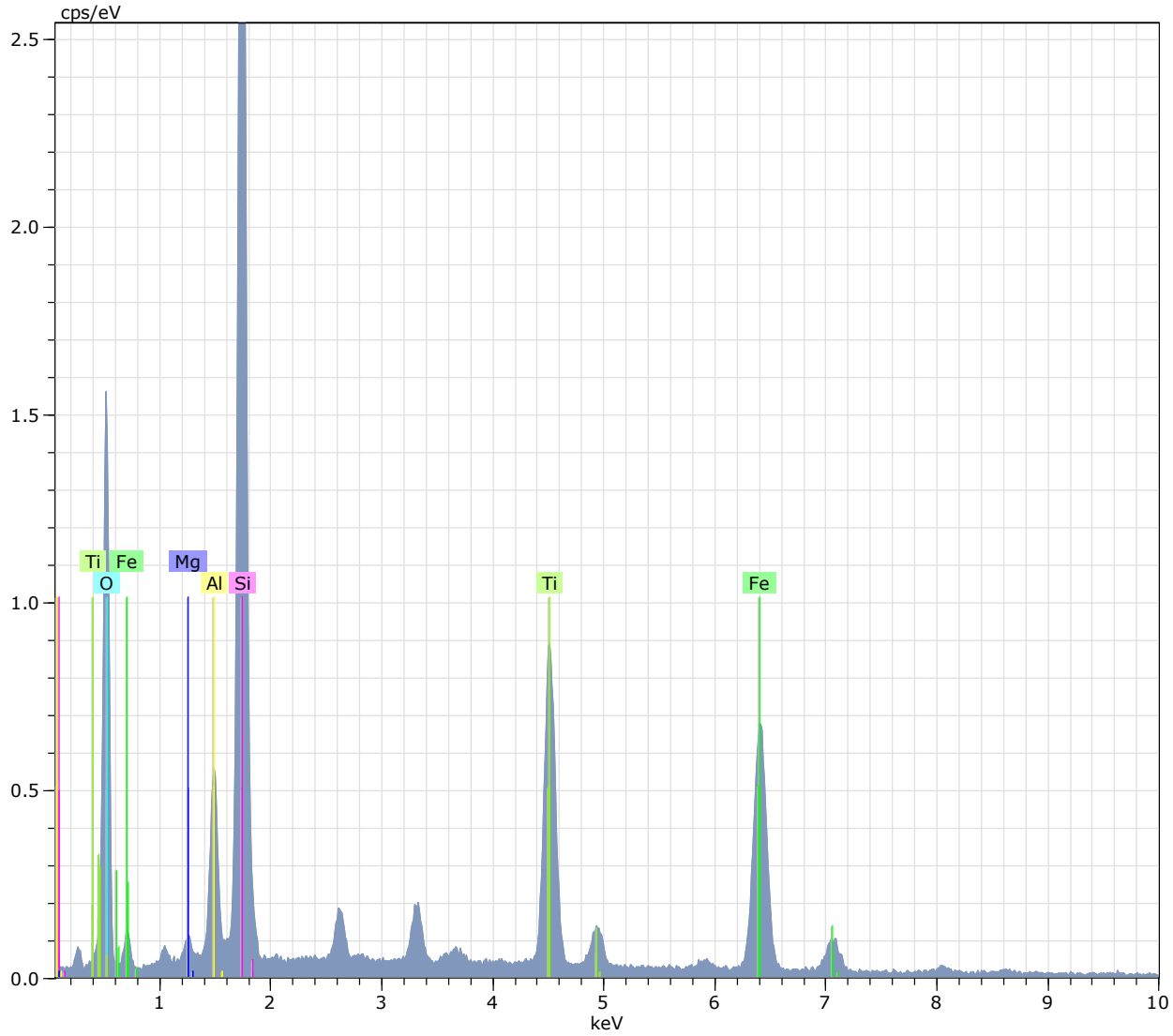

UTK-W2_33_ 1 Date:8/15/2016 10:23:07 AM HV:25.0kV Puls th.:1.42kcps

El	AN	Series	unn. C [wt.%]	norm. C [wt.%]	Atom. C [at.%]	Error (1 Sigma) [wt.%]
O	8	K-series	37.85	42.67	67.66	6.56
Fe	26	K-series	22.61	25.49	11.58	0.67
Ti	22	K-series	19.36	21.82	11.56	0.60
Si	14	K-series	6.92	7.80	7.05	0.36
Al	13	K-series	1.48	1.67	1.57	0.13
Mg	12	K-series	0.49	0.55	0.57	0.08
		Total:	88.71	100.00	100.00	

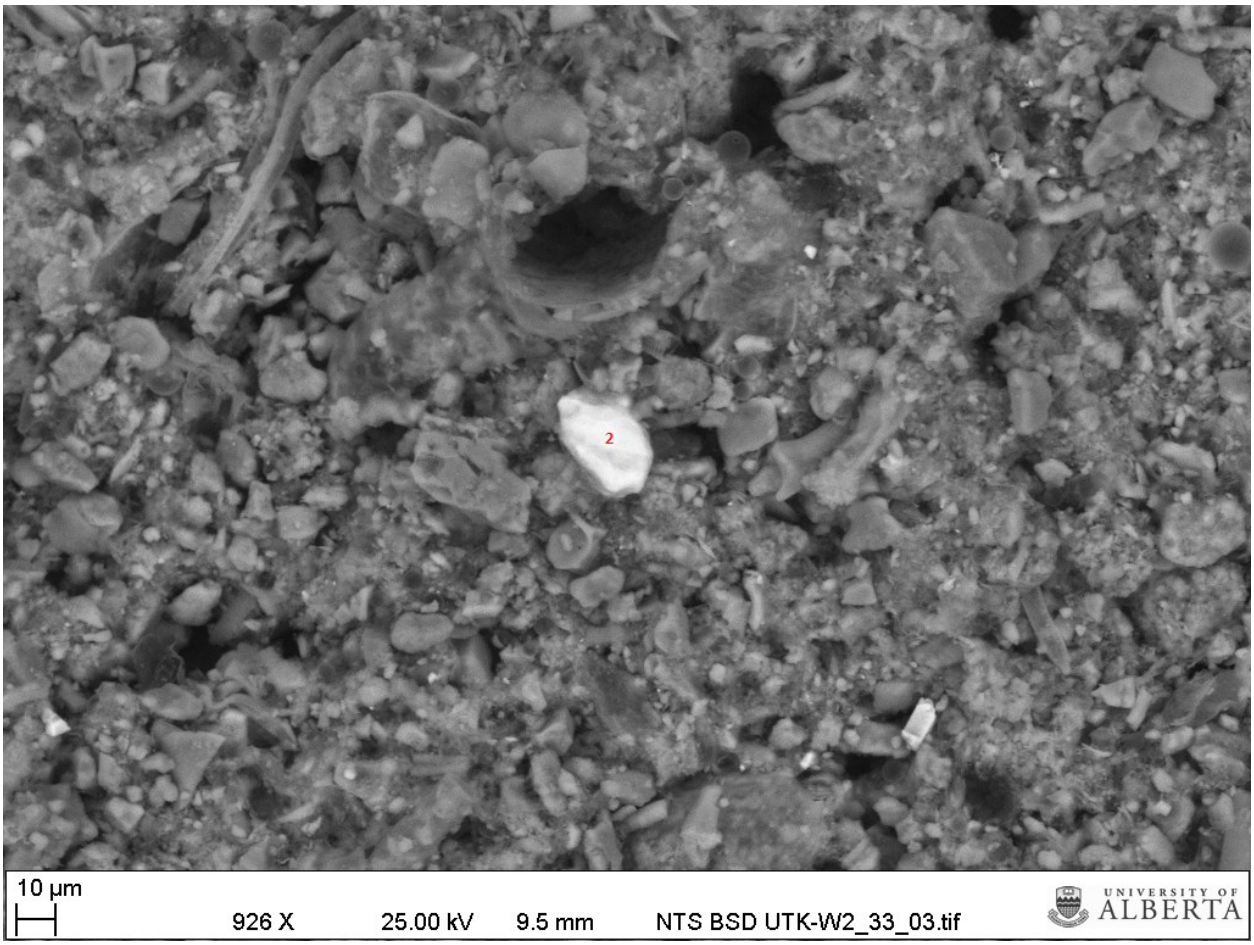
2
10 µm
926 X
25.00 kV
9.5 mm
NTS BSD UTK-W2_33_03.tif
UNIVERSITY OF ALBERTA

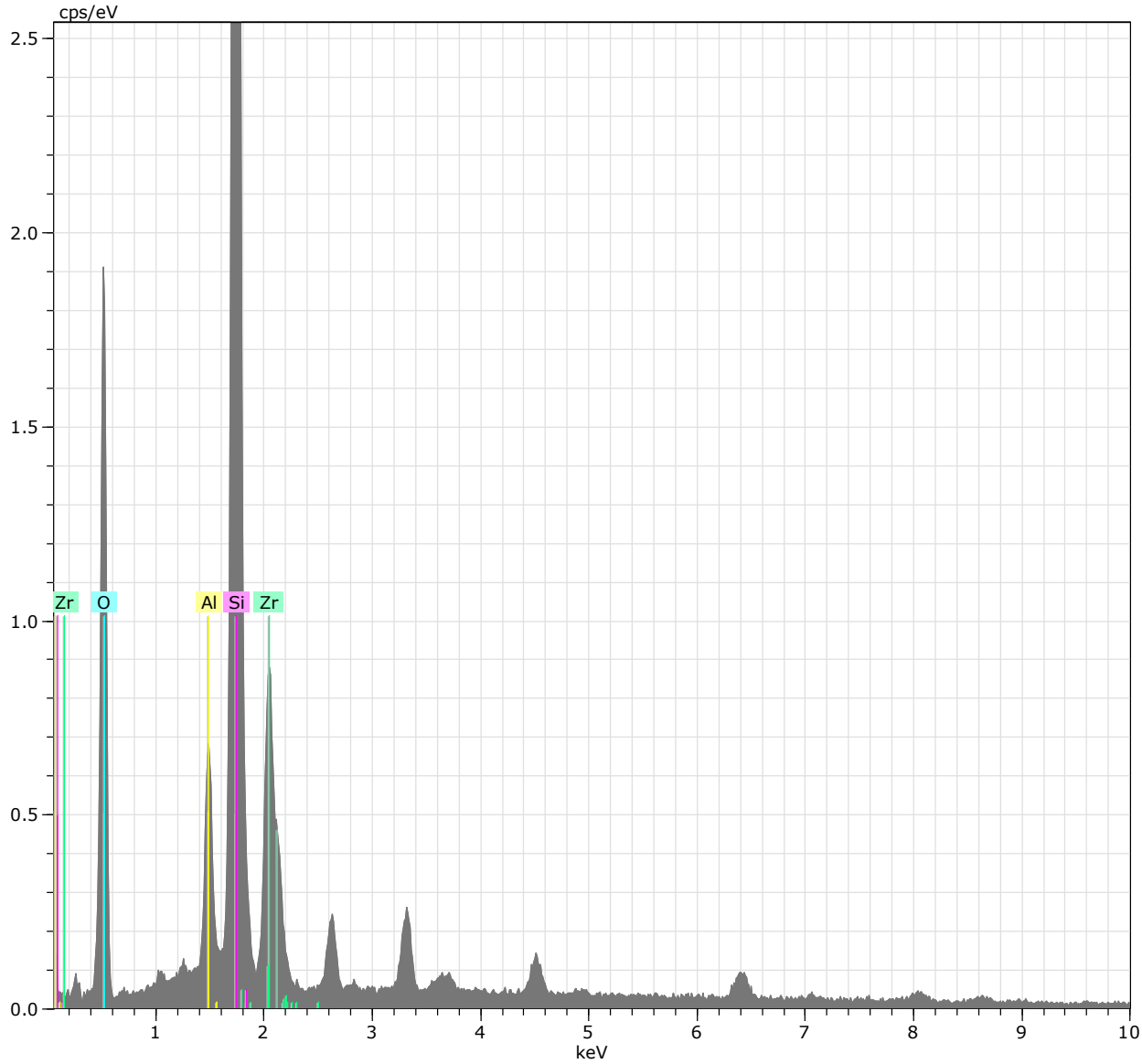

UTK-W2_33_ 2 Date:8/15/2016 10:27:56 AM HV:25.0kV Puls th.:1.66kcps

El	AN	Series	unn. C [wt.%]	norm. C [wt.%]	Atom. C [at.%]	Error (1 Sigma) [wt.%]
O	8	K-series	31.18	41.88	70.63	6.74
Zr	40	L-series	29.69	39.88	11.80	1.30
Si	14	K-series	12.71	17.07	16.40	0.63
Al	13	K-series	0.87	1.17	1.17	0.11
		Total:	74.46	100.00	100.00	

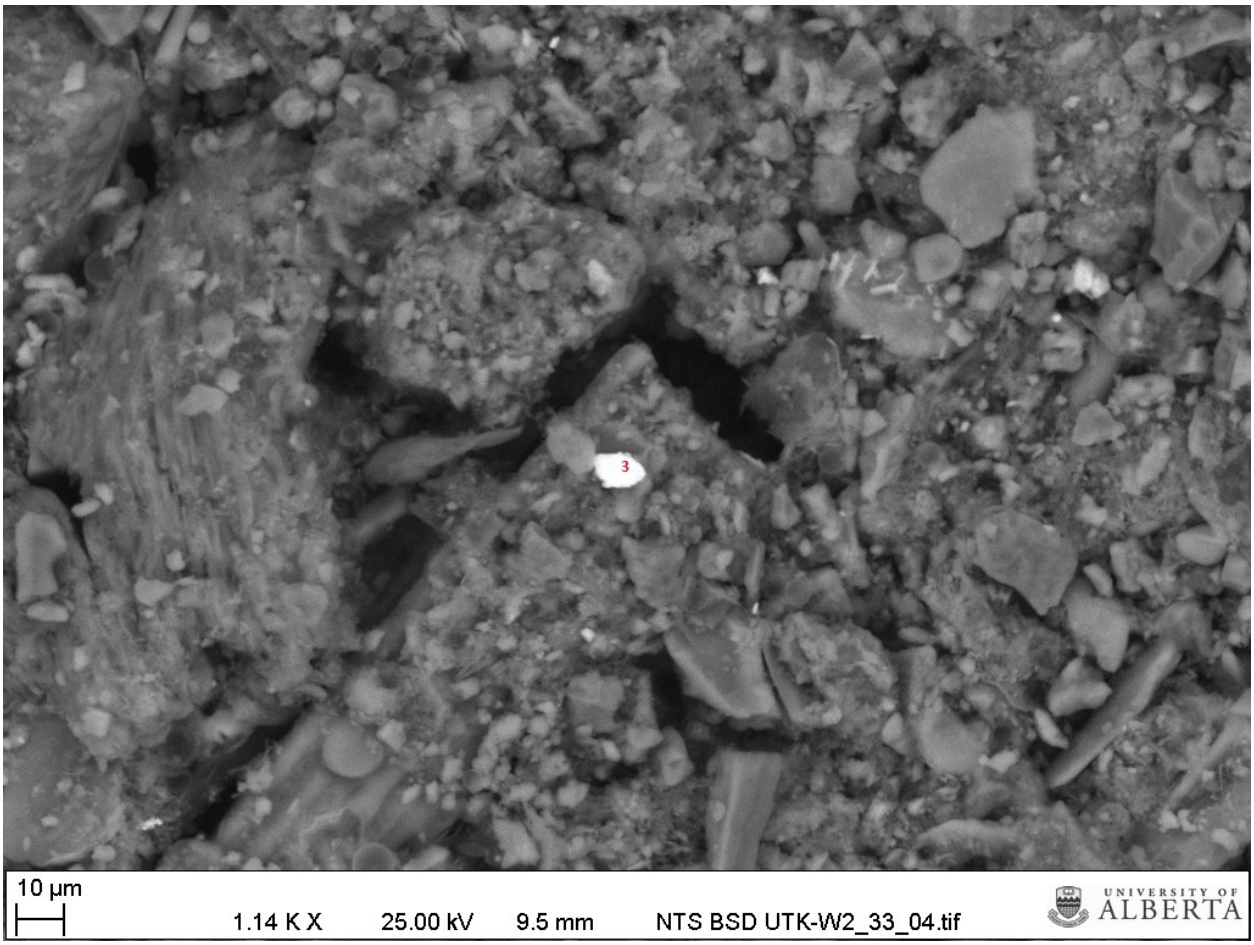
3
10 µm
1.14 K X
25.00 kV
9.5 mm
NTS BSD UTK-W2_33_04.tif
UNIVERSITY OF ALBERTA

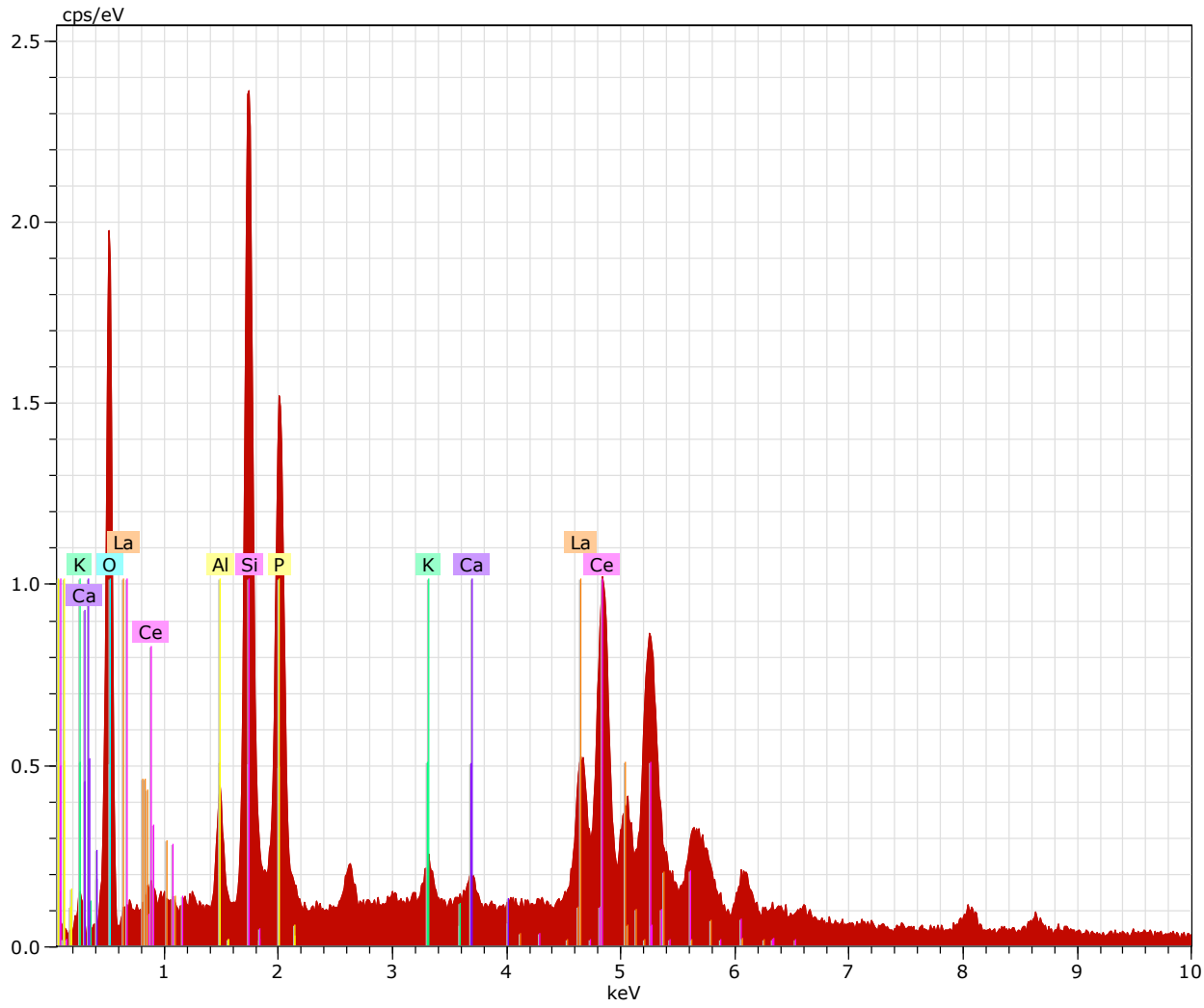

UTK-W2_33_ 3 Date:8/15/2016 10:32:38 AM HV:25.0kV Puls th.:2.26kcps

El	AN	Series	unn. C [wt.%]	norm. C [wt.%]	Atom. C [at.%]	Error (1 Sigma) [wt.%]
O	8	K-series	15.59	28.79	56.66	2.58
Ce	58	L-series	14.72	27.18	6.11	0.45
Si	14	K-series	8.08	14.91	16.72	0.40
P	15	K-series	6.91	12.75	12.97	0.33
La	57	L-series	6.30	11.64	2.64	0.23
Al	13	K-series	1.67	3.08	3.59	0.14
K	19	K-series	0.46	0.85	0.69	0.05
Ca	20	K-series	0.43	0.80	0.63	0.05
		Total:	54.15	100.00	100.00	